# Root responses to soil physical conditions and the role of root–particle contact

A thesis submitted in partial fulfilment of the requirements of the University of Abertay Dundee for the degree of Doctor of Philosophy

by

Sonja Schmidt MSc

University of Abertay Dundee

School of Contemporary Sciences

January 2011

**I certify that this thesis is the true and accurate version of the thesis approved by examiners.**

Signed..... Date.....
(Director of Studies)

# Declaration

I hereby declare that this thesis has been composed by myself and that it has not been accepted in any previous application for a degree. The work of which it is a record, is my own, unless otherwise stated. All verbatims have been distinguished by quotation marks and sources of information specifically acknowledged by means of references.

Sonja Schmidt

# Acknowledgements

I would like to express my sincere thanks to:

The SCRI and University of Abertay Dundee for funding my studentship. SCRI receives Grant-in-Aid from the Scottish Government Rural and Environment Research and Analysis Directorate.

My supervisors at SCRI: Prof. Dr Peter J. Gregory and Dr A. Glyn Bengough for their great guidance, support and motivation throughout the last 3½ years.

My supervisors at University of Abertay Dundee: Dr Wilfred Otten and Prof. Philippe Baveye, as well as my former supervisors Prof Iain M. Young and Dr Dmitri Grinev.

The team of Volume Graphics, especially Ms Daniela Handl, for their help with image analysis and development of a method to analyse root–particle contact.

Katrin McKenzie (BIOSS) for help with statistics.

Philip Smith (SCRI) for kindly proof reading my thesis.

My colleagues and friends at SCRI and in Dundee who kept me going throughout the last 3½ years and made my time in Dundee unforgettable.

Finally I would like to thank my sisters and parents, as well as my friends in Germany for their support and encouragement.

# Abstract

This thesis considers the elongation of root and shoots in relation to matric potential and soil strength in contrasting species. The role of root–particle contact for root and shoot elongation in relation to particle/aggregate size and bulk density at various matric potentials is discussed.

Root and shoot elongation of maize and lupin in soil and vermiculite at matric potentials ranging from -0.03 MPa to -1.6 MPa were investigated. Both root and shoot elongation rate of maize and lupin were significantly slower in vermiculite than in soil ($p < 0.001$). As vermiculite has very different particle size distribution and hydraulic properties from soil, the degree of contact between root and vermiculite was thought to provide a possible explanation for the slower elongation rates. A new method was developed to quantify root–particle contact using X-ray microtomography and verified using 'phantoms' (model systems of known dimensions). Root–particle contact was approximately 25 % greater in soil than in vermiculite. The greater root–particle contact in soil was thought to provide better growth conditions than in vermiculite. Root and shoot elongation were examined when plants were place in humid air above an osmotic solution (KCl) to evaluate the degree to which root elongation could occur in the absence of solution contact. No significant shoot elongation occurred and root elongation was more reduced than in vermiculite.

Hairless maize and barley mutants and their wildtypes were used to investigate further the effects of root–particle contact when water availability is limiting in both soil and vermiculite systems. Root elongation rates of the hairless mutants were slower than those

of the wildtypes, when the growth medium was wetter than -1.6 MPa. However the reduction in root elongation of hairless maize may have been due to pleiotropic effects slowing the elongation (the elongation rate relative to the maximum elongation rate was not significantly different).

The combined effects of mechanical impedance and decreasing matric potentials on root and shoot elongation were tested. Maize and lupin were grown in soil packed to five bulk densities (bulk densities 1.1, 1.2, 1.3, 1.4 and 1.5 g $cm^{-3}$) and wetted to three matric potentials ranging from -0.01 MPa to -1.2 MPa (Chapter 6). Root elongation rate decreased with increasing penetrometer resistance and maize was considerably more sensitive than lupin towards increase in these soil physical stresses. The effects of soil mechanical impedance dominated any improvement in root–soil contact. The averaged length of the root elongation zone (estimated from the distance between root hair zone and root tip) was linearly related to elongation rates. This is a possible method for estimating root elongation rates in situ.

To manipulate root–soil contact in loosely packed aggregates, seedlings were grown at various matric potentials in soils of different aggregate sizes (4–2 mm, 2–1 mm, 1–0.5 mm and <0.5 mm). The finer the aggregates were the faster the roots elongated, they also had better root–soil contact (72–79 % at <0.5 mm and 23–25 % at 4–2 mm).

A method was developed to investigate the role of liquid and solid contact with roots. Roots were exposed in different portions to the mist produced in an aeroponic system. In another experiment roots were placed above a water surface and supplied at different parts with water through cotton wool. Different portions of the total surface of the root

were in contact with liquid or solid phase. Root and shoot elongation were not significantly affected by the portion of root surface in contact with water or solid phase.

A good root-particle contact can improve plant growth when water availability is limiting growth but the effects of greater contact area are dependant on matric potential, plant species, and soil strength.

# Table of Contents

# List of Figures

# List of Tables

# 1 Background

## 1.1 Introduction

Crop productivity is highly dependant on a good supply of water and nutrients. With an increasing demand for food and variable soil water regimes associated with climate change and changing management practicies from ploughing to no tillage, greater understanding of the processes affecting root growth is particularly important.

To push their way through soils, roots need to overcome soil strength. Soil strength depends on permanent properties, such as particle size distribution, and variable properties, such as soil density and water potential. Soil strength varies with management and climate (rainfall) (Stone and Wires, 1990). Root growth in the field is often limited by physical stresses including mechanical impedance, water stress and oxygen deficiency. A better knowledge about the effects of single and combined stresses in drying soils is important for understanding water and nutrient uptake by plants. Until recently methods to investigate the root–soil interface have been destructive (Heeraman et al., 1997). Nowadays it is possible to gain an insight into root growth in opaque soils using X-ray microtomography (Gregory et al., 2003; Heeraman et al., 1997).

The following chapter summarizes general knowledge about root growth and the impacts of stresses occurring in drying soils on root growth. An overview of progress in root growth research using X-ray tomography is also given.

## 1.2 Root growth and physical stress

Soil strength generally increases as soil dries, typically from -0.005 MPa to -1.5 MPa. Soil strength and matric potential affect root growth of most crop plants (Yapa et al., 1988).

### 1.2.1 Theoretical framework of root growth

Roots have to overcome axial and radial stresses as well as frictional forces. The pressure that the root tip needs to exert to push its way through the soil depends on the resistance exerted by soil particles against displacement and deformation (Richards and Greacen, 1986). The force produced by the roots to deform the soil is often expressed as force per unit area – a pressure. To overcome the strength of the soil the growth pressure (Q) must exceed the soil pressure that restricts root growth. A classical explanation was that root elongation is induced by turgor pressure (P) and wall pressure (W) (Greacen and Oh, 1972). This is described in Equation 1-1:

$$0 = P + W + \sigma \qquad \textbf{Equation 1-1}$$

$\sigma$ = external resisting pressure of the soil, P = turgor pressure, W = cell wall pressure

In this equation the effects of soil properties on turgor pressure are not described. Greacen and Oh (1972) found a linear relation between the osmotic pressure and mechanical resistance of the soil with an intercept representing the threshold value of the wall pressure for cell elongation. They believed that the adjustment of turgor pressure provided the mechanism for roots to continue growth in hard soils. Other studies did not

necessarily agree with the study of Greacen and Oh (1972). Atwell and Newsome (1990) measured turgor pressures in the apical 15 mm of lupin (*Lupinus angustifolius*) grown in sandy loam at two bulk densities (1.6 g $cm^{-3}$ and 1.8 g $cm^{-3}$). The turgor pressure of plants grown at 1.6 g $cm^{-3}$ ranged between 0.213 and 0.530 MPa and at 1.8 g $cm^{-3}$ 0.210 and 0.570 MPa. Differences in turgor between the two treatments were not significant. Clark et al. (1996) reported an increase in turgor 5 mm from the apex of 4 and 5 day old pea roots which were mechanically impeded for one and two days. The effect was very small in 4 day old roots which were impeded for one day (0.04 MPa) but increased when impeded for two days (0.18 MPa). They concluded that the extent to which mechanical impedance affects turgor depends on the length of time for which it is imposed. It is assumed that an increase in turgor is caused by solute accumulation resulting from a decreased volume expansion. Bengough et al. (1997) found osmotic pressures of pea roots in compressed sand were 0.81 MPa and 0.64 MPa in loose sand. These differences disappeared 12 h after removing the roots from impeded sand, while root elongation remained slower than for unimpeded roots. They concluded that cell wall properties were more important than turgor in regulating root elongation rates. Bengough et al. (1997) modified the Lockhart equation (Equation 2-1) and included the effects of soil strength on cell expansion. They emphasized that turgor pressure, cell wall extensibility and cell wall yield threshold are physiological properties that depend on the external resisting pressure of the soil.

$$\frac{dl}{dt} = lm_{(\sigma)}\left[P_{(\sigma)} - Y_{(\sigma)} - \sigma\right] \qquad \textbf{Equation 1-2}$$

l = length of the elongating tissue, t = time, P = turgor pressure, $m_{(\sigma)}$ = cell wall extensibility, $Y_{(\sigma)}$ = cell wall yield threshold, $\sigma$ = external resisting pressure of the soil

Root growth pressure increases with soil strength, which depends on the water content. The permeability of the cell walls to water does not restrict the rate of cell expansion. The growth rate is therefore a function of turgor pressure (P), soil resistance and the rheological properties of the cell walls (Clark et al., 2003; Gregory, 2006).

The maximum growth pressure roots can produce differs between cultivars and species and seems to be temperature dependent (Bengough et al., 1994; Taylor and Ratliff, 1969; Whalley et al., 1994). Bengough et al. (1994) demonstrated that the maximum pressure was achieved twice as quickly at 25 °C as at 8 °C, while Whalley et al. (1994) found that maximum growth pressure of peas was lower at 15 °C and 20 °C than at 10 °C, 25 °C and 30 °C.

### 1.2.2 Effect of matric potential on root growth

The rate of root elongation is usually reduced when soil dries. The growth of roots is often not as much decreased as the decrease in shoot growth, so that the root–to–shoot ratio of such plants increases. Roots show enhanced geotropism when soil dries and water uptake is often enhanced by an increased rooting depth (Davies and Bacon, 2003).

Sharp et al. (1988) investigated the root growth of the tap root of maize (*Zea mays*) at different water potentials. Vermiculite was used as the growth medium. At dry water potentials the root continued slow rates of elongation, while shoot growth was completely inhibited. Sharp et al. (1988) determined the spatial distribution of root growth response. He found out that the length of the root elongation zone decreased progressively as the

matric potential decreased. The roots were marked with an ultrafine pen at approximately 1 mm intervals for 12 mm from the root apex. The maximum root growth rate moved apically with decreasing water potential and local growth rates throughout the majority of the zone were reduced except for the region closest to the apex.

### 1.2.3 Adaptation of roots to drought

#### 1.2.3.1 Morphological adaptations

Roots have an obvious role in moderating the supply of water through rooting depth and the quantity of roots in a particular layer. Roots show enhanced geotropism when soil dries out (Sharp and Davies, 1985). An increased rooting depth can significantly increase water uptake. A clear effect is only noticeable when plants are competing for the same reserves of soil water (Davies and Bacon, 2003). As soil water is restricted the root diameter changes. At dry water potentials and low mechanical impedance, it has been observed that the root diameter is thin. This is possibly an adaptation to a smaller carbohydrate supply (Sharp et al., 1988). In most soils with high mechanical impedance, roots increase in diameter behind the apex in drying soils (Spollen et al., 2000). Different species show different abilities to penetrate soil as mechanical impedance increases. Roots of many plants are restricted to cracks in soils of strong mechanical impedance and therefore often will be clustered in these fissures and cause local drying (Davies and Bacon, 2003). A shorter elongation zone is a consequence of a slower growth rate caused by shorter cortical cells and lower rate of cell production (Fraser et al., 1990).

Fine roots play an important role in drought resistance (McCully, 1999). In Brassicaceae, for example, short fine roots with radially swollen bases, matured xylem and inactive meristem develop and persist during drought (McCully, 1999). These fine roots develop numerous root hairs when watered and continue elongation. In other species drought leads to a greater number of lateral roots often in response to death of the parent root apical meristem (Brady et al., 1995; Jupp and Newman, 1987).

### 1.2.3.2 Physiological and biochemical adaptation of roots in drying soil

Root cell elongation of maize in the apical 2–3 mm was maintained when grown at -1.6 MPa (Sharp et al., 1988). The study of Voetberg and Sharp (1991) showed that an increase in proline deposition in the apical region contributed to an osmotic adjustment, but investigations of the spatial distribution of turgor and root growth at low potentials showed that turgor was greatly decreased at low matric potential (-1.6 MPa). Despite the decrease in turgor the longitudinal growth in the apical 2 mm was equal in wet and dry conditions. Spollen and Sharp (1991) suggested that changes in cell wall yielding occur, so that the root elongation in the apical region is maintained under dry conditions.

Xyloclucan endotransglycosylase (XET) was one of the first enzymes (expansin) found to regulate cell wall expansion. Wu et al. (1994) found that XET activity was greatly enhanced in the apical 5 mm of primary maize roots at dry matric potentials (-1.6 MPa), which suggested that cell walls in the apical region are more extensible at dry matric potentials. Further investigations of Wu et al. (1996) showed enhanced expansin activity in the very apex of maize roots at low water potential, which was well correlated with wall susceptibility to expansin.

Shoot growth is very sensitive to water–limited conditions. Previous studies have shown that the inhibition of growth is metabolically regulated, rather than a direct consequence of altered water status of the plant caused by drying soils (Sharp and Davies, 1989). Root growth is often less inhibited than shoot growth, or sometimes even promoted, in drying soils, which results in a better water supply under dry conditions (Sharp and Davies, 1989). Some plant species sustain root elongation at matric potentials drier than the wilting point (-1.6 MPa). Sharp et al. (1988) showed that maize roots elongated at 1 mm $h^{-1}$ at matric potentials drier than -1.6 MPa, while shoot growth was already inhibited at matric potentials lower than -0.8 MPa.

Abscisic acid (ABA) is increasingly implicated in coordinating the responses of roots and shoots to changes in soil water content (Sharp, 2002). ABA accumulates in root and shoot tissues under water limited conditions and it is often correlated with growth inhibition. Reduction in ABA production is correlated with a severe inhibition in root elongation compared to the wild type or untreated seedlings under dry conditions, but in wet conditions root elongation is minimally affected (Sharp et al., 2000). There is an interaction between water status of the soil and ABA concentration (Sharp et al., 1994), so that root elongation is not just a function of increase in ABA but a combination of ABA and change in environmental conditions. ABA has been shown to be involved in limiting ethylene production (Sharp et al., 2000; Spollen et al., 2000) and because of this interaction of shoot and root growth can be maintained rather than inhibited under certain conditions.

## 1.2.4 Plant responses to mechanical impedance

### 1.2.4.1 Root growth: morphological responses

#### *1.2.4.1.1 Mucilage exudation and sloughing of root cap cells*

Exudation of mucilage and sloughing of root cap cells reduce the frictional resistance to soil penetration. Bengough and McKenzie (1997) compared the penetration resistance of maize roots and a metal probe. The maize roots showed a lower penetration resistance than the metal probe. They suggested that root cap cells relieved the friction by detaching and forming a low friction lining to the cavity enlarged by the root. Cells slough from the root cap if the coefficient of friction between the cap cell and soil is lower than that between the cell and the root surface. Each sloughed cell reduces the frictional resistance (Bengough et al., 1997). Iijima et al. (2000) determined the number of maize root cap cells sloughed into sand for different levels of compaction. With increasing penetrometer resistance from 0.29 MPa to 5.2 MPa the number of sloughed root cap cells increased from 1930 to 3220 cells per day. The cells reduced the friction between the root cap and the surrounding soil particles. Iijima et al. (2004) quantified the contribution of mucilage and sloughing of border cells from the root cap for maize root growth in compacted soils. The impact of sloughing border cells (58 % of the lubricating effect) in reducing the mechanical impedance was greater than the effect of mucilage (42 % of the lubricating effect) (Iijima et al., 2004). The lubricating effect of mucilage depends on the degree of hydration (Iijima et al., 2004).

### *1.2.4.1.2 Root shape and diameter*

Mechanically impeded roots exhibit two very obvious features. They are shorter and thicker than roots grown in loose soil (Atwell, 1990b; Kirkegaard et al., 1992; Materechera et al., 1991). Lupin roots showed a radial thickening of about 15 % with increasing bulk density from 1.23 to 1.42 g $cm^{-3}$, while root elongation decreased by 38 % (Atwell, 1988). The amount of radial thickening depends on particular experimental conditions (Atwell, 1988). Radial thickening of impeded roots results in roots that are more resistant to buckling and probably decreases the axial stress in front of the root tip (Richards and Greacen, 1986; Whiteley et al., 1982). Atwell (1988) suggested that the reduction in cell elongation is a direct response of the meristematic zone to external pressure. The cells responsible for the thickening are mainly cortical cells. In lupin the diameter of the individual cells rather than the number of cells increased. Kirkegaard et al. (1992) investigated the growth of pigeonpea radicles and seedlings at different soil strengths. In a high strength root zone, root length was reduced by about 60 %. Similarly, Atwell (1990a) showed a reduction in root length of wheat from loosened soil to compact soil. Thickening of the compacted seminal root axes was caused by increased cell diameters of cortical cells. The length of cortical cells was smaller when roots grew in compacted soil. Croser et al. (2000) also investigated the effect of mechanical impedance on root growth of peas. Root elongation was slowed and the maximum elongation rate was reduced as strength increased. Recovery to the unimpeded rates occurred after 60 h following a transfer to a hydroponic system.

Inhibition of growth of the tap roots or seminal roots often leads to lateral root proliferation (Crossett et al., 1975). However, Atwell (1988) demonstrated that lupin roots grown in a sandy clay loam did not show this effect.

### 1.2.4.2 Metabolic changes

The concentration of metabolites and ions in roots reflects the rate of import and utilization and volume expansion of the cells. Atwell (1990b) investigated the changes in the major metabolites of roots growing through impeded soil. Compaction caused a reduction in N, K and the total concentration of solutes. In contrast the concentration of soluble sugar increased about 21 % through compaction. Atwell (1988) suggested that sugars accumulate through slower rates of cell volume expansion. Amino acids were less concentrated, possibly because of a deficiency either of total N or reduced N concentration in plants from compact soil (Atwell, 1990a). Atwell (1990c) investigated the pattern of assimilate transport to the roots of wheat in compact and loosened soil. The daily import of solutes was slower in compacted soil than in loosened soil. This caused a carbon saving to the plant from a restricted root system and altered utilization.

Less carbon was required to synthesize new seminal roots in loose soil than to synthesize an equivalent length of new seminal root in compacted soil. A decrease in seminal root axes in compacted soil was found (Atwell, 1990c) resulting in incomplete extraction of deep water and leached nutrients. Much of the additional carbon was used in synthesizing thicker roots and not for osmotically–active substances. The metabolic changes in wheat roots in impeded soil resulted in morphological changes rather than in increased turgor pressure (Atwell, 1990c).

### 1.2.4.3 Compression of soil around roots

Growing roots affect the soil around them in several different ways. The root compresses the soil mainly by radial expansion except if they grow into existing channels or fissures (Clark et al., 1996). Root tips can exert pressures up to 1 MPa and produce cap cells and mucilage (Clark et al., 1996). The stress applied by the root depends on the soil strength; the higher the bulk density the higher is the exerted stress. The stress is lower in regions distal from the root apex (Kirby and Bengough, 2002; Figure 1-1). As a result the greatest compression of soil appears close to the root apex. The changes of porosity close to the root can lead to changes in nutrient, air and water transport to the root surface (Bengough et al., 2003).

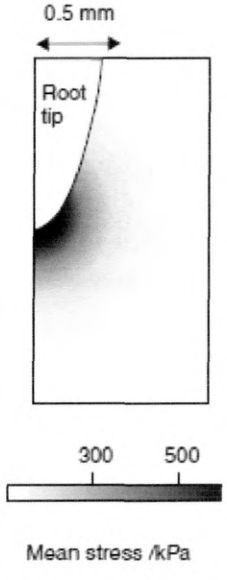


**Figure 1-1: Predicted mean stress near the root tip of a thin root analogue penetrating soil (from Kirby and Bengough, 2002).**

Bulk densities at the surface of maize, pea and wheat roots of about 1.7 to1.8 g $cm^{-3}$ were reported (Bruand et al., 1996), when the bulk density of the bulk soil was about 1.3 to 1.54 g $cm^{-3}$.

The relative increase in density at the root surface and the thickness of the soil that the root will compress depends on the root diameter and the compressibility of the soil. It is possible to calculate the amount of soil compression which is produced at different distances from a root. Dexter (1987) developed a simple model of soil compression around roots using the theory of the expansion of cylindrical cavities in plastic frictional media. His model showed that the resulting soil density or porosity varied exponentially with distance from the root surface, the porosity of the soil becomes more similar to the porosity of the undisturbed soil when the distance from the root surface increases (Equation 1-3):

$$\eta(r) = \eta_0 + (\eta_i - \eta_0)(1 - e^{-k(r-r_0)/r_0}) \qquad \textbf{Equation 1-3}$$

$\eta(r)$ = porosity at distance r from the root surface, $\eta_0$ = porosity in the zone of maximum compression at the root surface, $\eta_i$ = porosity of bulk soil, k = parameter describing the change in density with distance from the root surface and $r_0$ = root radius

This model requires a value for minimum porosity, which can be estimated by compressing the soil under a constant load, and a value of the parameter k, which is generally between 0.34 and 6 (Bruand et al., 1996; Dexter and Tanner, 1973; Richards and Greacen, 1986). The variation in k influences the rate of change of porosity outside the zone of maximum compression.

### 1.2.5 Root–soil contact

Root contact with the soil is essential for water and nutrient adsorption by plants. The root–soil contact is influenced by soil and root properties, like particle size, degree of soil compaction, root diameter and relative hydration (Nye, 1994; Tinker, 1976). In water–saturated and heavily compacted soils, problems with root gas exchange can occur (Veen et al., 1992), but incomplete root–soil contact due to soil structure or root shrinkage can reduce the uptake of water and nutrients (Veen et al., 1992).

The determination of the root–soil contact is rather difficult because soils are opaque. Van Noordwijk et al. (1992) showed that a thin–section technique could be used to derive the degree of root–soil contact. They grew maize in pots packed with aggregates obtained by sieving to different bulk densities ranging from 1.08 g $cm^{-3}$ to 1.50 g $cm^{-3}$. Thin sections were derived from vertical and horizontal blocks and photographic prints (enlargement x12) were made of the thin sections. Roots and roots–soil contact zones were drawn on transparencies used as overlays on the prints. Root parameters, such as number, cross sectional surface perimeter and perimeter of the soot soil contact zone were measured. The percentage of root–soil contact was derived from the root perimeter and the perimeter of root–soil contact zone. There was no visual appearance of shrinkage of roots which had intact epidermis, cortex and other tissues. Root lengths and number of root cross sections counted on horizontal and vertical thin sections were similar to those measured from duplicate soil samples where roots were washed from the soil (Van Noordwijk et al., 1992).

Kooistra et al. (1992) subsequently used this technique to determine the effect of bulk density on root–soil contact. Maize was grown at bulk densities of 1.08 g $cm^{-3}$, 1.32 g $cm^{-3}$, 1.43 g $cm^{-3}$, 1.50 g $cm^{-3}$ and 1.54 g $cm^{-3}$ at matric potentials between -10 kPa and -20 kPa. Their findings were that root–soil contact was increased by 45 % from the lowest to the greatest bulk density. Root–soil contact in the loosest soil was still 60 %, so that Kooistra et al. (1992) concluded that roots growing in loose soil preferentially grow down the wall of pores and have partial contact with the soil.

Veen et al. (1992) investigated in a third study whether poor root–soil contact affected root and shoot growth, nitrate and water uptake. Maize was grown at similar levels of soil compaction used in the study of Kooistra et al. (1992), as well as under restricted nitrogen supply. Root and shoot fresh weight increased with decreasing bulk density up to a bulk density of 1.32 g $cm^{-3}$ but lagged behind at the lowest bulk density of 1.08 g $cm^{-3}$, while root length increased constantly with decreasing bulk density. Water and nitrate uptake were also highest at the intermediate pore volume and slightly lower at the highest soil porosity. Root growth was restricted to the upper zones of the pots which were packed to the highest soil compaction and the root length was smaller than in less compacted soil. Water and nitrate uptake per unit root length decreased with decreasing root–soil contact (Veen et al., 1992).

The quantification of root–soil contact with the thin section technique only allows observations of root–soil contact in two dimensions and is rather time-consuming to determine root–soil contact for a whole root system. Carminati et al., (2009) used X-ray tomography to determine root–soil contact dynamics of white lupin (*Lupinus albus L.*)

under drying and wetting cycles in a sandy soil. Radii of roots and gaps between root and soil were determined by segmenting the tomogram into roots, gaps and soil. Changes in root diameter and diameter of pores hosting the root were determined under dry (volumetric water content = 0.025 $cm^3$ $cm^{-3}$) and wet (volumetric water content = 0.135 $cm^3$ $cm^{-3}$) conditions. The absolute change in root diameter was greater than that of the pore that the root grew into, and Carminati et al. (2009) concluded that gap dynamics are primarily controlled by swelling and shrinking of the root. The air gap formation around roots suggests changes in root–soil contact, but root–soil contact was not quantified.

## *1.3 Visualization of root systems using X-ray microtomography*

X-ray microtomography allows non-destructive observations of roots in opaque soils (Perret et al., 2007; Tracy et al., 2010). Several studies have observed roots using X-ray microtomography (Gregory et al., 2003; Heeraman et al., 1997; Kaestner et al., 2006; Lontoc–Roy et al., 2006; Perret et al., 2007). Depending on scan alignment of the CT scanner, the results may differ from the results of destructive methods. The quality of the images depends on the energy of the X-ray beam, the number of angular projections and the signal acquisition time per projection (Ketcham and Carlson, 2001). The more angular projections less noise can be expected, but scanning duration will be longer.

To estimate the fraction of the roots in voxels containing roots and soil the following approach can be used (Equation 1-4)

$$\mu_v = \sum_{i=m}^{m} f_i \mu_i$$ **Equation 1-4**

$\mu_v$ = voxel average linear attenuation coefficient, $f_i$ = voxel volume fraction of component i, $\mu_i$ = linear attenuation coefficient of component i

Equation 1-5 applies for a system containing soil and roots.

$$\mu_v = f_r \mu_r + f_m \mu_m$$ **Equation 1-5**

$\mu_v$ = voxel average linear attenuation coefficient, $f_r$ = voxel volume fraction of roots, $\mu_r$ = linear attenuation coefficient of roots, $f_m$ = voxel volume fraction of soil matrix, $\mu_m$ = linear attenuation coefficient of soil matrix

The $\mu_r$ represents living roots because of their water content. If it is assumed that the voxels are large enough compared with particle size then the matrix can be treated as a single phase and each voxel can be computed as (Equation 1-6).

$$f_m + f_r = 1$$ **Equation 1-6**

$f_m$ = voxel volume fraction of soil matrix, $f_r$ = voxel volume fraction of roots

Because the raw images of roots and the edges of soil particles have the same grey value, partial volume effects make it difficult to produce a threshold image which represents roots accurately (Kaestner et al., 2006). The images have three main features: sand grains, pores and roots. The grey values of the three compounds are ordered by density. Sand grains are represented by bright voxels and pores by dark voxels. Because the values for the roots are in between the values for soil and pores, it is difficult to reconstruct root networks satisfactorily even when using a connectivity algorithm. Kaestner et al. (2006)

enhanced the contrast between the roots and the embedding material by using a non–linear diffusion filter acting in three dimensions. The diffusion filter used strong gradients in the image as the barrier for smoothing. Thresholding was implemented using Rosin's threshold algorithm method for unimodal histograms. For extraction of the main features they also used a morphological connectivity algorithm. With this approach they were able to detect fine roots with diameters less than 0.5 mm.

Heeraman et al. (1997) used the quadratic mean root radius (QMRR) to estimate the root length by assuming that roots are cylindrical in shape. The following relationships were used. Total Volume ($V_t$) = Total number of voxels × voxel volume (v, $cm^3$); Air Cavity Volume ($C_v$) = No. of voxels consisting of air within column × v; Soil Matrix volume ($V_m$) = No. of matrix voxels × v; Root volume ($R_v$) = No. of root voxels × v; Root length ($R_l$) = $R_v/\pi \times (QMRR)^2$; and Root Length Volume ($L_v$) = $R_l/V_t$. Roots of beans (*Phaseolus vulgaris* L.), were grown for 14 days in sandy soil with uniform packing and water content, and scanned with a 420 kV X-ray source collimated through a narrow slit (0.2 mm in height and 0.2 mm in length; Heeraman et al., 1997). Heeraman et al. (1997) compared the results of the CT–scanning with data from destructive root measurements. The results showed an overestimation of root length of 21 to 42 % for the CT–scanning, which was probably caused by signal noise and large attenuation variations due to local variations in packing. Furthermore the contribution of air in voxels at the root–air interface was not considered which led to an overestimation of the root volume.

Gregory et al. (2003) investigated the root growth of wheat (*Triticum aestivum*) and rape (*Brassica napus*) by using a CT–Scanner. They found an underestimation of root length

and diameter of 10 % determined from 3-D volumetric images. The images were reconstructed from a slice a short distance from the seed. This allowed the root to be clearly distinguished from the seed but resulted in a small loss of root length. They determined the attenuation value for the voxels at the base of the seeds to set the binary thresholds which were able to differentiate biological materials. There was some overlap in values of image density for roots, soil and container. Therefore they applied a 3-D connectivity routine to connect neighbouring voxels of similar image density starting at the plane corresponding to the base of the seed and working down on each slice of data to improve root identification. A problem which occurred soon after germination was that the roots hit the container wall and were indistinguishable for the CT–scanner.

Perret et al. (2007) used bigger containers (0.23 × 0.14 m) compared to the containers Gregory et al. (2003) used (0.025 × 0.025 m). Before visualization of chickpea (*Cicer arietinum* L.) roots they optimized the scanner settings using a phantom core filled with different soil and material (including root segments). In comparison to the results of destructive analysis, the root length data showed an underestimation by the CT scan. These results are similar to Gregory et al. (2003) findings. Also the number of roots detected by CT scanning was less than by destructive determination. Root diameter determined from 3-D volumetric images ranged between 3.2 mm and 1.4 mm and was up to 0.8 mm greater than the actual root diameter. Air near the root caused this overestimation (Perret et al., 2007). The CT scanning delivered data about tortuosity which was not possible to obtain with the destructive method.

Lontoc–Roy et al. (2006) also used homogenised soil but different types of soil moisture combinations. The aim of their study was to isolate the root system from the soil and quantify root system complexity. Maize was grown in sandy soil and in loamy sand under dry and water saturated conditions. For data analysis they employed an algorithm developed in MATLAB (Math Works Inc., 2005) to separate roots from the soil by doing a 3-D neighbourhood analysis of the CT data. They compared the fractal dimension calculated by CT scanning with results from estimating the fractal dimension using 2-D photographs. The most accurate results (difference 7%) were found in dry homogenous sand. Pierret et al. (2003) visualised root growth and water uptake by using thin–slab systems. The advantage of thin–slab systems is that they provide high resolution images, but they are restricted to 2-D (Young et al., 2001).

Table 1-1 summarizes the different alignments and preparations for visualization of root systems using X-ray microtomography.

**Table 1-1: Overview over different studies of visualization in 3-D of root systems by using X-ray computed tomography.**

| Author / Year | CT Scanner Alignments | Root and growth medium | Conclusions |
|---|---|---|---|
| Heeraman et al., 1997 | 420 kV3 µA<br>Sample diameter 50 mm, resolution 160 µm | Bush bean (*Phaseolus vulgaris* L.) in air dried sandy soil (grav. water content 0.18 %) | Overestimation of root length by 21–42 % |
| Gregory et al., 2003 | 50 kV, 80 µm spot size, sample diameter 25 mm, resolution 100 µm | Wheat (*Triticum aestivum*) and rape (*Brassica napus*) in sandy soil sieved to < 250 µm, gav. water content 15 % | Underestimation of root length by 10 % and diameter |
| Lontoc–Roy et al., 2006 | 130 kV, 100 µm spot size, sample diameter 100 mm, resolution 120 µm | Maize (*Zea mays*) in sieved and homogenized sand and loamy sand, sieved to 2 mm | Most accurate results in homogeneous dry sand and water saturated loamy sand |
| Kaestner et al., 2006 | 80 kV, spot size 5 µm, sample diameter 36.9 mm, resolution 36 µm | Alders (*Alnus incana* L.) scanned in quartz sand | Root system is preserved, fine roots (diameter less than 0.5 mm) are visible |
| Perret et al., 2007 | 130 kV, spot size 100 µm, sample diameter 0.23 x 0.14 m, resolution 275 µm | Chickpea (*Cicer arietinum* L) in irrigated sand (single grain 0.5 mm) | Underestimating of root length by 10 % and root number; overestimating of root diameter by 0.8 mm |

Studies which had been done to quantify root parameters, such as length, diameter or number from 3-D volumetric images (Table 1-1), showed that X-ray tomography is a valuable method for visualising and quantifying roots in soil, but the technique can over– or underestimate those parameters, depending on voxel size, root diameter and soil particle distribution. The methods have improved with time so that the error was reduced from 21 % to 42 % (Heeraman et al., 1997) to 10 % (Gregory et al., 2003; Perret et al., 2007).

## 1.4 Aim, Objectives and Hypothesis

### 1.4.1 Summary of Literature

Effects of drying soils on root and shoot growth are well studied (Bengough et al., 2003; Bengough and Mullins, 1990; Eavis, 1972; Goss, 1977; Materechera et al., 1991; Sharp et al., 1988; Spollen et al., 2000; Spollen and Sharp, 1991; Taylor and Ratliff, 1969; Veen and Boone, 1990). Knowledge of the effects of matric potential on root growth was mainly obtained from studies in vermiculite because mechanical impedance could be neglected (Sharp et al., 1988; Spollen et al., 2000; Wu and Cosgrove, 2000). Vermiculite is different in properties to soil. It consists of large plate–like swelling particles with highly anisotropic conductivity characteristics. Furthermore it only contains tiny quantities of water at potentials limiting to root growth, and has a very high porosity, so that a greater root–particle contact in soil than in vermiculite could be expected, which is important for water supply to the roots. However, in drying soils combined stresses, such as water stress and mechanical impedance occur, but only a few studies have looked at these combined stresses (Taylor and Ratliff, 1969; Veen and Boone, 1990) and information about effects of root–soil contact are rare.

### 1.4.2 Aim and Objectives

The overall aim of this thesis was to investigate effects of matric potential and strength on root and shoot elongation and to determine the role of root–particle contact.

The objectives in this study were to:

- **measure root and shoot elongation rates of contrasting plant types in growth media of different particle/aggregate sizes, bulk densities and matric potentials.** Maize and lupin will be grown in soil (<2 mm), vermiculite and air at four matric/water potentials to test the effects of matric potentials on root and shoot elongation rates in different growth media (Chapter 4). It is hypothesized that root and shoot elongation rates will be fastest in soil and slowest in air, because roots have greater contact in soil and therefore better access to water and nutrients. Furthermore combined stresses of decreasing matric potential (-0.01 MPa and -1.2 MPa) and increasing bulk densities (1.1 g $cm^{-3}$ to 1.5 g $cm^{-3}$) and also matric potential (-0.03 MPa to -0.8 MPa) and decreasing aggregate sizes (4-2 mm, 2-1 mm, 1-0.5 mm and <0.5 mm) on root and shoot elongation will be investigated (Chapter 6). It is hypothesized that root and shoot elongation will be faster the finer the aggregates because root–soil contact will be better and the plant is better supplied with water and nutrients. However in very dry soil, roots in coarser soil will have an advantage because of less contact with the soil and therefore smaller water losses from the plant to the soil. Moreover it was hypothesized that an increase in bulk density up to 1.3 g $cm^{-3}$ will increase root and shoot elongation rate because root–soil contact will be increased. At greater bulk densities roots will be mechanical impeded and therefore will elongate more slowly.

- **utilize root hair mutants to assess the contribution of root hairs to root and shoot elongation in different growth media.** Hairless maize and barley mutants

and their wildtypes will be grown in soil (<2 mm) and vermiculite (Chapter 5) and in soil of various aggregate sizes (4-2 mm, 2-1 mm, 1-0.5 mm and <0.5 mm; Chapter 6) at matric potentials ranging from -0.03 MPa to -1.6 MPa. It is hypothezised that root elongation of hairless mutant plants will be slower than that of the wildtypes because root hairs increase root-particle contact and plants which are producing root hairs will be better supplied with water and nutrients.

- **develop a method for quantifying root–particle contact using X-ray microtomography.** Model systems (Phantoms) of root–particle contact will be built and scanned and the contact area calculated from known dimension of the Phantoms. These values will be compared with contact areas determined using the software VGStudio MAX to test the accuracy of the method (Chapter 3).

- **quantify root–particle contact of seedlings grown in various growth media using X-ray microtomography and evaluate their effects on root and shoot elongation.** 3–D volumetric images of maize and lupin seedlings grown in soil (<0.2 mm) and vermiculite at -0.03 MPa and -1.6 MPa (Chapter 4) and in different aggregate sizes at -0.03 MPa (Chapter 6) will be obtained and root–particle contact will be determined. It is hypothesized that root–particle contact is greater in media with small aggregates than in media with larger agregates, and that root–particle contact will be greater in soil than in vermiculite because of smaller particle size in soil than in vermiculite.

- **compare the affects of root contact with liquid or solid phase when plant growth is not limited by water availability.** Lupin and maize roots will be grown in an aeroponic system and above a water surface. Parts of the roots will be

covered to avoid root contact with the liquid phase or roots will be partly in contact with moist cotton wool (Chapter 7). It is hypothesized that root elongation rate will be slower the smaller the region of the root in contact with the liquid phase.

# 2 Materials and methods

## 2.1 Introduction

This chapter details techniques and material common to experiments throughout the project, with consideration given to limitations and restrictions of certain methods. Plant material and growth media used during this project are introduced and methods for determining various properties of the growth media, such as pH, penetrometer resistance and water retention characteristics, are discussed.

## 2.2 Plant material and germination

During this project maize (*Zea mays*, cv. KX0141 source: KWS Germany) and lupin (*Lupinus angustifolius*, VIOL source: PGRO UK) were used for comparison between a monocotyledon and a dicotyledon. Maize and lupin grow a thick primary root, which allowed visualization of the roots with X-ray microtomography at resolution of 34.9 μm. Hairless mutants of maize (*Zea mays*, rth3, source Frank Hochholdinger ZMBP, Eberhard Karls University Tübingen, Germany) and spring barley (*Hordeum vulgare*, brb), as well as their wildtypes (*Zea mays,* B73 and *Hordeum vulgare*, Pallas) were used in several experiments to study root growth in drying soils.

Maize and lupin seeds were sterilized in 0.2 % CaOCl for 10 min and rinsed in distilled water three times, while barley was soaked in distilled water for 5–6 h before sterilisation. Seeds were then placed between moist paper towels and stored in sealed dishes (23 × 23 × 2) at either 20 °C for maize and lupin or 12 °C for barley for three days.

## 2.3 Growth media

*Soil*

The soil used was a sandy loam. It was collected in 2006 from an arable field site (Bullion Field), situated at the Scottish Crop Research Institute (Loades et al., 2010) and stored. It is a Eutric Cambisol derived from undifferentiated sandstone, composed of 71 % sand, 19 % silt and 10 % clay (White at al. 2000). In this projwect the soil was air–dried and then sieved to 2 mm, except for one experiment where the effect of aggregate size on root and shoot growth was tested. For that experiment soil was sieved to 4–2 mm, 2–1 mm, 1–0.5 mm and <0.5 mm.

*Vermiculite*

Vermiculite V3 (Wiliam Sinclair Horticulture Ltd., Lincoln UK), an aluminium iron silicate, used in this study consisted of particles with diameters of 4.75 mm to 1.2 mm. the grading specifications can be found in Table 2-1.

**Table 2-1: Grading specification of vermiculite (grade 3) expressed as % by weight passing.**

| Grading Specification - % by weight passing | |
|---|---|
| 4.75 | 90–100 % |
| 3.36 | 70–90 % |
| 2.36 | 35–60 % |
| 1.2 | 5–20 % |

The particle density of vermiculite V3 was 0.07 g $cm^{-3}$ (± 10 to 15 %). Vermiculite was taken out of two different bags for the different experiments. In this thesis they will be

referred to as bag 1 and bag 2. Vermiculite was used as a growth medium because mechanical impedance can be negated. Fundamental studies on the effects of decreasing matric potential on root and shoot elongation rates were conducted in vermiculite (Sharp et al., 1988). This study, amongst others, investigated whether root and shoot elongation rates of maize, lupin and barley were similarly affected by decreasing matric potential in loosely packed soil and vermiculite.

### 2.3.1 pH

Soil pH is an important factor influencing root growth of plants (Islam et al., 1980; Tang et al., 1996; White, 1990). In acidic or alkaline soils nutrient availability can be reduced (Gregory, 2006; Islam et al., 1980; Tang et al., 1996). At pH below 4 sufficient membrane damage can occur, that leads to loss of previously adsorbed ions. An optimal pH for growth of maize was reported at 5.5 to 6.5 (Islam et al., 1980) while for lupin the optimal range is 5 to 5.5 (Tang et al., 1996).

The pH of soil and vermiculite was measured using a Mettler Toledo pH meter MP 230. Either 10 g of soil, sieved to 2 mm, or 1 g of vermiculite was mixed with 20 ml of 0.01 M $CaCl_2$-solution and stirred for 20 min. A smaller amount of vermiculite was chosen, because its greater water adsorption capacity compared to soil. Three samples of soil and vermiculite (bag 1) and five of vermiculite (bag 2) were measured. Each vermiculite sample (bag 2) was measured three times, while one reading of each soil and vermiculite (bag 1) sample was taken. The soil had a pH of 5.2 (±0.01), vermiculite (bag 1) 7.7 (±0.09) and vermiculite (bag 2) 7.7 (±0.03).

Different numbers of measurements for soil and vermiculite (bag 1) and vermiculite (bag 2) were done because readings of vermiculite took longer and measurements were carried out over a different period.

**Figure 2-1: Vermiculite untreated (left) and washed in $CaCl_2$-solution (right), weight 10 g of air dried vermiculite.**

The pH of vermiculite (bag 1 and bag 2) was outside of the optimal range for maize and lupin. Therefore measures to reduce the pH were explored. Vermiculite was washed with 0.1 M $CaCl_2$-solution to reduce pH, at the same time the pH of soil was increased with 3.5 g $CaCO_3$ per 1 kg soil. The pH of soil was increased to 7 (± 0.09) and that of vermiculite was decreased to 7 (±0.02). The structure of vermiculite collapsed, so that its physical properties changed too. The vermiculite was therefore used without lowering the pH. In general soil with pH 5.2 was used throughout all experiments, except for one experiment where root growth of maize and lupin at low and high pH was tested.

### 2.3.2 Penetrometer resistance

Penetrometers give a good estimate of resistance to root growth in soil, but the penetrometer resistance of the metal probe can be two to eight times greater than penetrometer resistance of a root (Bengough and Mullins, 1990). Most penetrometers are equipped with a metal probe with a conical tip fixed onto a cylindrical shaft, which is usually of smaller diameter than the cone (Bengough and Mullins, 1990). The penetrometer resistance is defined by the force required to push the penetrometer probe through the soil and the cross–sectional area of the penetrometer cone (Equation 2-1).

$$Q_{p.r} = \frac{F_{p.r}}{A_{p.r}} \qquad \textbf{Equation 2-1}$$

$Q_{p.r}$ = penetrometer resistance, $F_{p.r}$ = force required to push the penetrometer probe through the soil, $A_{p.r}$ = cross–sectional area of penetrometer cone

The penetrometer resistance of soil packed to various bulk densities was determined using a needle penetrometer (30° angle cone, 0.97 mm diameter with 0.8 mm relieved shaft) on a mechanical test machine (Instron 5540, Instron Merlin Software, Instron Cooperation, High Wycombe, UK) with a penetration rate of 4 mm $min^{-1}$ and to a depth of 1.5 cm. Soil was wetted to three gravimetric water contents (Table 2-7) that corresponded to matric potentials of -0.01 MPa, -0.4 MPa and -1.2 MPa and then packed to five different bulk densities (1.1 g $cm^{-3}$, 1.2 g $cm^{-3}$, 1.3 g $cm^{-3}$, 1.4 g $cm^{-3}$ and 1.5 g $cm^{-3}$) in plastic cores with a diameter of 5 cm and heights of 12 cm (-1.2 MPa), 17 cm (-0.4 MPa) and 22 cm (-0.01 MPa) using a hydraulic press. The maximum load of 5 N, to prevent damage to the probe, was exceeded at a matric potential -0.4 MPa and

bulk density 1.5 g $cm^{-3}$, so that penetrometer resistance was not determined for these samples.

Figure 2-2 shows average penetrometer resistances at the five bulk densities and three matric potentials. Penetrometer resistance increased with increasing dry bulk density and was least affected by density in the wettest soil treatment (-0.01 MPa). Those findings agree with those from Vaz et al., (2001) and Mirreh and Ketcheso (1972). Greatest penetrometer resistances were measured for the intermediate matric potential and exceeded the load of 5 N at a bulk density of 1.5 g $cm^{-3}$. Studies of others (Lapen et al., 2004; Vaz et al., 2001; Whitmore and Whalley, 2009) showed an increase in penetrometer resistance with decreasing water content. Thus the penetrometer resistance of soils at -1.1 MPa was initially expected to be greater than at -0.4 MPa.

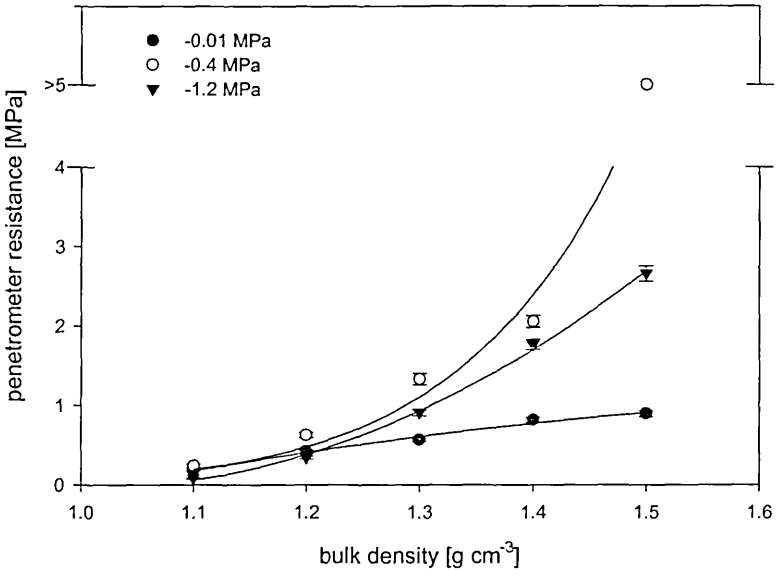


**Figure 2-2: Average penetrometer resistance at bulk densities of 1.1, 1.2, 1.3, 1.4 and 1.5 gcm$^{-3}$ for soil wetted to matric potential of -0.01, -0.4 and -1.2 MPa.**

However, Vaz et al. (2001) and Lapen et al. (2004) measured the penetrometer resistance of undisturbed samples from the field, while in this study the soil was packed at given soil water contents and so the driest soil was drier than the optimal water content for soil packing and particle cohesion forces. Hence penetrometer resistance was smaller than would have been achieved if wet packed soil equilibrated to a matric potential of -1.1 MPa. Harris et al. (2003) packed this soil at water contents of 12 to 29 g 100g$^{-1}$ to various bulk densities.

### 2.3.3 Adjustment of matric potentials

In the following chapters, water contents of soil and vermiculite were adjusted to achieve particular matric potentials. Water retention curves of loosely packed soil (sieved to 2 mm) and vermiculite, as well as of soils packed to bulk densities ranging from

1.1 g $cm^{-3}$ to 1.5 g $cm^{-3}$ and soil sieved to particle sizes of 4–2 mm, 2–1 mm, 1–0.5 mm and <0.5 mm were determined. Three methods of measuring matric potential were used: psychrometer, tensiometer and filter paper. Gravimetric water contents from the resulting water retention curves were used to adjust matric potentials. This section shows the water retention curves for the various growth media used.

#### 2.3.3.1 Methods for determining matric potentials and resulting water retention curves

Matric potential can be used as an indicator for plant available water in the soil. The water potential is defined as the potential energy of water per unit mass of water in the system and can be described by the sum of gravitational, matric, osmotic and pressure potentials. Matric potential is defined by the adsorptive forces binding water to a matrix. Osmotic potential depends on the concentration of dissolved substances and describes the ability of water to penetrate a semi permeable membrane. The pressure potential is influenced by the hydrostatic or pneumatic pressure. The matric potentials for soil and vermiculite used in this project were determined using three methods:

*Psychrometer*

Psychrometers sense the relative humidity of vapour in equilibrium with the liquid phase in soils. The relationship between water potential and the vapour pressure of air is described in Equation 2-2.

$$\psi = \frac{RT\rho_w}{M} \times \ln \frac{p}{p_0}$$ **Equation 2-2**

$\Psi$ = water potential, R = gas constant (8.31 J $mol^{-1}$ $K^{-1}$ or 0.008314 kPa $m^3$ $mol^{-1}$ $K^{-1}$), T = sample temperature in Kelvin (K), $\rho_w$ = density of water (1 kg $m^{-3}$), M = molecular weight of water (0.018 kg $mol^{-1}$), p = vapour pressure, $p_0$ = saturation vapour pressure

When the osmotic potential is negligible, the soil water potential determined by a psychrometer is essentially equal to the soil matric potential (Or and Wraith, 2002).

Two types of psychrometer were used to measure the matric potential of growth media: Tru Psi thermocouple psychrometer (Decagon Devices, Inc) and the WP4–T Dewpoint Potential Meter (Decagon Devices, Inc). A thermocouple psychrometer consists of a fine–wire bimetallic double junction of two dissimilar metals. When the two junctions are exposed to different temperatures a voltage is generated (Seedbeck effect). In the **Tru Psi thermocouple psychrometer** the temperature of one junction is lowered by wetting it from a supply of water, while the other one is kept dry. The water potential that corresponds to a pair of wet and dry junction can be measured using a thermocouple that has been calibrated over salt solutions of known concentrations at same temperature. NaCl- and KCl-solutions are commonly used to calibrate psychrometers. The vapour pressure of a solution can be expressed with Raoult's law (Equation 2-3).

$$p_{sol} = m_s p_0$$ **Equation 2-3**

m = mole fraction of the solvent, $p_{sol}$ = vapour pressure of solution, $p_0$ = saturation vapour pressure

The partial vapour pressure of a salt in solution is equal to the mole fraction of this salt times the saturation vapour pressure of the pure solvent.

KCl-solutions ranging from 0.00625 to 0.4 molarities were used to calibrate the Tru Psi thermocouple psychrometer (Figure 2-3). The water potential of the calibration solution was calculated from the microvolt output (Equation 2-4).

$$\psi_{cal} = \frac{mV(T_{sample} + 273)}{293} \qquad \textbf{Equation 2-4}$$

The calibration curve showed in increase in water potential with increasing microvolt output and increasing KCl-concentration. A linear regression was fitted through the calibration data (Figure 2-3). The intercept and gradient were used to calculate the matric potential of samples (Equation 2-5).

$$\psi_{sample} = mV \times REG_{grad} + REG_{int} \qquad \textbf{Equation 2-5}$$

Because of temperature differences of the actual samples from the average temperature during calibration a temperature correction for matric potential was performed (Equation 2-6).

$$\psi_{corr} = \psi_{sample}(1 - 0.025(T_{sample} - T_{cal})) \qquad \textbf{Equation 2-6}$$

mV = measured microvolts, $\Psi_{cal}$ = water potential corredponding to KCl-solution, $\Psi_{sample}$ = matric potential of sample calculated from mV output without temperature correction, $\Psi_{corr}$ = matric potential after temperature correction, $T_{sample}$ = temperature of sample, $T_{cal}$ = average temperature during calibration $REG_{grad}$ = gradient of linear regression line of calibration, $REG_{int}$ = intercept of linear regression line of calibration

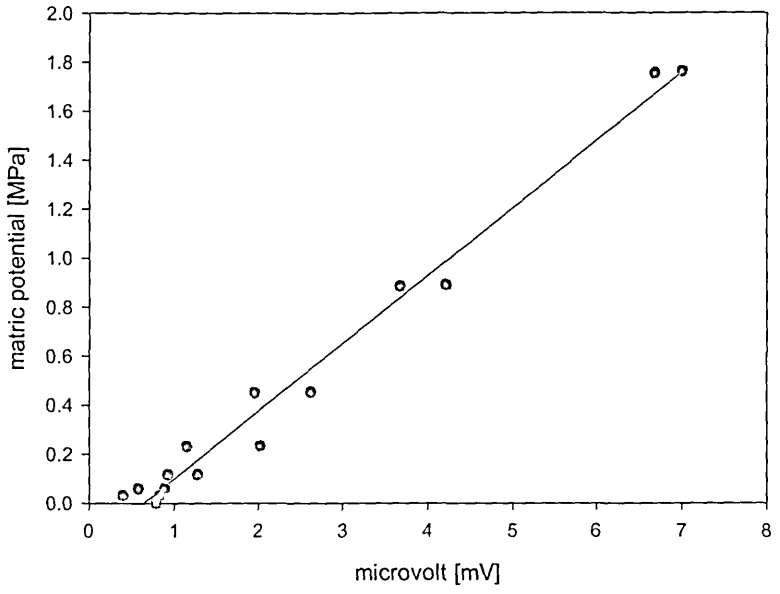


**Figure 2-3: Calibration curve for Tru Psi thermocouple psychrometer determined with KCl-solutions. Linear regression $\Psi = 0.2962x-0.2962$, $r^2 = 0.99$.**

Samples were wetted to various water contents and placed in the Tru Psi psychrometer (Figure 2-4) and then left for 30 min until vapour and thermal equilibrium was reached.

**Figure 2-4: Tru Psi thermocouple psychrometer (Decagon Devices) with 9 sample holders (metal cups).**

The sample chamber holds up to 9 metal cups (1.5 ml) plus one special cup holding a water reservoir for wetting one junction of the thermocouple. With a custom made cone a dent was made in the soil to prevent contact between the thermocouple and the soil and vermiculite.

The microvolt output was recorded and the corresponding matric potential was calculated with Equations 2-5 and 2.6.

In the **WP4–T Dewpoint Potential Meter** the sample equilibrated with the headspace of a sealed chamber that contains a mirror and a means of detecting condensation on it. At equilibrium, the water potential of the air in the chamber is the same as the water potential of the sample. The appearance of condensation on the mirror is detected by a photodetector cell. A beam of light is directed onto the mirror and the photodetector cell senses changes in reflection resulting from condensation (Decagon Devices, Inc).

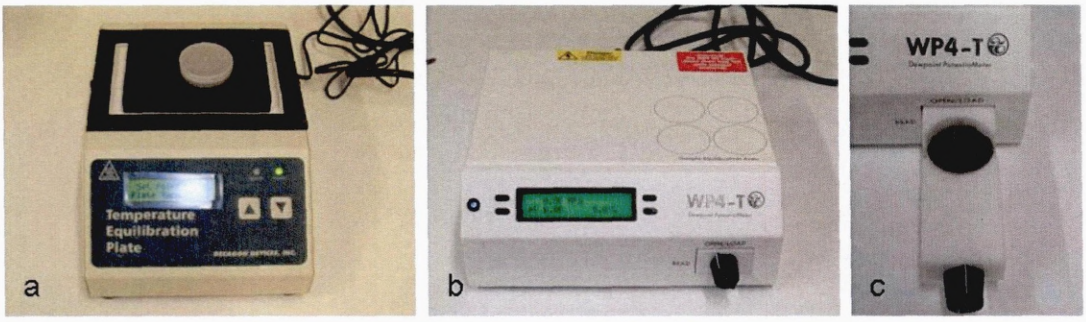


**Figure 2-5: Temperature equilibration plate (a) and WP4–T Dewpoint Potential Meter (b) with sample drawer (c).**

The accuracy of the WP4–T Dewpoint Potential Meter was tested using a 0.05 M KCl-solution, where the corresponding water potential is -0.232 MPa. Samples were wetted to various water contents (see below) and placed on a temperature equilibration plate (Figure 2-5) to adjust to a temperature of 20°C before placing them in the psychrometer (Figure 2-5) to measure the matric potential. The sample cup carried a volume of 15 ml. To prevent contamination of the sample chamber, sample cups were half filled approximately to a bulk density of 0.9 g $cm^{-3}$.

*Tensiometer*

A tensiometer consists of a porous ceramic vessel connected to a pressure transducer, with all parts of the system water–filled. Hydraulic connection arises between soil water and the water within the vessel via the pores inside the vessel. Water moves into or out of the vessel until the negative pressure inside the cup equals the matric potential of the soil. Water–filled tensiometers have a lower measuring limit of about -85 kPa because, at more negative potentials, trapped air enters the system and hydraulic connectivity is broken (Gardner et al., 1991).

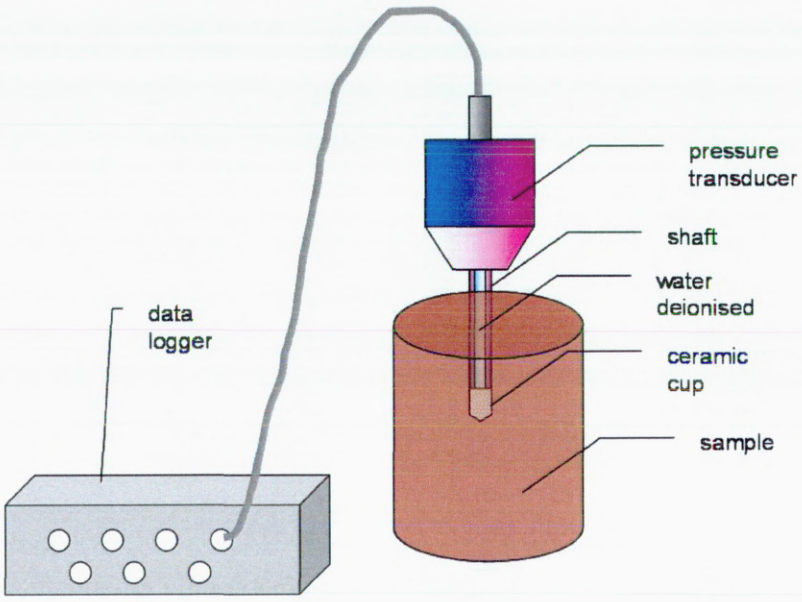


**Figure 2-6: Schematic drawing of tensiometer measurement.**

A **SWT5 tensiometer** (Delta–t Devices Ltd.) with a pressure transducer and data logger was used. The growth medium, wetted to various water contents (see below) was packed in cylindrical containers (height 10 cm, diameter 3 cm). The tensiometer was then placed in the growth medium so that the ceramic cup was in contact with it. The value for matric potential was recorded when the reading stabilized.

*Filter paper method*

The third method used to determine matric potentials of growth media was the filter paper method. At equilibrium, the matric potential of a filter paper placed in the growth medium corresponds to the matric potential of the growth medium. The filter paper used for the measurements was **Whatmann 42** (diameter 55 mm). Work by others had shown that Whatmann 42 seemed to be the most accurate filter paper to determine the matric potential (Leong et al., 2002; Sibley and Williams, 1990). The corresponding water

contents of filter paper at specific suctions were determined by placing saturated filter paper on tension tables and pressure plates at suctions ranging from 0.0005 MPa to 1.5 MPa. Dry filter papers and filter paper after equilibration for different times on tension tables or pressure plates at different suctions were weighed to determine the water content of the filter papers. The water content of the filter paper corresponded to a suction value as shown in Figure 2-7.

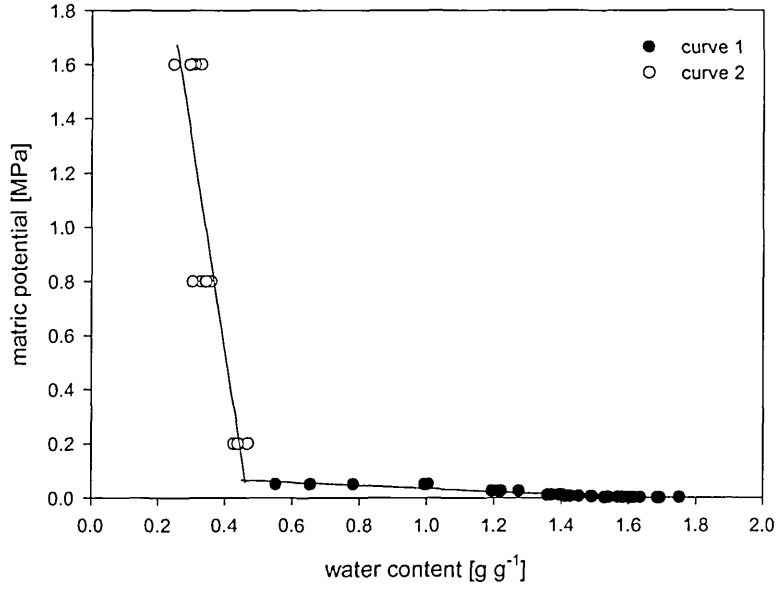


**Figure 2-7: Fitted calibration lines for the water content [g $g^{-1}$] of the filter paper at corresponding suction [MPa], linear regression for lower matric potential $\Psi = -7.8175\Theta_g + 3.6668$, $r^2 = 0.80$ and for upper matric potential $\Psi = -0.0562\Theta_g + 0.0911$, $r^2 = 0.90$. Water content on X-axis as known variable.**

Two separate linear regressions for lower and upper ranges of matric potential were fitted through the data, as is common with most other authors (Deka et al., 1995; Greacen et al., 1989; Hamblin and Tennant, 1987).

The matric potential of the growth medium was measured by placing the saturated filter paper in contact with the growth medium in a sealed plastic container (Figure 2-8).

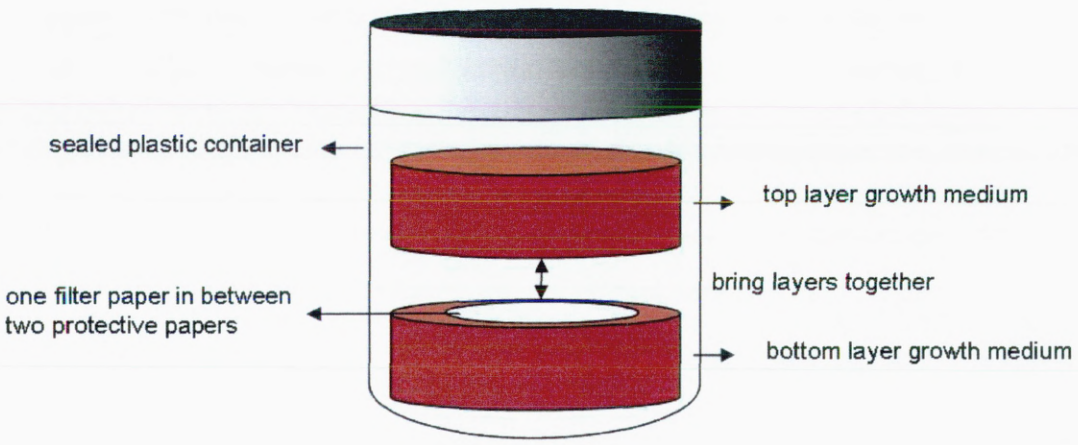


**Figure 2-8: Schematic drawing of determining matric potential with filter paper. Filter paper is placed between two layers of growth medium.**

To avoid soil particles sticking to the filter paper, it was cut to 50 mm diameter and placed between two filter papers of a diameter of 55 mm. After an equilibration time of 7 days at 20 °C the water content for the filter paper was determined. The water content of the filter paper was converted to matric potential using the calibration lines in Figure 2-7.

*Vermiculite and soil sieved to 2 mm*

Water retention curves for vermiculite of both bags were determined by using psychrometers and tensiometers. The corresponding matric potential to adjusted water contents of vermiculite from bag 1 were determined using a WP4–T Dewpoint Potential Meter (psychrometer) and the SWT5 tensiometer.

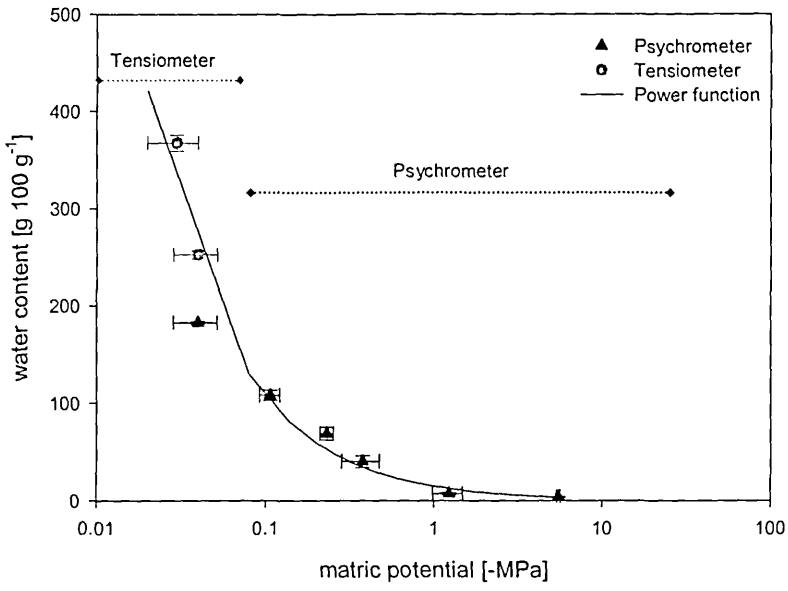


**Figure 2-9: Water retention curve for vermiculite (bag 1) determined by psychrometer and tensiometer. Power function $\Theta_g = 14.182\Psi^{-0.8904}$, $r^2 = 0.91$.**

The psychrometer was used for water contents up to 200 g $100g^{-1}$, while the tensiometer was used for water contents from 250 g $100g^{-1}$ to 375 g $100g^{-1}$. Water contents ranged between 5 g $100g^{-1}$ to 375 g $100g^{-1}$. The resulting water retention curve is shown in Figure 2-9. A power function resulted in better correlations than the van Genuchten-Mualem model. Three replications of each treatment were measured and the actual water content per sample was determined by weighing the wet samples and after drying at 105 °C for 24 h.

The water retention curve for vermiculite (bag 2) was determined using the Tru Psi thermocouple psychrometer. Water contents of the vermiculite were adjusted ranging between 5 g $100g^{-1}$and 350 g $100g^{-1}$. Three replications of each treatment were measured

and the actual water content per sample was determined. The resulting water retention curve is demonstrated in Figure 2-10.

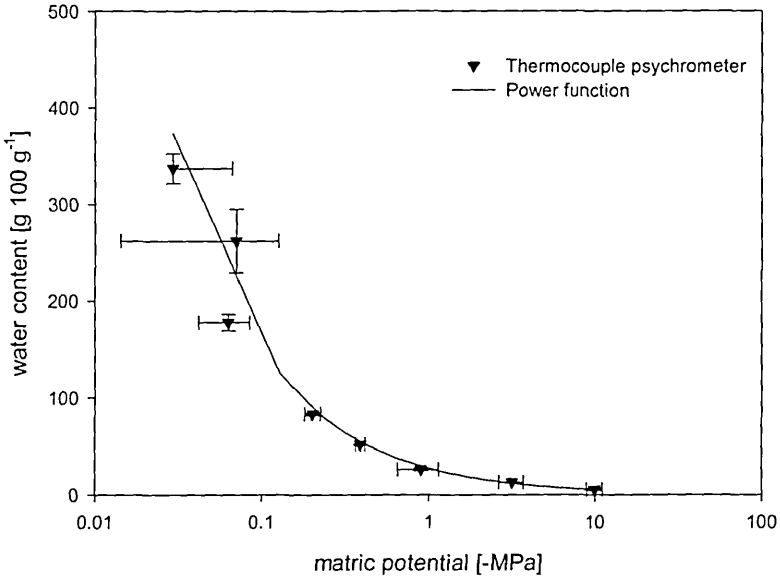


**Figure 2-10: Water retention curve for vermiculite (bag 2) determined by psychrometer. Power function $\Theta_g = 27.634\Psi^{-0.8904}$, $r^2 = 0.92$.**

Water retention data for loosely packed soil (bulk density approximately 0.9 g $cm^{-3}$) were determined using the WP4–T Dewpoint water potential meter, SWT5 tensiometer and filter paper. Soil was wetted to water contents ranging from 5 g $100g^{-1}$ to 25 g $100g^{-1}$. The WP4–T Dewpoint potential meter was used up to water contents of 15 g $100g^{-1}$. Measurements with the tensiometer were performed in soil of 20 g $100g^{-1}$, 22.5 g $100g^{-1}$ and 25 g $100g^{-1}$, while filter paper was used for water contents between 5 g $100g^{-1}$ and 22.5 g $100g^{-1}$. Three replicates for each water content and method were measured.

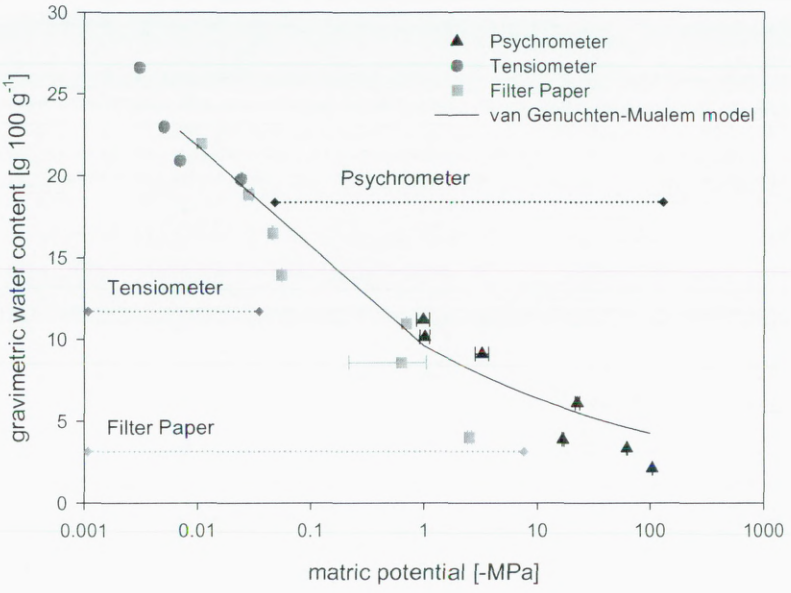


**Figure 2-11: Water retention curve for soil sieved to 2 mm determined by WP4–T water potential meter, SWT5 tensiometer and filter paper method. Van Genuchten-Mualem model fitted $\Theta_{(\Psi)}=\Theta_r+(\Theta_s-\Theta_r)/[1+(\alpha|\Psi|)^n]^m$, $r^2=0.88$.**

Figure 2-11 is the water retention curve for soil sieved to 2 mm measured by all three methods.

**Table 2-2: Parameters of van Genuchtem–Mualem model (m=1-1/n, $\Theta_{(\Psi)}=\Theta_r+(\Theta_s-\Theta_r)/[1+(\alpha|\Psi|)^n]^m$) fitted through soil water retention data. Data collected with WP4–T water potential meter, SWT5 tensiometer and filter paper method. Soil sieved to 2mm.**

| van Genuchtem Mualem model (m=1-1/n) | |
|---|---|
| parameter | soil |
| $\Theta_r$ | 0 |
| $\Theta_s$ | 31.54 |
| a | 822.06 |
| n | 1.17710 |
| $r^2$ | 0.88 |

The van Genuchten-Mualem model (m = 1-1/n) was fitted through the data, where the parameters for the model were determined using RETC (Table 2-2). A good fit of model through the raw data was achieved ($r^2 = 0.88$).

The resulting water retention curves for vermiculite and soil were used to adjust the matric potential at -0.03 MPa, -0.2 MPa, -0.81 MPa and -1.6 MPa. The corresponding water contents at those matric potentials are in Table 2-3.

**Table 2-3: Corresponding water contents for vermiculite bag 1 and bag 2 calculated from power functions and soil calculated from van Genuchten-Mualem mode: $\Theta_{(\Psi)} = \Theta_r + (\Theta s - \Theta r)/[1+(\alpha|\Psi|)^n]^m$ at matric potentials of -0.03 MPa, -0.2 MPa, -0.81 MPa and -1.6 MPa.**

| Matric potential [MPa] | Water content vermiculite bag 1 [g 100 $g^{-1}$] | Water content vermiculite bag 2 [g 100 $g^{-1}$] | Water content soil [g 100 $g^{-1}$] |
|---|---|---|---|
| -0.03 | 321 | 366 | 18 |
| -0.2 | 59 | 90 | 13 |
| -0.81 | 17 | 32 | 10 |
| -1.6 | 9 | 19 | 8 |

The corresponding water contents for all four matric potentials were greater in vermiculite than in soil. Furthermore vermiculite from bag 1 was drier at similar matric potentials compared to vermiculite from bag 2.

*Effect of aggregate sizes*

Soil was sieved to four aggregate sizes (4–2 mm, 2–1 mm, 1–0.5 mm and <0.5 mm) using soil sieves of appropriate sizes. Water retention curves for soil of each aggregate

size were determined using a WP4–T Dewpoint water potential meter and SWT5 tensiometers. Psychrometer readings were taken for gravimetric water contents ranging from 5 g $100g^{-1}$ to 12.5 g $100g^{-1}$ and tensiometer readings were taken for water contents ranging from 15 g $100g^{-1}$ to 25 g $100g^{-1}$. Three replicates for each treatment (aggregate size and gravimetric water content) were measured.

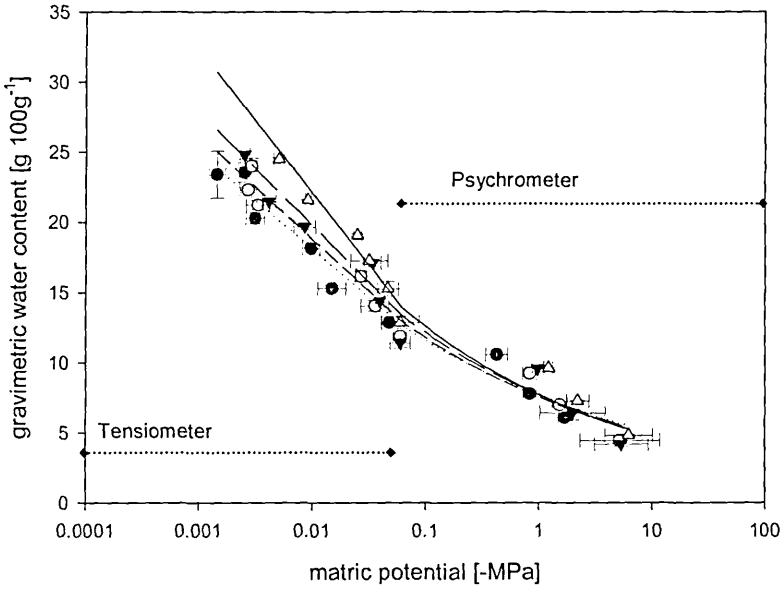


**Figure 2-12: Water retention curves for soil sieved to 4–2 mm, 2–1 mm, 1–0.5 mm and <0.5 mm determined by psychrometer and tensiometer. Van Genuchten-Mualem model fitted ($m = 1-1/n$, $\Theta_{(\Psi)}=\Theta_r+(\Theta_s-\Theta_r)/[1+(\alpha|\Psi|)^n]^m$).**

The water retention curves for the four aggregate sizes are shown in Figure 2-12. The van Genuchten-Mualem model was fitted to each aggregate size; parameters are in Table 2-4.

The drier the soil, the more similar were the water contents corresponding to similar matric potentials for the four aggregate sizes. The effect of aggregate size on water content increased with greater matric potentials (Table 2-5).

**Table 2-4: Parameter of van Genuchtem–Mualem model ($m=1-1/n$; $\Theta_{(\Psi)} = \Theta_r+(\Theta_s-\Theta_r)/[1+(\alpha|\Psi|)^n]^m$) fitted through soil water retention data of soil sieved to four aggregate sizes (4–2 mm, 2–1 mm, 1–0.5 mm and <0.5 mm). Data collected with WP4–T water potential meter.**

| Van Genuchtem Mualem model (m=1-1/n) | | | | |
|---|---|---|---|---|
| parameter | soil 4–2 mm | soil 2–1 mm | soil 1–0.5 mm | soil <0.5 mm |
| $\Theta_r$ | 0 | 0 | 0 | 0 |
| $\Theta_s$ | 29.766 | 29.830 | 32.758 | 61.136 |
| $\alpha$ | 1882.44 | 1214.89 | 1510.09 | 17532.06 |
| n | 1.1802 | 1.19386 | 1.19832 | 1.20367 |
| $r^2$ | 0.97 | 0.96 | 0.97 | 0.96 |

Aggregate sizes and water content had a significant effect on matric potential ($p < 0.001$).

**Table 2-5: Corresponding water contents for vermiculite bag 1 and bag 2 at matric potentials of -0.03 MPa, -0.2 MPa, -0.81 MPa and -1.6 MPa, calculated from power function fitted through water retention data.**

| Matric potential [MPa] | soil 4–2mm | soil 2–1mm | soil 1–0.5mm | soil <0.5mm |
|---|---|---|---|---|
| -0.03 | 14.37 | 14.82 | 15.35 | 17.06 |
| -0.2 | 10.22 | 10.28 | 10.55 | 11.6 |
| -0.81 | 7.95 | 7.84 | 8.00 | 8.72 |

The finer the particle size the more water was needed to adjust similar matric potentials compared to coarser soil. The water retention curves were used to adjust matric potentials to -0.03 MPa, -0.2 MPa and -0.81 MPa. The corresponding water contents are presented in Table 2-5.

*Effect of bulk density*

The water retention curves for soil sieved to 2 mm and packed to five bulk densities are shown in Figure 2-13.

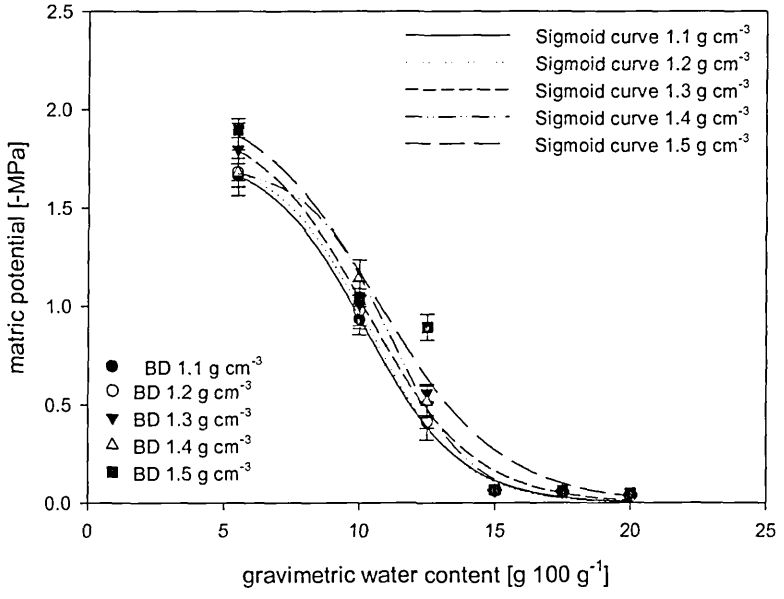


**Figure 2-13: Water retention curves for soil sieved to 2 mm and packed to bulk densities of 1.1, 1.2, 1.3, 1.4 and 1.5 g cm$^{-3}$ determined by filter paper method. Sigmoid curve (3 parameter) $\Psi = a/(1+\exp(-(\Theta_g-x_0)/b))$.**

Matric potentials for water contents ranging from 5 g 100g$^{-1}$ to 20 g 100g$^{-1}$ were determined using the filter paper method. Sigmoid curves were fitted through the raw data of every bulk density. The parameters of the curve fitting are shown in Table 2-6. Sigmoid curves showed a good fit with $r^2$–values between 0.96 to 0.98 ($p < 0.001$).

**Table 2-6: Parameters of sigmoidal curve fitting for water retention curves of soil sieved to 2 mm and packed to bulk densities of 1.1, 1.2, 1.3, 1.4 and 1.5 g $cm^{-3}$.**

| Bulk density | $r^2$ | Parameter a | Parameter $x_0$ | Parameter b | Probability value Gradient |
|---|---|---|---|---|---|
| 1.1 g $cm^{-3}$ | 0.97 | 1.7846 | 10.1947 | -1.7929 | <0.001 |
| SE of parameter | | 0.1261 | 0.4397 | 0.3292 | |
| 1.2 g $cm^{-3}$ | 0.98 | 1.7704 | 10.3793 | -1.6867 | <0.001 |
| SE of parameter | | 0.1101 | 0.3750 | 0.2962 | |
| 1.3 g $cm^{-3}$ | 0.96 | 1.9524 | 10.2520 | -1.9842 | <0.001 |
| SE of parameter | | 0.1410 | 0.4723 | 0.3307 | |
| 1.4 g $cm^{-3}$ | 0.96 | 1.7145 | 11.1017 | -1.5091 | <0.001 |
| SE of parameter | | 0.0871 | 0.2908 | 0.2333 | |
| 1.5 g $cm^{-3}$ | 0.97 | 2.0667 | 10.6377 | -2.2987 | <0.001 |
| SE of parameter | | 0.1508 | 0.5179 | 0.1508 | |

The water retention curves were used to adjust soil to matric potentials of -0.01 MPa, -0.4 MPa and -1.1 MPa. The corresponding water contents are shown in Table 2-7.

**Table 2-7: Corresponding water contents at matric potentials of -0.01 MPa, -0.4 MPa and -1.2 MPa for soil sieved to 2 mm and packed to bulk densities of 1.1, 1.2, 1.3, 1.4 and 1.5 g $cm^{-3}$ determined from sigmoid curves (3 parameter) $\Psi = a/(1+\exp(-(\Theta_g-x_0)/b))$.**

| Bulk density | Water content [g 100 $g^{-1}$] -0.01 MPa | | Water content [g 100 $g^{-1}$] -0.4 MPa | | Water content [g 100 $g^{-1}$] -1.2 MPa | |
|---|---|---|---|---|---|---|
| 1.1 g $cm^{-3}$ | 19 | ± 0.78 | 12 | ± 0.38 | 9 | ± 0.2 |
| 1.2 g $cm^{-3}$ | 19 | ± 0.66 | 13 | ± 0.25 | 9 | ± 0.05 |
| 1.3 g $cm^{-3}$ | 21 | ± 0.09 | 13 | ± 0.005 | 9 | ± 0.15 |
| 1.4 g $cm^{-3}$ | 19* | ± 1.28 | 13 | ± 0.16 | 10 | ± 0.36 |
| 1.5 g $cm^{-3}$ | 23 | ± 2.46 | 13 | ± 0.42 | 10 | ± 0.05 |

*as a result of curve fitting

The greater the bulk density the more water was needed to achieve similar matric potentials, except at a bulk density of 1.4 g $cm^{-3}$, when the water content to adjust to a matric potential of -0.01 MPa was less than that of soil packed to 1.3 g $cm^{-3}$.

### 2.3.3.2 Air humidity

Relative air humidity was employed as another environmental factor influencing root growth. The relative air humidity is expressed in the ratio of vapour partial pressure of the air to saturation vapour partial pressure of the air at actual air temperature (Equation 2-7).

$$\varphi = \frac{p_{sol}}{p_{sat}} \times 100\% \qquad \textbf{Equation 2-7}$$

$\varphi$ = relative air humidity, $p_{sol}$ = vapour partial pressure of solution, $p_{sat}$ = saturation vapour pressure at actual temperature

The fact that salt concentrations in solutions alter the vapour partial pressure and therefore the water potential (see above) was used to manipulate water potential above KCl-solutions of different concentrations.

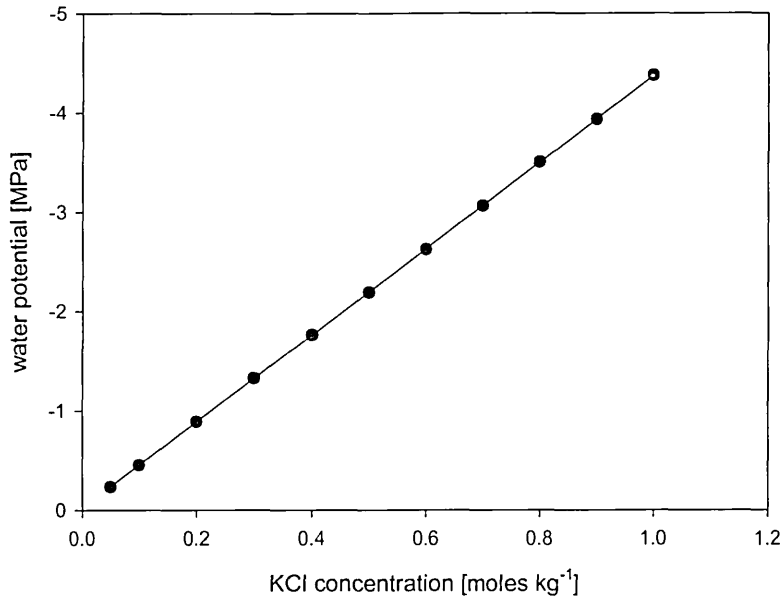


**Figure 2-14: Linear regression of KCl-solution and its corresponding water potential. $\Psi$=-4.3522×KCl+(-0.0164), $r^2$ = 1 (Operators manual for WP4 and WP4–T potential meter, version 4, Decagon devices Inc.).**

The molarities corresponding to -0.03 MPa, -0.2 MPa, -0.81 MPa and -1.6 MPa were obtained from the WP4–T Dewpoint water potential meter calibration standards for KCl. The calibration data are plotted in Figure 2-14. The greater the KCl-concentration the greater the water potential.

**Table 2-8: KCl-concentrations corresponding to water potentials of -0.03 MPa, -0.2 MPa, -0.81 MPa and -1.6 MPa.**

| Water potential [MPa] | KCl-concentration [Moles $l^{-1}$] |
|---|---|
| -0.03 | 0.0031 |
| -0.2 | 0.0422 |
| -0.81 | 0.1823 |
| -1.6 | 0.3638 |

The KCl-concentrations to adjust water potentials of -0.03 MPa, -0.2 MPa, -0.81 MPa and -1.6 MPa are presented in Table 2-8. To obtain an environment of different relative humidity, KCl-solutions were enclosed in sealed plastic containers (height 10 cm, diameter 9 cm). The container walls were lined with KCl-solution soaked paper towel.

### 2.3.3.3 Discussion

Methods for determining water retention curves of different growth media are discussed. The first growth medium investigated was vermiculite. Two water retention curves for vermiculite were determined, because vermiculite was used from different bags. The matric potential measurements for bag 1 were conducted using the WP4–T Dewpoint Potential Meter while for bag 2 the Tru Psi thermocouple psychrometer was used. Both methods use the principle of detecting the water potential by sensing the relative humidity of vapour in equilibrium with the liquid phase in soils. Measurement accuracy for the WP4–T Dewpoint Potential Meter (±0.1) is less than for the Tru Psi thermocouple psychrometer (±0.03). Nevertheless water potential measurements conducted by older models of these two instruments compared favourably (Gee et al., 1992). Besides, the output of both samples was checked with KCl-solutions. The vermiculite from bag 1 was

generally drier than from bag 2 at similar matric potentials. The particle size distribution might have varied between the two bags, given the fact that they were purchased at different times and therefore from different batches. Even so the particle size distribution of both bags was grade 3; some variation in particle size could have appeared due to the fact that the different particle sizes forming grade 3 ranged between 10 and 25 %.

Water retention curves for soil sieved to 2 mm and loosely packed was determined using three methods (WP4–T Dewpoint Potential Meter, SWT5 tensiometer and filter paper). The advantage of combining psychrometer and tensiometer readings is, that psychrometers are highly accurate at dry potentials up to -300 MPa (Decagon Devices Inc.1998–2003), while tensiometers are better for matric potentials up to -100 kPa (Or and Wraith, 2002). Filter paper results agreed well with tensiometer readings but were below the psychrometer readings. Studies where psychrometer readings were compared with other methods to determine matric potential resulted in greater suction values for psychrometer readings compared with other methods (Leong et al., 2002; Madsen et al., 1986). Madsen et al. (1986) measured soil matric potential of soil samples that were equilibrated on pressure plates at a suction of -1.5 MPa. Matric potential measured with the psychrometer was consistently wetter than -1.5 MPa.

The samples of filter paper were left for 7 days and the most negative matric potentials that were determined were -2.6 MPa. Six days of equilibration time for the filter paper is usually long enough to get accurate results for potentials up to -2.5 MPa. Psychrometer readings were significantly lower ($p < 0.001$) at water contents of 5 g $100g^{-1}$ than the potential determined by filter paper method (-2.6 MPa). Therefore a longer equilibration

time for the filter paper might have been necessary at low water contents, which would have altered the results. The van Genuchten-Mualem model was fitted to the combined data of all three methods. For comparison of the effects of matric potential of both growth media (soil and vermiculite) it would have been desirable to use similar methodology for determining the water retention curves. Even if so there is an uncertainty that all three methods would give completely consistent results, various studies have proven that all three methods are appropriate for determining water retention curves (Campbell, 1988; Deka et al., 1995; Hamblin and Tennant, 1987; Leong et al., 2002).

Water retention curves for soil sieved to groups of aggregate fraction between 4–2 mm, 2–1 mm, 1–0.5 mm and <0.5 mm showed similar water retention at dry matric potentials, but with decreasing aggregate size water retention increased at wet matric potentials. Similar results were found by Liepiec et al., (2007), who investigated the effect of aggregate size on water retention and pore structure. Earlier studies showed grouping effects; depending on the soil type aggregates of greater size showed smaller differences in water retention, but groups of small aggregates were significantly different from larger aggregates. Witmuss and Mazurek (1958) investigated water retention of aggregate fractions of a silty clay soil. Aggregates ranging from 0.07 mm to 4.8 mm had similar water retention, while aggregates <0.07 mm had different retention for matric potentials ranging from 0 MPa to -1.5 MPa. Tamboli (1964) observed similarities in water retention of aggregates of 2–3 mm, 3–5 mm, 5–9.5 mm and 9.5–12 mm of a silty loam, while water retention for 1–2 mm and 1–0.5 mm was smaller than for larger fractions. Amemiya (1965) also found water retention of aggregate fractions to be similar when they ranged between 1 mm and 5 mm, but found significant differences of aggregate

fraction of 1–0.5 mm compared to larger fractions. Different aggregate fractions in one sample caused either increase or decrease in water retention. Abrol and Palta (1970) observed an unvaried decrease in water retention of aggregate fractions with aggregate size in the range of matric potential from -0.045 MPa to -1 MPa. Differences in water retention with aggregate size not only depend on aggregate size, but also soil type. The soil used in this study was a sandy loam, while in most in the above mentioned studies silty loams or clays were used.

Changes in bulk density also altered water retention significantly ($p < 0.001$) when soil was drier than 15 g $100g^{-1}$. The general trend was when soil was more compacted matric potential increased at same water content, except that at 10 g $100g^{-1}$ water content the matric potential of soil packed to 1.4 g $cm^{-3}$ was lower than for 1.3 g $cm^{-3}$. Hill and Summer (1967) found that for a sandy loam with increasing bulk density the water holding capacity increased at large suctions, but showed an opposite effect at small suctions. The results presented here, did not show a similar effect, but the magnitude of water holding capacities of soil packed to different bulk densities decreased.

## 2.4 Statistical Analysis

Data were anlysed using several software packages. RETC was used to determine the parameter for fitting the van Genuchten-Mualem model through water retention data of soil. Power function and sigmoid curves were fitted through water retention data using SigmaPlot $11^{th}$ Edition, when the van Genuchten-Mualem model poorly fitted the data. Exponential growth curves and linear regressions of root elongation rates and root diameter or distance between root tip and root hair zone were also fitted using SigmaPlot

11th Edition. Microsoft Excel was used to determine root and shoot elongation rates and the root length increase of maize, lupin and barley. In GenStat 12th Edition data were tested for normal distribution and a general analysis of variance for different sample treatments was conducted to determine the statistical significance of data.

## 2.5 Summary

This Chapter presented plant material and growth media used throughout this thesis. Sterilization processes for maize, lupin and barley, and soil and vermiculite were introduced. Methods for determining the pH, penetrometer resistance and water retention curves of growth media were presented.

The pH of vermiculite was significantly higher than that for soil, and outside the optimal range for maize and lupin growth. Attempts to reduce the pH failed, because the structure collapsed.

Penetrometer resistances were measured for soil packed to different bulk densities and matric potentials. Soil at intermediate water content showed the greatest penetrometer resistance, probably because the driest soil had water contents well below the optimal water content for compacting soils.

Water retention curves were determined for vermiculite and soil. Different methods (Psychrometer, tensiometer and filter paper) were used. The water retention curves were used to adjust matric potentials for further experiments. All methods proved valuable for determining matric potentials. Furthermore KCl-solutions were used to create environments of different relative air humidities.

# 3 X-ray microtomography: development of methods for quantifying contact areas of roots with the gaseous, liquid and solid phases in soil

## 3.1 Introduction

X-ray computed tomography (X-ray CT) provides non–invasive or non–destructive three–dimensional images. In the last two decades X-ray tomography has been applied to study soil properties and the spatial distribution of roots (Gregory et al., 2003; Heeraman et al., 1997; Kaestner et al., 2006; Lontoc–Roy et al., 2006; Perret et al., 2007). When X-ray tomography was first used to investigate root growth in soils rather low resolutions were obtained (more than 100 μm). Scanners are nowadays available, which have been developed specifically for materials research and resolutions up to 5 μm are possible. With the development in X-ray tomography roots in soils can be studied in greater detail. Carminati et al. (2009) studied root–soil contact dynamics of lupin plants under drying and wetting cycles using X-ray tomography and found that with drying soil roots lose contact due to root shrinkage but re–establish contact when soil was wetted. Processes at the root–soil interface are still poorly understood, but with X-ray tomography new possibilities open up to study water transport and water uptake by roots.

The development of a method to quantify root–particle contact from 3-D volumetric images is presented and advantages and limitations are discussed. Preliminary results for quantifying water in porous media and the contact of roots with the three phases: gaseous, liquid and solid using 3-D volumetric images are presented and discussed.

### 3.1.1 X-rays

In X-ray tomography the transmission of radiation through a three dimensional object is used to produce a two dimensional image of the internal features of the object.

X-rays are generated by a source which consists of a cathode and an anode inside a vacuum tube. When the cathode is heated an electrical potential between cathode and anode forces electrons to accelerate towards the anode. As these electrons impinge on a heavy metal (target) they interact with the atoms of the target. These interactions result in a conversion of kinetic energy into thermal and electromagnetic energy in the form of X-rays. X-rays interact with atomic electrons, with nucleons and with electric fields associated with atomic electrons and/or atomic nuclei of matter. X-rays can be completely adsorbed or scattered elastically or inelastically. The following interactions between X-ray photons and matter are common: Photoelectric adsorption, Compton Scattering and Pair production. The process of transferring the total energy of an incoming X-ray to an inner electron of a material, causing the electron to be ejected is called photoelectric adsorption. Compton Scattering differs from adsorption, because the incoming photon affects outer electrons by ejecting them and losing just part of its own energy. In pair production the photon interacts with a nucleus and is transformed into a positron–electron pair. In this case no excess photon energy is transferred into kinetic energy (Heeraman et al., 1997). These interactions result in a reduction in intensity of an X-ray beam.

### 3.1.2 Attenuation

The reduction in intensity of an X-ray when it passes through an object is called attenuation. The attenuation of an X-ray beam as it passes through an object depends on its electron density and packing density, and the energy of the radiation (Asseng et al., 2000).

The attenuation of a monoenergetic beam through a homogeneous material is given by Beer's law (Equation 3-1).

$$I = I_0 \exp[-\mu x] \qquad \textbf{Equation 3-1}$$

I = intensity of transmitted beam, $I_0$ = initial X-ray intensity, $\mu$ = linear attenuation coefficient and x = length of the X-ray path

Equation 3-2 applies for an inhomogeneous material where each increment (i) reflects a single material.

$$I = I_0 \exp[\Sigma(-\mu_i x_i)] \qquad \textbf{Equation 3-2}$$

I = attenuation of a monoenergetic beam, $I_0$ = initial X-ray intensity, $\mu$ = linear attenuation coefficient and x = length of the X-ray path, i = single material

The linear attenuation coefficient depends on the density of the material ($\rho$) and the mass attenuation coefficient ($\mu^*$) (Equation 3-3).

$$\mu = \rho\mu^* \qquad \textbf{Equation 3-3}$$

$\mu$ = linear attenuation coefficient, $\rho$ = density of material, $\mu^*$ = mass attenuation coefficient

Because the attenuation coefficient is a strong function of X-ray energy, the total range of the effective X-ray spectrum needs to be considered

$$I = \int I_0(E) \exp\left[\sum_i (-\mu_i(E) x_i)\right] dE \qquad \textbf{Equation 3-4}$$

I = attenuation of X-ray beam, $I_0$ = initial X-ray intensity, $\mu$ = linear attenuation coefficient and x = length of the X-ray path, i = single material

Equation 3-4 is difficult to solve for industrial tomography, because the precise X-ray spectrum is usually only estimated rather than measured. Moreover, most reconstruction strategies solve Equation 3-2 by assigning a single value to each pixel rather than an energy dependent range.

### 3.1.3 3-D volumetric image acquisition

X-rays are detected after passing through an object by a detector system (Figure 3-1). At first photographic films were used as detectors, but with respect to computed tomography digital storage charge–couple device cameras and flat panel systems are more commonly employed.

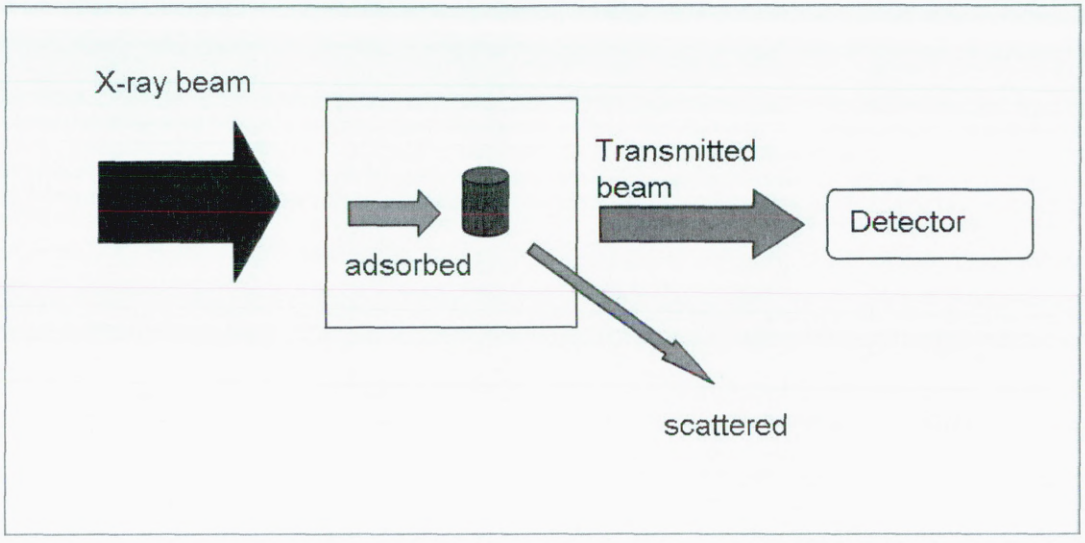


**Figure 3-1: Attenuation of a narrow beam of radiation by adsorption and scattering (after Aylmore, 1993).**

The focal spot size resolution of a CT system defines, amongst others, the spatial resolution by determining the numbers of possible source detector paths which cross a certain point in the object being scanned. The penetrative ability of an X-ray beam and its expected relative attenuation when passing through materials of different densities is dependent on the energy spectrum. High energy X-ray beams go through more effectively, but are less sensitive to changes in the material density and composition (Ketcham and Carlson, 2001).

To cover all angles of measurement either the X-ray beam and the detector move in synchrony around the subject or the sample is on a mechanical turntable that allows samples to rotate (Gregory et al., 2003). Four generations of computed tomography systems exist. They differ mostly in configuration of the source and detectors. The first-generation directs a pencil beam through the object to a single detector. Source and detector are moving around the object, repeating the scan process from different angular

orientations. In the second-generation a fan beam is applied and the single detector is replaced by a linear or accurate series of detectors. In a typical third-generation CT, beam and detector are wide enough to encompass the entire object. The sample can be removed from the centre of the fan beam to scan larger objects or smaller objects can be moved closer to the source, so that an increased resolution leads to a visualization of smaller subsections. Part of the object is then outside the fan beam, but the centre of rotation is within it. As the object rotates all of it passes the fan beam, so that the reconstruction of a whole image is possible (Ketcham and Carlson, 2001). Fourth-generation scanners consist of a fixed complete ring of detectors and a single X-ray source (Ketcham and Carlson, 2001).

Calibration of the X-ray signal, read by the detector, is necessary to establish the characteristics of the X-ray beam. One principle of calibration is 'offset and gain', where the detector readings with X-rays off and with X-rays on (scanning alignments used for scanning the object) are determined.

### 3.1.4 Reconstruction

Reconstruction techniques are necessary to obtain three dimensional images of cross sections of the scanned object projection. The most widespread reconstruction technique is the filtered back–projection. The projection data are convolved with a filter and each view is superimposed over a square grid at an angle corresponding to its acquisition angle. The outcome of the reconstructing process is a numerical map consisting of the values of attenuation coefficient $\mu_{(x,y)}$ corresponding to each voxel (CT number or CT

value). The range of CT number or CT values is determined by the computer system. The most common scale used to date has been 12 bit, which results in 4096 possible values; in industrial scanners these correspond to a greyscale in the created or exported image files. The Hounsfield scale has been developed in medical scanners to characterise the density of living tissues and can be used to represent CT values (Equation 3-5; Duliu, 1999; Rogasik et al., 1999).

$$HU = \frac{\mu_{(x,y)} - \mu_w}{\mu_w} \times 1000$$ **Equation 3-5**

HU = Hounsfield Unit, $\mu_{(x,y)}$ = value of attenuation coefficient corresponding to each voxel, $\mu_w$ = linear attenuation coefficient of water

The attenuation coefficient for water is 0, while the attenuation coefficient for air is 1000. Thus the higher the attenuation coefficient, the higher is also the Hounsfield Unit (Duliu, 1999).

### 3.1.5 Artefacts

Image analysis of 3-D volumetric images depends highly on the quality of the images. The quality is constrained by scanning artefacts, such as beam hardening, ring artefacts and partial volume effects.

Beam hardening is the most commonly occurring artefact in tomographic imaging. It is caused by a polychromatic X-ray beam, which has a wide range of energies. Unless X-rays are produced by radioactive decay, they are always polychromatic. The edges of an

object appear to be brighter than the centre, because of an increase in the mean X-ray energy of the beam while passing through the object. The lower–energy X-rays are attenuated more readily than higher-energy X-rays (Ketcham and Carlson, 2001). The effective attenuation coefficient of any material declines, so that short ray paths are attenuated more than long ray paths. This causes an artificial darkening at the centre of long ray paths and a corresponding brightening at the edge of the object (Ketcham and Carlson, 2001). To avoid this problem, a high energy X-ray beam can be used so that beam hardening can be ignored. But it must be noted that in using a high–energetic X-ray beam, the contrast between different materials may not be noticeable anymore, because high energy beams are less sensitive to attenuation. Another possibility is to pre-harden the X-ray beam by passing it through an attenuation filter. Beam filtration can lead to decreased intensity of the X-ray signal and therefore to an increase in the noise of the images (Ketcham and Carlson, 2001).

Ring Artefacts occur in third-generation scanning and are caused by shifts in outputs from individual detectors, which detect the corresponding ray or rays in each view. They appear as a number of concentric rings superimposed on the structures being scanned. Temperature instability can lead to drifts in detector element sensitivity in between the white–field calibration. Changes in beam strength can lead to those shifts, too, as well as a differential sensitivity to varying beam hardness (Ketcham and Carlson, 2001). Grey levels in the reconstructed images are influenced by these ring artefacts and quantitative analysis is hampered and noise reduction and image segmentation become more difficult. The effects of variation in temperature and beam strength can be overcome by controlling

experimental conditions and recalibration of the system. It is more difficult to overcome ring artefacts produced by beam hardening. If the calibration of the detector response is done by 'offset and gain' the relative response of the detector can change when the beam is significantly changed by passing through the object. Different views of an uneven object can reflect different grades of beam hardening, which leads to partial rings. If arrangements are made to reduce beam hardening, ring artefacts will usually decrease as well. Software remedies can spot and remove ring artefacts before reconstruction.

Partial volume effects hamper quantitative image analysis of 3-D volumetric images obtained through X-ray scanning. Each pixel in a CT image represents the attenuation properties of a specific volume. Depending on the resolution, a voxel may represent more than one material and the CT value is an average value for those properties. This is called the partial volume effect. All material boundaries are blurred to some extent so that any one voxel can affect CT values of surrounding voxels. These factors can lead to ill-defined boundaries of objects and hence difficulties in segmentation and interpretation of the CT data (Ketcham and Carlson, 2001).

## *3.2 Materials and methods*

### 3.2.1 X-ray system

3-D volumetric images in this thesis were obtained using a Metris X–Tek HMX CT scanner with a Varian Paxscan 2520 V detector and a 225 kV X-ray source (http://www.nikonmetrology.com) giving a resolution of up to 5 μm. The energy of the beam was as required for the electron density of the materials. The alignments for the

different scans are discussed in each appropriate section. A molybdenum target was used and, where needed, a 0.1 mm aluminium filter was applied to filter soft X-rays and minimize beam hardening (see details in each section). Metris software CT Pro v2.0 was used for reconstruction which uses a filtered back–projection algorithm.

### 3.2.2 Image analysis: Root–particle contact

The software VGStudio MAX v2.0 and v2.1 (http://www.volumegraphics.com) was used to develop and optimize a method for analysing root–particle contact from 3-D volumetric images. In this section two different methods of analysing root–particle contact are presented, because during the process of developing and optimizing this method the software VGStudio MAX v2.0 was replaced with a newer version (2.1). The data presented in VGStudio MAX are referred to as volumes.

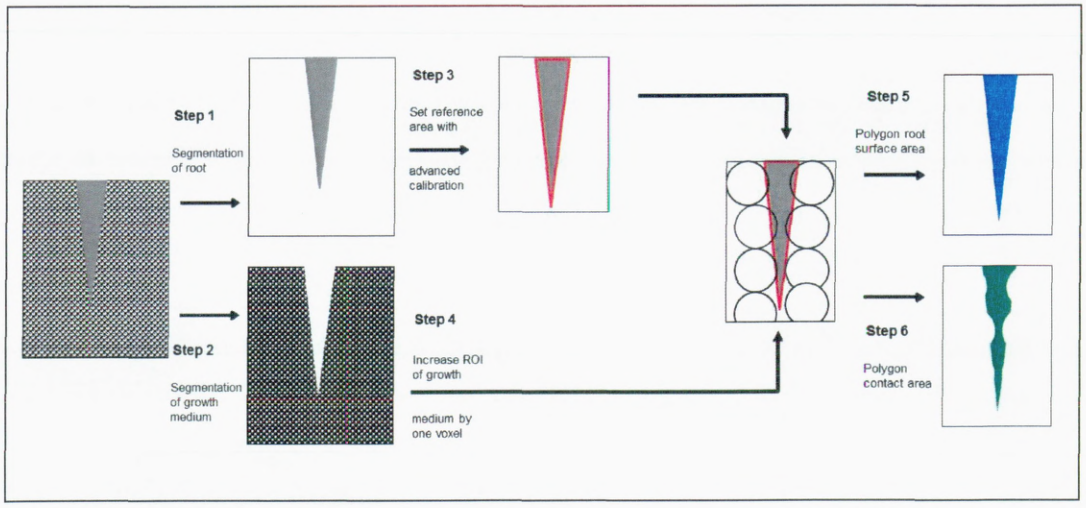


**Figure 3-2: Scheme for determining root–particle contact areas using VGStudio MAX v2.0.**

The **first method** was applied in VGStudio MAX v2.0 (Figure 3-2). To determine the contact area between root and growth medium, six main steps of image analysis were

conducted. In **step 1,** voxels representing the root volume were segmented from the sample volume. The root volume was thresholded using 3-D volume segmentation tools ("region grower"), which identify and extract voxels belonging to calculated ranges of greyscale values. Noise was reduced using an opening/closing tool. In **step 2** the growth medium was thresholded from the sample volume choosing grey scale values representing the solid phase using the segmentation tool "region grower" and "opening/closing" tools. These segmentation processes resulted in two regions of interest (ROI), one of the root volume and the other of the growth medium. The boundary of the root surface was calibrated so that voxels inside the calibrated region of interest were considered for further analysis in VGStudio MAX (**Step 3**). This was achieved using an "advanced calibration tool" which identifies voxels within 0.3 mm of the border of the region of interest representing root volume and then calculates an average grey scale value for the root surface (red line in Figure 3-2). This root surface constitutes a reference area that is subsequently used as the basis for estimating root–particle contact. **Step 4** uses the growth medium region of interest. This region of interest is extended by one voxel using the "erosion/dilate" tool and those voxels located inside the reference area (determined in **step 3**) constitute the root–particle contact. In the next step (**step 5**) polygonal meshes were superimposed over both the root surface and the voxels located inside the reference area with the "surface extraction" tool. This allowed the determination of the surface area of the root (closed surface) as well as the contact area between root and particles (open surface) (**step 6**). The contact area was expressed as a percentage of the total surface area of the root. The alignments in VGStudio MAX v2.0

for producing polygonal meshes differed for the root (closed surface) and the contact area (open surface) which resulted in different start and end points of the polygonal meshes.

The **second method** to investigate root–particle contact was conducted in VGStudio MAX v2.1 (Figure 3-3)

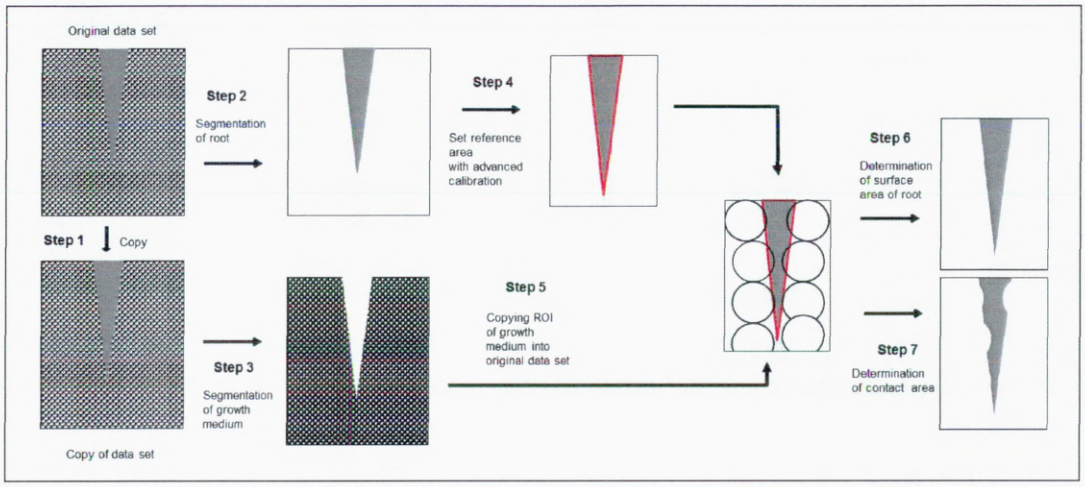


**Figure 3-3: Scheme for determining root–particle contact areas using VGStudio MAX v2.1.**

Before producing regions of interest for root and growth medium, a copy of the data set was generated (**step 1**). Similar to the first method, a region of interest for the root volume was produced by segmenting the voxels in the original data set, allowing the root volume to be defined (**step 2**) using the 'region grower' tool. In the copy of the data set, the region of interest for the growth medium was segmented (**step 3**). In the original data set the surface area of the root was determined from the root region of interest using the "advanced calibration tool" (**step 4**). The region of interest of the growth medium in the copied data set was extended by one voxel and then copied into the original data set to ensure that voxels accounting for root–particle contact were located in the reference area (**step 5**). The surface area of the root was determined from the region of interest

representing the segmented root volume (**step 6**). Voxels of the growth medium region of interest which were located in the reference area constitute the contact area (**step 7**). The contact between root and growth matrix was expressed as a percentage of the total root surface area.

When setting the reference area of objects in VGStudio MAX v2.0 and v2.1 the option to calibrate for single and multiple materials was given. The single material option was chosen when root–particle contact was analysed in VGStudio MAX v2.0, while in VGStudio MAX v2.1 multiple materials was selected because during the development of the method it was found that errors in surface areas of objects with known dimensions decreased when this option was selected.

### 3.2.2.1 Phantoms

Model systems (Phantoms) of root–soil contact with known dimensions were built to calculate systematic errors in the methodology for estimating the root–particle contact. In the first phantom (Figure 3-4), an acrylic rod (1.5 mm diameter, length 9.61 mm, representing the root) was placed on top of two cellulose acetate beads (3 mm diameter, representing soil particles). The Phantom was scanned at 64 kv and 485 µA with 2855 projections and a resolution of 18 µm was obtained (Figure 3-5 a).

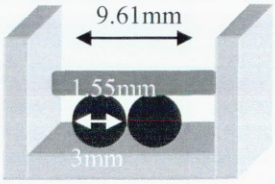


**Figure 3-4: Phantom 1 acrylic rod (representing the root) in contact with two cellulose acetate beads (representing particles).**

Volumes and surface areas of rod and beads were calculated from micrometer readings plus assumed cylindrical and spherical geometry. These were compared with values determined by analysis of 3-D volumetric images using the software VGStudio MAX v2.0 (3.2.2, Figure 3-2). To determine the contact area between roots and growth medium the surface area of the root needed to be determined. To test the accuracy of the method the surface areas of rod and beads were determined after segmentation from the regions of interest and from polygonal meshes (Figure 3-5), which were produced from the region of interest. The effects of various parameters on surface area estimates were performed.

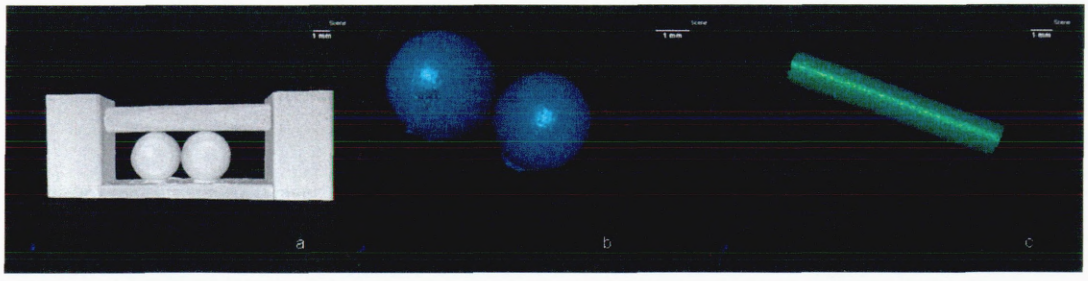


**Figure 3-5: Phantom rod in contact with two beads (a), segmented beads (normal polygonal mesh) and segmented rod (normal polygonal mesh).**

The 2-D cross sections through the rod were used to assess the error caused by the segmentation of the cylindrical surface into voxels of dimensions of 18 µm, and the subsequent generation of the polygonal mesh with normal or small triangles. In Figure

3-6 images of the cross sections of the rod are shown, taken from 3-D volumetric images of the polygonal meshes of normal (a) and small (b) triangles. Perimeters of circles were determined using the software ImageJ 1.43t (http://rsbweb.nih.gov/ij/).

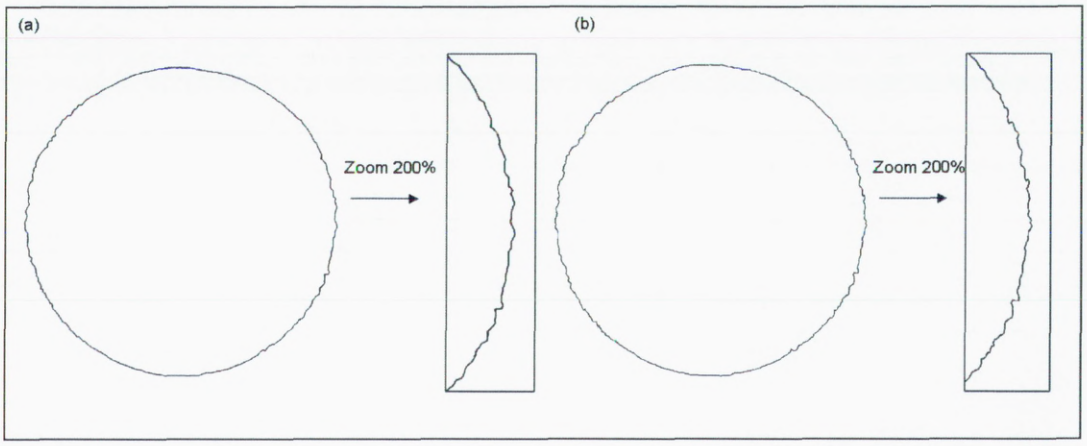


**Figure 3-6: 2-D cross sections of rod from polygonal meshes using normal and small triangles, and section zoomed in by 200 %.**

From the number of voxels of the cross section the diameter of circles was calculated and the length of the perimeter of a perfect circle with this diameter was calculated. The calculated values of perimeter were also compared with the perimeter determined with ImageJ 1.43t.

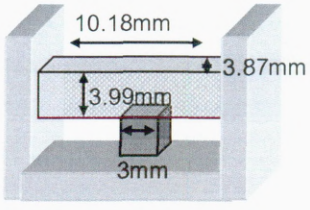


**Figure 3-7: Phantom 2, a modelsystem for root–particle contact; a polypropylethylene bar (3.99 × 3.87 × 10.18 mm, representing the root) in contact with acrylic cube (3 × 3 × 3 mm, representing a particle).**

To provide a geometrically simpler system, a second phantom was built. This phantom had square dimensions (Figure 3-7). A bar (representing the root), cut out of a polypropylethylene sheet, was in contact with an acrylic cube (growth medium), cut from a bar. For calculating the contact area of the two materials complete (100 %) contact between bar and cube was assumed. Three replicates of this phantom were made.

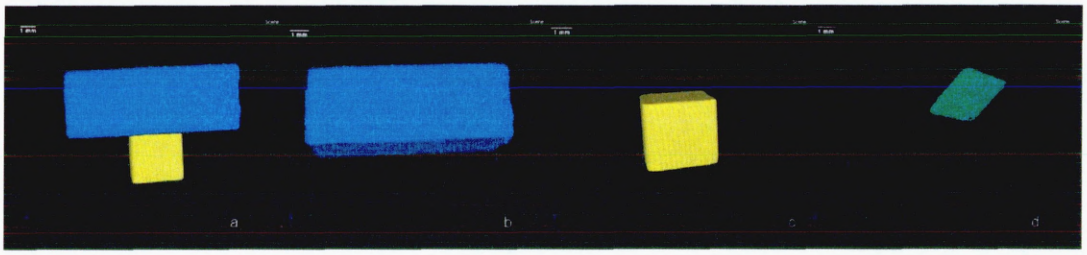


**Figure 3-8: False coloured 3-D volumetric images of phantom polypropylethylene bar in contact with acrylic cube (a), segmented bar (b) and cube (c) and, contact area (d) determined with VGStudio MAX v2.1. Resolution 34.9 µm.**

These phantoms were scanned (Figure 3-8) at 92 kV and 94 µA with 1088 projections. A 0.1 aluminium filter was used. A resolution of 34.9 µm was achieved. 3-D volumetric images were analysed using VGStudio MAX version 2.1 (3.2.2., Figure 3-3). Bar and cube were segmented (Figure 3-8). Contact areas of bar and cube for the square phantoms of similar dimensions were determined (Figure 3-8) before and after filtering the data set with a median filter of 3.

## *3.3 Results*

### 3.3.1 Phantoms

Figure 3-9 shows surface areas and volumes of rod and two beads of Phantom 1. The results present the calculated surface area of rod and two beads and the values determined

by image analysis. The surface areas determined from regions of interest and from two different polygonal meshes are shown. The surface area determined by image analysis was much greater than the calculated values.

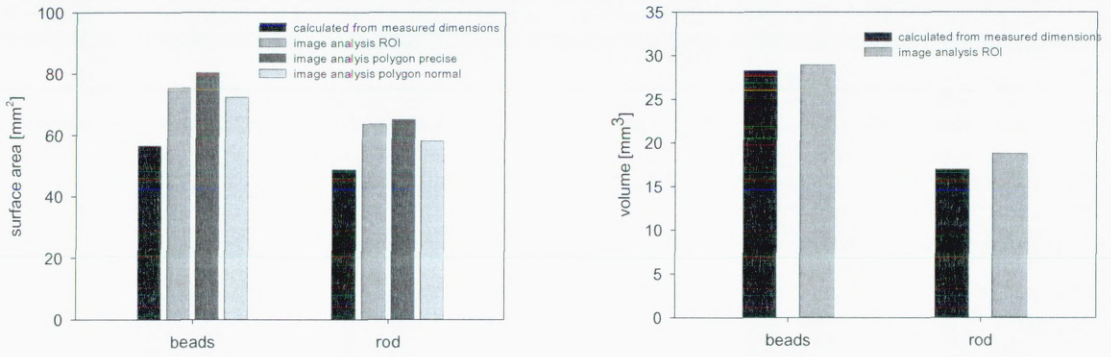


**Figure 3-9: Surface areas and volumes from calculation and image analysis of beads and rod of Phantom 1. Surface areas from image analysis from region of interest (ROI), and from polygonal meshes of small triangle size (precise) and normal triangle size (normal). Volumes are calculated from measured dimensions and from image analysis of the ROI.**

Greatest variance was between the calculated values and values determined from a precise polygonal mesh. Surface area and volume were both overestimated by image analysis although the overestimation of volume was less than that for surface area.

The length of perimeters calculated and analysed in ImageJ 1.43t of cross sections from the rod is shown in Figure 3-10. Scanning, reconstruction and image analysis caused an overestimation of 7.7 % to 9.4 %. The bigger the triangles of the polygonal mesh, the smaller the error.

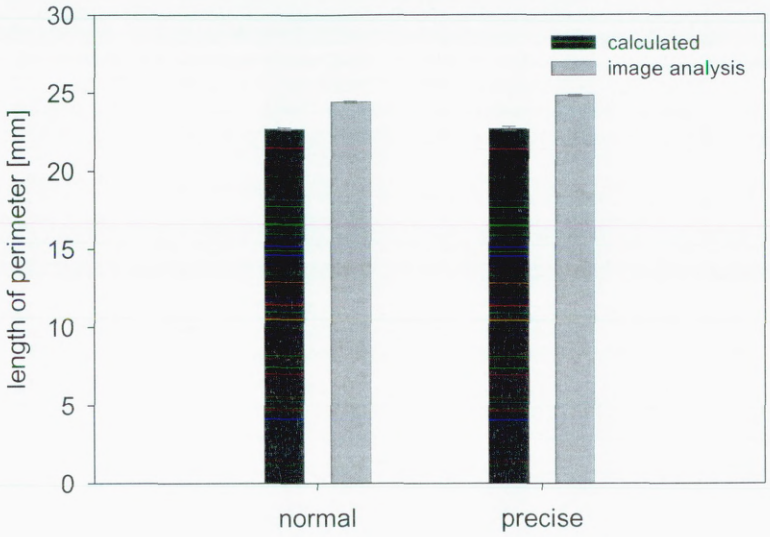


**Figure 3-10: Perimeter of 2-D cross section of rod calculated.**

Filtering the scan with a median filter of 3 also influenced differences between calculated values and results of image analysis (Figure 3-11). The surface areas of the bar of phantom 2 were greater for image analysis than those calculated; the error increased from 7 % to 11 % when the data set was not filtered. The error in surface error of the cube was smaller than for the bar (unfiltered, overestimation of 1.4 %; filtered, underestimation of 2.6 %). Filtering the data altered surface area values of the cube significantly ($p = 0.047$), but had no effect on the surface area of the bar ($p = 0.401$).

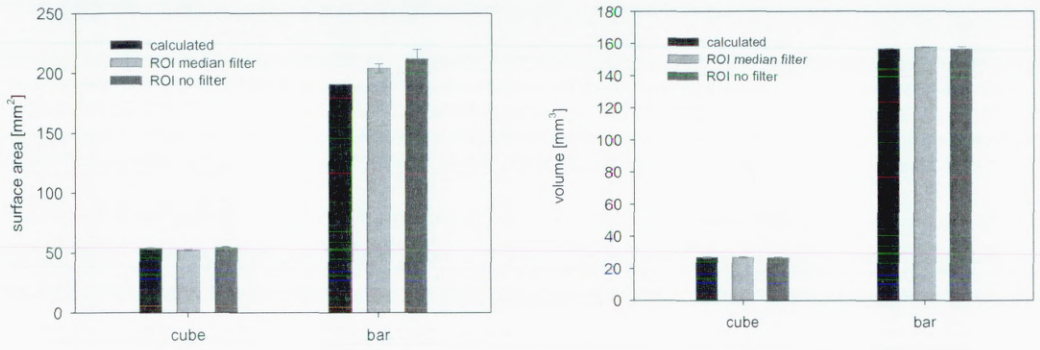


**Figure 3-11: Surface areas and volumes from calculation of measured dimension and image analysis of cube and bar of Phantom 2. Surface areas and volumes from image analysis from region of interest (ROI) before and after filtering with a median filter of 3.**

Determination of the volume of the bar and cube using VGStudio MAX v2.1 resulted in values that differed less than 0.3 % from the calculated data. Filtering had no significant effect on the volume data ($p = 0.512$ and 0.894).

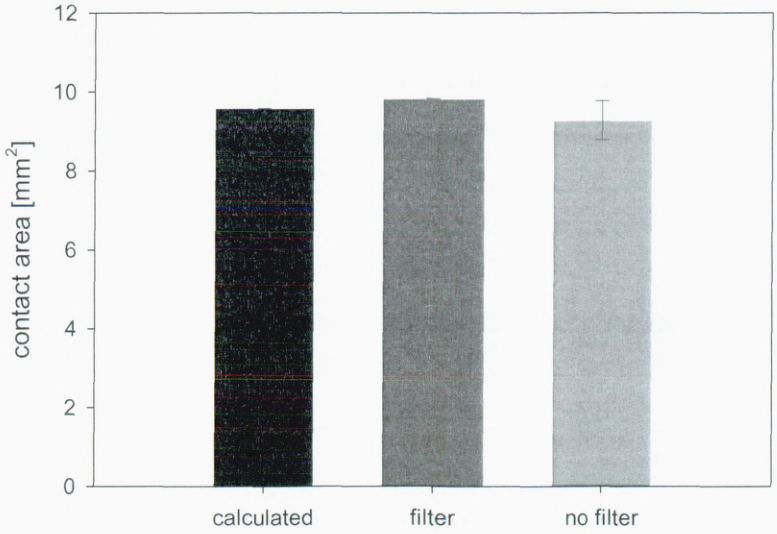


**Figure 3-12: Contact area of cube and bar of Phantom 2 from calculation and image analysis before and after filtering with median filter.**

The contact between bar and cube determined by image analysis of unfiltered 3-D data sets differed about 3.2 %, and for filtered data sets about 2.5 %, from calculated values. Greater variation for the three phantoms (type 2) was found with unfiltered data.

## 3.4 Discussion

In this chapter image analysis of 3-D volumetric images was undertaken using VGStudio MAX v2.0 and v2.1. Phantoms were scanned to estimate the accuracy of the methods. Surface area and volume determined by image analysis was compared with values calculated from measured dimensions. Surface areas of the different objects of the two phantoms were overestimated. To a certain extent the overestimation was due to artefacts occurring during the scanning process. Beam hardening was unavoidable using a polychromatic beam and made the segmentation process more difficult, because the edges of the phantom appeared brighter. Partial volume effects also might have added to the surface area by counting voxel which were partly representing other phases/materials of the object analysed. At a scale of 34.9 µm and 18 µm two or more materials might have been represented by one voxel. This effect might have been increased by the brighter edges due to beam hardening.

When the reference area was set to calculate surface areas, the region of interest representing the rod was chosen for calibration purposes. Voxels up to a distance of 0.3 mm in all three dimensions of the border line of the region of interest were considered. The calibration line was the result of average greyscale values of the neighbouring voxels. The calibration line was judged to be the outer border of the object.

Brighter voxels at the edges could have caused the calibration line to be further out than the actual voxels representing the objects. The surface areas determined by VGStudio MAX v.2.0 were significantly greater than those calculated from the dimensions of beads and rod. Besides beam hardening and partial volume effects, the fact that round objects were represented by squared voxels might have added to the greater surface areas. Image analysis in 2-D cross sections of the rod showed that the perimeter increased by about 5 % compared to the actual diameter. Furthermore, the calibration process was subvoxel precise, while regions of interest were voxel precise, so that the calibration line cut through some voxels to draw the outer border of objects. The algorithm for determining surface areas of regions of interest took outer borders of the voxels crossed by the calibration line into account for determining surface areas instead of following the calibration line which was the correct border of the object.

Moreover in version 2.0 'single material' in the alignments was chosen for calibrating an object, but the phantom was made of multiple materials, so that the alignment 'multiple materials' would have been correct. The alignments caused sub volumes, which added to the region of interest and therefore to the surface area. During the analysis process in VGStudio MAX v2.1 it was discovered that the choice of 'multiple material' decreased the error. The software VGStudio MAX v2.0 was not available anymore, so that the error could not be corrected for the samples analysed in version 2.0.

For determining a contact area, in VGStudio MAX v2.0 polygonal meshes needed to be produced. Those polygonal meshes were fitting the surface area of an extracted object within a certain tolerance. The range in tolerance depended on the size of the polygonal

mesh (and therefore the number of triangles). The bigger the triangles the greater the tolerance. The size and number of triangles influenced the estimation of surface area of objects. The finer mesh caused a greater error in surface area compared to calculated values, because it follows more accurately the characteristics of the region of interest, while the coarser mesh probably smoothed the surface area, as demonstrated in Figure 3-6. The error in determining the volume of a reference object from 3-D volumetric images compared to calculated values was smaller than for surface area because more voxels were considered for the volume, so that edge effects were only small compared to surface determination, where only voxels on the reference area border were considered, so that results for the surface area were significantly affected by edge effects.

The error in surface area was greatly reduced using the more advanced version 2.1 for image analysis. The algorithm for calculating the surface area of regions of interest was changed in version 2.1, so that only the calibration line accounted for surface area. Furthermore, the contact area could be determined from the region of interests and losing detail by producing a polygonal mesh from the region of interest was prevented. The use of 'single material' for calibration was changed to 'multiple materials', so that no subvolumes appeared. The error in surface area might also have been smaller because for that study square phantoms were chosen for modelling the root–soil contact. Voxels fit the shape of a square object better than for round objects. A square phantom was chosen in preference to the cylinder–spheres phantom, because the contact area could be calculated, assuming complete contact, without knowing the force between the two objects. The assumption of complete contact was made because at a resolution of

34.9 μm fine irregularities in the surface were not visible. A median filter of 3 reduced the error in surface area estimates. Median filtering is a common method for noise reduction (Soille, 2003). The surface areas of cube and bar were determined by VGStudio MAX v.2.1. The results for surface area determined by image analysis differed between 1.4 and 11 %. The error in surface area estimates was greater for the bar compared to the cube. The cube was cut from a square rod, so that it had to be cut to the right size on two sides, while the bar was cut out of a sheet, so that the end product had four cut sides. Although the phantom was polished, the cut sides remained less smooth. The dimensions of the cube and bar were measured with a caliper but an uncertainty remains in the measurements of the phantom. The more cut sides the greater the probability of error in dimensions. The error in surface area stated might be smaller than that reported because of inaccuracies in the dimensions of the phantoms. Three phantoms were built to estimate the variability in dimensions of bar and cube. The standard error in surface area was greater for the cube than for the bar which suggests that the number of cut sides did not influence the accuracy of the phantom. Despite these uncertainties and source of error, it was shown throughout this work that the contact area can be quantified with high accuracy (within 3%) using VGStudio MAX v2.1.

## 3.5 Summary

This Chapter presented a method for determining root–particle contact from X-ray microtomographs using VGStudio MAX. Model systems of root–particle contact where

the dimensions were known were used to test the accuracy of the method. Root–particle contact could be determined with an accuracy of 3 %.

In conclusion, X-ray microtomography and 3-D image analysis algorithms are useful tools to study the root–soil interface and determine contact areas, but require both careful optimisation of image quality and the development of rigorous image analysis protocols that minimise elements of subjectivity. A valuable method for quantifying root–particle contact was developed and was used for later studies.

# 4 Effects of matric potential and growth medium on root and shoot elongation

## 4.1 Introduction

Root growth is often decreased when soil dries out. The reduction of growth is often not as much as the reduction in shoot growth, so that the root–to–shoot ratio of plants increases (Sharp et al., 1988).

Roots have a role in moderating the supply of water through rooting depth and the quantity of roots in a particular layer. Roots show enhanced gravitropism when soil dries (Sharp and Davies, 1985) and an increased rooting depth can significantly increase water uptake, although a clear effect of rooting depth is often only noticeable when plants are competing for the same reserves of soil water (Davies and Bacon, 2003). Water uptake by roots is possible up to a matric potential of about -1.5 MPa. At this matric potential the wilting point of many mesophytic plants is reached. Root growth rate is reduced substantially by matric potentials drier than -1.5 MPa (Bengough et al., 2006). Investigations by Sharp et al. (1988) of the primary root growth of maize at different matric potentials in vermiculite showed a decrease of elongation rate with decreasing matric potential. Maize root elongation was maintained preferentially towards the apex and unaffected in the apical 2–3 mm when matric potentials were as dry as -1.6 MPa. A shorter elongation zone was a consequence of a slower growth rate caused by shorter cortical cells and a slower rate of cell production (Fraser et al., 1990). The distance between root tip and the root hair zone can be used to estimate the length of the elongation zone (Pagès et al., 2009). As soil water supply is restricted, root diameter also changes. Sharp et al. (1988) found that roots in dry vermiculite, where no mechanical impedance hinders root elongation, were thinner than in wet vermiculite (Sharp et al.,

1988). It is believed that this change in morphology is adaptive to water stress and resources can be used to further extend root growth (Sharp et al., 1990). Root growth is often less inhibited than shoot growth, or sometimes even promoted, in drying soils, which is likely to result in a better water supply if water is available at depth (Sponchiado et al., 1989). Shoot growth is sensitive to water-limited conditions. Previous studies have shown that the inhibition of shoot growth is largely a consequence of hormonal interactions of ABA and ethylene rather than by direct consequences of altered water status caused by drying soils (Sharp et al., 2000).

Water transport to roots becomes more important for the plant as soil dries. An essential factor for root growth is a good contact with the growth medium for nutrient and water uptake (Veen et al., 1992). Root–soil contact is influenced by soil and root properties, like particle size, degree of soil compaction, root diameter and relative hydration (Van Noordwijk et al., 1992; Nye, 1994; Tinker, 1976). In water-saturated and heavily compacted soils, problems with root gas exchange can occur (Veen et al., 1992). Conversely, incomplete root–soil contact due to soil structure or root shrinkage can reduce the uptake of water and nutrients (Veen et al., 1992). Van Noordwijk et al, (1992) used thin–sections to evaluate root–soil contact which was used by Veen et al. (1992), who investigated whether poor root–soil contact affected shoot growth, nitrate and water uptake. Maize was grown at five different levels of soil compaction and with a restricted nitrogen supply. Shoot growth was slightly lower at a porosity of 59.6 % than at a porosity of 50.6 % and decreased with further increase in bulk density. Water and nitrate uptake were also highest at the intermediate pore volume (50.6 %) and slightly lower at the highest soil porosity (59.6 %). Root growth was restricted to the upper zones of the

pots which were packed to a bulk density of 1.54 g $cm^{-3}$ and specific root length per plant was 3.45 m $g^{-1}$, smaller than in the least compacted soil (1.08 g $cm^{-3}$). Veen et al. (1992) also found a decrease of 5 μL $h^{-1}$ $m^{-1}$ in water adsorption and of 5.9 mmol $m^{-1}$ per unit root length in nitrate uptake from compacted to loose soil as a result of decreasing root–soil contact. When soil dries, gaps form between the root and soil due to root shrinking, so that root–soil contact decreases (Carminati et al., 2009). Under conditions of poor root–soil contact, vapour transport for plant growth might become more important. Studies of seed germination with different seed–soil contacts and soil matric potentials showed that vapour transport played a major role in water supply for germinating seeds (Wuest et al., 1999; Wuest, 2002).

The work of Sharp and co–workers gave insight into how plant growth is influenced by changes in matric potential. Nevertheless, this work was mainly done in vermiculite so that mechanical impedance would not affect root elongation. Vermiculite has different particle size and water retention properties compared to soil. Furthermore information about processes at the root–soil interface and the role of root–soil contact and vapour transport for root growth in drying soils is poor. The work in this Chapter investigated the effects of growing media at different matric potentials on root and shoot growth. Three different growth media (soil, vermiculite and humid air) were used to investigate root and shoot growth at different matric potentials. It was hypothesized that root and shoot elongation is faster in soil than in vermiculite and air, because of better water availability due to a different structure of soil and vermiculite hence a greater root–particle contact in soil. The effect of root–particle contact will be more important in drier soils because fewer pores will be water filled and water transport via liquid films towards the roots

becomes more important. Root and shoot growth of maize and lupin in soil, vermiculite and air were investigated at matric potentials in the range of field capacity to permanent wilting point.

## 4.2 Materials and methods

### 4.2.1 Root and shoot growth of maize and lupin in soil and vermiculite at a range of matric potentials between -0.03 MPa and -1.6 MPa

Pre-germinated maize and lupin seeds with 10 mm long radicles were moved into a dishes (23 × 23 × 2 cm) filled with either soil or vermiculite wetted to water contents corresponding to the following potentials (Table 2-2): -0.03 MPa, -0.2 MPa, -0.81 MPa and -1.6 MPa. Five seedlings per dish were placed on top of the growth medium and covered with a lid. The dishes were stored upright, so that the radicles were facing downwards, for 96 h in an incubator at 20 °C in darkness. Matric potentials might have changed throughout the experiment, but because plants were grown in darkness in a sealed container for only four days these changes were assumed to be minimal.

Soil was packed at a bulk density of approximately 0.9 g $cm^{-3}$. Root and shoot lengths were measured every day with a ruler. Root and shoot elongation rates were calculated from the root length increase (Equation 4-1).

$$E = \frac{\left(L_{(n)} - L_{(n-1)}\right)}{d}$$ **Equation 4-1**

E = root or shoot elongation rate [cm $d^{-1}$], L = root/shoot length [cm], n = time [d] after placing seeds into growth medium

The average root and shoot elongation rates were determined from the total root and shoot growth during 96 h (Equation 4-2).

$$E = \frac{\left(L_{(end)} - L_{(start)}\right)}{t} \qquad \textbf{Equation 4-2}$$

E = root or shoot elongation rate [mm $h^{-1}$], L = root/shoot length [mm], t = time of growth period [h]

Root diameter and distance between root tip and root hair zone were measured after 96 h using a stereomicroscope (Leica MZ FL III) equipped with an eyepiece graticule.

It was investigated whether pH affected root elongation in soil, because vermiculite and soil differed in pH, but also in structure. Pre-germinated maize and lupin seedlings were placed in similar dishes as mentioned above, filled with soil of pH 5.2 or 6.9 at matric potentials of either -0.03 MPa, -0.2 MPa, -0.81 MPa or -1.6 MPa. Five seedlings per dish were placed on top of the soil and covered with a lid. The dishes were placed in an incubator at 20 °C in darkness for 96 h and root growth during this period was measured.

### 4.2.2 Root–particle contact

Root–particle contact of maize and lupin roots in soil and vermiculite wetted to initial water contents corresponding to matric potentials of -0.03 MPa and -1.6 MPa (Table 2-2) was investigated using X-ray computed tomography. 3-D volumetric images were taken of seedlings growing in soil and in vermiculite using the XTEK HMX 225.

Cylindrical plastic containers (10 cm tall and 3 cm in diameter) were packed with either soil (bulk density 0.9 g $cm^{-3}$) or vermiculite (bulk density 0.07 g $cm^{-3}$) at water contents of 18 g $g^{-1}$ (soil) and 321 g $g^{-1}$ (vermiculite) corresponding to a matric potential of -0.03 MPa or 8 g $g^{-1}$ (soil) and 9 g $g^{-1}$ (vermiculite) corresponding to a matric potential of -1.6 MPa. Pre-germinated maize or lupin seed with 1–2 cm long radicles were placed in containers and stored at 20°C in darkness for 24 h before they were scanned at 145 kV and 140 µA. A resolution of 34.9 µm was achieved. 2855 projections were taken. A 0.1 mm aluminium filter was used to reduce beam hardening.

Root–soil contact was determined using VGStudio MAX v2.1 (see Chapter 3). Three replicates of each treatment (2 × plant species, 2 × growth media and 2 × matric potentials) were prepared and scanned, which resulted in 14 scans in total. Root–particle contact was determined from a subregion of the scans to avoid beam hardening effects and because seeds and shoots had similar grey scale values as roots so the subregion excluded the seed and shoots and represented a volume in the centre of the tube of approximately 1280 $mm^3$ (8 mm × 8 mm × 20 mm). Maize roots tended to grow down container walls, so that root volumes used for image analysis varied per scan.

### 4.2.3 Root and shoot growth in air at a range of matric potentials between -0.03 MPa and -1.6 MPa

Root and shoot elongation of maize and lupin in air at different relative humidity (-0.03 MPa, -0.2 MPa, -0.81 MPa and -1.6 MPa) was investigated. The seeds were placed in sealed jars (diameter 9 cm; height 10 cm, one seed per jar). A nylon mesh was stretched over a plastic cylinder (diameter 5 cm; 6 cm height) and one seedling per jar

was placed on the mesh so that the radicle was not touching any surface. KCl-solution was used to adjust the relative humidity of the air. The jars were stored in an incubator at 20 °C in darkness for 48h. Three replicates for every treatment (plant species and air humidity) were measured.

The weight of the seed and the root and shoot length before and after 48 h were determined. The weight increase contributing to root and shoot growth was calculated, assuming that the root is cylindrical of length (l) and volume (V) (Equation 4-3).

$$V = r^2 \times \pi \times l$$ **Equation 4-3**

Furthermore, it was assumed that the root and shoot tissues consist of 90 % water (Equation 4-4).

$$V_{90} = \frac{V}{90} \times 100$$ **Equation 4-4**

To determine the contribution of water intake to root and shoot growth, the weight increase was determined (Equation 4-5).

$$w_{alt} = w_e - w_s$$ **Equation 4-5**

The length of tissue was calculated in mm (Equation 4-6).

$$l_{cal} = \frac{w_{alt}}{V_{90} \times 1000}$$ **Equation 4-6**

V = volume of plant growth, r = average radius of root and shoot, l = length (here 1mm), $V_{90}$ = Volume of water to produce 1mm of root or shoot tissue, $w_{alt}$ = weight change of seedling, $w_s$ = weight of seedling at

start of experiment, $w_e$ = weight of seedling at end of experiment, $l_{cal}$ = length calculated from weight change of seedling

The average root and shoot elongation rates (Equation 4-2) over 48 h were compared with those in soil and vermiculite (4.2.14.2.3).

## *4.3 Results*

### 4.3.1 Root and shoot elongation rates of maize and lupin in soil and vermiculite at a range of matric potentials

Root length was significantly influenced by time ($p < 0.001$), matric potential ($p < 0.001$), growth medium ($p < 0.001$) and plant species ($p < 0.001$; Figure 4-1). Root length of maize increased faster the wetter the growth medium, so that root length of maize grown in soil for 96 h was 12.26 ±0.21 cm at -0.03 MPa and 4.30 ±0.41 cm at -1.6 MPa. Maize root length in vermiculite (max. 8.85 ±0.65 cm) was shorter than that in soil (max. 12.26 ±0.21 cm) at all matric potentials over the 96 h period.

Lupin root length was shorter the drier the matric potential of the growth medium (Figure 4-1). No differences in root length of roots grown in soil at -0.03 MPa (max. 8.75 ±0.82 cm) and -0.2 MPa (9.5 ±0.33cm) were found, but in vermiculite roots grown at -0.03 MPa (max. 7.48 ±0.95cm) were longer than roots grown in vermiculite at matric potentials drier than -0.03 MPa (max. 4.25 ±0.24 cm; 4.10 ±0.24 cm and 3.8 ±0.24 cm). Lupin roots grown in vermiculite -0.2 MPa, -0.81 MPa and -1.6 MPa had similar root lengths from day one to day four.

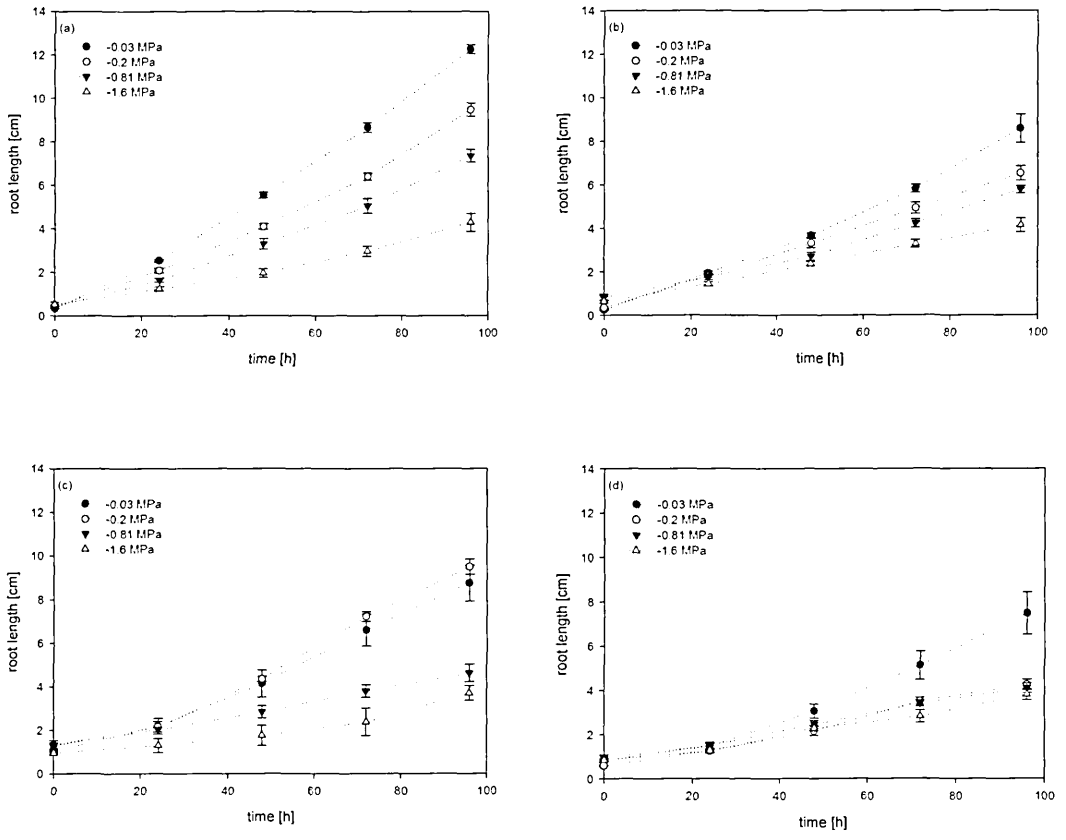


**Figure 4-1: Root length of maize (a, b) and lupin (c, d) as a function of time in soil (a, c) and vermiculite (b, d) at matric potentials of -0.03 MPa, -0.2 MPa, -0.81 MPa and -1.6 MPa. Data are means ±SE (n = 5).**

Root elongation rates per day of maize increased with time in soil and in vermiculite (Table 4-1). Root elongation rates of maize in soil were greater than those in vermiculite when soil was wetter than -1.6 MPa. The drier the growth medium the smaller the differences in elongation rate between soil and vermiculite.

**Table 4-1: Root elongation rates per day of maize in soil and vermiculite [cm $d^{-1}$] at matric potentials of -0.03 MPa, -0.2 MPa, -0.81 MPa and -1.6 MPa. Data are means ±SE (n = 5).**

| | Root elongation rate of maize in soil [cm $d^{-1}$] | | | | | | | |
|---|---|---|---|---|---|---|---|---|
| Time [h] | -0.03 MPa | | -0.2 MPa | | -0.81 MPa | | -1.6 MPa | |
| 0–24 | 2.26 | ±0.11 | 1.66 | ±0.07 | 1.22 | ±0.08 | 0.73 | ±0.11 |
| 24–48 | 3.00 | ±0.13 | 2.02 | ±0.06 | 1.66 | ±0.16 | 0.66 | ±0.13 |
| 48–72 | 3.66 | ±0.81 | 2.30 | ±0.18 | 1.76 | ±0.21 | 0.88 | ±0.89 |
| 72–96 | 3.60 | ±0.64 | 3.08 | ±0.17 | 2.30 | ±0.21 | 1.13 | ±0.64 |
| | Root elongation rate of maize in vermiculite [cm $d^{-1}$] | | | | | | | |
| Time [h] | -0.03 MPa | | -0.2 MPa | | -0.81 MPa | | -1.6 MPa | |
| 0–24 | 1.74 | ±0.10 | 1.46 | ±0.051 | 0.94 | ±0.12 | 0.78 | ±0.10 |
| 24–48 | 1.72 | ±0.13 | 1.50 | ±0.16 | 0.94 | ±0.12 | 0.88 | ±0.13 |
| 48–72 | 2.58 | ±0.27 | 1.62 | ±0.12 | 1.38 | ±0.12 | 0.93 | ±0.27 |
| 72–96 | 2.76 | ±0.44 | 1.60 | ±0.11 | 1.55 | ±0.09 | 0.75 | ±0.44 |

Root elongation rates of lupin grown in soil and vermiculite at matric potentials ranging from -0.03 MPa to -1.6 MPa increased, when wetter than -0.2 MPa in soil or wetter than -0.03 MPa in vermiculite (Table 4-2). Maximum root elongation rates of lupin were slower by 1.2 cm $d^{-1}$ than maximum root elongation rates of maize.

**Table 4-2: Root elongation rates per day of lupin in soil and vermiculite [cm $d^{-1}$] at matric potentials of -0.03 MPa, -0.2 MPa, -0.81 MPa and -1.6 MPa. Data are means ±SE (n = 5).**

| | Root elongation rate of lupin in soil [cm $d^{-1}$] | | | | | | | |
|---|---|---|---|---|---|---|---|---|
| Time [h] | -0.03 MPa | | -0.2 MPa | | -0.81 MPa | | -1.6 MPa | |
| 0–24 | 1.16 | ±0.24 | 0.84 | ±0.13 | 0.72 | ±0.06 | 0.70 | ±0.06 |
| 24–48 | 1.96 | ±0.28 | 1.32 | ±0.68 | 0.82 | ±0.21 | 0.55 | ±0.04 |
| 48–72 | 2.46 | ±0.31 | 2.30 | ±0.60 | 0.96 | ±0.08 | 0.70 | ±0.16 |
| 72–96 | 2.13 | ±0.19 | 1.82 | ±0.47 | 0.82 | ±0.13 | 0.80 | ±0.23 |
| | Root elongation rate of lupin in vermiculite [cm $d^{-1}$] | | | | | | | |
| Time [h] | -0.03 MPa | | -0.2 MPa | | -0.81 MPa | | -1.6 MPa | |
| 0–24 | 0.66 | ±0.12 | 0.66 | ±0.12 | 0.56 | ±0.15 | 0.48 | ±0.08 |
| 24–48 | 1.58 | ±0.29 | 0.90 | ±0.14 | 0.96 | ±0.07 | 0.74 | ±0.05 |
| 48–72 | 2.06 | ±0.31 | 0.64 | ±0.57 | 0.94 | ±0.13 | 0.64 | ±0.12 |
| 72–96 | 2.36 | ±0.32 | 0.60 | ±0.18 | 0.70 | ±0.11 | 0.80 | ±0.29 |

Root elongation rates during 96 h decreased with decreasing matric potential in soil and vermiculite. Maize root elongation rates were faster in soil than in vermiculite at all matric potentials. Growth material ($p < 0.001$) and matric potential ($p < 0.001$) had significant effects on root elongation rates of maize (Figure 4-2). Root elongation rates of roots grown in soil slowed more steadily than in vermiculite. In vermiculite maize root elongation slowed down the greatest from -0.03 MPa to -0.2 MPa (0.46 mm $h^{-1}$).

Lupin root elongation rates were also significantly affected by matric potential ($p < 0.001$) and growth material ($p < 0.001$). Root elongation rates decreased with decreasing matric potential and slowed down significantly in vermiculite between matric potentials of -0.03 MPa to -0.2 MPa (0.69 mm $h^{-1}$ to 0.35 mm $h^{-1}$), while in soil the effect was greatest between matric potentials of -0.2 MPa and -0.81 MPa (from 0.90 mm $h^{-1}$ to 0.39 mm $h^{-1}$).

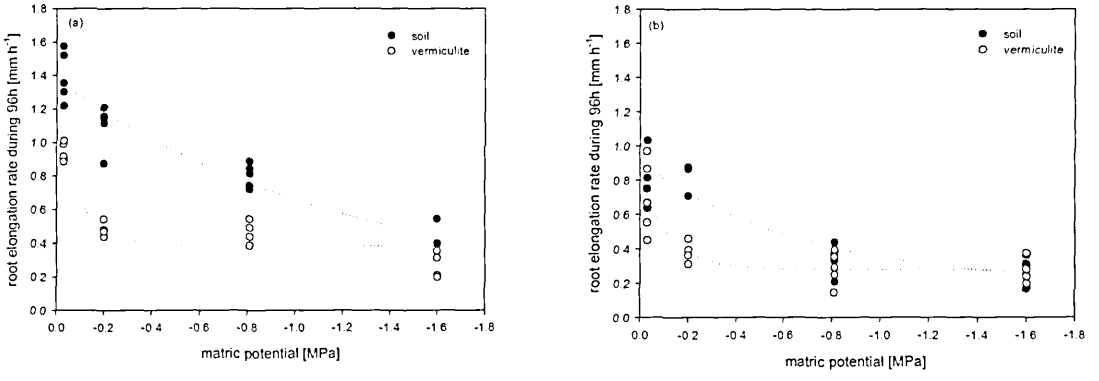


**Figure 4-2: Average root elongation rates during 96 h of maize (a) and lupin (b) roots grown in soil and vermiculite at matric potentials of -0.03 MPa, -0.2 MPa, -0.81 MPa and -1.6 MPa. The dotted lines are simple exponential curves: maize in soil $E=0.08+1.29\times2.33^{\Psi}$; maize in vermiculite $E=0.34+0.76\times32929.65^{\Psi}$; lupin in soil $E=0.18+0.72\times4.16^{\Psi}$; lupin in vermiculite $E=0.28+0.54\times4026.75^{\Psi}$.**

The drier the growth medium, the shorter the shoot until a matric potential of -1.6 MPa. At this potential no shoot growth occurred. Maize and lupin shoots grew longer in soil than in vermiculite (Figure 4-3).

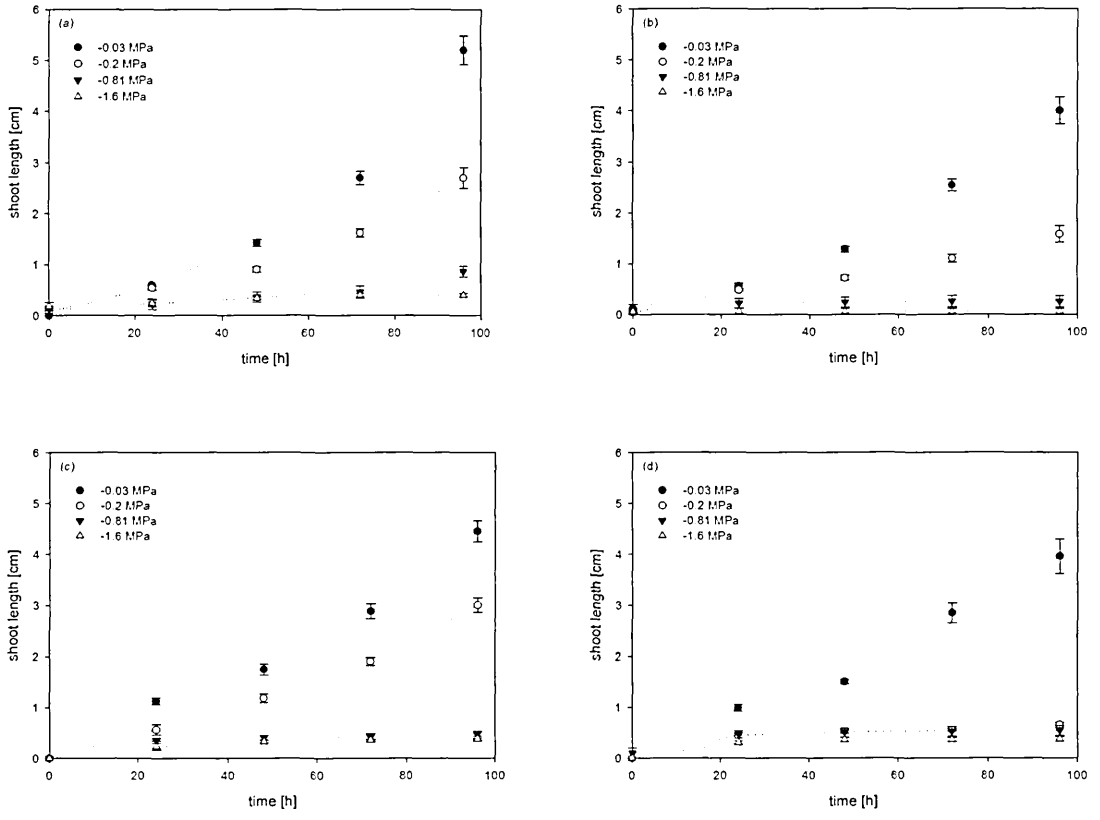


**Figure 4-3: Shoot length of maize (a, b) and lupin (c, d) as a function of time in soil (a, c) and vermiculite (b, d) at matric potentials of -0.03 MPa, -0.2 MPa, -0.81 MPa and -1.6 MPa. Data are means ±SE (n = 5).**

Shoot elongation rate changed significantly with time and matric potential ($p < 0.001$), but also growth medium affected shoot growth ($p < 0.001$). Shoot elongation rates of maize increased by 1.9 cm $d^{-1}$ (soil) or 1.02 cm $d^{-1}$ (vermiculite) from day one to day four in soil or vermiculite of -0.03 MPa (Table 4-3).

**Table 4-3: Shoot elongation rates per day of maize in soil and vermiculite [cm $d^{-1}$] at matric potentials of -0.03 MPa, -0.2 MPa, -0.81 MPa and -1.6 MPa. Data are means ±SE (n = 5).**

| | Shoot elongation rate of maize in soil [cm $d^{-1}$] | | | | | | | |
|---|---|---|---|---|---|---|---|---|
| Time [h] | -0.03 MPa | | -0.2 MPa | | -0.81 MPa | | -1.6 MPa | |
| 0–24 | 0.60 | ±0.00 | 0.46 | ±0.10 | 0.10 | ±0.04 | 0.05 | ±0.04 |
| 24–48 | 0.82 | ±0.08 | 0.36 | ±0.02 | 0.14 | ±0.07 | 0.12 | ±0.05 |
| 48–72 | 1.28 | ±0.10 | 0.72 | ±0.07 | 0.10 | ±0.03 | 0.03 | ±0.02 |
| 72–96 | 2.50 | ±0.23 | 1.08 | ±0.13 | 0.40 | ±0.11 | 0.03 | ±0.00 |
| | Shoot elongation rate of maize in vermiculite [cm $d^{-1}$] | | | | | | | |
| Time [h] | -0.03 MPa | | -0.2 MPa | | -0.81 MPa | | -1.6 MPa | |
| 0–24 | 0.44 | ±0.02 | 0.44 | ±0.04 | 0.18 | ±0.08 | 0.00 | ±0.00 |
| 24–48 | 0.72 | ±0.04 | 0.24 | ±0.04 | 0.02 | ±0.02 | 0.00 | ±0.00 |
| 48–72 | 1.26 | ±0.07 | 0.38 | ±0.07 | 0.02 | ±0.02 | 0.00 | ±0.00 |
| 72–96 | 1.46 | ±0.14 | 0.48 | ±0.11 | 0.00 | ±0.00 | 0.00 | ±0.00 |

Shoot elongation rates in soil decreased with time when soil was drier than -0.81 MPa while in vermiculite shoot elongation rates decreased when it was drier than -0.2 MPa. No shoot growth of maize was determined in vermiculite at -1.6 MPa.

Shoot elongation rates of lupin grown in soil decreased with time when soil was drier than -0.2 MPa. Shoots elongated fastest in the first 24 h in vermiculite drier than -0.03 MPa (Table 4-4) and stopped growing in vermiculite at -1.6 MPa after 48 h.

**Table 4-4: Shoot elongation rates per day of lupin in soil and vermiculite [cm $d^{-1}$] at matric potentials of -0.03 MPa, -0.2 MPa, -0.81 MPa and -1.6 MPa. Data are means ±SE (n = 5).**

| | Shoot elongation rate of lupin in soil [cm $d^{-1}$] | | | | | | | |
|---|---|---|---|---|---|---|---|---|
| Time [h] | -0.03 MPa | | -0.2 MPa | | -0.81 MPa | | -1.6 MPa | |
| 0–24 | 1.12 | ±0.08 | 0.60 | ±0.06 | 0.36 | ±0.02 | 0.20 | ±0.07 |
| 24–48 | 0.62 | ±0.05 | 0.60 | ±0.08 | 0.04 | ±0.02 | 0.18 | ±0.09 |
| 48–72 | 1.14 | ±0.10 | 0.80 | ±0.11 | 0.02 | ±0.02 | 0.03 | ±0.02 |
| 72–96 | 1.50 | ±0.19 | 1.10 | ±0.20 | 0.06 | ±0.02 | 0.00 | ±0.02 |
| | Shoot elongation rate of lupin in vermiculite [cm $d^{-1}$] | | | | | | | |
| Time [h] | -0.03 MPa | | -0.2 MPa | | -0.81 MPa | | -1.6 MPa | |
| 0–24 | 0.98 | ±0.08 | 0.36 | ±0.05 | 0.44 | ±0.06 | 0.33 | ±0.03 |
| 24–48 | 0.52 | ±0.06 | 0.04 | ±0.02 | 0.08 | ±0.02 | 0.04 | ±0.06 |
| 48–72 | 1.34 | ±0.21 | 0.02 | ±0.03 | 0.05 | ±0.02 | 0.06 | ±0.00 |
| 72–96 | 1.12 | ±0.25 | 0.02 | ±0.04 | 0.10 | ±0.02 | 0.00 | ±0.00 |

Shoot elongation over 96 h slowed with drier matric potentials in both growth media (Figure 4-4). Shoot elongation rates of maize were greater in soil than in vermiculite and decreased with decreasing matric potential. Matric potential and growth medium had a significant effect on root elongation rates of maize ($p < 0.001$) and lupin ($p < 0.001$). Shoot elongation rate of maize and lupin was much faster in soil at -0.2 MPa than in vermiculite. Maize shoots grown in soil elongated at this matric potential at a rate of 0.33 ±0.02 mm $h^{-1}$ and in vermiculite at a rate of 0.12 ±0.008 mm $h^{-1}$. Shoot elongation rate of lupin at this matric potential in soil was 0.25 ±0.03mm $h^{-1}$ and in vermiculite 0.06 ±0.005 mm $h^{-1}$.

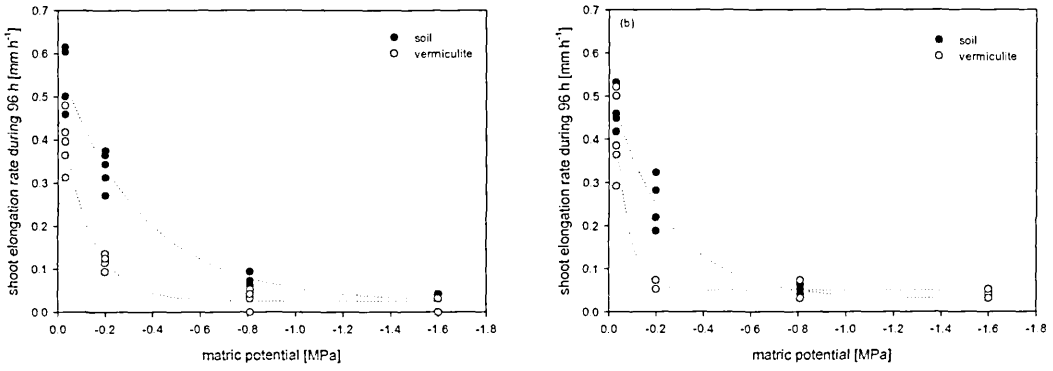


**Figure 4-4: Average shoot elongation [mm $h^{-1}$] rates during 96 h of maize (a) and lupin (b) roots grown in soil and vermiculite at matric potentials of -0.03 MPa, -0.2 MPa, -0.81 MPa and -1.6 MPa. The dotted lines are exponential growth curves: maize in soil $E=0.02+0.56\times17.77^{\Psi}$; maize in vermiculite $E = 0.02+0.47\times2708.48^{\Psi}$; lupin in soil $E = 0.03+0.49\times55^{\Psi}$; lupin in vermiculite $E = 0.05+0.61\times\exp(17.34\times\Psi)$.**

The relationship between root elongation rate and distance between root tip and root hair zone are shown in Figure 4-5. Linear relationships between elongation rate and distance between root tip and root hair zone were found for maize ($r^2 = 0.74$, $p < 0.001$ in soil and $r^2 = 0.79$ ($p < 0.001$ in vermiculite) and lupin ($r^2 = 0.82$, $p < 0.001$ in soil and $r^2 = 0.80$, $p < 0.001$ in vermiculite) grown in soil and vermiculite. The faster the root elongated the greater the distance between root tip and root hair zone.

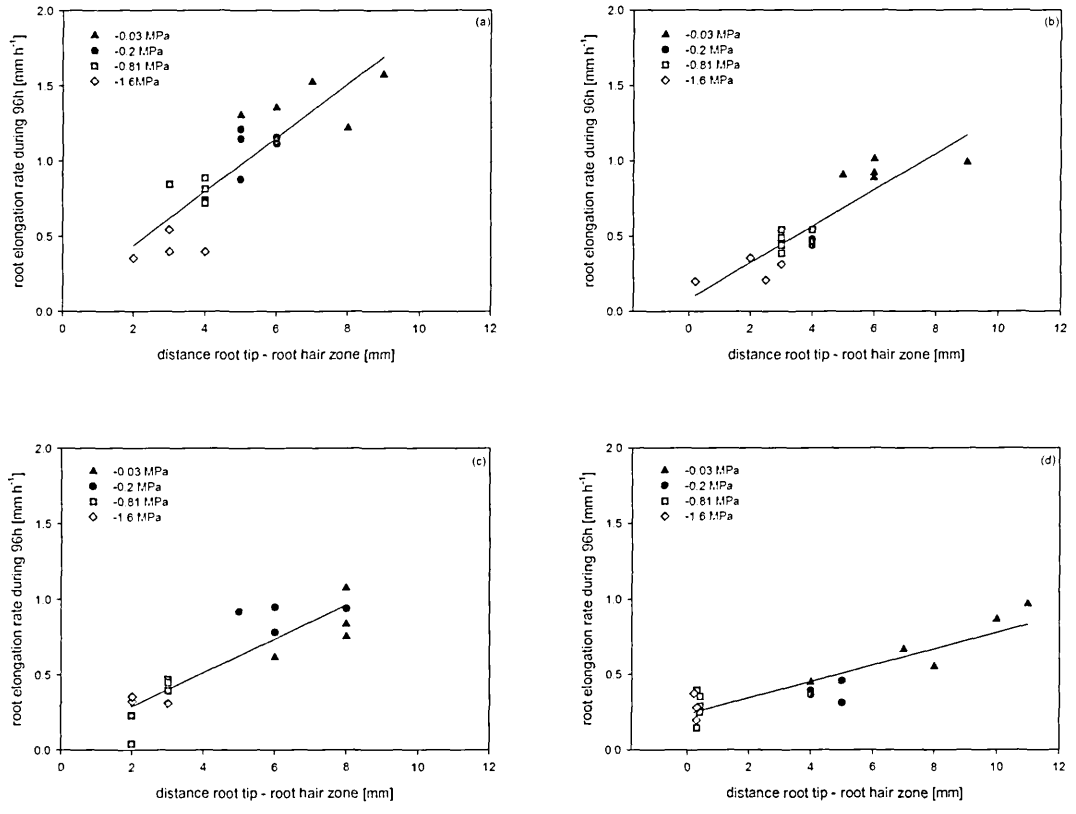


**Figure 4-5: Distance between root tip and root hair zone vs average root elongation rate during 96 h of maize (a, b) and lupin (c, d) in soil (a, c) and vermiculite (b, d) wetted to -0.03 MPa, -0.2 MPa, -0.81 MPa and -1.6 MPa. The lines are linear regressions. $R^2$ values are given in Table 4-5.**

The gradients for the lines of maize and lupin grown in soil (maize 0.18; lupin 0.11) were greater than those grown in vermiculite (maize 0.12; lupin 0.054), and those for maize (0.18 and 0.12) were greater than those for lupin (0.11 and 0.054; Table 4-5).

Matric potential ($p < 0.001$) and plant species ($p = 0.045$) had significant effects on root diameter, but growth medium did not ($p = 0.331$).

**Table 4-5: Curve fitting parameters for linear regression and correlation coefficients between root elongation rate and distance between root tip and root hair zone for maize and lupin grown in loose packed soil at matric potentials of -0.03 to -1.6 MPa.**

| Plant | Growth medium | $r^2$ | Intercept | SE Inter–cept | Probability value Intercept | Gradient | SE Gradient | Probability value Gradient |
|---|---|---|---|---|---|---|---|---|
| Maize | Soil | 0.69 | 0.093 | 0.14 | 0.52 | 0.18 | 0.027 | <0.001 |
| Lupin | Soil | 0.75 | 0.085 | 0.083 | 0.32 | 0.11 | 0.015 | <0.001 |
| Maize | Vermiculite | 0.79 | 0.082 | 0.065 | 0.23 | 0.12 | 0.015 | <0.001 |
| Lupin | Vermiculite | 0.80 | 0.23 | 0.035 | <0.001 | 0.054 | 0.0069 | <0.001 |

In drier soil roots tended to be thinner and elongated more slowly than in wetter soil (Figure 4-6).

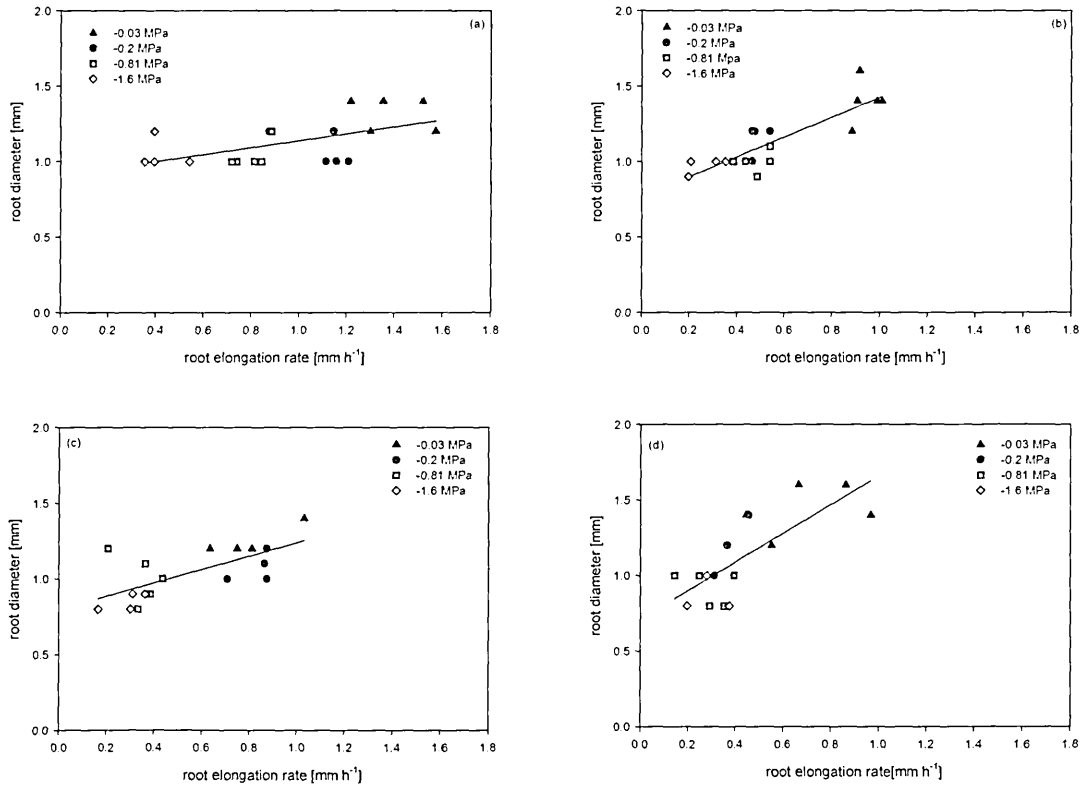


**Figure 4-6: Root diameter vs elongation rate during 96 h of maize (a, b) and lupin (c, d) in soil (a, c) and vermiculite (b, d) wetted to -0.03 MPa, -0.2 MPa, -0.81 MPa and -1.6 MPa. The lines are linear regressions. $R^2$ values are given in Table 4-6.**

Root diameter and root elongation rate were linearly correlated for maize and lupin (Table 4-6). The correlation was greater in vermiculite (maize $r^2 = 0.77$; lupin $r^2 = 0.56$) than in soil (maize $r^2 = 0.28$, lupin $r^2 = 0.44$).

**Table 4-6: Curve fitting parameters for linear regression and correlation coefficients between root elongation rate and root diameter for maize and lupin grown in loose packed soil at matric potentials of -0.03 to -1.6 MPa.**

| Plant | Growth medium | $r^2$ | Intercept | SE Inter–cept | Probability value Intercept | Gradient | SE Gradient | Probability value Gradient |
|---|---|---|---|---|---|---|---|---|
| Maize | Soil | 0.28 | 0.91 | 0.08 | <0.001 | 0.23 | 0.08 | 0.012 |
| Lupin | Soil | 0.44 | 0.81 | 0.07 | <0.001 | 0.44 | 0.12 | 0.002 |
| Maize | Vermiculite | 0.72 | 0.77 | 0.59 | <0.001 | 0.66 | 0.10 | <0.001 |
| Lupin | Vermiculite | 0.56 | 0.71 | 0.10 | <0.001 | 0.95 | 0.21 | <0.001 |

Root growth of maize and lupin in soil of pH 5.2 and 6.9 was measured after a period of 96 h (Figure 4-7).

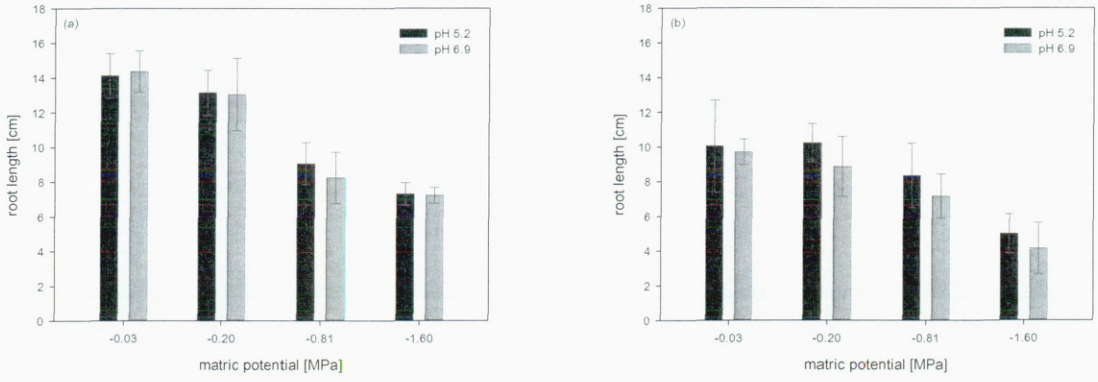


**Figure 4-7: Root length of maize (a) and lupin (b) in soil of pH 5.2 and 6.9 and matric potentials of -0.03, -0.2, -0.81 and -1.6 MPa after 96 h. Data are means ±SE (n = 5).**

Neither maize ($p = 0.48$) nor lupin ($p = 0.091$) lengths were significantly affected by pH of the soil at any matric potentials, but lupin showed a greater sensitivity towards an increase in pH than maize.

### 4.3.2 Root and shoot growth of maize and lupin in soil and vermiculite and air at a range of matric potentials

Figure 4-8 shows root and shoot elongation rates of maize and lupin in soil, vermiculite and humid air. The root elongation rate of maize and lupin increased in all growth media with increasing matric potential. Maize elongation rates were highly significantly influenced by matric potential ($p < 0.001$) and the growth medium ($p < 0.001$).

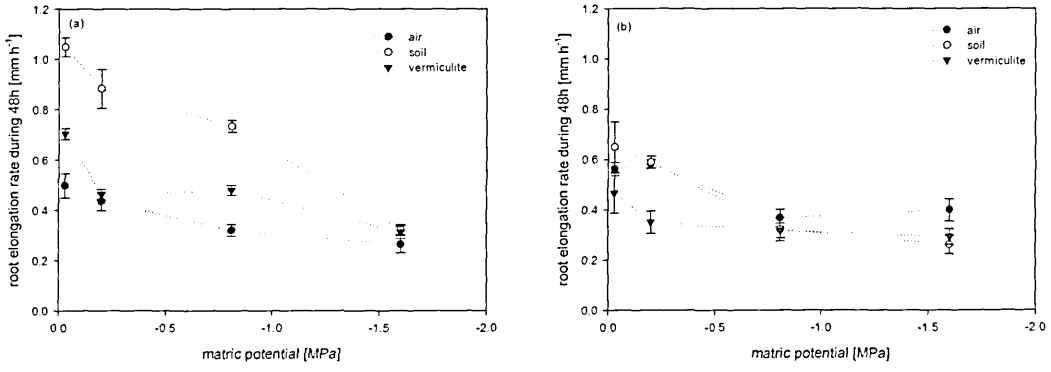


**Figure 4-8: Average root elongation rate of maize (a) and lupin (b) [mm $h^{-1}$] after 48 h in soil, vermiculite and air at matric/water potential of -0.03 MPa, -0.2 MPa, -0.81 MPa and -1.6 MPa.**

Roots elongated faster in soil than in vermiculite or air when matric potentials were above -1.6 MPa. Maize roots elongated slowest in air and fastest in soil. Lupin elongation rates were not affected by growth medium ($p = 0.543$), but decreasing matric potential slowed root elongation significantly ($p < 0.001$).

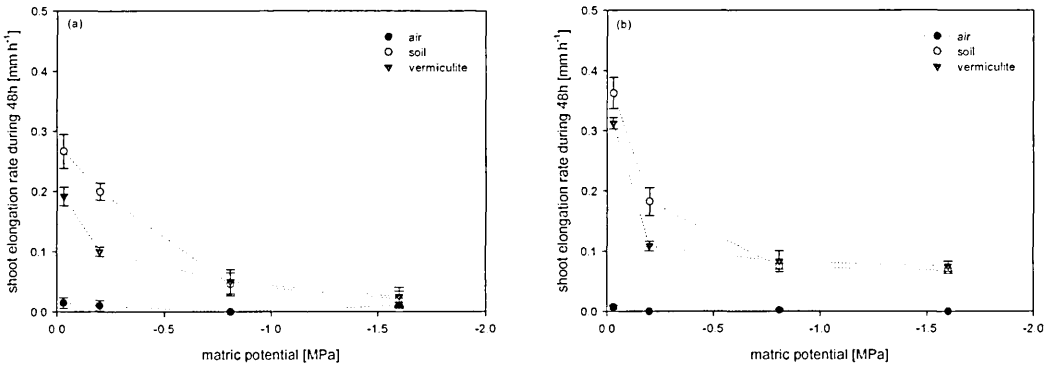


**Figure 4-9: Average shoot elongation rate of maize (a) and lupin (b) [mm $h^{-1}$] after 48 h in soil, vermiculite and air at matric/water potential of -0.03 MPa, -0.2 MPa, -0.81 MPa and -1.6 MPa.**

Shoot elongation rates of maize and lupin in soil, vermiculite and air responded similarly (Figure 4-9). Elongation rate increased in soil and vermiculite with increasing matric potential, while in air elongation was inhibited at all matric potentials. At the lowest matric potential (-1.6 MPa) no significant shoot growth was recorded. Shoot elongation rates of lupin were faster in soil and vermiculite than those of maize. Both growth medium ($P < 0.001$) and matric potential ($p < 0.001$) had significant effects on shoot elongation rates. Nevertheless maize and lupin showed significantly different growth responses to growth medium and matric potential ($p < 0.001$).

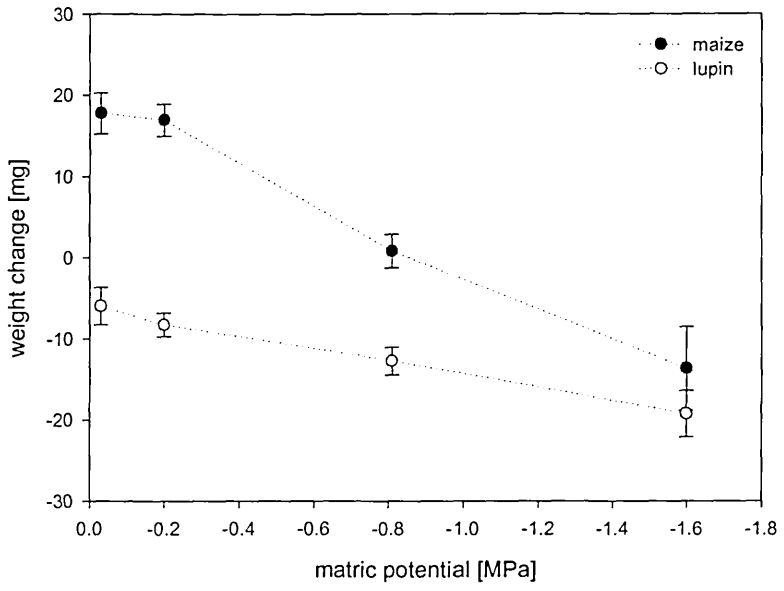


**Figure 4-10: Weight change of maize and lupin seedlings grown at four different air humidity (water potentials of -0.03 MPa, -0.2 MPa, -0.81 MPa and -1.6 MPa) during 48 h. Dashed line shows the zero point on y-scale.**

The weight changes of seedlings grown in humid air are shown in Figure 4-10. Lupin lost weight at all four matric potentials, while maize gained weight at water potentials greater than -0.81 MPa.

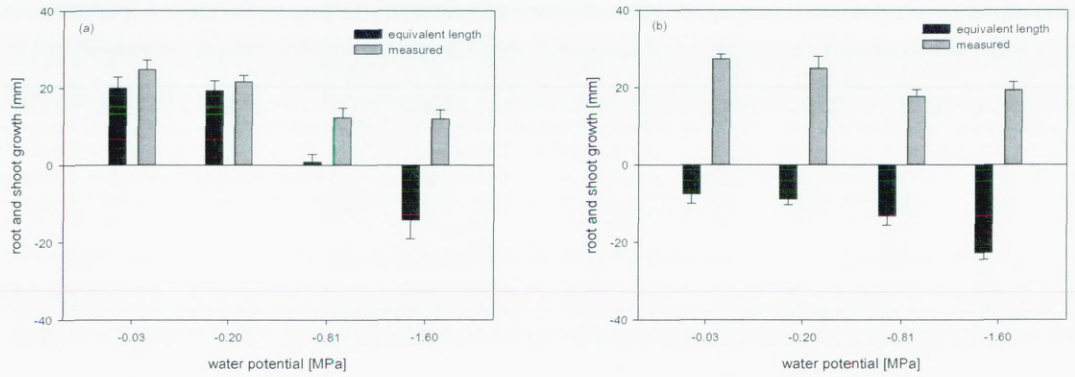


**Figure 4-11: Root and shoot growth of maize (a) and lupin (b) measured for roots grown in humid air for 48 h. Also shown is the equivalent change in length corresponding to that calculated from weight change of the seedlings during 48h.**

Lupin did not gain any water from the surrounding (Figure 4-11), but increased its root and shoot length more than maize, presumably due to redistribution of its water internally from the cotyledons. Maize gained water when grown in air wetter than -1.6 MPa, but the increase in weight of the seedlings was not enough for shoot and root elongation during 48 h.

### 4.3.3 Root–particle contact

Root–particle contact was determined from 3-D volumetric images. An example of frontal plane of sections of 3-D volumetric images of maize and lupin grown in soil and vermiculite at -0.03 MPa are shown in Figure 4-12.

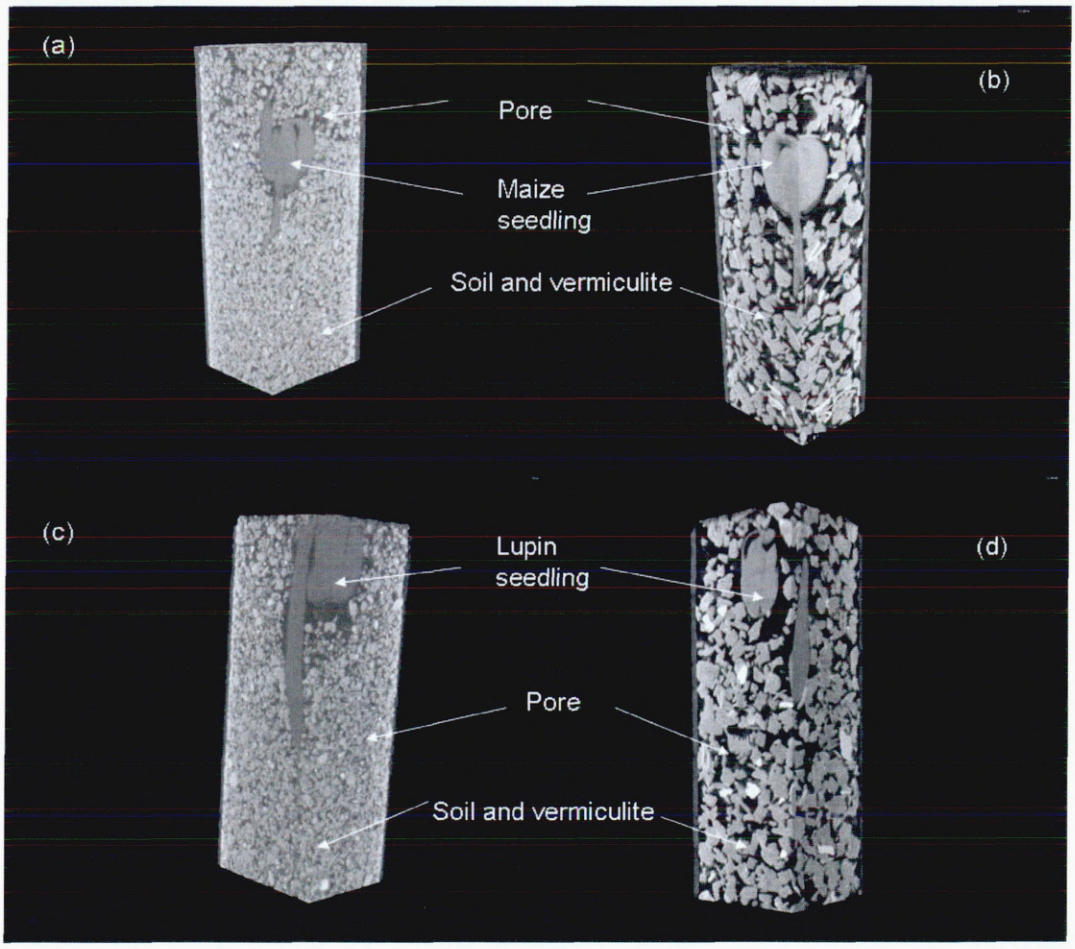


**Figure 4-12: Frontal plane of sections of 3-D volumetric images: maize (a, b) and lupin (c, d) seedlings in soil (a, c) and vermiculite (b, d) at -0.03 MPa. Resolution 34.9 µm.**

The different structures of soil and vermiculite are clearly distinguishable and there was greater contact of roots in soil compared to vermiculite. Contact areas were determined from regions of interest (ROI) of the root and soil particles (Figure 4-13).

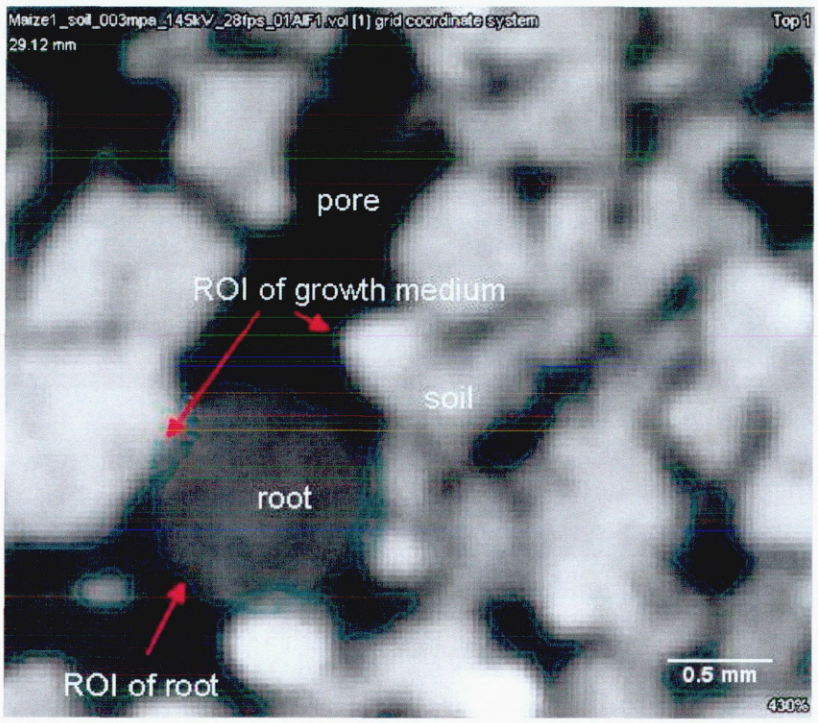


**Figure 4-13: Two dimensional cross section of maize root in soil sieved to 2 mm with region of interest (ROI) around root and soil particles.**

Where regions of interest were overlapping, an area (contact area) was determined (Figure 4-13) and compared with the surface area of the root. An example for root volumes in soil and vermiculite of segmented maize and lupin roots and their contact areas with growth media are shown in Figure 4-14. The contact area of the roots grown in soil was greater than that of the roots grown in vermiculite.

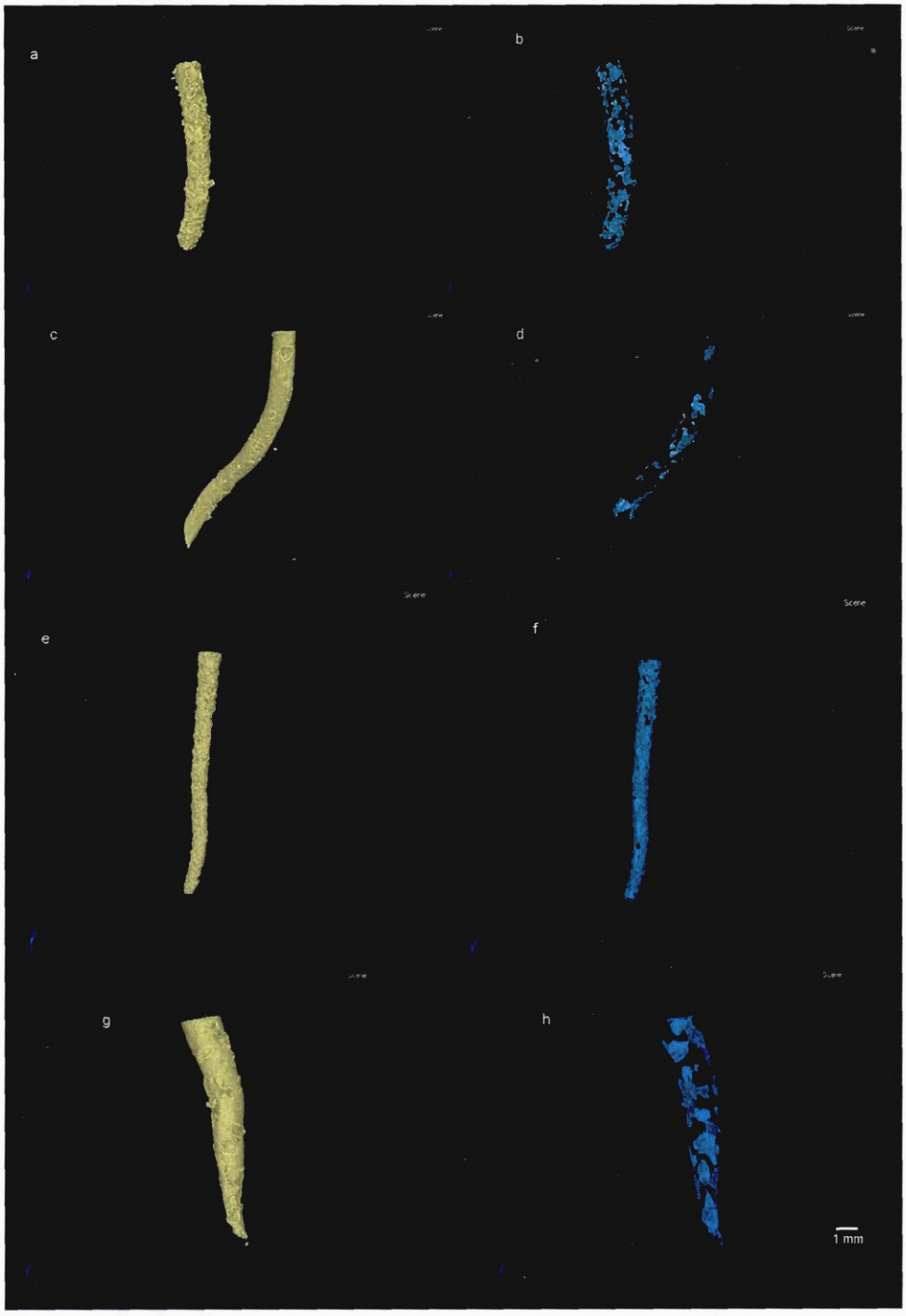


**Figure 4-14: False coloured images of segmented root volume of maize (a, c) and lupin (e, g) in soil sieved to 2 mm (a, e) and vermiculite (e, g) and root–particle contact area (b maize in soil, d maize in vermiculite, f lupin in soil, h lupin in vermiculite) determined from 3-D–volumetric images in VGStudio MAX v2.1.**

Root volumes used for image analysis differed per sample because of different growth rates of roots in soil and vermiculite and because maize tended to grow down container walls, so that a great proportion of the root was not considered. The volumes of roots considered for contact analysis were greater for lupin than for maize (Table 4-7). Greater root volumes of lupin at -0.03 MPa were determined than at -1.6 MPa because of greater root elongation rates. Maize root also elongated faster at -0.03 MPa than at -1.6 MPa but roots grew preferentially down the container walls and portions of the roots were therefore not considered for root–particle contact determination, as indicated in the root volumes used (Table 4-7).

**Table 4-7: Root volume determined from region of interest in VGStudio Max v2.1 used from which root–particle contact was determined.**

| Plant species | Growth material | Ψ [MPa] | Root volume $mm^3$ | SE |
|---|---|---|---|---|
| Maize | Soil | -0.03 | 11.87 | ±0.82 |
| Maize | Soil | -1.6 | 21.05 | ±5.56 |
| Maize | Vermiculite | -0.03 | 14.54 | ±1.22 |
| Maize | Vermiculite | -1.6 | 13.32 | ±3.32 |
| Lupin | Soil | -0.03 | 34.37 | ±0.80 |
| Lupin | Soil | -1.6 | 26.49 | ±6.05 |
| Lupin | Vermiculite | -0.03 | 50.45 | ±5.09 |
| Lupin | Vermiculite | -1.6 | 34.50 | ±7.34 |

Maize and lupin had greater contact in soil than in vermiculite ($p < 0.001$; Figure 4-15). Lupin had significantly greater contact with the growth medium than maize ($p = 0.005$) but matric potential had no effect on root soil contact ($p = 0.903$).

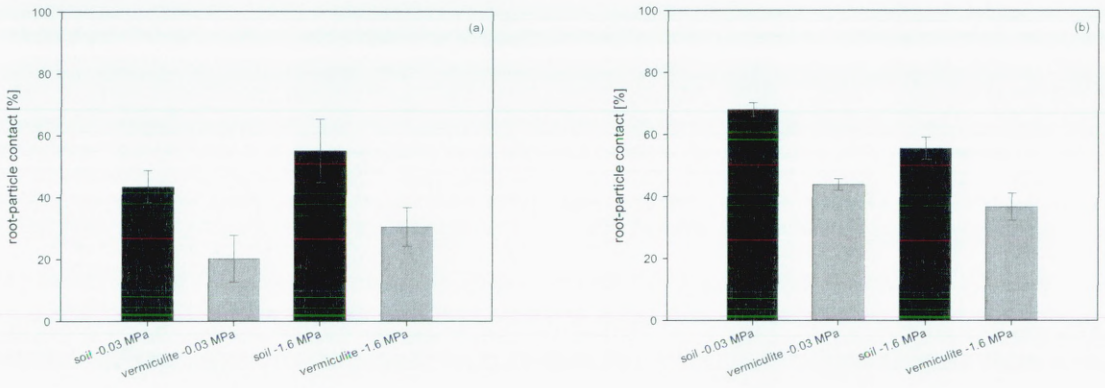


**Figure 4-15: Root–particle contact of maize (a) and lupin (b) grown at -0.03 MPa and -1.6 MPa for 24h in soil and vermiculite. The contact area is shown as % of the surface area of the root. Data are means with SE (n = 3).**

Root–particle contact of maize roots in soil was approximately 23 to 25 % greater than in vermiculite, while lupin root–particle contact was 18 to 25 % greater in soil.

## 4.4 Discussion

*Differences in root and shoot elongation in soil and vermiculite*

The effect of decreasing matric potential on root and shoot elongation was studied extensively Sharp and co-workers (Sharp et al., 1988; Spollen et al., 2000; Spollen and Sharp, 1991; Voetberg and Sharp, 1991; Wu et al., 1994; Wu et al., 1996; Wu and Cosgrove, 2000). In most of these studies plants were grown in vermiculite (to minimize effects of mechanical impedance), but vermiculite is very different in particle size and structure than soil. Root and shoot elongation rates of seedlings grown in soil and vermiculite at four matric potentials ranging from -0.03 MPa to -1.6 MPa were compared to investigate whether the growth medium affects plant growth at the same matric potentials.

Both roots and shoots grew slower in vermiculite than in soil. Root elongation slowed with decreasing matric potential which was found by several researchers (Evans and Etherington, 1991; Materechera et al., 1991; Mirreh and Ketcheso, 1973; Sharp et al., 1988; Taylor and Ratliff, 1969; Whalley et al., 1998; Wu et al., 1993). Elongation of roots grown in vermiculite slowed down the most when matric potential decreased from -0.03 MPa to -0.2 MPa, which agrees with the findings of Sharp et al. (1988). However, root elongation in soil decreased more steadily as a function of matric potential (Figure 4-2). This suggests that seedlings grown in vermiculite are more sensitive towards initial changes in matric potential than seedlings grown in soil. This might be caused by a smaller area of the root in contact with the particles and therefore with water filled pores and films around the particles. Shoot elongation of maize was also slower in vermiculite than in soil: the shoot elongation stopped after 24 h in vermiculite at -0.81 MPa, while in soil shoot growth continued growing for 48 h at matric potentials of -1.6 MPa.

This hypothesis that greater root–particle contact is associated with increasing root elongation rate was supported by the root–particle results determined from 3-D volumetric images. Greater root–particle contact and faster elongation rates were found in soil than in vermiculite. The section of the roots used to analyse root–particle contact were of different sizes, because some roots grew down the container wall. Those parts of the root were not included in the image analysis process and the lengths of root sections analysed differed between the plant species, matric potentials and growth materials. Lupin had greater root–particle contact than maize in both growth media, but because roots of lupin grew in the centre of the plastic container longer sections of lupin roots compared with sections of maize roots were used for root–particle analysis. Root

diameter measured 1 cm from the root tip of lupin was significantly thinner than those of maize at matric potentials drier than 0.2 MPa, but root–particle contact was greater.

It cannot be ruled out that chemical properties of the soil and vermiculite influenced root elongation (Findenegg, 1987; Tang et al., 1996). The pH of vermiculite was higher (7.7) than that of soil (5.2, Chapter 2). Higher pH might reduce growth (Tang et al., 1996; Tang et al., 1993; White, 1990). The increase in root diameter with increasing matric potential was greater in vermiculite than soil. Tang et al. (1993) showed that roots of lupin (*Lupinus angustifolius*) grown in an aerated nutrient solution of pH 7.5 were stunted and thicker than those of lupin grown at pH 5.2. However, maize and lupin elongation rates were similar in soil of pH 6.9 to those grown in soil of pH 5.2.

*Root and shoot growth in humid air*

To test the importance of root–particle contact further, a second experiment was conducted. Pre-germinated seeds were placed in jars with water potentials similar to matric potentials in soil and vermiculite. Root elongation rates were smaller than those found in soil and vermiculite suggesting the importance of root–soil contact for growth. However, the seedlings were placed several cm from the water surface, while vapour transport is more important at small distances of 1–2 mm (Owen, 1952; Wuest, 2002). Furthermore, a gradient in water potential with distance from the water surface to the seed might occur when roots take up or give up water, because of the great distance (Wuest, 2002), so that a uncertainty of the water potential around the root exists.

The weight change of seedlings indicated that not enough water was taken up by the seedling to explain the growth. Some seedlings lost weight suggesting that water was given up to the environment, but still root growth was recorded. The seedlings were germinated on moist paper towel before they were placed in humid air and probably stored water in the cotyledon which was used for growth. No shoot elongation occurred, indicating that all seedlings grown in air were experiencing water stress. Sharp et al., 1988 found no shoot growth of maize in very dry soil (-1.6 MPa), while roots were still elongating.

*Growth responses of maize and lupin towards decreasing matric potential*

Maize and lupin were used in both experiments to investigate if they are differently affected by changes in matric potential. Lupin was less sensitive than maize towards changes in matric potential. The seedlings used in this study were pre-germinated on moist paper towel, so that seedlings imbibed water. Volumes of lupin seeds increased more than those of maize seeds, so it might be that lupin seeds stored more water and used the water stored in the seedling for plant growth while maize was reacting earlier stage towards changes in water accessibility. Similar root elongation rates of lupin in air compared to those in soil and in vermiculite were found, while maize root elongation was significant slower in air than in vermiculite and soil.

Read and Gregory (1997) reported that mucilage in lupin roots was distributed along its flanks, while for maize roots mucilage and detached cells were found predominantly around the root tip. They suggested that mucilage plays a major role in the maintenance of root–soil contact in drying soils and therefore maintaining hydraulic conductivity.

Lupin might be less sensitive to decreases in matric potential because of a greater surface area covered in mucilage and therefore a better water supply. Greater water uptake rate per unit root length of lupin compared to cereals were suggested by Hamblin and Tennant (1987), which could have also contributed to a greater tolerance towards changes in matric potential.

*Prediction of root elongation rates from root diameter and distance between root tip and root hair zone*

Elongation rates of maize and lupin were strongly linearly correlated with the distance between root tip and root hair zone, while root diameter was poorly correlated with elongation rate. The gradient of the linear regression of elongation rate and distance between root tip and root hair zone were steeper for maize than for lupin, as well as steeper in soil than in vermiculite. This is probably due to slower root elongation of lupin and its greater resistance to soil physical stress. Pagès et al. (2009) and Watt et al. (2003) showed that root elongation and distance between root tip and root hair zone of maize and wheat are linearly correlated. Pagès et al. (2009) used sand and peat as the growth medium and reduced elongation rates by turning the sample holder transiently, whilst Watt et al. (2003) examined two different soil compaction treatments. Pagès et al. (2009) also investigated if the root diameter is correlated to root elongation rates, but found that elongation rate variability for a given root diameter was rather large. However, no information existed in the Pagès or Watt studies to show if these relationships apply under water stress or combinations of water stress and impedance.

For both maize and lupin, root elongation rates of seedlings grown in vermiculite were better linearly correlated with the root diameter than with root diameter of those grown in soil. This might be exacerbated because of greater pH effects in vermiculite: Tang et al. (1993) reported thicker cell diameters in lupin roots grown at a pH of 7.5, which might lead to a thicker root. Root elongation rate increases with increasing distance between root tip and root hair zone because of more rapidly elongating cells. Pagès et al. (2009) implied that the time required for a cell formed in the meristem to reach the next development stage (here producing root hairs) is constant. Watt et al. (2003) in contrast showed that root hairs of mechanically impeded roots develop faster than those of unimpeded roots. Nevertheless, this relationship could be useful to predict elongation rates in field sites, but in drying soils water stress is often combined with increasing mechanical impedance. Therefore it would be useful to test if this linear relation can be found in water stressed and mechanically impeded roots.

## 4.5 Summary

In this chapter the root and shoot elongation rates of maize and lupin in soil, vermiculite and air at four matric potentials ranging from -0.03 MPa to -1.6 MPa were presented and the root–particle contact of maize and lupin plants in loosely packed soil (<2 mm) and vermiculite was determined using X-ray microtomographs.

Root and shoot elongation decreased with decreasing matric potential, but the effects of matric potential was dependant on growth medium and plant species. Root and shoot elongation rates were found to be faster in soil compared with vermiculite and air.

Furthermore maize root and shoot elongation was more sensitive towards changes in matric potentials and growth medium than lupin.

Greater root–particle contact in soil compared with vermiculite was found. It was concluded that a greater root–particle contact in soil than in vermiculite offered better growth conditions.

Root elongation rates of both maize and lupin were linearly correlated to the distance between root tip and root hair zone. This parameter offers a quick way to determine root elongation rates of plants grown in field conditions.

# 5 Effects of root hairs and matric potential on root and shoot elongation of maize and barley grown in soil and vermiculite

## 5.1 Introduction

In drying soils root contact with the soil is essential for water and nutrient adsorption by plants. The contact between root and soil is influenced by soil and root properties, like particle size, degree of soil compaction, root diameter, root hairs and relative hydration (Nye, 1994; Tinker, 1976). Root hairs can increase the volume of soil in contact with the root and play an important role in acquisition of water and nutrients (Gilroy and Jones, 2000).

Root hairs are produced behind the zone of elongation as specialised projections from modified epidermal cells. Root hairs usually first appear as small protuberances near the apical end of an epidermal cell but, if the epidermal cell elongates further, the root hair can be found somewhat distant from the apical end of the cell. In nearly all dicots, some monocots, and all ferns, all epidermal cells seem to be capable of forming root hairs, but in some plants only certain of the root epidermal cells can form root hairs (trichoblasts), while other cells seem incapable of producing root hairs (atrichoblast) (Gregory, 2006). Root hair initiation and subsequent growth is genetically, hormonally and environmentally regulated. Following initiation, the tip of the root hair starts growing. In *Arabidopsis* root surface area was increased sevenfold, when plants were grown in P-deficient soil compared to P-sufficient soil with root hairs contributing 91 % of the total root surface area (Bates and Lynch, 1996). Root hairs vary in length and frequency along a root typically 0.1 mm to 1.5 mm long and 5 μm to 20 μm in diameter. Root hair numbers can differ from 2 per $mm^2$ for tree roots to 50–100 per $mm^2$ of root length in

some grasses. Root hairs are usually viable for only a few days, so that the root hair zone is relatively short (Gregory, 2006).

Mutations that alter root hair morphology are of great value for studying the role of root hairs in nutrient and water uptake. Gahoonia and Nielsen (2003) used a root hairless mutant of barley (bald root barley *brb*) and the wildtype (Pallas) to quantify the importance of root hairs for P uptake from soils. The wildtype took up twice as much as the hairless mutant. In low P-soil the hairless mutant did not survive, whereas the wildtype continued to grow. The wildtype depleted twice as much P from the rhizosphere as the hairless mutant. The P depletion profile was extended by 0.8 mm, which was similar to the root hair length. Phosphorus is highly immobile and insoluble in soils (Holford, 1997), so that good root–soil contact is important for its uptake. White and Kirkegaard (2010) observed more root hairs which were also longer when roots grew in large pores relatively to the root diameter and hence a greater root–soil contact. They assumed that water uptake was increased by a greater root–soil contact caused by root hairs, although the contribution in water uptake is uncertain, because it is unknown how root hairs can penetrate the soil pore walls.

Water uptake can also be assisted by root hairs (Hofer, 1991). Segal et al. (2008) investigated the water uptake of hairless barley mutants and the wildtype using magnetic resonance imaging (MRI). The wildtype took up more water than the hairless mutant. They hypothesized that this result was not due to the greater root surface area per se (because the soil water potential between root hairs quickly reaches values close to that

of the root) but rather the increase in root diameter was the reason, which was supported by characteristic water profiles.

Studies in Chapter 4 indicated that a greater root–particle contact in soil compared to vermiculite had a positive effect on root and shoot elongation rates when the matric potential was wetter than wilting point. To test if root hairs increase root and shoot elongation when water is limiting root growth, hairless maize and barley and the wildtypes were grown in both media at various matric potentials. It was hypothesized that roots and shoots of the wildtype will elongate faster because of increasing root–particle contact and a better supply with water. Furthermore it was hypothesized that root hairs would have a greater effect on root and shoot elongation in vermiculite because of its greater particle size and therefore less root–particle contact.

## *5.2 Materials and methods*

### 5.2.1 Root and shoot elongation of wildtype and hairless maize and barley mutants in soil and vermiculite at a range of matric potentials between -0.03 MPa and -1.6 MPa

Root and shoot elongation of hairless barley (*brb*) and maize (*rth3*) mutants and their wildtypes (barley: Pallas; maize: B73) in soil and vermiculite at four matric potentials (-0.03 MPa, -0.2 MPa, -0.81 MPa and-1.6 MPa) was investigated. Pre-germinated barley and maize seeds with 1 mm to 2 mm long radicles were placed into square petri dishes (23 × 23 × 2 cm) which were filled either with soil or vermiculite wetted to one of the four matric potential. Five seeds per petri dish were placed in darkness in an incubator at

either 12 °C for barley or 20 °C for maize for four days. Root and shoot lengths were measured each day with a ruler. Daily root and shoot growth rates and average elongations rates during 96 h of maize were calculated using Equations 4-1 and 4-2.

Root and shoot lengths of maize were measured every day and root and shoot elongation rates were determined. Additionally the growth rates of maize roots grown in soil and vermiculite were set in relation to growth rates on cotton wool (Equation 5-1).

$$E_{(\%)} = \frac{E_{gm}}{E_{\max}} \times 100 \qquad \textbf{Equation 5-1}$$

$E_{(\%)}$ = percentage of maximum elongation rate, $E_{gm}$ = elongation rate in soil or vermiculite, $E_{max}$ = maximum elongation rate (measured on moist cotton wool)

Barley seedlings developed between 2 and 9 seminal roots from germination to the end of the experiment. The length of each barley root was recorded daily. The rates of daily total root length increase per seedling were determined (Equation 5-2).

$$RITRL = \frac{\left(L_{1(n)} - L_{1(n-1)}\right) + \left(L_{2(n)} - L_{2(n-1)}\right) + \cdots + \left(L_{m(n)} - L_{m(n-1)}\right)}{n} \qquad \textbf{Equation 5-2}$$

RITRL = rate of increase in total root length [cm $d^{-1}$], L = root length, m = number of root, n = number of days after placing seeds into growth medium

The average elongation rates during 96 h presented for barley were calculated from the cumulative root length increase per seed (Equation 5-3).

$$RITRL = \frac{(L_{1(end)} - L_{1(start)}) + (L_{2(end)} - L_{2(start)}) + \cdots + (L_{m(end)} - L_{m(start)})}{t} \qquad \textbf{Equation 5-3}$$

RITRL = average rate of increase in total root length during 96 h [mm $h^{-1}$], L = root length [mm], t = time of growth period [h], m = max. root number per seed

The hairless maize mutant showed a slower germination rate than its wildtype, therefore it was tested whether the primary roots of the hairless maize mutant elongated slower than those of the wildtype (for example, due to a pleitropic effect of the mutation). Five pre-germinated seeds of the hairless mutant or the wildtype were placed in between moist cotton wool in a square petri dish (23 × 23 × 2 cm) and stored for four days in an incubator at 20 °C.

## *5.3 Results*

### 5.3.1 Root and shoot elongation of hairless maize mutants and wildtype in soil and vermiculite at a range of matric potentials

*Root elongation of maize*

The root and shoot lengths of maize are shown in Figure 5-1. Roots of the wildtype elongated approximately 10 to 20 % faster than the hairless mutant. The difference in root length between wildtype and hairless mutant increased with time. Root ($p < 0.001$) and shoot length ($p = 0.009$) of the hairless mutant were significantly shorter than for the wildtype, although the rate of shoot elongation was similar for both ($p = 0.304$).

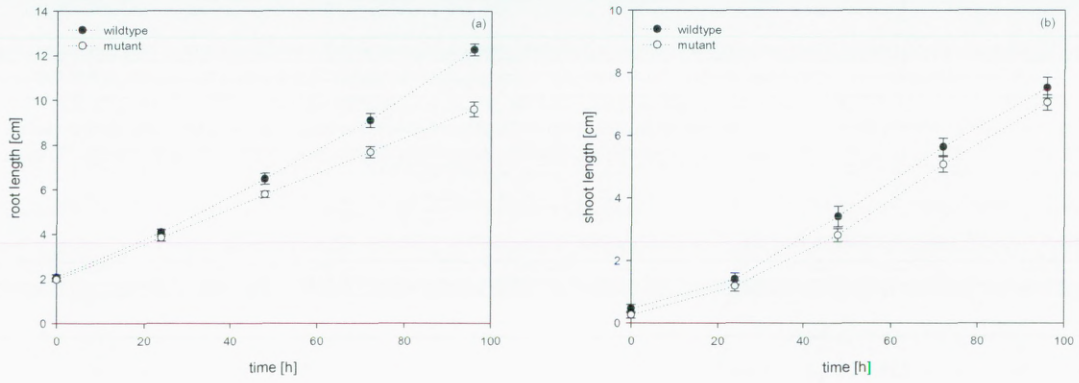


**Figure 5-1: Root length of primary root (a) and shoot length (b) of wildtype and hairless maize mutant on moist cotton wool during 96 h of growth. Data are means ±SE (n = 5).**

The average root elongation rate during a growth period of 96 h was significantly greater for the wildtype than for the hairless mutant ($p < 0.001$; Figure 5-2).

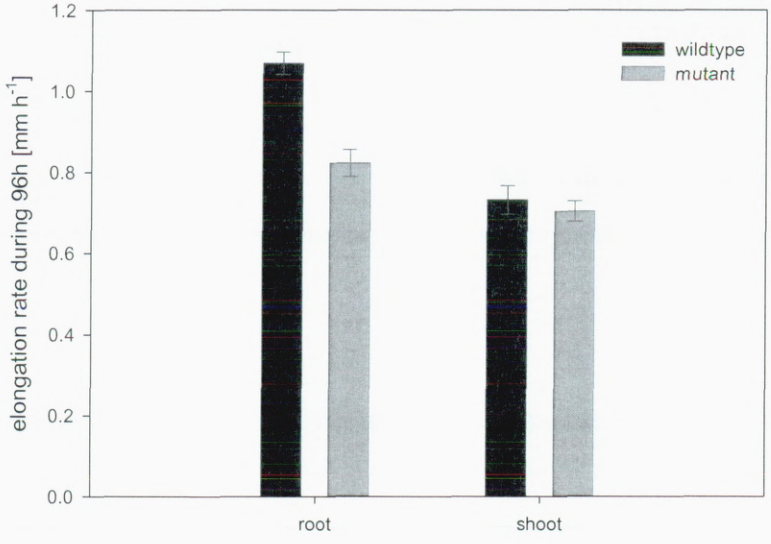


**Figure 5-2: Average root and shoot elongation rates of maize wildtype and the hairless mutant during 96 h of growth on moist cotton wool at 20 °C. Mean values ±SE (n =5).**

Figure 5-3 shows root lengths of wildtype and the hairless maize mutant grown in soil and vermiculite. Roots of the wildtype were longer than those of the hairless mutant with greater differences in soil than in vermiculite. Root length decreased with decreasing matric potential. The hairless mutant had similar root lengths at -0.03 MPa and -0.2 MPa, although, in vermiculite roots of maize wildtype were longer at -0.2 MPa than at -0.03 MPa.

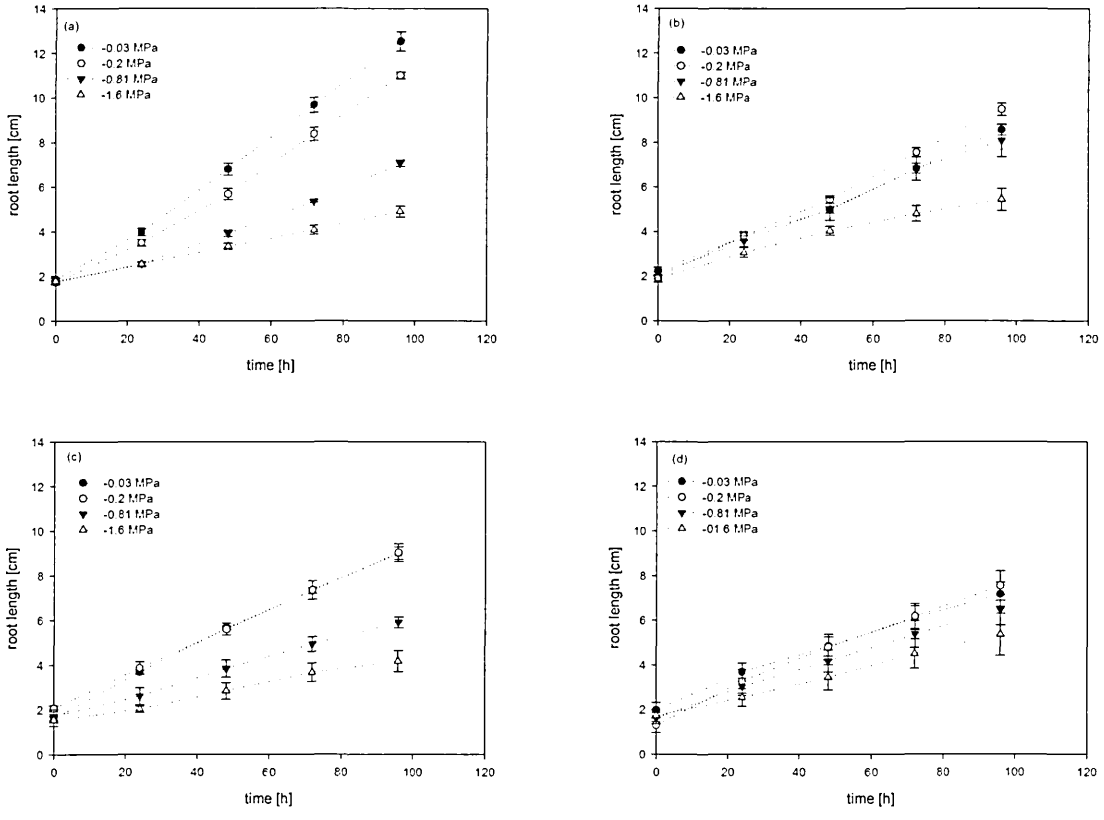


**Figure 5-3: Root length of maize wildtype (a, b) and the hairless maize mutant (c, d) as a function of time in soil (a, c) and vermiculite (b, d) at matric potentials of -0.03 MPa, -0.2 MPa, -0.81 MPa and -1.6 MPa. Data are means ±SE (n = 5).**

The rate of root elongation of the wildtype grown in soil increased in time at matric potentials wetter than -1.6 MPa (Table 5-1). Root elongation rate was significantly influenced by time ($p < 0.001$). Root elongation rate in vermiculite did not change with time when matric potential was wetter then -1.6 MPa. At -1.6 MPa root elongation rate decreased at -1.6 MPa by 45 % from day one to day four. Root elongation rate remained relatively constant with time ($p = 0.123$; Table 5-1).

**Table 5-1: Root elongation rates per day of maize wildtype in soil and vermiculite [cm $d^{-1}$] at matric potentials of -0.03 MPa, -0.2 MPa, -0.81 MPa and -1.6 MPa. Mean values ±SE are presented (n = 5).**

| | Root elongation rate of maize wildtype in soil [cm $d^{-1}$] | | | | | | | |
|---|---|---|---|---|---|---|---|---|
| Time [h] | -0.03 MPa | | -0.2 MPa | | -0.81 MPa | | -1.6 MPa | |
| 0–24 | 2.12 | ±0.092 | 1.78 | ±0.15 | 0.80 | ±0.063 | 0.78 | ±0.12 |
| 24–48 | 2.82 | ±0.14 | 2.18 | ±0.15 | 1.38 | ±0.073 | 0.78 | ±0.11 |
| 48–72 | 2.88 | ±0.12 | 2.7 | ±0.076 | 1.44 | ±0.12 | 0.74 | ±0.13 |
| 72–96 | 2.84 | ±0.21 | 2.62 | ±0.29 | 1.7 | ±0.14 | 0.82 | ±0.073 |
| | Root elongation rate of maize wildtype in vermiculite [cm $d^{-1}$] | | | | | | | |
| Time [h] | -0.03 MPa | | -0.2 MPa | | -0.81 MPa | | -1.6 MPa | |
| 0–24 | 1.54 | ±0.08 | 1.84 | ±0.09 | 1.44 | ±0.18 | 1.16 | ±0.16 |
| 24–48 | 1.2 | ±0.06 | 1.64 | ±0.10 | 1.46 | ±0.29 | 0.98 | ±0.21 |
| 48–72 | 1.84 | ±0.08 | 2.1 | ±0.09 | 1.8 | ±0.37 | 0.76 | ±0.23 |
| 72–96 | 1.74 | ±0.07 | 1.94 | ±0.10 | 1.26 | ±0.25 | 0.64 | ±0.23 |

Root elongation rate of the hairless maize mutant in soil at -0.03 MPa decreased from day one to day four (Table 5-2). Fastest root elongation rates of hairless maize were determined at -0.03 MPa after 24 h. In vermiculite root elongation rates of the hairless mutant decreased significantly with time when the vermiculite was wetter than -1.6 MPa ($p = 0.015$).

**Table 5-2: Root elongation rates per day of hairless maize in soil and vermiculite [cm $d^{-1}$] at matric potentials of -0.03 MPa, -0.2 MPa, -0.81 MPa and -1.6 MPa. Mean values ±SE are presented (n = 5).**

| | Root elongation rate of hairless maize mutant in soil [cm $d^{-1}$] | | | | | | | |
|---|---|---|---|---|---|---|---|---|
| Time [h] | -0.03 MPa | | -0.2 MPa | | -0.81 MPa | | -1.6 MPa | |
| 0–24 | 2.06 | ±0.08 | 1.80 | ±0.26 | 0.88 | ±0.09 | 0.48 | ±0.18 |
| 24–48 | 1.98 | ±0.08 | 1.74 | ±0.30 | 1.24 | ±0.02 | 0.82 | ±0.27 |
| 48–72 | 1.68 | ±0.12 | 1.76 | ±0.13 | 1.1 | ±0.13 | 0.84 | ±0.05 |
| 72–96 | 1.68 | ±0.17 | 1.68 | ±0.12 | 0.98 | ±0.13 | 0.5 | ±0.08 |
| | Root elongation rate of hairless maize mutant in vermiculite [cm $d^{-1}$] | | | | | | | |
| Time [h] | -0.03 MPa | | -0.2 MPa | | -0.81 MPa | | -1.6 MPa | |
| 0–24 | 1.70 | ±0.09 | 1.97 | ±0.21 | 1.23 | ±0.17 | 0.82 | ±0.16 |
| 24–48 | 1.15 | ±0.03 | 1.53 | ±0.05 | 1.15 | ±0.12 | 0.90 | ±0.18 |
| 48–72 | 1.28 | ±0.15 | 1.37 | ±0.11 | 1.20 | ±0.27 | 1.06 | ±0.29 |
| 72–96 | 1.05 | ±0.06 | 1.37 | ±0.11 | 1.08 | ±0.11 | 0.70 | ±0.21 |

Figure 5-4 shows the average root elongation rates of the wildtype and hairless mutant over 96 h. Root elongation rate was fastest for the wildtype grown at -0.03 MPa and was greater for the wildtype than the mutant at all matric potentials wetter than -1.6 MPa. Large differences in root elongation rates of wildtype and hairless mutant were found in soil wetter than -0.81 MPa.

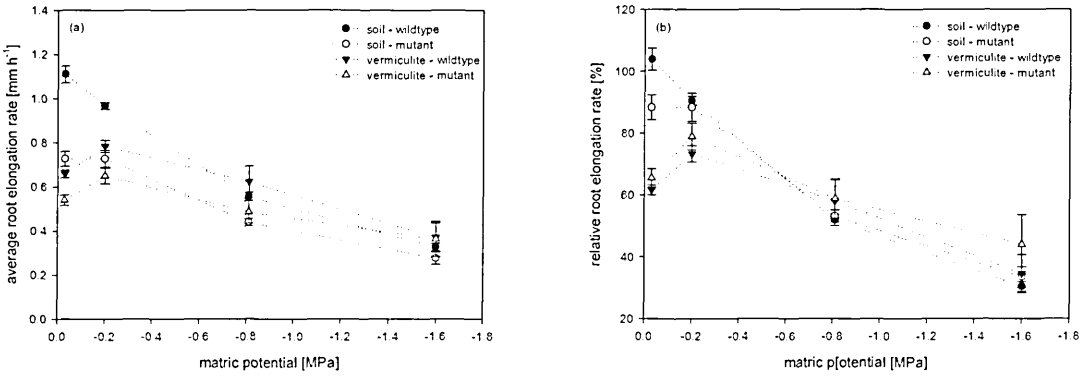


**Figure 5-4: Average root elongation rate of maize wildtype and hairless mutant (b) during 96 h in soil and vermiculite at a matric potential of -0.03 MPa, -0.2 MPa, -0.81 MPa and -1.6 MPa and root elongation rates in relation to maximum root elongation rates of roots grown on well moistened cotton wool (b). Mean values ±SE are presented (n = 5).**

Root elongation rates of hairless maize mutant and wildtype ($p < 0.001$) differed significantly and matric potential and growth medium had a significant effect ($p < 0.001$). Root elongation rate was faster in soil than vermiculite when soil was wetter than -0.81 MPa. Root elongation rates of the wildtype were faster than for the hairless mutant in both media. Because root growth of the hairless mutant showed a possible pleiotropic effect, average root elongation rates were expressed relative to those grown on moist cotton wool (Figure 5-4). There were no differences between the wildtype and the hairless mutant in relative root elongation rates ($p = 0.504$). Root elongation rates were slower in vermiculite at -0.03 MPa than at -0.2 MPa. This was possibly caused by the pH of the vermiculite (as discussed in Chapter 2).

*Shoot elongation of maize*

Shoot lengths are shown in Figure 5-5. Shoot lengths of wildtype and hairless mutants were shorter as matric potential decreased. Shoots of the wildtype grown in soil at -0.03 MPa were shorter than in vermiculite, but when the soil was drier than -0.03 MPa shoot lengths of plants grown in soil and vermiculite were similar. Shoot length increased with time at matric potentials wetter than -0.81 MPa, but at drier potentials there were no growth in either soil or vermiculite.

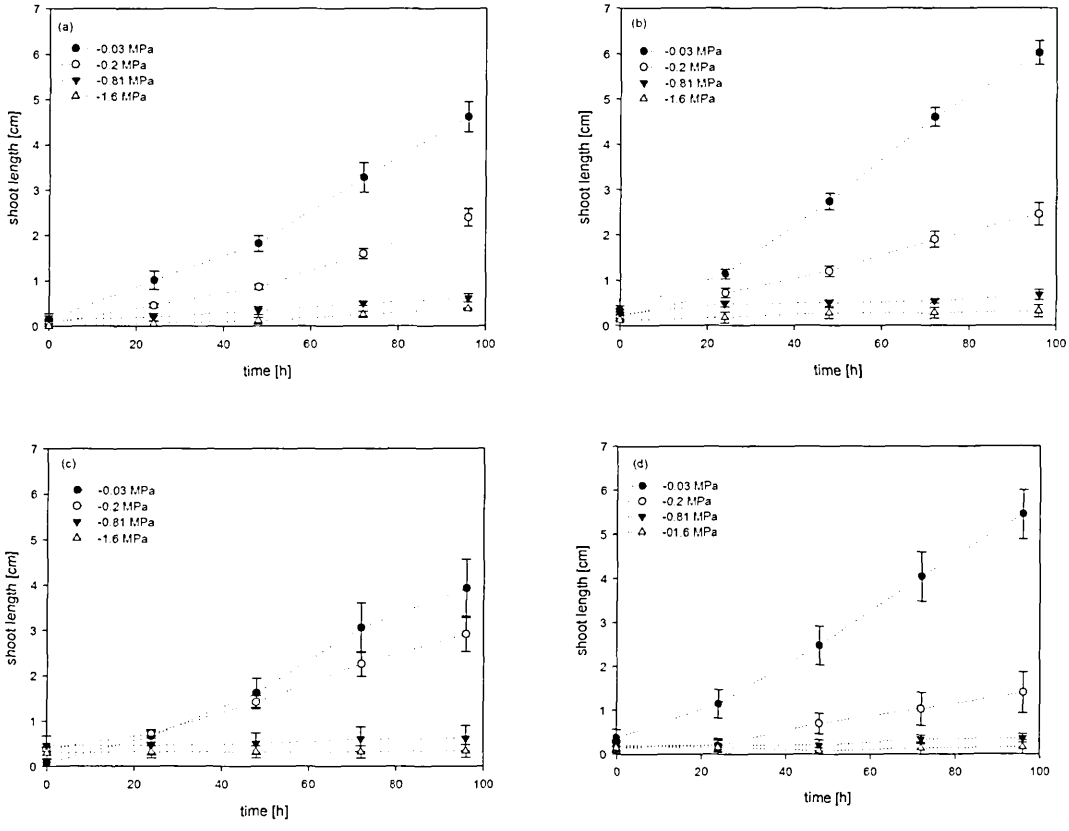


**Figure 5-5: Shoot length of maize wildtype (a, b) and hairless maize mutant (c, d) as a function of time in soil (a, c) and vermiculite (b, d) at matric potentials of -0.03 MPa, -0.2 MPa, -0.81 MPa and -1.6 MPa. Data are means ±SE (n = 5).**

Shoot elongation rate of the wildtype in soil at -0.03 MPa was greatest on day three (Table 5-3). Shoot elongation rates of plants grown in the wettest vermiculite were faster than in soil, but at drier potentials it was similar to those in soil.

**Table 5-3: Shoot elongation rates per day of maize wildtype in soil and vermiculite [cm $d^{-1}$] at matric potentials of -0.03 MPa, -0.2 MPa, -0.81 MPa and -1.6 MPa. Mean values ±SE are presented (n = 5).**

| | Shoot elongation rate of maize wildtype in soil [cm $d^{-1}$] | | | | | | | |
|---|---|---|---|---|---|---|---|---|
| Time [h] | -0.03 MPa | | -0.2 MPa | | -0.81 MPa | | -1.6 MPa | |
| 0–24 | 0.88 | ±0.15 | 0.40 | ±0.097 | 0.06 | ±0.06 | 0.06 | ±0.060 |
| 24–48 | 0.80 | ±0.095 | 0.40 | ±0.043 | 0.14 | ±0.068 | 0.06 | ±0.060 |
| 48–72 | 1.46 | ±0.25 | 0.74 | ±0.037 | 0.16 | ±0.068 | 0.14 | ±0.068 |
| 72–96 | 1.34 | ±0.11 | 0.80 | ±0.077 | 0.12 | ±0.049 | 0.120 | ±0.049 |
| | Shoot elongation rate of maize wildtype in vermiculite [cm $d^{-1}$] | | | | | | | |
| Time [h] | -0.03 MPa | | -0.2 MPa | | -0.81 MPa | | -1.6 MPa | |
| 0–24 | 0.80 | ±0.071 | 0.52 | ±0.097 | 0.22 | ±0.058 | 0.06 | ±0.06 |
| 24–48 | 1.60 | ±0.077 | 0.48 | ±0.13 | 0.02 | ±0.029 | 0.10 | ±0.077 |
| 48–72 | 1.86 | ±0.093 | 0.70 | ±0.16 | 0.04 | ±0.025 | 0.00 | ±0.00 |
| 72–96 | 1.42 | ±0.097 | 0.56 | ±0.076 | 0.14 | ±0.067 | 0.04 | ±0.04 |

The rate of shoot elongation decreased with decreasing matric potentials and was significantly affected by time ($p < 0.001$) and matric potential ($p < 0.001$), but not by the growth medium ($p = 0.509$). Daily root elongation rates were significantly different for the wildtype compared to the hairless mutant ($p < 0.001$) in vermiculite, but not in soil ($p = 0.179$; Table 5-4).

**Table 5-4: Shoot elongation rates per day of the hairless maize mutant in soil and vermiculite [cm $d^{-1}$] at matric potentials of -0.03 MPa, -0.2 MPa, -0.81 MPa and -1.6 MPa. Mean values ±SE are presented (n = 5).**

| | Shoot elongation rate of hairless maize in soil [cm $d^{-1}$] | | | | | | | |
|---|---|---|---|---|---|---|---|---|
| Time [h] | -0.03 MPa | | -0.2 MPa | | -0.81 MPa | | -1.6 MPa | |
| 0–24 | 0.58 | ±0.06 | 0.34 | ±0.08 | 0.00 | ±0.00 | 0.02 | ±0.02 |
| 24–48 | 0.96 | ±0.20 | 0.70 | ±0.06 | 0.04 | ±0.02 | 0.00 | ±0.00 |
| 48–72 | 1.44 | ±0.31 | 0.84 | ±0.14 | 0.10 | ±0.04 | 0.00 | ±0.00 |
| 72–96 | 1.15 | ±0.15 | 0.66 | ±0.14 | 0.02 | ±0.02 | 0.02 | ±0.02 |
| | Shoot elongation rate of hairless maize in vermiculite [cm $d^{-1}$] | | | | | | | |
| Time [h] | -0.03 MPa | | -0.2 MPa | | -0.81 MPa | | -1.6 MPa | |
| 0–24 | 0.78 | ±0.14 | 0.03 | ±0.03 | 0.00 | ±0.00 | 0.02 | ±0.02 |
| 24–48 | 1.33 | ±0.14 | 0.50 | ±0.08 | 0.00 | ±0.00 | 0.03 | ±0.03 |
| 48–72 | 1.58 | ±0.17 | 0.33 | ±0.14 | 0.14 | ±0.09 | 0.07 | ±0.07 |
| 72–96 | 1.40 | ±0.08 | 0.37 | ±0.09 | 0.02 | ±0.02 | 0.02 | ±0.02 |

The hairless mutant and wildtype (Table 5-4) had similar shoot elongation rates in soil and vermiculite at -0.03 MPa and there was negligible elongation in both media of -0.81 MPa and -1.6 MPa. In soil, shoot elongation rate of the hairless mutant was slower than that of the wildtype when soil was drier than -0.2 MPa.

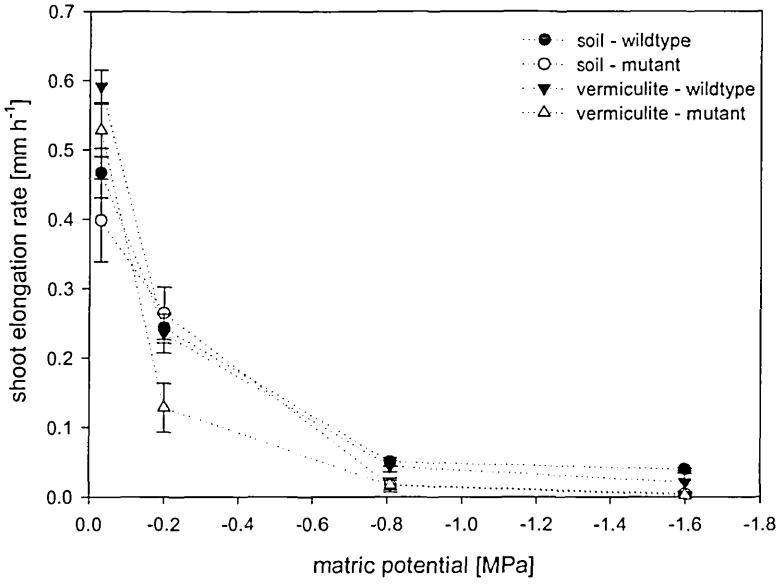


**Figure 5-6: Average shoot elongation rate of maize wildtype and hairless mutant during 96 h in soil and vermiculite at a matric potential of -0.03 MPa, -0.2 MPa, -0.81 MPa and -1.6 MPa. Mean values ±SE are presented (n = 5).**

Shoots of the wildtype were elongating significantly faster than those of the hairless mutants ($p = 0.002$), but no significantly differences of plants grown in soil or vermiculite were found ($p = 0.405$).

### 5.3.2 Root and shoot elongation of hairless barley mutants and wildtype in soil and vermiculite at a range of matric potentials

*Barley root elongation*

The number of seminal roots of barley seedlings increased significantly with time ($p < 0.001$; Figure 5-7) and seedlings had more roots the wetter the growth medium was ($p < 0.001$). The wildtype grew significantly more seminal roots in soil at -0.81 MPa

($p < 0.001$) and -1.6 MPa ($p < 0.001$) and in vermiculite at -0.81 MPa ($p < 0.001$) than the hairless mutant. In vermiculite at -0.03 MPa both the wildtype and the hairless mutant had more roots than in soil, but when the growth medium was drier significantly more roots were produced in soil ($p < 0.001$).

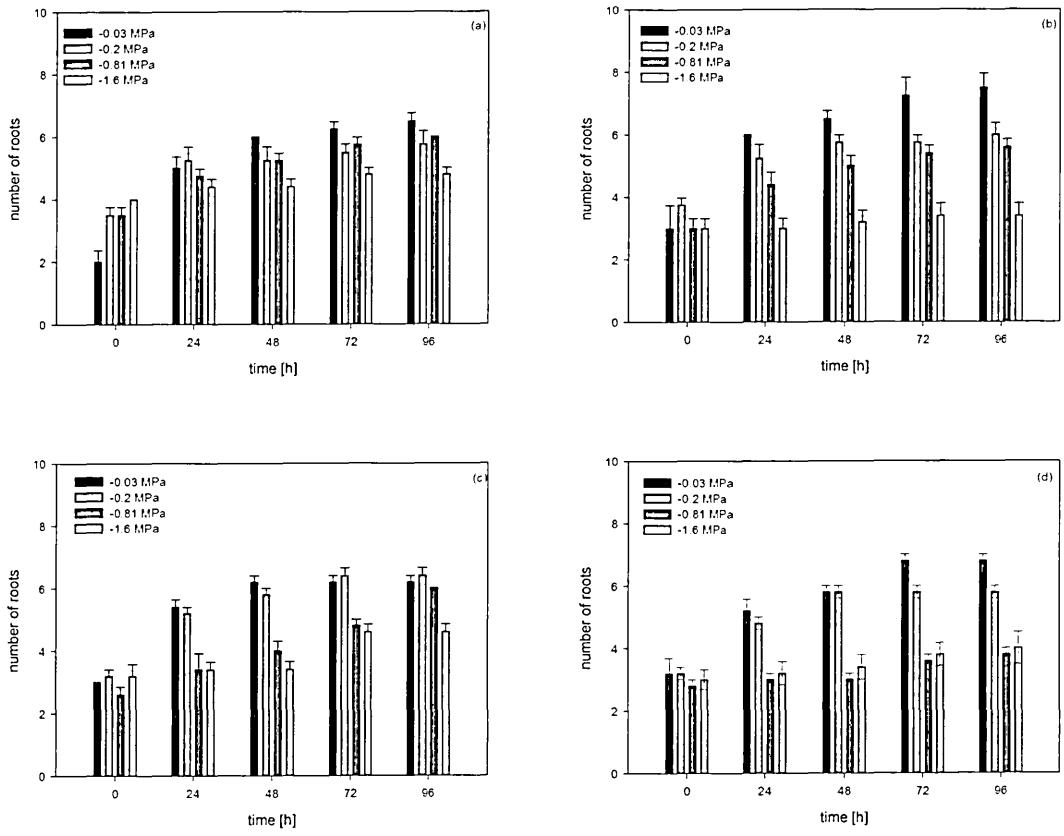


**Figure 5-7: Emergence of roots of barley wildtype (a, b) and hairless mutant (c, d) with time in soil (a, c) and vermiculite (b, d) at matric potentials of -0.03 MPa, -0.2 MPa, -0.81 MPa and -1.6 MPa. Data are means ±SE (n = 5).**

Roots which appeared first were significantly longer than roots which developed later ($p < 0.001$; Figure 5-8, Figure 5-9). The emergence of seminal roots was slowed in drier

growth media ($p < 0.001$) – but more so in vermiculite than in soil and for the hairless mutant ($p < 0.001$).

Roots of the hairless mutant grown in soil at -0.03 MPa ($p = 0.019$) were significantly longer than those of the wildtype, but at potentials drier than -0.2 MPa roots of the wildtype were longer than those of the hairless mutant ($p < 0.001$) (Figure 5-8). All seminal roots grew after 48 h at a constant rate.

Root elongation rates of wildtype and hairless mutant in vermiculite decreased in time when they were grown at potentials wetter than -0.81 MPa. Roots of the wildtype were significantly longer than those of the hairless mutant at -0.03 MPa ($p < 0.001$) -0.81 MPa ($p < 0.001$). No significant differences in root length between both wildtype and hairless mutant at -0.2 MPa were found ($p = 0.47$) while roots of the hairless mutants were longer than those of the wildtype at -1.6 MPa ($p = 0.045$).

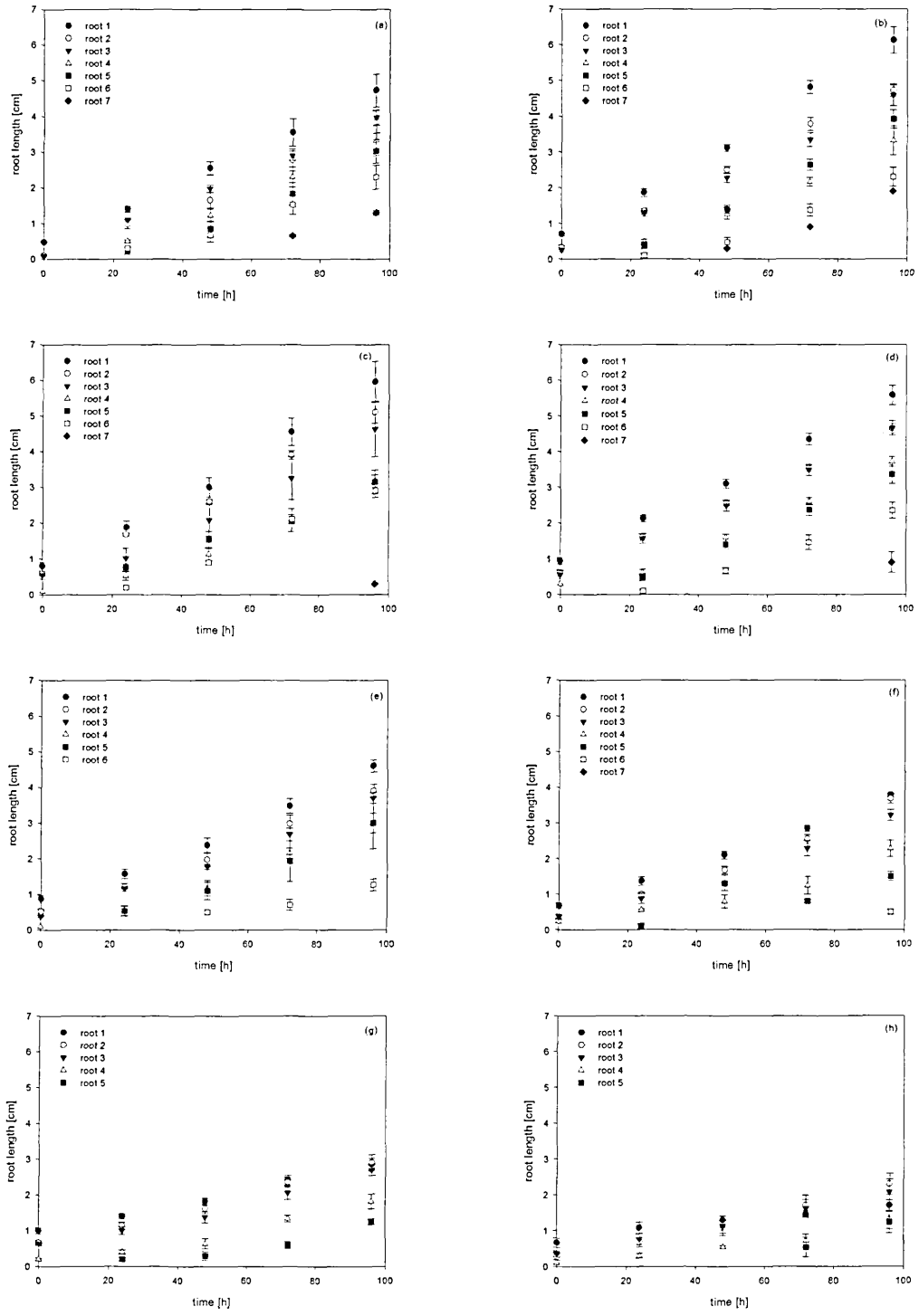


**Figure 5-8: Root length of each seminal barley root of wildtype (a, c, e, g) and hairless mutant (b, d, f, h) as a function of time in soil at matric potentials of -0.03 MPa, -0.2 MPa, -0.81 MPa and -1.6 MPa. Data are means ±SE (n = 5).**

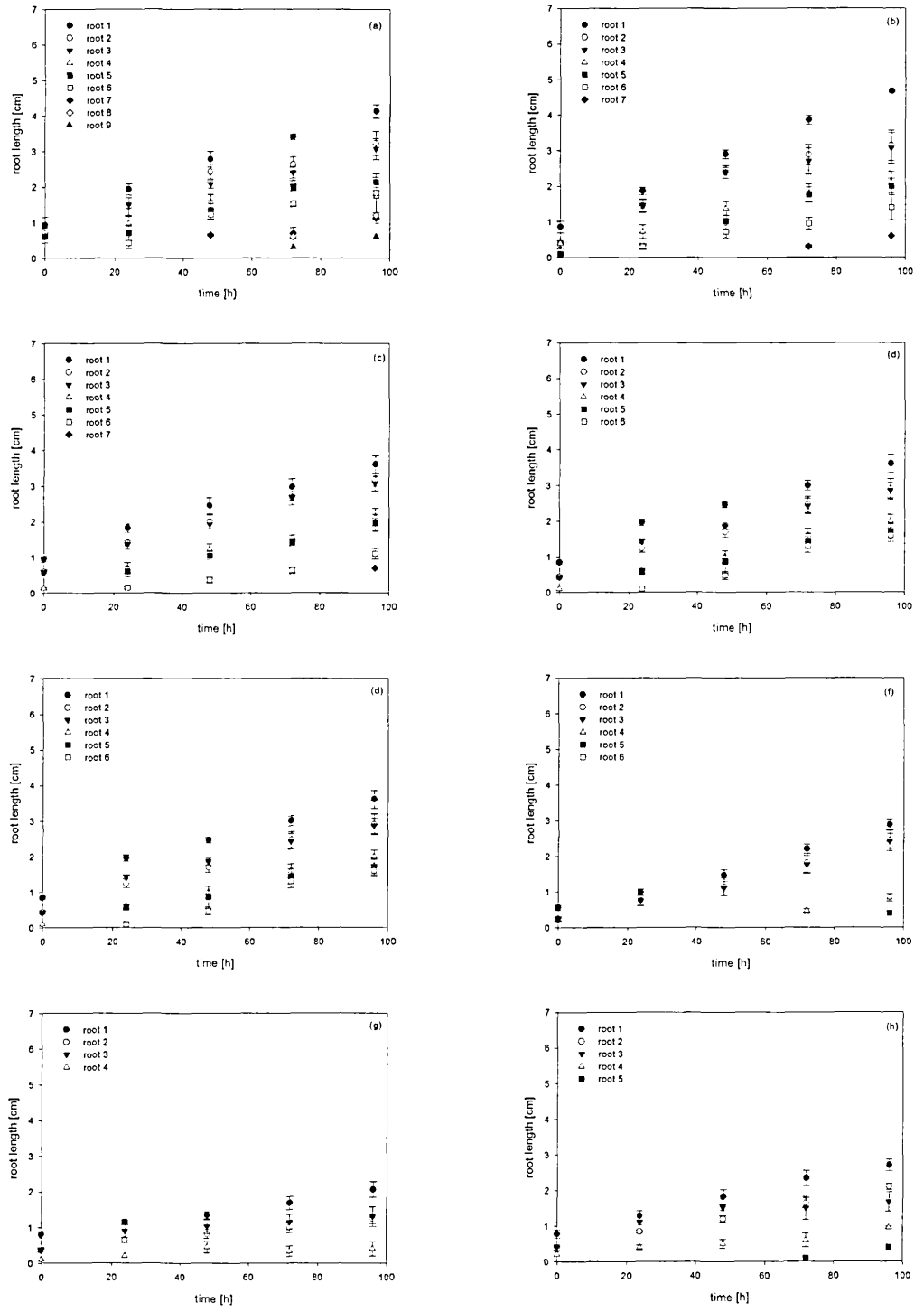


**Figure 5-9: Root length of each seminal barley root of wildtype (a, c, e, g) and hairless mutant (b, d, f, h) as a function of time in vermiculite at matric potentials of -0.03 MPa, -0.2 MPa, -0.81 MPa and -1.6 MPa. Data are means ±SE (n = 5).**

Figure 5-10 shows total root length barley wildtype and hairless mutant in soil and vermiculite. Total root lengths of the hairless barley mutant were significant shorter when soil was drier than -0.2 MPa ($p < 0.001$). Roots of both plant types were shorter in vermiculite than in soil ($p < 0.001$).

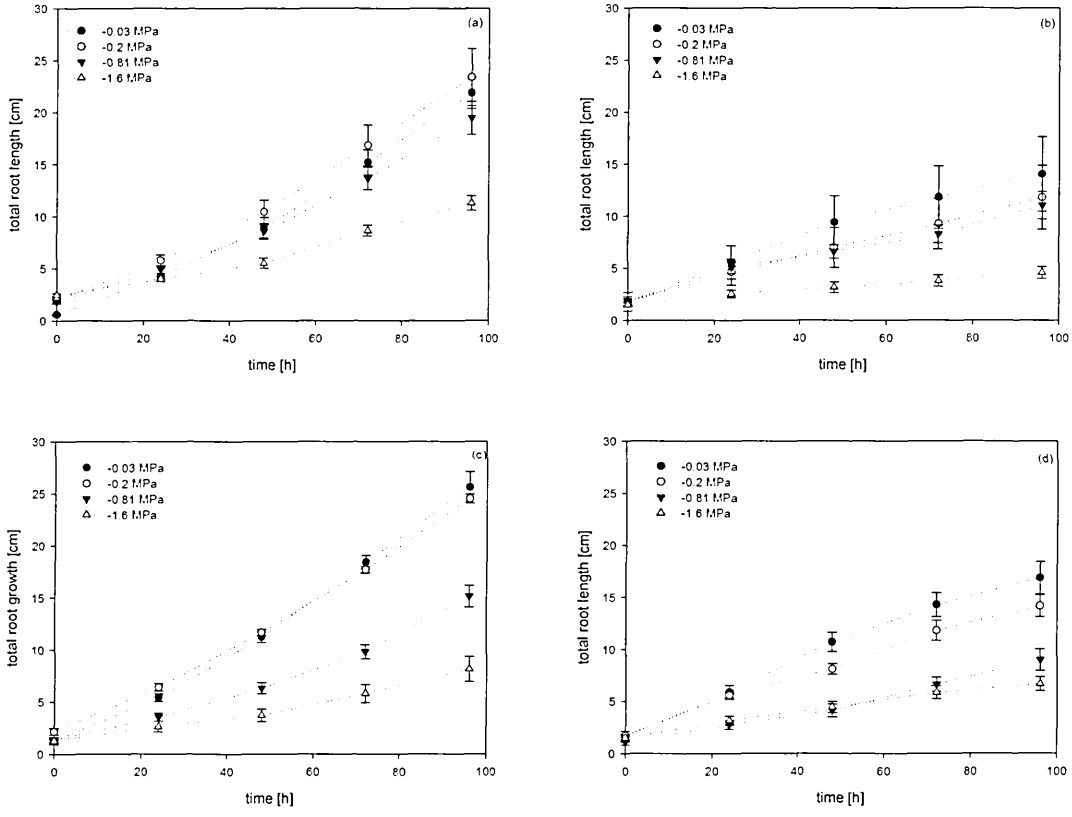


**Figure 5-10: Root length barley wildtype (a, b) and the hairless maize mutant (*brb*) (c, d) as a function of time in soil (a, c) and vermiculite (b, d) at matric potentials of -0.03 MPa, -0.2 MPa, -0.81 MPa and -1.6 MPa. Mean values ±SE are presented (n = 5).**

The rate of increase in total root length of the barley wildtype increased in time at all matric potentials, while in vermiculite the rate generally decreased (Table 5-5) especially

at -0.03 MPa. The greatest rates of increase in total root length were found in the wettest soil at -0.03 MPa.

**Table 5-5: Rate of increase in total root length per day of the barley wildtype in soil and vermiculite [cm $d^{-1}$] at matric potentials of -0.03 MPa, -0.2 MPa, -0.81 MPa and -1.6 MPa. Mean values ±SE are presented (n = 5).**

| | Rate of increase in total root length of barley wildtype in soil [cm $d^{-1}$] | | | | | | | |
|---|---|---|---|---|---|---|---|---|
| Time [h] | -0.03 MPa | | -0.2 MPa | | -0.81 MPa | | -1.6 MPa | |
| 0–24 | 3.65 | ±0.26 | 3.80 | ±0.42 | 3.08 | ±0.21 | 1.52 | ±0.23 |
| 24–48 | 4.70 | ±0.69 | 4.68 | ±0.63 | 3.63 | ±0.19 | 1.54 | ±0.26 |
| 48–72 | 6.13 | ±0.31 | 6.38 | ±0.85 | 5.13 | ±0.21 | 3.14 | ±0.14 |
| 72–96 | 6.45 | ±0.66 | 6.55 | ±0.86 | 5.80 | ±0.31 | 2.62 | ±0.23 |
| | Rate of increase in total root length of barley wildtype in vermiculite [cm $d^{-1}$] | | | | | | | |
| Time [h] | -0.03 MPa | | -0.2 MPa | | -0.81 MPa | | -1.6 MPa | |
| 0–24 | 4.75 | ±0.06 | 3.58 | ±0.40 | 3.22 | ±0.14 | 1.06 | ±0.37 |
| 24–48 | 4.78 | ±0.49 | 2.93 | ±0.38 | 1.72 | ±0.27 | 0.62 | ±0.23 |
| 48–72 | 2.95 | ±0.77 | 2.88 | ±0.10 | 2.14 | ±0.30 | 0.64 | ±0.24 |
| 72–96 | 2.7 | ±0.66 | 3.18 | ±0.19 | 2.86 | ±0.47 | 0.78 | ±0.12 |

Rate of increase in total root length of the hairless mutant grown in soil increased with time at all matric potentials (Table 5-6). The greatest rate was determined at -0.03 MPa and lowest at -1.6 MPa as with the wildtype the rate of root growth of the hairless mutant decreased with time in vermiculite.

Rate of increase in total root length per day of wildtype and hairless mutant were significantly influenced by growth medium ($p < 0.001$), matric potential ($p < 0.001$) and time ($p = 0.009$), and also the presence of root hairs ($p = 0.025$).

**Table 5-6: Rate of increase in total root length per day of the hairless barley mutant (*brb*) in soil and vermiculite [cm $d^{-1}$] at matric potentials of -0.03 MPa, -0.2 MPa, -0.81 MPa and -1.6 MPa. Mean values ±SE are presented (n = 5).**

| | Rate of increase in total root length of hairless barley in soil [cm $d^{-1}$] | | | | | | | |
|---|---|---|---|---|---|---|---|---|
| Time [h] | -0.03 MPa | | -0.2 MPa | | -0.81 MPa | | -1.6 MPa | |
| 0–24 | 3.98 | ±0.30 | 4.24 | ±0.28 | 2.12 | ±0.21 | 1.38 | ±0.19 |
| 24–48 | 5.70 | ±0.19 | 5.28 | ±0.20 | 2.72 | ±0.28 | 1.08 | ±0.13 |
| 48–72 | 7.08 | ±0.19 | 6.00 | ±0.25 | 3.54 | ±0.19 | 2.10 | ±0.40 |
| 72–96 | 6.45 | ±1.00 | 6.82 | ±0.38 | 5.28 | ±0.16 | 2.32 | ±0.42 |
| | Rate of increase in total root length of maize wildtype in vermiculite [cm $d^{-1}$] | | | | | | | |
| Time [h] | -0.03 MPa | | -0.2 MPa | | -0.81 MPa | | -1.6 MPa | |
| 0–24 | 4.18 | ±0.25 | 3.88 | ±0.16 | 1.50 | ±0.20 | 1.66 | ±0.19 |
| 24–48 | 5.53 | ±1.04 | 2.48 | ±0.36 | 1.22 | ±0.30 | 1.28 | ±0.17 |
| 48–72 | 3.95 | ±0.84 | 3.72 | ±0.76 | 2.32 | ±0.20 | 1.40 | ±0.20 |
| 72–96 | 2.63 | ±0.59 | 2.38 | ±0.36 | 2.20 | ±0.18 | 1.02 | ±0.53 |

Figure 5-13 shows the root elongation rates calculated from total root length increase during 96 h of barley wildtype and hairless mutant. Growth medium ($p < 0.001$) and matric potential ($p < 0.001$) influenced the rate of root length increase significantly with roots of the wildtype elongating faster in soil than in vermiculite at a matric potential of -0.81 MPa. Few differences were found in wetter soil between the two plant types. The hairless mutant showed the opposite response to matric potential and growth medium, growing faster in vermiculite at -1.6 MPa ($p = 0.014$). Overall, rates of root length increase were greater in soil than in vermiculite.

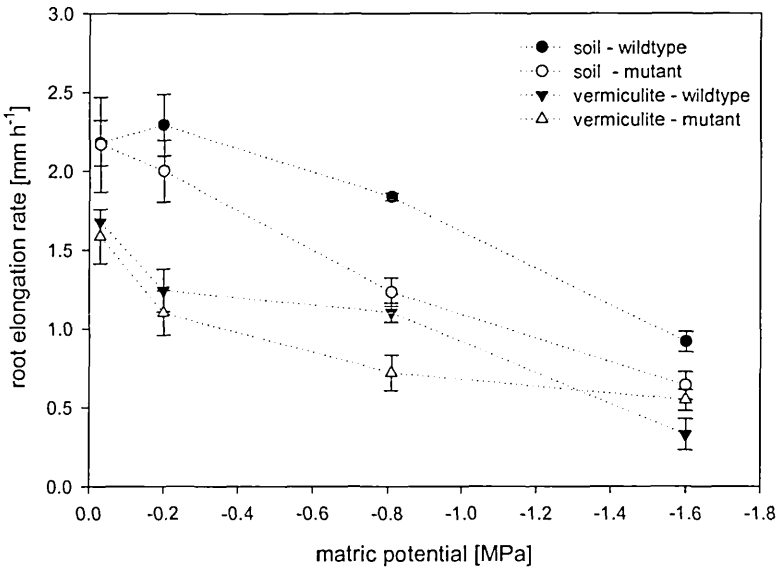


**Figure 5-11: Average rate of root length increase of barley wildtype and hairless mutant (*brb*) during 96 h in soil and vermiculite at a matric potential of -0.03 MPa, -0.2 MPa, -0.81 MPa and -1.6 MPa. Root elongation rates are calculated from total root length increase during 96 h. Mean values ±SE are presented (n = 5).**

*Shoot elongation of barley*

Shoot lengths of barley wildtype and hairless mutant are shown in Figure 5-12. There was no shoot growth at -0.81 MPa or -1.6 MPa during the first 48 h for both barley wildtype and hairless mutant. Shoot length was greater in soil than in vermiculite. The rate of shoot growth was greatest of the wildtype in soil at -0.2 MPa, while in vermiculite, the longest shoots were found at -0.03 MPa. Shoots of the hairless barley mutant were longer in soil than in vermiculite. There were no differences in shoot length in soil at -0.03 MPa and -0.2 MPa ($p = 0.645$), while in vermiculite at -0.03 MPa shoot length was significant longer than at -0.2 MPa ($p < 0.001$).

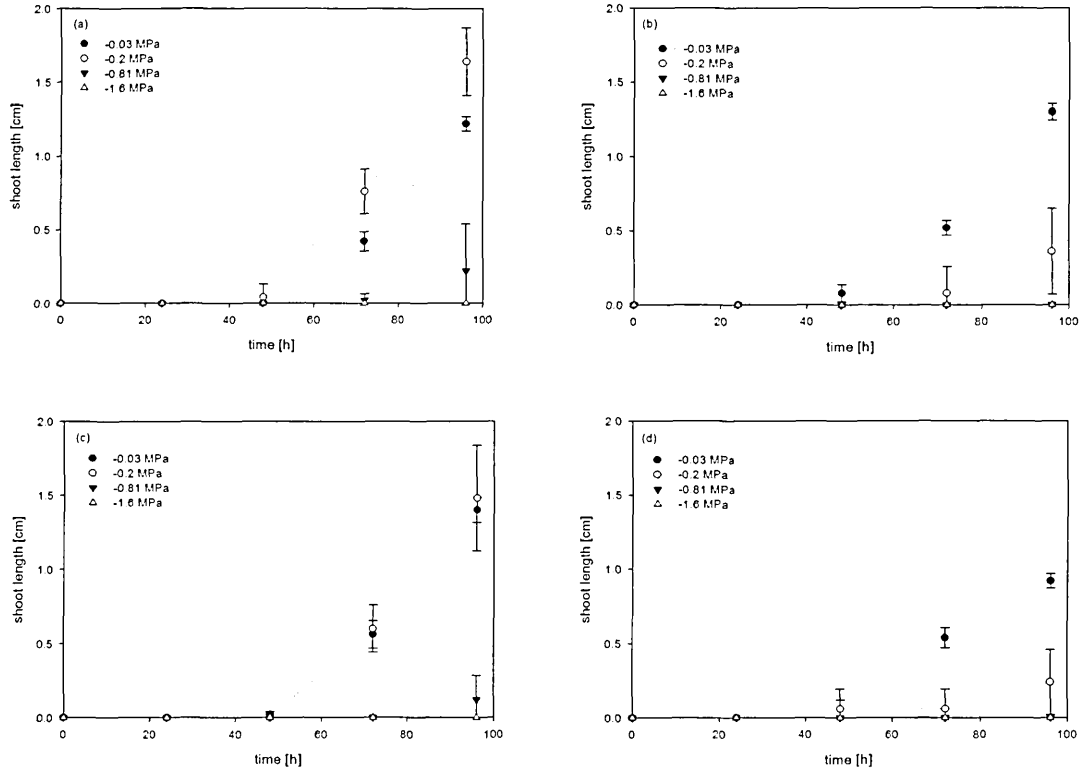


**Figure 5-12: Shoot length of barley wildtype (a, b) and hairless mutant (brb) (c, d) as a function of time in soil (a, c) and vermiculite (b, d) at a matric potential of -0.03 MPa, -0.2 MPa, -0.81 MPa and -1.6 MPa. Root elongation rates are calculated from total root length increase during 96 h. Mean values ±SE are presented (n = 5).**

Shoot elongation increased significantly after 48 h in soil for both wildtype and hairless mutant when matric potentials were higher than -0.81 MPa ($P < 0.001$; Table 5-7). There was no shoot elongation in vermiculite drier than -0.2 MPa and in soil drier than -0.81.

**Table 5-7: Shoot elongation rates per day of the barley wildtype in soil and vermiculite [cm $d^{-1}$] at matric potentials of -0.03 MPa, -0.2 MPa, -0.81 MPa and -1.6 MPa. Mean values ±SE are presented (n = 5).**

| | Shoot elongation rate of barley wildtype in soil [cm $d^{-1}$] | | | | | | | |
|---|---|---|---|---|---|---|---|---|
| Time [h] | -0.03 MPa | | -0.2 MPa | | -0.81 MPa | | -1.6 MPa | |
| 0–24 | 0.00 | ±0.00 | 0.00 | ±0.00 | 0.00 | ±0.00 | 0.00 | ±0.00 |
| 24–48 | 0.00 | ±0.00 | 0.04 | ±0.04 | 0.00 | ±0.00 | 0.00 | ±0.00 |
| 48–72 | 0.42 | ±0.066 | 0.72 | ±0.073 | 0.02 | ±0.02 | 0.00 | ±0.00 |
| 72–96 | 0.80 | ±0.055 | 0.88 | ±0.049 | 0.20 | ±0.13 | 0.00 | ±0.00 |
| | Shoot elongation rate of barley wildtype in vermiculite [cm $d^{-1}$] | | | | | | | |
| Time [h] | -0.03 MPa | | -0.2 MPa | | -0.81 MPa | | -1.6 MPa | |
| 0–24 | 0.00 | ±0.00 | 0.00 | ±0.00 | 0.00 | ±0.00 | 0.00 | ±0.00 |
| 24–48 | 0.08 | ±0.06 | 0.00 | ±0.00 | 0.00 | ±0.00 | 0.00 | ±0.00 |
| 48–72 | 0.44 | ±0.02 | 0.08 | ±0.08 | 0.00 | ±0.00 | 0.00 | ±0.00 |
| 72–96 | 0.78 | ±0.04 | 0.28 | ±0.07 | 0.00 | ±0.00 | 0.00 | ±0.00 |

The hairless mutant and the wildtype showed similar shoot elongation rates in soil at -0.03 MPa. There was no shoot growth of the hairless mutant at -0.81 MPa and -1.6 MPa, but the shoots of the wildtype grew after 72 h.

**Table 5-8: Shoot elongation rates per day of the hairless barley mutant (*brb*) in soil and vermiculite [cm $d^{-1}$] at matric potentials of -0.03 MPa, -0.2 MPa, -0.81 MPa and -1.6 MPa. Mean values ±SE are presented (n = 5).**

| | Shoot elongation rate of hairless barley in soil [cm $d^{-1}$] | | | | | | | |
|---|---|---|---|---|---|---|---|---|
| Time [h] | -0.03 MPa | | -0.2 MPa | | -0.81 MPa | | -1.6 MPa | |
| 0–24 | 0.00 | ±0.00 | 0.00 | ±0.00 | 0.00 | ±0.00 | 0.00 | ±0.00 |
| 24–48 | 0.02 | ±0.02 | 0.00 | ±0.00 | 0.00 | ±0.00 | 0.00 | ±0.00 |
| 48–72 | 0.54 | ±0.075 | 0.60 | ±0.071 | 0.00 | ±0.00 | 0.00 | ±0.00 |
| 72–96 | 0.84 | ±0.06 | 0.88 | ±0.11 | 0.12 | ±0.073 | 0.00 | ±0.00 |
| | Shoot elongation rate of hairless barley in vermiculite [cm $d^{-1}$] | | | | | | | |
| Time [h] | -0.03 MPa | | -0.2 MPa | | -0.81 MPa | | -1.6 MPa | |
| 0–24 | 0.00 | ±0.00 | 0.00 | ±0.00 | 0.00 | ±0.00 | 0.00 | ±0.00 |
| 24–48 | 0.06 | ±0.06 | 0.06 | ±0.06 | 0.00 | ±0.00 | 0.00 | ±0.00 |
| 48–72 | 0.48 | ±0.02 | 0.00 | ±0.00 | 0.00 | ±0.00 | 0.00 | ±0.00 |
| 72–96 | 0.38 | ±0.06 | 0.18 | ±0.05 | 0.00 | ±0.00 | 0.00 | ±0.00 |

Shoot elongation rates were significant faster with time when grown at -0.03 MPa and -0.2 MPa, but no significant differences for wildtype and hairless mutant were found ($p = 0.08$) although shoot growth was faster in soil than in vermiculite.

Figure 5-13 shows root elongation rates calculated from total root growth in 96 h for barley wildtype and hairless mutant, as well as shoot elongation rates.

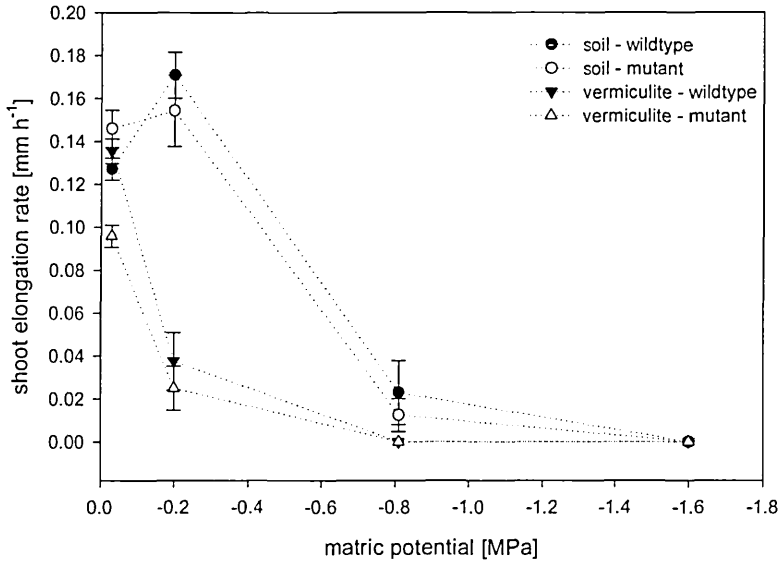


**Figure 5-13: Average shoot elongation rates of barley wildtype and hairless mutant (*brb*) during 96 h in soil and vermiculite at a matric potential of -0.03 MPa, -0.2 MPa, -0.81 MPa and -1.6 MPa. Mean values ±SE are presented (n = 5).**

Shoot elongation rate was significantly affected by growth medium ($p < 0.001$) and matric potential ($p < 0.001$), but not by the root hair mutation ($p = 0.079$). Shoot elongation decreased with decreasing matric potential. Shoots elongated faster in soil than in vermiculite.

## 5.4 Discussion

*Maize root and shoot elongation of the wildtype and the hairless mutant at different matric potentials*

Maize wildtype and a hairless mutant were used to investigate the effect of root hairs on root elongation at various matric potentials. Root and shoot elongation rates of wildtype and hairless mutants of seedlings grown on moist cotton wool were determined to test whether root and shoot elongation rates were affected by the mutation. It was assumed that the seedlings between two layers of cotton wool were unstressed. Roots of the wildtype elongated faster on moist cotton wool than the mutant, but root elongation rates of seedlings grown between two layers of moist cotton wool were slower than those determined in the wettest soil treatment. Therefore, it remains uncertain if seedlings were stressed on moist cotton wool or not, and if differences in growth were or were not caused by the mutation. Hochholdinger et al. (2004) reported similar phenotypes of the wildtype and hairless maize mutant except for the development of root hairs, but did not determine root elongation rates.

The hypothesis that root hairs improve water availability especially when soil dries could not be confirmed by the results of root elongation rates relative to the maximum elongation rate on cotton wool. The wildtype grew faster only at -0.03 MPa in soil when the relative results were considered. At drier potentials root hairs might not have developed properly (Schnall and Quatrano, 1992; Worrall and Roughley, 1976). Worrall

and Roughly (1976) reported abnormally short and swollen root hairs of clover roots at matric potentials of -0.36 MPa.

Significantly slower root elongation rates (absolute values) of the hairless mutant compared with the wildtype were determined when the growth medium was wetter than -1.6 MPa which would confirm the hypothesis that root hairs improve root–particle contact and therefore the access to water. The interpretation of the results is highly dependant on whether the hairless mutant shows pleiotropy. Therefore it is uncertain whether roots of the hairless mutant elongated more slowly because of the genetic mutation or because of root–particle contact.

*Barley root and shoot elongation of the wildtype and the hairless mutant at different matric potentials*

Earlier studies with the wildtype (Pallas) and hairless mutant (*brb*) have shown that when water and nutrient supply is adequate, phenotypes only differed in the formation of root hairs (Gahoonia and Nielsen, 1997) so no obvious pleiotropic effects were observed. Gahoonia and Nielsen (2003) reported similar root mats after 7 days of grown in vermiculite, but actual root length or root elongation rates were not reported.

The rates of total root length increase of the wildtype were greater than those of the hairless mutants in soil drier than -0.03 MPa, but rates of the total root length increase were significantly slower at -0.03 MPa for the wildtype. The number of roots emerged after germination was significantly lower for the wildtype than for the wildtype at this matric potential, which probably affected the rate of increase in total root length.

Nevertheless, shoot elongation rates of the wildtype were faster than those of the hairless mutant at -0.03 MPa which suggests that the hairless mutant sensed a more unfavourable growth environment than the wildtype. Shoot growth is often more inhibited than root growth in drying soils (Sharp et al., 2000), which is rather a consequence of root–to–shoot signalling then a change in water status.

The differences in total root length increase between the wildtype and the hairless mutant were greater in the drier treatments. This suggests that greater root–particle contact may be more important when water supply is limited. However at -1.6 MPa was no significant increase in total root length found, probably because the growth medium was too dry for root hairs to develop properly, so root–particle contact was not significantly improved (Schnall and Quatrano, 1992; Worrall and Roughley, 1976). White and Kirkegaard (2010) showed that wheat roots which were grown in large pores developed abundant root hairs which were either in contact with other roots clumped together or the pore wall and so increased root–soil contact. The root hair density increased the poorer the contact between root and pore wall was. Other studies showed that root hairs are important for the uptake of nutrients of low diffusivity, such as phosphorous (Gahoonia and Nielsen, 2003) and zinc (Genc et al., 2007), which suggests that root–soil contact was greater for roots which developed root hairs. Gahoonia and Nielsen (2003) found that the wildtype of barley (Pallas) depleted twice as much phosphorous than its hairless mutant (*brb*); moreover the hairless mutant died after 30 days grown in a soil of low phosphorous availability.

The wildtype developed significantly more roots than the hairless mutant when soil was drier than -0.02 MPa. This may have been because the water supply was better due to a better contact with the growth medium. Roots of the wildtype were also longer than those of the hairless mutant, so that the greater total root length achieved was a result of both more root tips and root tips which were elongating faster. No shoot elongation at the two drier potentials was found and this is consistent with observations that shoot elongation rate is often more reduced than root elongation (Sharp et al., 1988) when water is limiting plant growth.

*Root and shoot elongation rates in soil and vermiculite*

It was initially expected that root elongation in vermiculite might be even more affected by the presence of root hairs because of greater size of vermiculite particles and therefore smaller root–particle contact. However, root hairs had no effect on the root elongation rate of maize relative to unstressed roots (Figure 5-4) in vermiculite and even so roots of the barley wildtype in vermiculite grew faster than those of the mutant; differences between wildtype and the hairless mutant were less than in soil (Figure 5-11). This might have been caused by root hair being stunted by the alkaline conditions in vermiculite (Chapter 2; Ewens and Leigh, 1985) and thus being less advantageous than in soil. Ewans and Leigh (1985) reported shorter root hairs of wheat roots when pH was <7. The rate of increase in total root length for barley at -0.03 MPa was slower than at -0.2 MPa (Figure 5-10). These results suggest that not water availability was limiting root elongation. Root growth might have been reduced because of more alkaline growth conditions in wetter soil (Tang et al., 1996; White, 1990).

*Root and shoot elongation of maize and barley in comparison*

Root elongation rates of barley wildtype were greater than those of the hairless mutant, while the relative maize root elongation rates were not significantly affected by the presence of root hairs. Segal et al. (2008) implied that greater water uptake due to appearance of root hairs is caused by an expansion of the effective root diameter. Barley has smaller root diameters than maize; the effect of root hairs might therefore be proportionately greater for barley than for maize. Furthermore greater seed size of maize may have caused less sensitivity towards decreases in matric potential because more water was stored in maize seeds than in barley seeds, so that even at -1.6 MPa shoots of maize elongated while barley shoots did not grow at potentials drier than -0.2 MPa.

## 5.5 Summary

The effects of root hairs of maize and barley on root and shoot elongation rates in soil and vermiculite at four different matric potentials were tested. Hairless maize and barley seedlings and their wildtypes were grown in soil or vermiculite at matric potentials of -0.03 MPa, -0.2 MPa, -0.81 MPa and -1.6 MPa and root and shoot elongation rates were compared.

Maize root and shoot elongation rates of the wildtype (with root hairs) were significantly faster than those of the hairless mutant when the growth medium was wetter than -0.81 MPa, but slower root elongation rates of the hairless mutant caused by the mutation could not be excluded. There were no significant differences in root elongation rate when rates relative to the maximum root elongation rates were considered.

The rates of total root length increase of the wildtype of barley were greater than those of the hairless mutant when the growth medium was wetter than -1.6 MPa, which was a result of more and longer roots.

In conlusion, root hairs can improve growth conditions when water supply is limiting probably because of a better contact with the growth medium, but the effects of root hairs are dependant on plant species and matric potential of the growth medium.

# 6 Effects of bulk density and aggregate size on root–soil contact and root and shoot elongation

## 6.1 Introduction

Soils provide water and nutrients for plants to grow, as well as sufficient mechanical strength to provide anchorage for the plant throughout its life. Hard soils can mechanically impede roots and slow their elongation rate (Bengough and Mullins, 1991; Taylor and Ratliff, 1969), while in very loose soil root–soil contact might be insufficient for water and nutrient uptake (Veen et al., 1992).

Almost all roots growing in soil experience mechanical impedance to a certain degree, if continuous pores of appropriate diameter do not exist, so that roots need to exert a force to deform the soil. The force required to deform soil is often presented per unit surface area, as growth pressure. The pressure will increase with increasing soil strength due to drying, or if the bulk density of the soil increases (Bengough et al., 1997). In hard and compacted soils roots grow thicker (Kirby and Bengough, 2002; Materechera et al., 1991). Bengough et al. (1997) reported root diameter of impeded and unimpeded roots at different positions of the root (up to 10 mm from the apex) and found that root diameter of impeded roots continued to increase, while the root diameter of unimpeded roots was the same from 2 mm from the apex to 10 mm from the apex. The thickening of the root diameter is mainly due to an expansion of cell diameter in the cortex, as well as an increase in number of cortical cells (Croser et al., 2000). Cortical cells expand radially because of microfibril reorientation in the primary cell wall (Bengough et al., 2011). It was suggested that thicker roots penetrate hard soils better because they are more resistant to buckling (Whiteley et al., 1982) and because of stress relief in the axial direction (Kirby and Bengough, 2002).

Root elongation rate is slowed when roots are mechanically impeded (Bengough et al., 1994; Bengough and Mullins, 1991). Bengough and Mullins (1991) found a 50 % to 60 % reduction in root elongation, when root penetration resistance was between 0.26 MPa to 0.47 MPa (corresponding penetrometer resistance between 4.5 to 7.5 times greater). Root elongation rate of impeded roots is reduced because fewer cells are produced and root mitotic activity is slowed down (Croser et al., 1999). Mechanical impedance has a persistent effect on root growth, which is caused by cell wall stiffening (Croser et al., 1999). For example, impeded pea roots took 60 h after being transferred into hydroponic cultures to reach the elongation rates of the previously unimpeded roots (Croser et al., 2000). The maximum growth pressure a root can exert to penetrate soils depends on the turgor pressure in the expanding cells, which varies with soil matric potential. Whalley et al. (1998) studied the effect of osmotic potential on maximum root growth pressure and found a linear decrease in maximum growth pressure from 0.66 MPa to 0.35 MPa when osmotic potential decreased from 0 to -0.45 MPa. In compacted and wet soils hypoxia (too little oxygen) is likely to limit root growth, when air–filled pore space is less than 10 % (daSilva et al., 1994).

Soil can be too loose as well as too compacted (Boone, 1988; Veen et al., 1992). In very loosely packed soil, root–soil contact might be insufficient for water and nutrient uptake. Atkinson et al. (2009) showed that crop establishment of winter wheat (*Triticum aestivum*) was significantly reduced with increasing pore space and concluded that poor seed–soil contact caused decreased crop establishment. Veen et al. (1992) investigated the effect of root–soil contact at five bulk densities (1.54 g $cm^{-3}$, 1.50 g $cm^{-3}$, 1.43 g $cm^{-3}$, 1.32 g $cm^{-3}$ and 1.08 g $cm^{-3}$) on root and shoot growth. Shoot growth decreased with

increasing bulk density from 1.32 g $cm^{-3}$ to 1.50 g $cm^{-3}$, but was slightly less at 1.08 g $cm^{-3}$. Root fresh weight decreased as well up from 1.32 g $cm^{-3}$ to 1.50 g $cm^{-3}$, while the total root length decreased with increasing bulk density. Root–soil contact increased with increasing bulk density (Kooistra et al., 1992).

Another aspect of soil structure that affects plant growth is the aggregation of soils. Several studies showed a decrease in total root length with increasing aggregate size (detailed in Table 6-1). Donald et al. (1987) studied root and shoot growth of maize in silt loam soil sieved to four aggregate size fractions (<1.6 mm, 1.6–3.2 mm, 3.2–6.4 mm and 6.4–12.8 mm). They found a decrease in shoot dry weight as aggregate size increased from <1.6 mm to 1.6–3.2 mm and total root length was reduced by 60 % from the finest to the coarsest system, but the primary root and nodal roots were longer in coarser soil than in finer. Roots tend to penetrate coarser aggregates more often than finer aggregates. Samples with coarser aggregates showed a greater penetrometer resistance than finer aggregates. The changes in root and shoot growth could not be explained by water status nor nutrient supply. Premalal and Deen (2006) found similar responses of root growth when aggregate size increased. They used artificial aggregates made out of burned montmorillinite. The aggregates were either <0.2 mm or 2–7 mm fraction and water and nutrients were supplied by a hydroponic system. Maize was sampled at 5, 7 and 10–leaf stage and differences in total root length disappeared with time.

**Table 6-1: Overview over different studies investigating effects of aggregate size on shoot and root elongation.**

| Author / Year | Plant species and age | Aggregate size and material | PR | Ψ | Findings |
|---|---|---|---|---|---|
| Schneider and Gupta, 1985 | Maize | Loam, silt loam, clay loam<br>geometric mean 0.5 mm to 11.1 mm | N/A | -10 kPa<br>to<br>-500 kPa | Maize emergence faster in smaller aggregate size |
| Donald et al., 1987 | Maize<br>18 days | Loam soil:<br><1.6 mm to 12.8 mm | Increase in PR with increasing aggregate size from 0.38 MPa to MPa 1.83 MPa | -3<br>to<br>-20 kPa | Main axis: increase in length with increasing aggregate size<br>Total length: decrease in length with increasing aggregate size |
| Logsdon et al., 1987 | Maize<br>4–7 days | Silt loam:<br><1 mm to 6 mm | N/A | Watered daily | Root length decrease and diameter increase with increasing aggregate size |
| Misra et al., 1988 | Cotton and sunflower<br>15 days | Soil:<br>1 mm to 19 mm | Individual penetrometer resistance for single aggregates increases with aggregate size from 0.2 MPa to 1.2 MPa | One water content used<br>0.28 g $g^{-1}$ | Decrease in total root length and root hair length increase with increasing aggregate size |
| Alexander and Miller, 1991 | Maize<br>8 to 16 days | 0.075 mm to4–8 mm | N/A | -5<br>to<br>-25 kPa | Total root length decreased with increasing aggregate size |
| Premalal and Deen, 2006 | Maize grown unt 5-, 7- and 10 leaf stage | Burned montmorillonite <2 mm and 2-7 mm | N/A | Hydroponic system | Decrease in total root length with increasing aggregate size, but less severe when root was older |

Previous chapters indicated greater root–particle contact is correlated with a faster root and shoot growth. Soil (sieved to 2 mm) and vermiculite were used as the growth media;

greater root–particle contact of roots in soil than in vermiculite was found, as well as faster root and shoot elongation rates. The problem with comparison of growth rates of plants grown in soil or vermiculite is that vermiculite differs, not only in particle size but also in chemical properties. To investigate the effects of soil structure on root and shoot elongation further when water is limiting root growth, two experiments were conducted.

For the first experiment maize and lupin were grown in soil packed to five bulk densities and three matric potentials and root and shoot growth rates were determined. It was hypothesized that with increasing bulk density the root–soil contact increases, but also mechanical impedance, so that root and shoot elongation rates will be greatest at an intermediate bulk density. Moreover, the drier the soil the fewer pores are water filled and root–soil contact becomes more important for water uptake. However, mechanical impedance also increases and the maximum growth pressure that a root can exceed decreases with decreasing matric potential, so that root and shoot elongation in drier and more compacted soil will be slowed.

The second experiment was conducted in soil aggregates of four sizes, wetted to three matric potentials. Finer aggregate size will improve water availability of roots because of a finer pore size and better root–soil contact, which will lead to faster root and shoot elongation rates. The drier the soil the greater the effect of aggregate size on root elongation, because when the degree of saturation decreases larger pores empty and become non–conducting.

Maize and lupin were chosen for the growth studies to investigate differences between monocots and dicots. Lupin was expected to be less sensitive to mechanical impedance, aggregate size and drought stress than maize, because lupin can exert greater growth pressures take up more water per unit root length than maize. Furthermore it will be tested whether root hairs can improve growth conditions in soils with high porosity. It is hypothesized that roots with root hairs will grow faster because of a greater root surface area for taking up water and a better root–soil contact.

## *6.2 Materials and methods*

### 6.2.1 Particle sizes and bulk densities

For the first experiment soil was wetted to three gravimetric water contents (Table 2-6) that corresponding to matric potentials of -0.01 MPa, -0.4 MPa and -1.2 MPa and then packed to five different bulk densities (1.1, 1.2, 1.3, 1.4 and 1.5 g $cm^{-3}$) in plastic cores with a diameter of 5 cm and heights of 12 cm (-1.2 MPa), 17 cm (-0.4 MPa) and 22 cm (-0.01 MPa) using a hydraulic press. Germinated seedlings of maize and lupin with 1–2 cm long radicles were placed into 1 cm deep holes made using a 2 mm drill bit in the soil of five different bulk densities.

For the second experiment soil (sandy loam) was sieved to four different aggregate groups: 4–2 mm, 2–1 mm, 1–0.5 mm and <0.5 mm and wetted to water contents (Table 2-3) corresponding to matric potentials of -0.03 MPa, -0.2 MPa and -0.81 MPa. Soil was filled in similar plastic cores as mentioned above (height of 12 cm, -0.81 MPa; 17 cm,

-0.2 MPa; 22 cm, -0.03 MPa). Maize and lupin, as well as hairless maize mutant and the wildtype were used in this experiment.

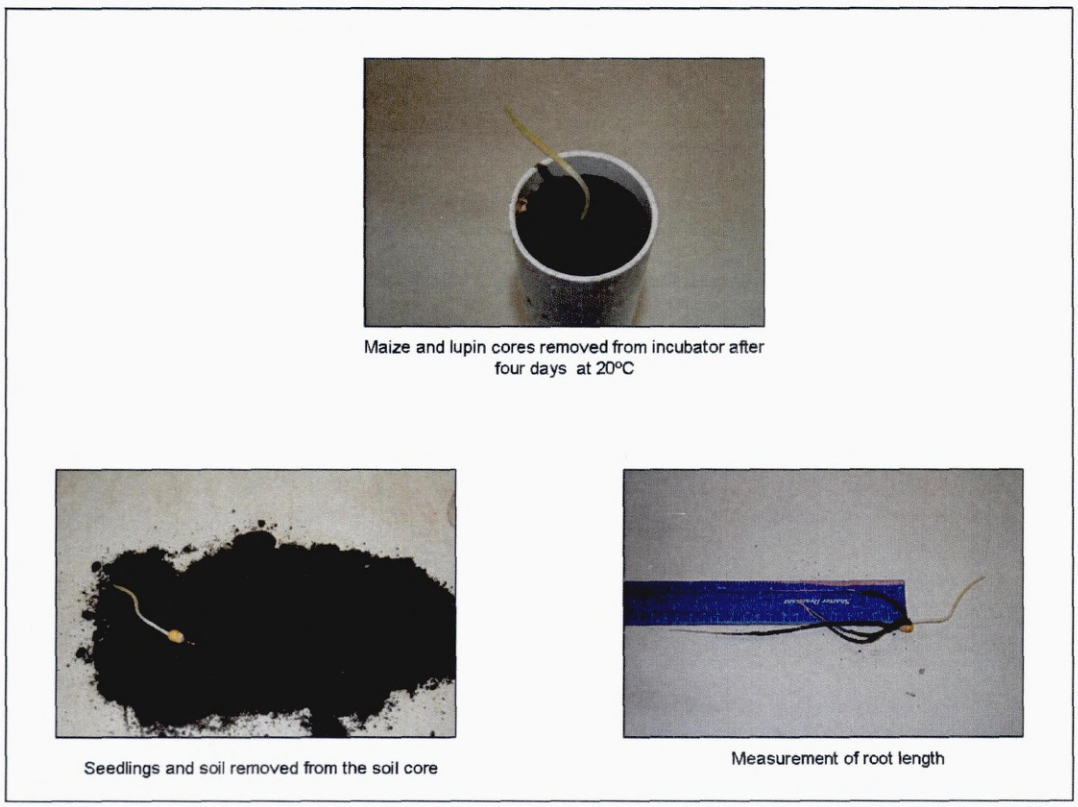


**Figure 6-1: Sampling of seedlings after four days of root growth.**

Seedlings were then grown in darkness at 20°C. The length of the radicles was measured with a ruler on the day of planting. After four days roots were excavated from the pots and measured again (Figure 6-1). The average root elongation rate was determined by dividing the root length increase by 96 h (Equation 4-2). Root diameter and distance between root tip and root hair zone were measured after 96 h by using a stereomicroscope (Leica MZ FL III) equipped with a graticule scale. The elongation rates of wildtype and hairless maize mutant were set in relation to the fastest elongation rate observed for either

wildtype or hairless mutant in soil, because a pleitropic effect (single gene influences multiple phenotypic traits) could not be excluded.

Images of germinated maize and lupin root tips were taken using the stereomicroscope (Leica MZ FL III). Lupin was grown for two more days on moist paper towel and another image of the root tip of the root tip of lupin was taken.

## 6.3 Results

### 6.3.1 Effects of bulk density on root and shoot growth

The root elongation rates are shown in Figure 6-2. Root elongation rates of both plant species decreased significantly with increasing penetrometer resistance as well as with decreasing matric potential ($p < 0.001$). Maize ($p < 0.001$) was more sensitive to matric potential than lupin ($p = 0.03$). Maize and lupin elongation rates slowed rapidly when a penetrometer resistance of approx 0.5 MPa was exceeded. Maize elongated faster than lupin until a penetrometer resistance of approx. 1.4 MPa and ceased when a penetrometer resistance of approx. 2.5 MPa was exceeded. Lupin root elongation stopped when penetrometer resistance was >3.5 MPa.

Shoot elongation rates were not affected by penetrometer resistance ($p = 0.10$), but were significantly reduced as matric potential decreased ($p < 0.001$; Figure 6-2). Lupin shoots elongated slower than maize ($p = 0.013$), but both ceased elongation when penetrometer resistance exceeded 5 MPa.

Root diameter increased significantly with increasing penetrometer resistance ($p < 0.001$; Figure 6-2). Maize (2.6 ±0.27 mm) and lupin (2.5 ±0.15 mm) roots were thickest at penetrometer resistances >5 MPa.

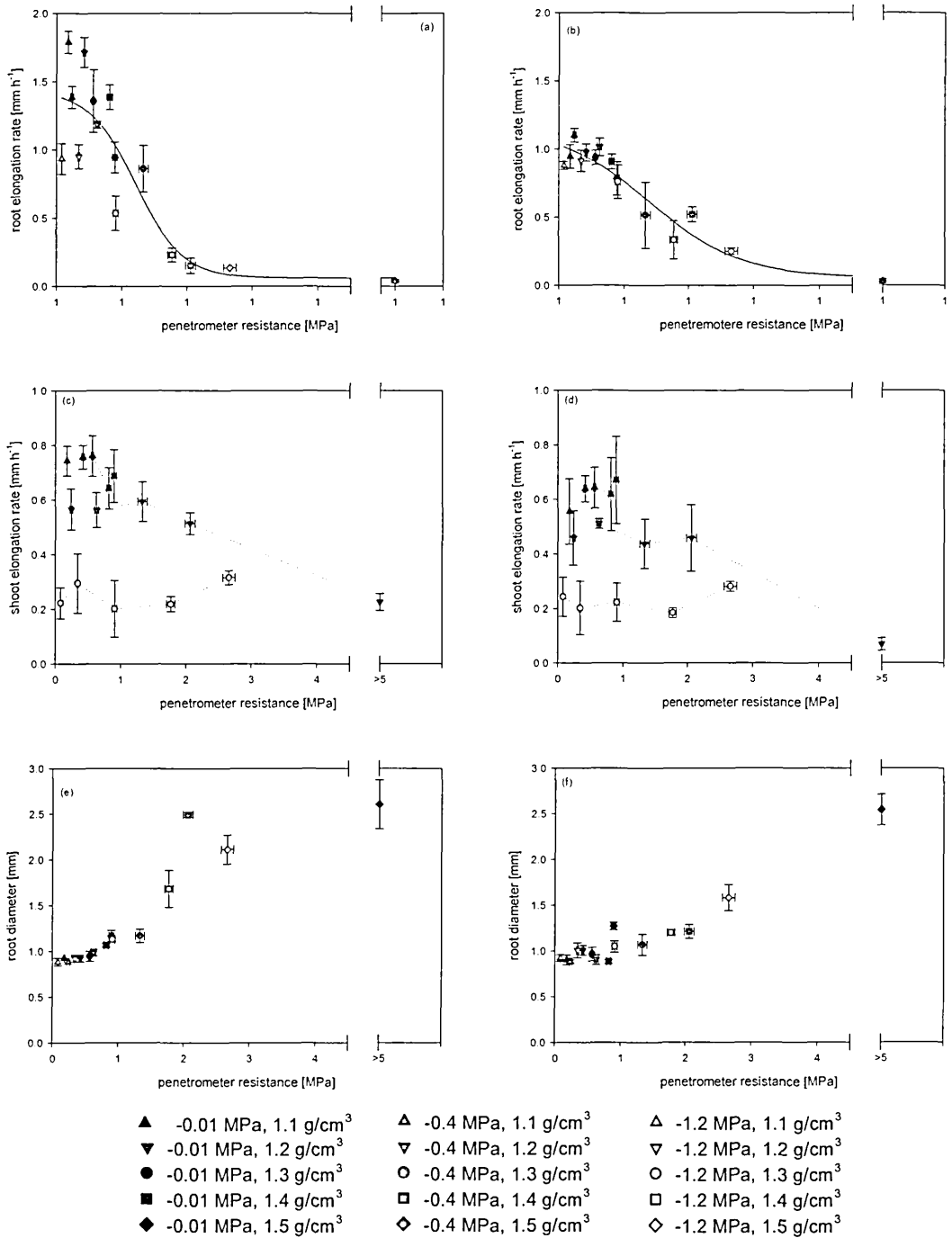


**Figure 6-2: Root (a, b) and shoot (c, d) elongation rates and diameters (e, f) of maize (a, c, e) and lupin (b, d, f) vs penetrometer resistance at matric potentials of -0.01 MPa, -0.4 MPa and -1.2 MPa. Data are means ±SE (n =3).**

The relationships between root elongation rate and distance between root tip and root hair zone are shown in Figure 6-3.

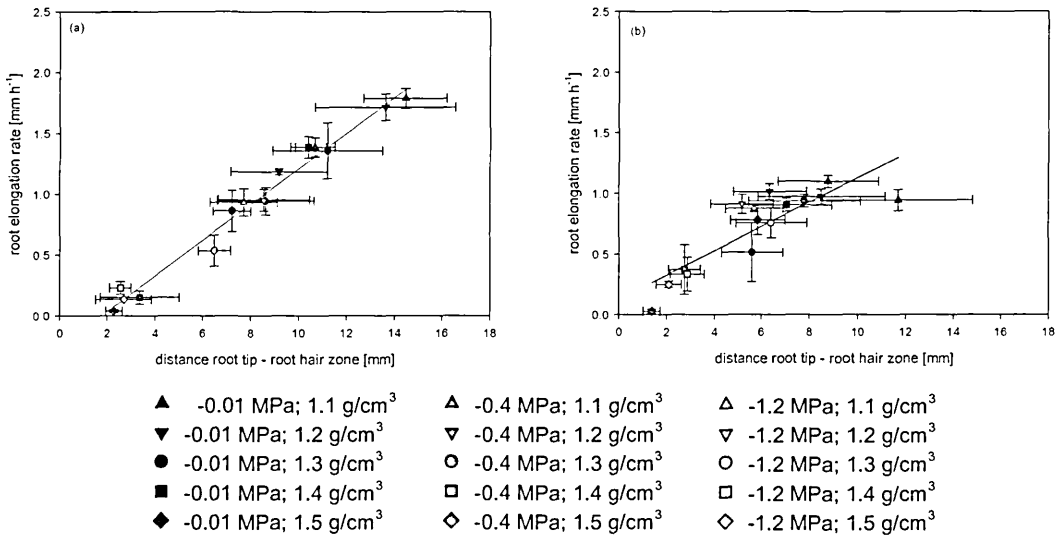


**Figure 6-3: Distance between root tip and root hair zone vs average root elongation rate during 96 h of maize (a) and lupin (b) roots grown in soil wetted to different matric potentials -0.01 MPa, -0.4 MPa and -1.2 MPa and packed to 5 bulk densities: 1.1 g $cm^{-3}$, 1.2 g $cm^{-3}$, 1.3 g $cm^{-3}$, 1.4 g $cm^{-3}$ and 1.5 g $cm^{-3}$. Data are means ±SE (n = 3).**

Linear relationships were found for both maize (mean values $r^2 = 0.98$, raw data $r^2 = 0.58$, $p < 0.001$) and lupin (mean values $r^2 = 0.70$, raw data $r^2 = 0.31$ $p < 0.001$). The data for lupin were more scattered than for maize and both plant species had larger variances in distance between root tip and root hair zone.

The linear regressions shown in Figure 6-3 were fitted through the mean values; information of the intercept and the gradient are shown in Table 6-2. Additional information is given of the intercept and gradient of linear regression fitted through the raw data.

**Table 6-2: Curve fitting parameters for linear regression and correlation coefficients between root elongation rate and distance between root tip and root hair zone (fitted through raw and mean data) for maize and lupin at bulk densities of 1.1 g $cm^{-3}$ to 1.5 g $cm^{-3}$ and matric potentials of -0.01 MPa, -0.4 MPa and -1.2 MPa.**

| Plant | Data | $r^2$ | Intercept | SE Inter–cept | Probability value Intercept | Gradient | SE Gradient | Probability value Gradient |
|---|---|---|---|---|---|---|---|---|
| Maize | means | 0.98 | -0.25 | 0.052 | <0.001 | 0.15 | 0.0059 | <0.001 |
| Maize | raw | 0.58 | 0.11 | 0.13 | 0.401 | 0.10 | 0.014 | <0.001 |
| Lupin | means | 0.70 | 0.13 | 0.11 | 0.273 | 0.10 | 0.017 | <0.001 |
| Lupin | raw | 0.31 | 0.41 | 0.084 | <0.001 | 0.054 | 0.012 | <0.001 |

The gradient for the line fitted through the maize data was greater than for the line fitted through the lupin data (maize means 0.15, raw data 0.10; lupin means 0.10, raw data 0.054). The lines fitted through mean values were steeper than when lines would have been fitted through the raw data (Table 6-2).

**Table 6-3: Curve fitting parameter of exponential curve for maize and lupin grown in soil of different bulk densities (1.1, 1.2, 1.3, 1.4, 1.5 g $cm^{-3}$) and matric potentials (-0.01, -0.4 and -1.2 MPa); $EI = a+b\times r^x$ and correlation coefficients with x = distance between root tip and root hair zone.**

| | $r^2$ | Parameter a | Parameter b | Parameter r | SE of observation | Probability value Gradient |
|---|---|---|---|---|---|---|
| Maize | 0.66 | 1.793 | -2.342 | 0.8658 | 0.33 | <0.001 |
| SE of parameter | | 0.315 | 0.266 | 0.047 | | |
| Lupin | 0.46 | 0.9507 | -1.422 | 0.615 | 0.26 | <0.001 |
| SE of parameter | | 0.0767 | 0.390 | 0.106 | | |

Exponential curves fitted through the raw data showed better correlation for both plants (Table 6-3) than linear regressions (Table 6-2).

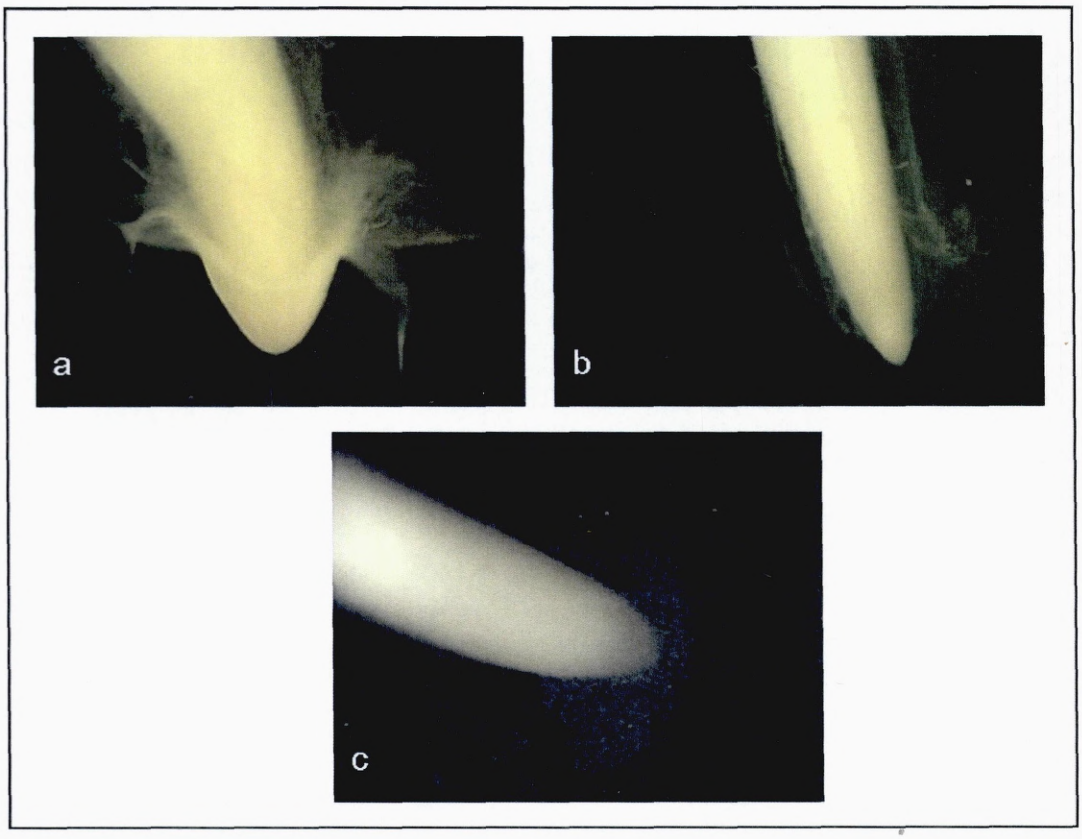


**Figure 6-4: Root tip of lupin after germination surrounded with borderlike cells (a), lupin two days later when borderlike cells have fallen off tip, root is covered with mucilage (b) and maize root tip with mucilage (c).**

Images of lupin and maize root tips are shown in Figure 6-4. Root tips of lupin and maize differ from each other. The tip of 1–2 cm long lupin radicles was surrounded by borderlike cells which fell when grown for a longer period, but further along the root axis those borderlike cells remained. Maize root tip in contrast was releasing mucilage and border cells.

### 6.3.2 Effects of aggregate size on root and shoot elongation

Figure 6-5 shows the effect of aggregate size on root and shoot elongation rates.

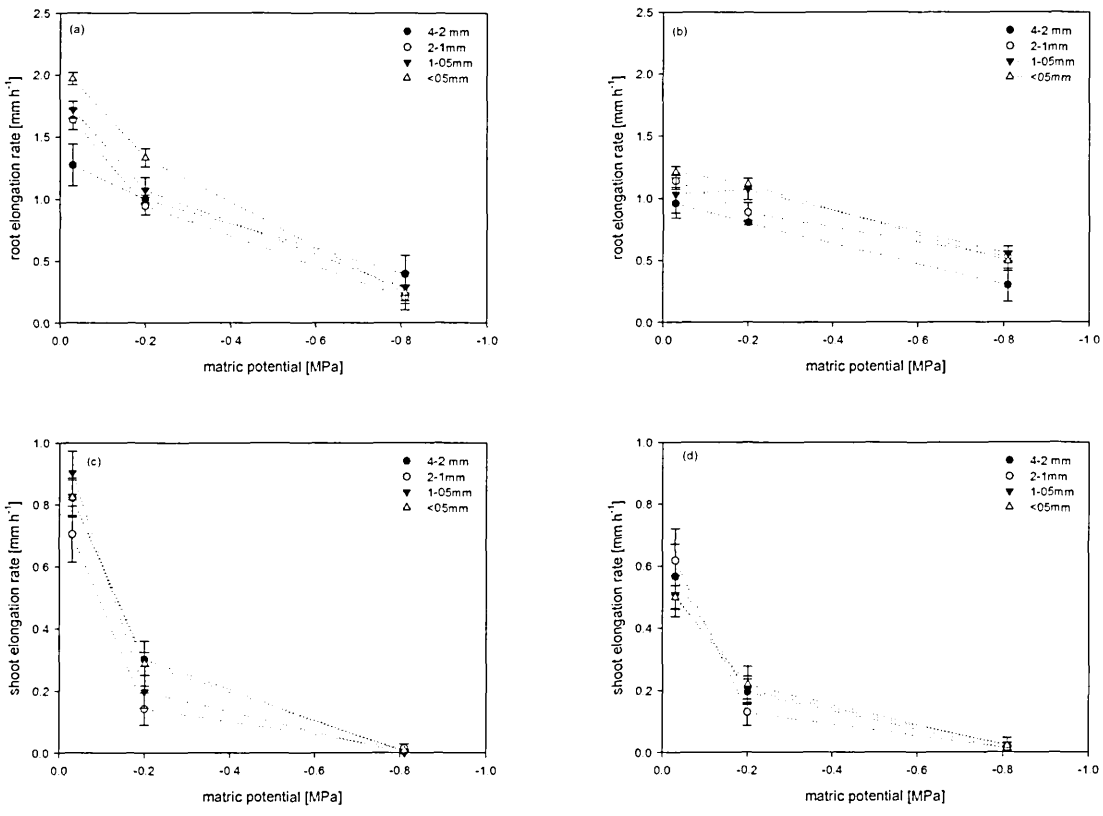


**Figure 6-5: Root and shoot elongation rate of maize (a, c) and lupin (b, d) in soil of various aggregate sizes (4–2 mm, 2–1 mm, 1–0.5 mm and <0.5 mm) and matric potentials (-0.03 MPa, -0.2 MPa and -0.81 MPa). Data are means ±SE (n =3).**

Root elongation of maize and lupin slowed in drier soil. Maize ($p = 0.002$) and lupin ($p = 0.008$) root elongation rates were significantly affected by aggregate size, the coarser the aggregates the slower the root elongation rates. For example, at an aggregate sizes of 4–2 mm the elongation rate of maize was 1.3 ±0.17 mm $h^{-1}$, whereas with aggregates <0.5 mm the rate was 1.97 ±0.049 mm $h^{-1}$. At a matric potential of -0.81 MPa root elongation of maize was greatest at an aggregate size of 4–2 mm (0.39 ±0.15 mm $h^{-1}$). Lupin roots elongated also fastest (1.21 ±0.04 mm $h^{-1}$) in the finest (<0.5 mm) aggregates and slowest (0.96 ±0.12 mm $h^{-1}$) in the coarsest aggregates (4–2 mm).

Maize and lupin shoot elongation rates decreased in drier soil ($p < 0.001$), but were unaffected by aggregate size (maize $p = 0.132$; lupin $p = 0.99$). Maize shoots elongated faster than lupin shoots (maximum rate for maize $0.82 \pm 0.06$ mm $h^{-1}$; lupin $0.57 \pm 0.11$ mm $h^{-1}$; $p < 0.001$).

Root elongation of maize wildtype and hairless maize mutant slowed with decreasing matric potential (Figure 6-6). Root elongation rates were faster in finer soil than in coarser soil ($p < 0.001$). Elongation rates of the hairless mutant were significantly slower than of the wildtype ($p < 0.001$), when the absolute values of root elongation rates were compared. However, no differences were determined when root elongation rates relative to the maximum elongation rates measured in this experiment were considered ($p = 0.224$).

Shoot elongation rate was significant changed by matric potential ($p < 0.001$) and aggregate size ($p = 0.003$). Furthermore, shoot elongation of the hairless mutant was significantly slower than the wildtype ($p < 0.001$). Shoot elongation rates of maize wildtype (0.88 mm $h^{-1}$, $\pm 0.05$) and hairless mutant (0.77 mm $h^{-1}$, $\pm 0.03$) were greatest in soil of aggregates <0.5 mm at -0.03 MPa (Figure 6-6). No elongation occurred at a matric potential of -0.81 MPa.

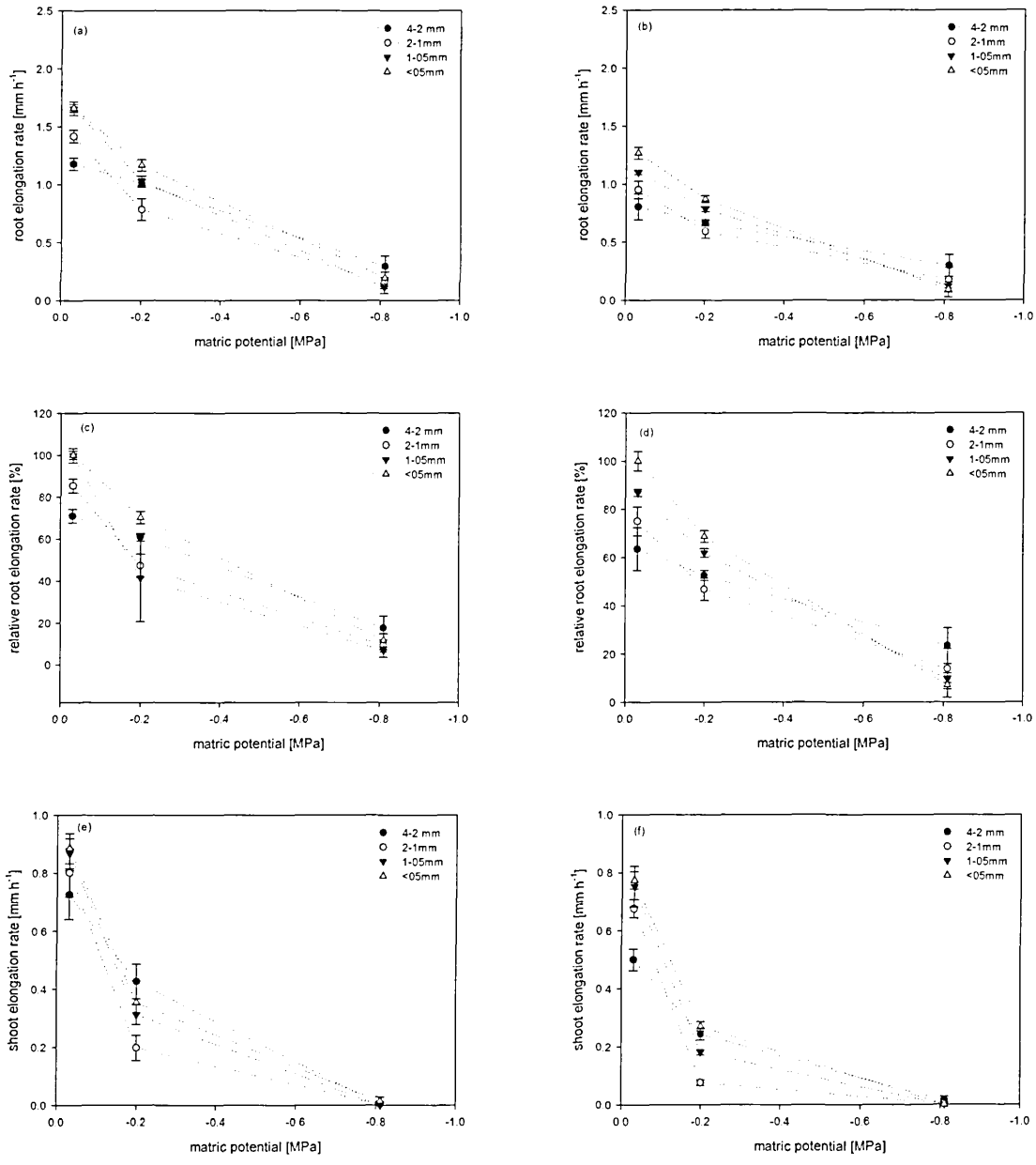


**Figure 6-6: Root and shoot elongation rate of maize wildtype (a, e) and hairless mutant (b, f) in soil of various aggregate sizes (4–2 mm, 2–1 mm, 1–0.5 mm and <0.5 mm) and matric potentials (-0.03 MPa, -0.2 MPa and -0.81 MPa), as well as the relative root elongation rates of wildtype (c) and hairless mutant (d) to root elongation rates of roots in soil at -0.03 MPa. Data are means ±SE (n = 3).**

Root diameter of lupin increased with increasing aggregate size ($p = 0.013$; Figure 6-6). Average root diameter of lupin in aggregates <0.5 mm was 0.93 ±0.03 mm while at 4–

2 mm, the average diameter was 1.04 ±0.032 mm. Matric potential did not affect the diameter (p = 0.705).

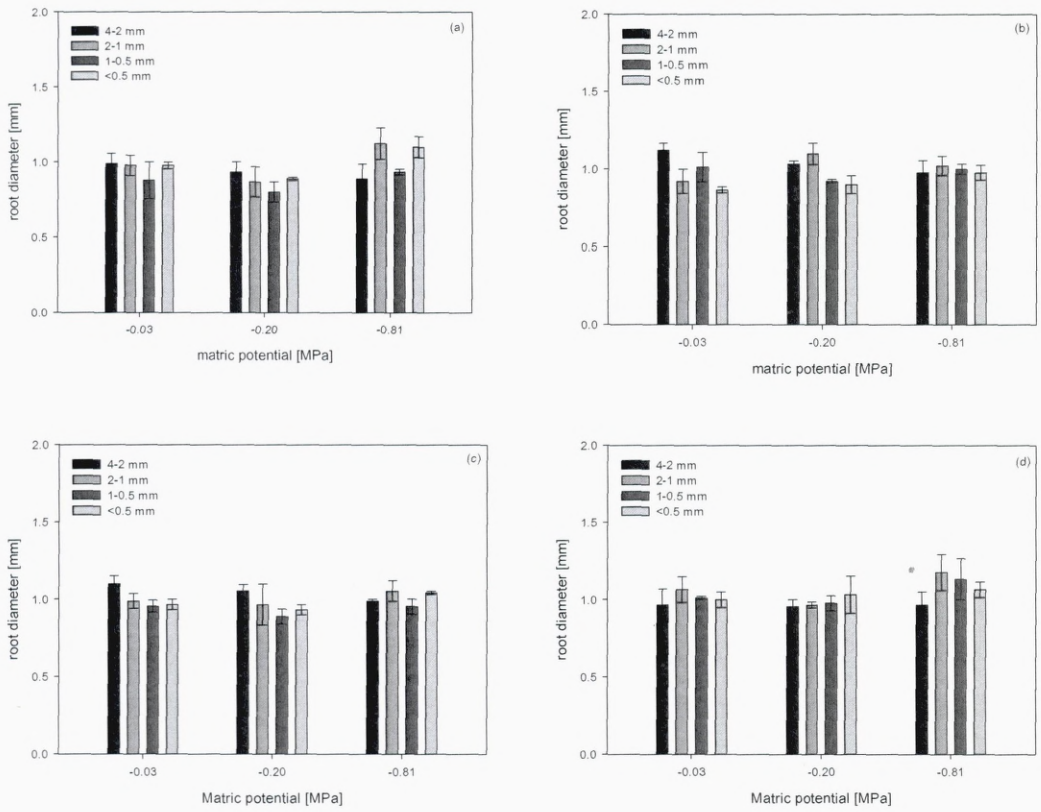


**Figure 6-7: Root diameter of maize (a), lupin (b), maize wildtype (c) and hairless mutant (d) grown in soil aggregates of 4–2 mm, 2–1 mm, 1–0.5 mm and <0.5 mm diameter and matric potentials of -0.03 MPa, -0.2 MPa and -0.81 MPa; measured 1 cm from root tip. Data are means ±SE (n = 3).**

In contrast, aggregate size did not change the root diameter of maize (p = 0.211), maize wildtype (p = 0.117) and the hairless maize mutant (p = 0.441).

### 6.3.3 Root–soil contact

Three dimensional volumetric images were taken of maize and lupin grown in the four aggregate sizes (Figure 6-8). Different aggregate sizes are clearly distinguishable, as is the greater contact of the root with the soil as aggregate size decreases.

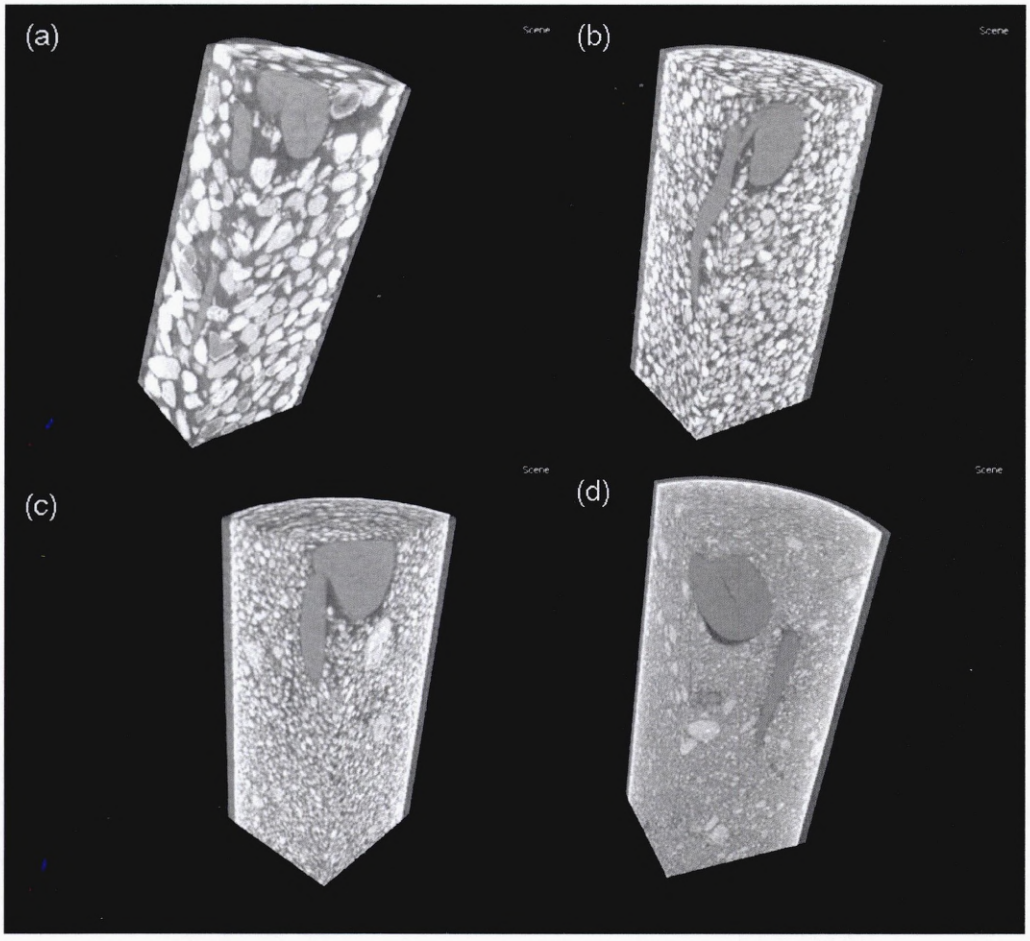


**Figure 6-8: Frontal plane of sections of 3-D volumetric images: Lupin seedlings grown in soil at -0.03 MPa and sieved to aggregate sizes of 4–2 mm (a), 2–1 mm (b) , 1–0.5 mm (c) and <0.5 mm (d) for a day. Resolution 34.9 µm.**

The 3-D volumetric images of roots were used to segment root sections (Figure 6-9) and determine root–soil contact as described in Chapter 3. A greater contact area of roots with soil was visible for finer aggregates than for coarser aggregates.

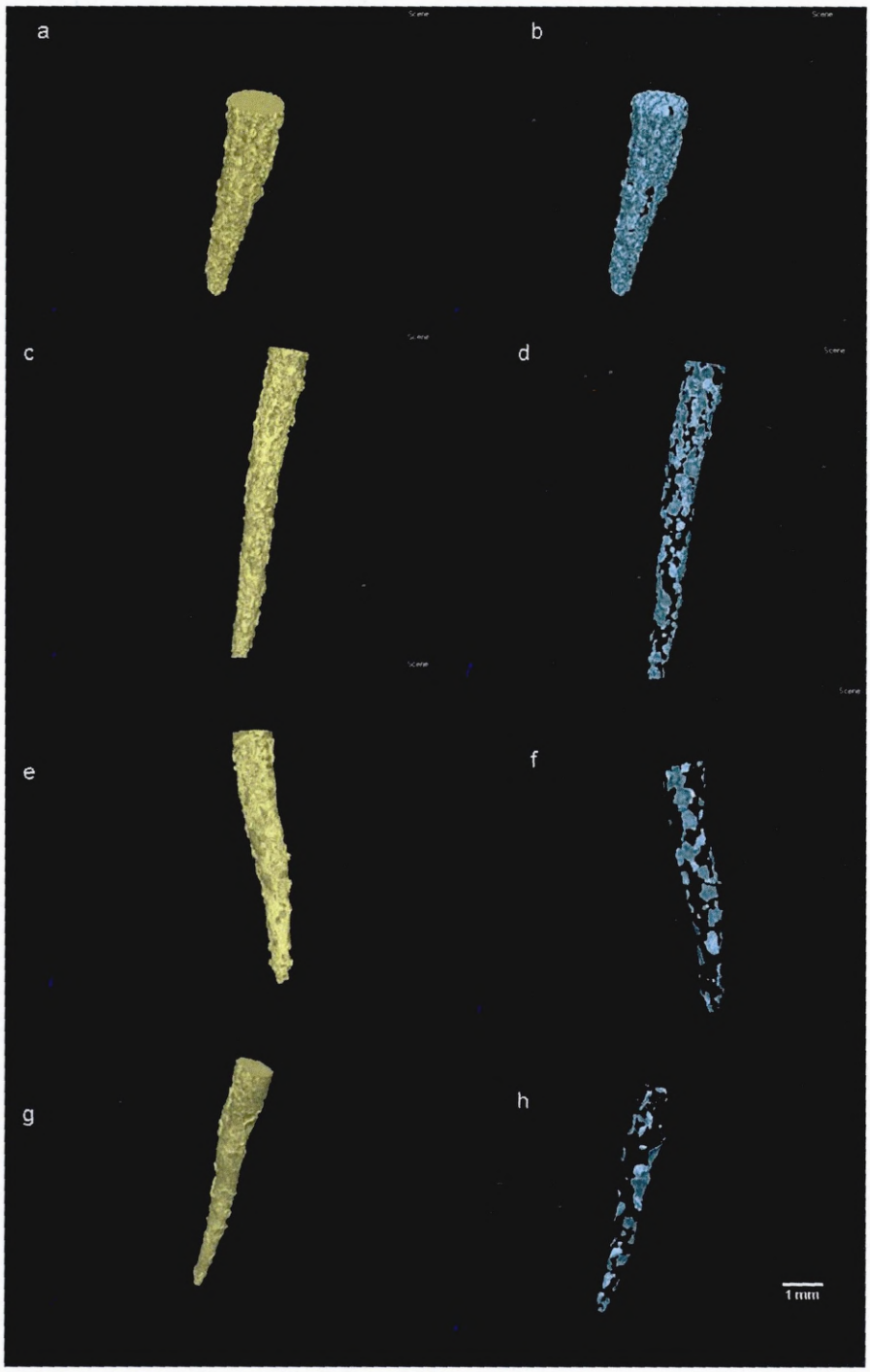


**Figure 6-9: False coloured images of segmented root volume of lupin in soil sieved to <0.5 mm (a), 1-0.5 mm (c), 2-1 mm (e) and 4–2 mm (f) and their root–soil contact areas (b <0.5 mm; d 1-0.5 mm, f 2-1 mm and g 4–2 mm) determined from 3-D-volumetric images in VGStudio MAX v2.1. Images are false coloured.**

Root–soil contact decreased significantly ($p < 0.001$) with increasing aggregate size. Root–soil contact was greatest in soil <0.5 mm (maize 79 ±2.5 %; lupin 72 ±9.7 %) and smallest at 4–2 mm (maize 25 ±2.7 %; and lupin 23 ±1.9 %). Root–soil contact was similar for maize and lupin ($p = 0.147$) for each aggregate size.

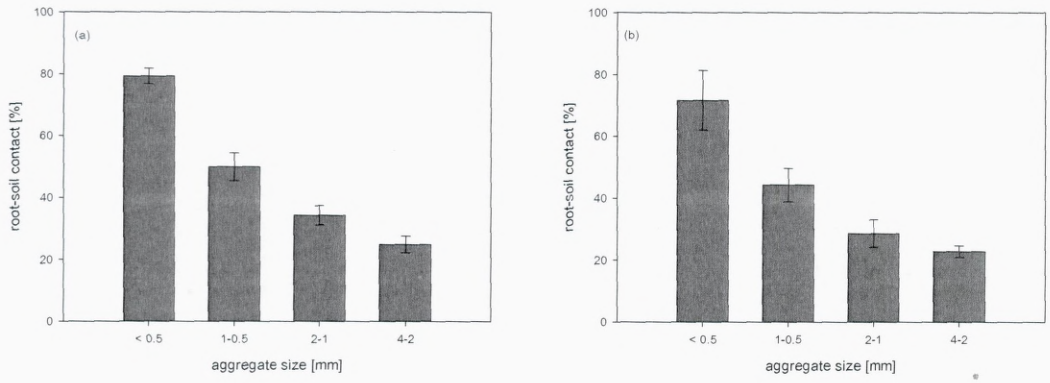


**Figure 6-10: Root-soil contact [%] of maize (a) and lupin (b) in soil of aggregate sizes of <0.5 mm, 1–0.5 mm, 2–1 mm and 4–2 mm. Data are means ±SE (n = 3).**

Root elongation rate of maize and lupin increased with increasing root–soil contact. Maize showed greater sensitivity towards changes in root–soil contact than maize. Both, maize and lupin showed greatest increase in root elongation rate when root–soil contact increased from approximately 25 % to approximately 35 %.

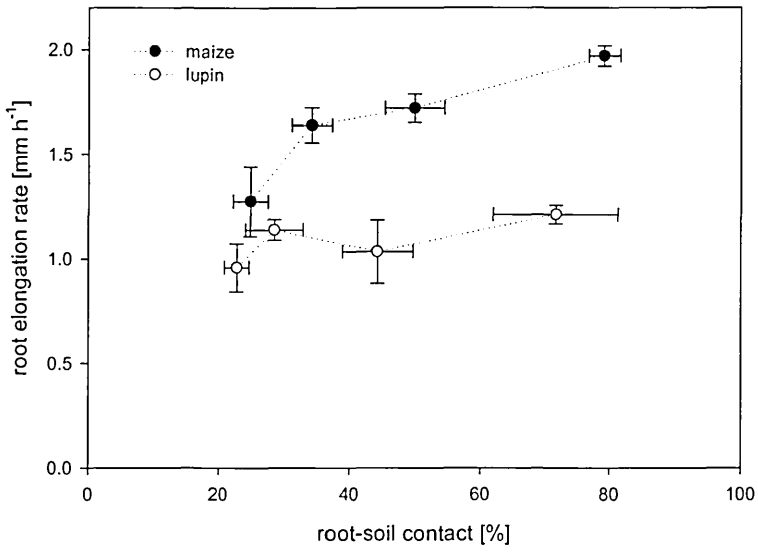


**Figure 6-11: Root–soil contact vs root elongation rate of maize and lupin seedlings grown in aggregate sizes of 4-2 mm, 2-1 mm, 1-0.5 mm and <0.5 mm at -0.03 MPa. Data of root-soil contact were derived from different samples than data of root elongation rates.**

## 6.4 Discussion

*Effects of bulk density and matric potential on root and shoot elongation*

The first experiment combined the stresses of limiting water and soil strength. Root elongation rates of maize and lupin were slowed when penetrometer resistance increased and matric potential decreased, which agrees with the findings of several other studies (Bengough and Mullins, 1991; Eavis, 1972; Goss, 1977; Materechera et al., 1991; Sharp et al., 1988; Taylor and Ratliff, 1969; Veen et al., 1992). Only a few studies have considered the combined stresses of water stress and mechanical impedance (Mirreh and Ketcheso, 1973; Taylor and Ratliff, 1969; Veen et al., 1992) for example Taylor and Ratliff (1969) studied root elongation rates of cotton and peanut at various water contents at matric potentials ranging from -0.017 MPa to -1.25 MPa and penetrometer resistances of 0.005 to 2.0 MPa.

The hypothesis that an intermediate bulk density will offer the best growth condition for roots did not apply, instead root elongation decreased with increasing bulk density and penetrometer resistance. This shows that mechanical impedance decreased root elongation, dominating any effect of better root–soil contact. Similar results have been recorded for root elongation rates of barley (Stirzaker et al., 1996), maize (Veen et al., 1992), cotton and peanut (Taylor and Ratliff, 1969). For shoot elongation in this study, it was unaffected by penetrometer resistances below 5 MPa, which agrees with results of pigeonpea found by Kirkegaard et al. (1992). However, Veen et al. (1992) reported slightly slower shoot elongation rates of maize in the lowest bulk density of 1.08 g $cm^3$ (Veen et al., 1992).

Maize and lupin showed different sensitivity to soil physical limitations. Maize root elongation was significantly decreased in drier soil, while lupin showed no sensitivity towards changes in matric potential (Figure 6-2), which agrees with findings in Chapter 4. The different growth responses of maize and lupin to changes in matric potential are discussed in more detail in Chapter 4. Furthermore lupin was also less sensitive to an increase in penetrometer resistance than maize, such that maize root elongation was halved at a penetrometer resistance of approximately 1.3 MPa, while lupin root elongation showed similar decrease at 1.8 MPa. These findings agree broadly with results of Taylor and Ratliff (1969) and Veen and Boone (1990), who reported reductions in root elongation of 50 % for cotton, maize and peanut when penetrometer resistance was between 0.8 MPa and 2 MPa. Materechera et al. (1991) suggested that dicotyledons generate greater maximum growth pressure than monocotyledons, but Clark and Barraclough (1999) found similar maximum growth pressure for maize and lupin, so that

maximum axial root growth pressure does not explain the different growth responses of maize and lupin to mechanical impedance.

Root tips of maize and lupin differ in shape as shown in Figure 6-4. The root tip of the young lupin primary root is surrounded by long strings of borderlike cells and mucilage, which changes the form of the root tip from narrowly pointed to a blunter shape. This is in contrast to maize, which exudes mucilage and releases individual border cells from its tip. Maize roots exude mucilage around the root tip while lupin mucilage tends to accumulate around the flanks of the root too (Read and Gregory, 1997). Both, mucilage and border cells have a lubricating effect and decrease soil mechanical impedances (Iijima et al., 2004). Lupin may initially be less sensitive to mechanical impedance because of a greater lubricating effect due to mucilage around a greater surface of the root than maize. The thick layer of border cells may also act as a hydraulic border between the lupin root tip and the soil – to a greater extent than in maize.

*Prediction of root elongation rates from distance between root tip and root hair zone*

The relationship between root elongation rate and distance between root tip and root hair zone was determined for a wide range of soil physical conditions. Watt et al. (2003) and Pagès et al. (2009) showed a strong correlation between root elongation rate and the distance between root tip and root hair zone: Root elongation of maize in the study of Pagès et al. (2009) was transiently reduced by rotating the cylinder pots in which the plants were grown, whilst Watt et al. (2003) conducted experiments with wheat in loose and compacted soil. The results in this Chapter showed root elongation rate was better correlated to the distance between root tip and root hair zone for maize than for lupin.

Pagès et al. (2009) suggested that the differentiation period of cells requires a specific time, while the study from Watt et al. (2003) showed that the cells of mechanically impeded roots differentiate sooner than cells of roots grown in loose soil. It is difficult to say what leads to a shorter elongation zone in stressed roots, but it is known that in mechanically impeded roots cell walls become stiffer in axial direction and corresponding root elongation zones are shortened (Bengough et al., 2006). Root elongation zones are also shortened in water stressed roots, but local growth rates (strain rate mm $mm^{-1}$ $h^{-1}$) are maintained in the apical region, which is probably due to softening of the cell walls in the axial direction (Sharp et al., 1988; Wu et al., 1996).

The linear relation between the distance of root tip and root hair zone and root elongation rate can be a used to predict root elongation rates for excavated root tips of plants grown in field or lab conditions. This distance between root tip and root hair zone should be averaged for several root tips to predict elongation rates, because mean values showed better linear correlations than the individual raw data (where an exponential curve offers a slightly better fit). Maize had greater correlation values than lupin, which suggests that elongation rates of roots grown under stress condition are more predictable than for lupin – this is probably because of the greater sensitivity of maize towards both decrease in matric potential and increase in mechanical impedance.

*Effects of aggregate size on root–soil contact and root and shoot elongation*

In the second experiment the effect of aggregate sizes on root–soil contact root and shoot elongation was studied when soil was wetted to different matric potentials. Maize and lupin were grown in aggregates of 4–2 mm, 2–1 mm, 1–0.5 mm and <0.5 mm. Many

studies have looked at the impact of aggregate size on total root length under the aspect of mechanical impedance (see Table 6-1) but relatively little information is available of the effect of aggregate size and matric potential on root and shoot elongation. It was hypothesized that, when soil becomes drier smaller aggregate size will have improved root–soil contact. Root elongation in the two wettest treatments decreased with increasing aggregate size, whilst for the driest treatment no differences in root elongation between aggregate sizes were found.

It was thought initially that a greater mechanical impedance of coarser aggregates may have caused the decrease in root elongation observed (Donald et al., 1987). This would explain why shoot elongation was not affected by aggregate size, as shoot elongation is more sensitive to matric potential than soil strength (Sharp et al., 1988). However root diameters were similar in all aggregate fractions, suggesting that the roots did not experience large mechanical impedance (Kirby and Bengough, 2002; Materechera et al., 1991).

Image analysis of 3-D volumetric images of roots in different aggregate sizes showed there was greater root–soil contact in finer aggregate sizes. It is possible that in relatively wet soils greater root–soil contact is advantageous, whereas in drier soil, good root–soil contact may sometimes represent a disadvantage. In the wetter treatments good root–soil contact would allow faster uptake of both water and nutrients, and increased diffusion of any growth inhibitors away from the root cap. This was also supported by the results of root elongation rates of maize and lupin in relation to root–soil contact. Relatively small

increases in root–soil contact (approximately 10-15 %) when root–soil contact was poor lead to significantly faster root elongation rate (Figure 6-11).

In drier soil poor root–soil contact may tend to hydraulically isolate the root from the soil.Carminati et al. (2009) determined a decrease in root–soil contact of lupin roots in drying soil caused by shrinkage of the roots, which probably prevented water loss from the plant. Thus, roots in soil of 4–2 mm and matric potential of -0.81 MPa might have elongated faster than in finer soils because of a smaller root–soil contact and therefore fewer water losses from plant to soil.

*Effect of root hairs in soil of different aggregate fractions on root elongation*

Root elongation of maize wildtype was greater than for the mutant, and it is well established that root hairs can improve water and nutrient uptake (Gahoonia and Nielsen, 2003; Genc et al., 2007; Itoh and Barber, 1983). Observation of root elongation of wildtype and hairless mutant on moist cotton wool showed slower root elongation of the hairless mutant which indicated a pleiotropic effect (mutational gene alters more than one phenotypical characteristic) on the hairless mutant. Hence, root elongation rates of each treatment were normalised by the fastest root elongation rate of either the wildtype or the hairless mutant [it should be noted that root elongation rates of roots on moist cotton wool did not reach values of roots grown in the wettest soil treatment]. These root elongation rates did not vary between wildtype and hairless mutants as a function of matric potential and aggregate size. Hochholdinger et al. (2004) reported similar phenotypes of the wildtype and the mutant except for root hairs, but did not report root elongation rates directly.

## 6.5 Summary

In this Chapter the effects of combined stresses, such as water stress and mechanical impedance on root and shoot elongation rate of maize and lupin were considered. Maize and lupin were grown in soil packed to five different bulk densities (1.1 g $cm^{-3}$ to 1.5 g $cm^{-3}$) and wetted to water contents corresponding to three matric potentials of -0.01 MPa, -0.4 MPa and -1.2 MPa. The effects of matric potential and mechanical impedance were strongly dependant on plant species. Root elongation rates of maize were significantly affected by a decrease in matric potential and increase in penetrometer resistance, while lupin was significantly reduced by increasing soil strength but not by decreasing matric potential. Linear correlations of root elongation rate and the distances between root tip and root hair zone for maize and lupin were found. This relationship can be used as an indicator of root elongation rate, but the estimation is dependant on plant species.

Shoot elongation rates of both maize and lupin were significantly decreased with decreasing matric potential and increasing penetrometer resistance. The greater root–soil contact with increasing bulk density did not improve the growth conditions in this case as the root elongation rate was reduced by mechanical impedance.

Furthermore the role of root–soil contact in soils of limiting water availability was tested. Maize and lupin were grown in soil of four aggregate sizes (4-2 mm, 2-1 mm, 1-0.5 mm and <0.5 mm) wetted to three matric potentials (-0.03 MPa, -0.2 MPa, -0.81 MPa and -1.6 MPa). Root and shoot elongation rate increased with decreasing aggregate size when soil was wetter than -0.81 MPa and a greater root–soil contact was determined with finer

aggregate sizes. It was concluded that a greater root–soil contact can improve growth conditions when mechanical impedance is not limiting root growth.

# 7 Effects of root surface area contributing to water uptake on root and shoot elongation

## 7.1 Introduction

The importance of the different pathways of water flow in non–transpiring seedling roots is not clear. This is partly because of the anatomical complexity of root structure which varies with plant species and age, as well as changes in root tissue caused by environmental stresses (Gregory, 2006). Three pathways for water transport across living tissue exist (Figure 7-1): a) through the cell walls (apoplastic flow); b) from cell to cell, along the symplasm through plasmodesmata (symplastic flow); and c) across membranes (transcellular flow). The apoplast includes cell walls, intercellular space and the lumena of trachery elements, while the symplast is the continuum of cytoplasm interconnected by plasmodesmata and excluding the vacuoles (Steudle and Peterson, 1998). The third pathway for water flow is when water flows through the cells bypassing membranes (Steudle and Peterson, 1998). Symplastic flow and the transcellular flow are difficult to measure separately and are therefore 'summarized' as the cell–to–cell component of transport (Steudle, 2000). It is likely that water flows through a combination of pathways, so that it might travel within the symplast for some distance and then may cross the plasmamembrane and travel via the transcellular path (Steudle and Peterson, 1998).

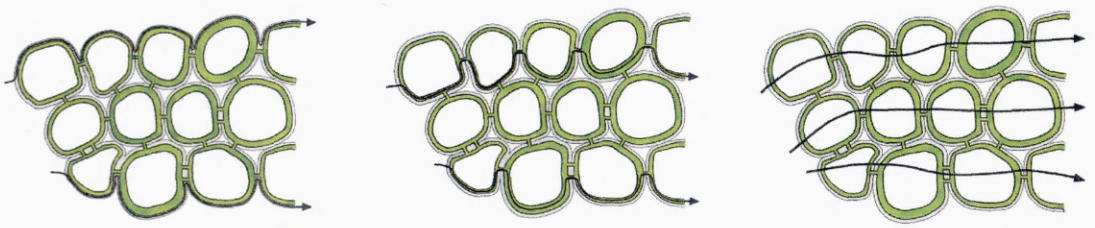

(a) Apoplastic path (b) Symplastic path (c) Transcellular path

**Figure 7-1: Routes of water flow in plant tissue. The tissue is represented by four cell layers arranged in series. (a) Denotes the apoplastic path (cell walls, grey) around protoplasts. The symplastic path (b) is mediated by plasmodesmata which bridge the cell walls between adjacent cells so that a cytoplasmic continuum is formed (green). During the passage along the apoplast and symplast, no membranes have to be crossed. On the transcellular path (c), two plasma membranes have to be crossed per cell layer. The transcellular path is used especially by water which has a high membrane permeability (Copy from Steudle and Peterson, *Journal of Experimental Botany;* Oxford University Press, 1998).**

The amount of water taken up by a root is highly dependent on the hydraulic conductance of the root, which varies with plant species and development age (Gallardo et al., 1996; Rieger and Litvin, 1999). Suberin lamellae and Casparian bands in the apoplast of the endodermis (and in some species in the exodermis) are an impedance to water flow (Gregory, 2006) and increase when plants are stressed (Steudle, 2000). Rieger and Litvin (1999) compared the hydraulic conductivity of two woody and three herbaceous species and found that with increasing diameter the hydraulic conductivity decreased and that the thickness of the cortex had a greater impact on hydraulic conductivity than root diameter. Suberization of cells had some effect on hydraulic conductivity but was less than the thickness of the cortex. Zimmermann and Steudle (1998) have shown that the hydraulic conductivity of maize seedlings was 3–4 times larger when there was no exodermis (roots grown in hydroponics) as compared with roots having an exodermis (roots grown in aeroponics).

Water uptake of roots differs with plant species (Steudle and Peterson, 1998). Monocots and dicots showed differences in water uptake per total root length per unit ground area when grown under different drought stress conditions (Gallardo et al., 1996; Hamblin and Tennant, 1987). Hamblin and Tennant (1987) compared water uptake of spring wheat, barley, lupin and field pea and suggested that the greater water uptake per unit root length for lupin and field pea compared to spring wheat and barley occurred because of the larger metaxylem vessels of the dicots, which give a much lower axial resistance.

Water uptake differs also along the root main axis. Sanderson (1983) studied water uptake of different regions along the primary axis of barley and found that water uptake increased in the first 4–5 cm and decreased towards the zone of lateral emergence, while a relatively constant rate was maintained along the rest of the axis (Sanderson, 1983; Varney and Canny, 1993). Varney and Canny (1993) suggested that water uptake is also affected by root surface area, because maize root branches had a greater surface area and collected more water than the root axis. Roots were grown in a nutrient dye mist using an aeroponic system and the rate of accumulation of dye at sites on the root was translated into a flux of water into the root.

Good root–soil contact is believed to increase water uptake per unit surface area of root (Herkelrath et al., 1977; Veen et al., 1992). Veen et al. (1992) investigated root–soil contact and water uptake of maize in soil of different porosities at matric potentials of -0.01 MPa. Water uptake per unit root surface area decreased with decreasing root–soil contact (Veen et al., 1992).

In the case of non–transpiring seedling roots, water uptake will be driven largely by osmotic potential in the cells of the root and epidermis (Kramer and Boyer, 1995). Water will be required for cell expansion and may be accompanied by growth induced changes in water potential. The elongation of roots may be decreased by changes in cell wall stiffness that depends on the physical environment (strength and matric potential) of the root (Bengough et al., 2006; Wu et al., 1996). Thus the local environment of different regions of the root surface may affect elongation to different extents. Diffusion of root–sourced growth inhibitors away from the root may also affect root elongation (Stirzaker et al., 1996)

Previous chapters have indicated that root–soil contact is important for root and shoot elongation. The aim of this chapter was to find a method to test if contact between root, solid and water affects root and shoot elongation. An aeroponic system was used to supply young maize and lupin seedlings with water. Plant roots were exposed to a fine mist of water and roots were covered at different positions and different lengths with sealed plastic tubes to avoid contact with the mist. It was hypothesized that the greater the root surface area exposed to the mist the faster the root and shoot elongation. Moreover it was hypothesized that when root sections closer to the tip are exposed to free water, root and shoot elongation will be faster. In addition total root length was exposed to the mist and different contact with a solid phase was given. It was assumed that contact between root and solid phase would not increase root and shoot elongation because transport to and from the root surface would not change. In a second experiment roots were placed above a water surface and supplied with water at different positions and lengths through moist cotton wool. It was hypothesized, that the greater the surface area covered in moist

cotton wool the faster root and shoot elongation would be, because the plant would sense a more favourable growth environment.

## 7.2 Materials and methods

### 7.2.1 Experiments in aeroponic system

*Aeroponic system*

An aeroponic system was designed for growing maize and lupin seedlings (Figure 7-2). A plastic–tank (77 cm × 40.5 cm × 27 cm, volume 20 l) was filled with 10 l water and a triple membrane mister unit (Lotus Water Garden Products Ltd, Burnley, UK) was placed in the water. A fine cool mist of 3–5 μm diameter droplets was produced and circulated by a ventilation system to ensure equal distribution of the mist. Air circulation was provided by a fan and blown into the system through a tube. The air was released 5 cm above the water surface through four holes 15 cm from each other across the tank.

Seedlings were placed on top of a mesh, which was stretched over a mesh pot. The mesh pots were placed above the water surface, so that radicles were exposed to the mist. The tank was covered with a lid to keep the moisture inside. The temperature in the chamber increased because the mister unit released heat and the water temperature increased. Therefore an open water reservoir outside the system was installed. Water was pumped from the aeroponic system into the water reservoir with a pump (Maxi Jet 1000 l $h^{-1}$) and circulated back into the aeroponic tank by gravity (Figure 7-2) to reduce temperature increase. Temperature was controlled to 20 °C within 3 °C.

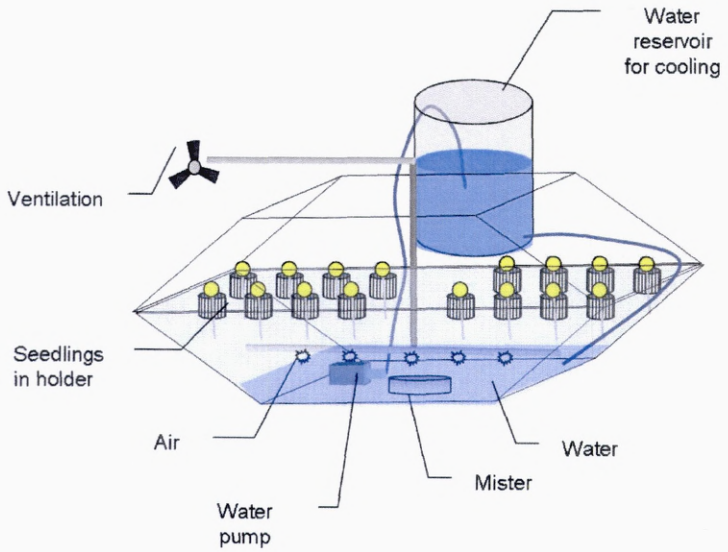


**Figure 7-2: Schematic drawing of aeroponic system with mister unit, ventilation and cooling.**

The distribution of mist was tested by placing 12 germinated lupin and 12 germinated maize seedlings in the aeroponic system in a growth chamber at 20 °C for 24 h. Two seedlings of both plants were placed alternately in each row in horizontal direction (Figure 7-2). Root length of the primary root was recorded at the start and after 24 h.

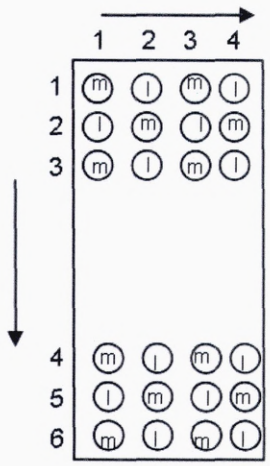


**Figure 7-3: Schematic drawing of distribution of maize (m) and lupin (l) in horizontal and vertical direction in aeroponic system.**

The average root elongation rate for each row in vertical and in horizontal directions was determined using Equation 4-2.

*Seedling preparation*

The contribution of different parts of a root to root and shoot elongation was examined. Germinated maize and lupin seedlings with 1.5 to 2.5 cm long radicles were covered with a 1 cm plastic tube with a diameter of 3 mm (taken from a 1 ml Pasteur disposable pipette) at three different positions (Figure 7-4): root tip, 1 cm from root tip and directly below the seed. The tube ends were covered with Nescofilm to keep the mist out; a small hole was made in the Nescofilm to allow the root through. A treatment where the root was not covered was used as control. Seedlings were supported by a funnel-shaped plastic head to keep the seedling in position. Three replicates of each treatment were randomly distributed in the aeroponic system.

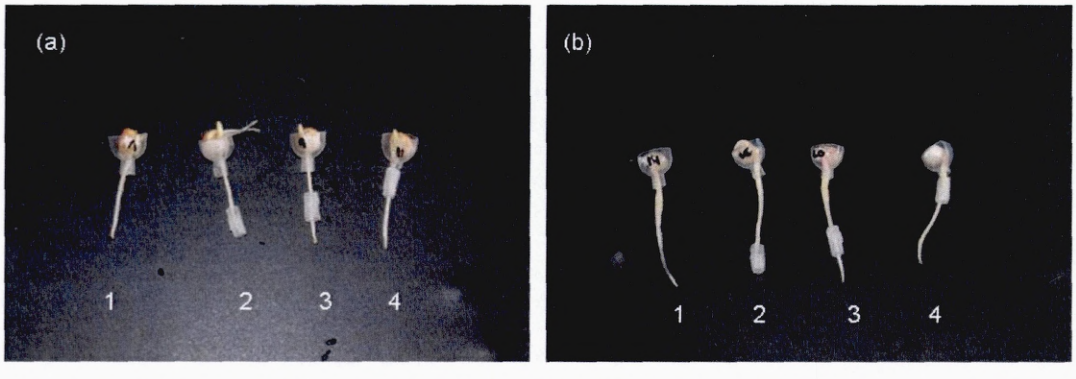


**Figure 7-4: Maize (a) and lupin (b) seedlings with 1.5–2.5 cm long primary roots; parts of the root are covered with 1 cm plastic tubes and a control treatment with no coverage. The root is either covered at the root tip (2), 1 cm above the root tip (3) or below the seed (4). The ends of the tube are sealed with Nescofilm.**

In another experiment root elongation rates were determined when maize and lupin roots were grown in tubes of different diameter to allow different amounts of contact with the solid phase (Figure 7-5) Disposable pipettes of 0.5 ml (diameter 2 mm), 1 ml (diameter 4 mm) and 3 ml (diameter 6 mm) were cut to 6.5 cm length. The walls of the top 1.5 cm were removed except for 1 mm wide ribbons on opposite sides to keep the tube in place (Figure 7-5). Seedlings with 1.5 mm to 2 mm long radicles were placed in the funnel-shaped head of the pipettes and the root tip was placed inside the tube. Roots which were without a tube were placed as a control in the aeroponic system. Three replications of each treatment plus control were distributed randomly in the aeroponic system.

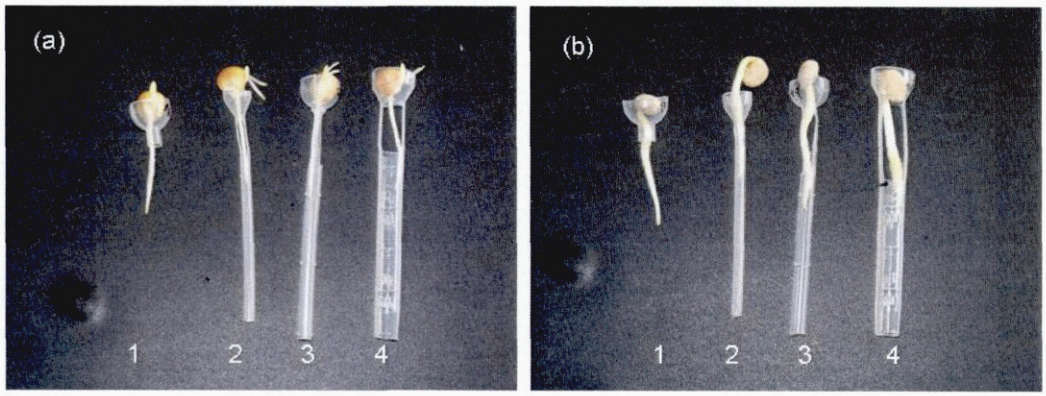


**Figure 7-5: Maize (a) and lupin (b) seedlings with 1.5–2.5 cm long primary roots; root tip placed in to tubes of 2 mm (2), 4 mm (3) and 6 mm (4) diameter to allow elongation down the tube and a control treatment (1) where the root is not place in a tube.**

An additional experiment was conducted where maize and lupin seedlings with 2 mm to 2.5 mm long radicles were placed in tubes of 4 mm diameter. The tubes were cut to 1 cm or 2 cm length. The inside of the tube walls were lined with moist cotton wool (Figure 7-6). Four replicates of each treatment and control were placed randomly in the aeroponic system.

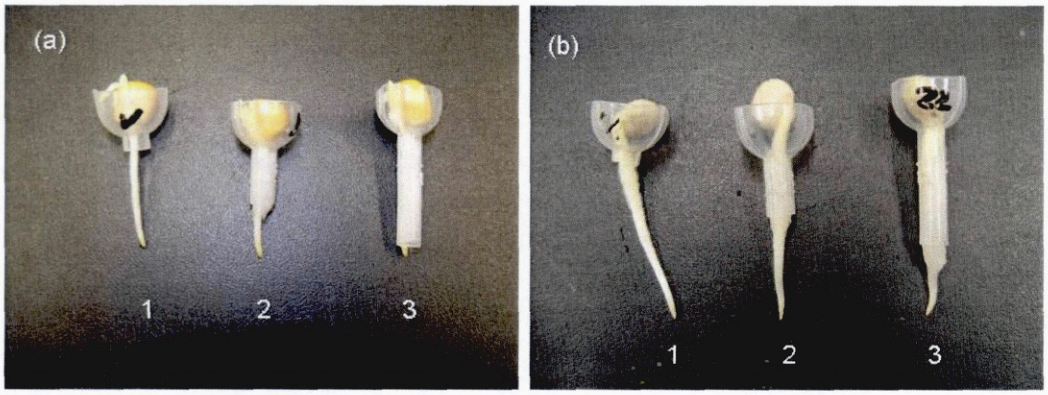


**Figure 7-6: Maize (a) and lupin (b) seedlings with 1.5–2.5 cm long primary roots; roots are placed in tubes (4 mm diameter) of 1 cm (2) or 2 cm (3) length equipped with moist cotton wool and a control treatment (1).**

All three experiments were placed in a growth cabinet at 20 (±3) °C and left for 48 h in darkness. The variation in temperature was caused by the heat output of the aeroponic system. Root and shoot length were measured with a ruler at the start and after 48 h and root elongation rates were determined (Chapter 4.2.1, Equation 4-2).

### 7.2.2 Experiments above water surface

*Growth environment*

A plastic-tank (77 cm × 40.5 cm × 27 cm) was filled with 10 l water. Maize and lupin seedlings were placed on top of a mesh, which was stretched over a mesh pot. The mesh pots were placed above the water surface and the tank was covered with a lid to keep the moisture inside (Figure 7-7). The tank was placed in a growth chamber at 20 °C in darkness.

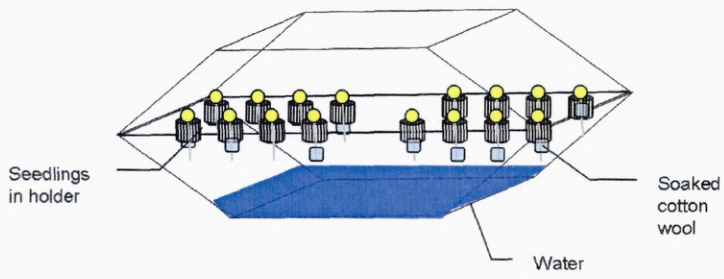


**Figure 7-7: Schematic drawing of seedlings equipped with moist cotton wool placed above water surface in a tank covered with a lid.**

*Seedlings preparation*

Germinated maize and lupin seedlings were covered with a plastic tube of 1 cm length and 1.2 cm in diameter at either root tip, 1 cm from root tip or below the seed; there was also a control treatment with no cover (Figure 7-8). The inside of the tube was lined with moist cotton wool and the ends of the tubes were sealed with Nescofilm to avoid evaporation. The tubes were supported by a thread which kept the tube in place but which extended with root growth. Four replicates of each treatment were randomly placed in the growth chamber.

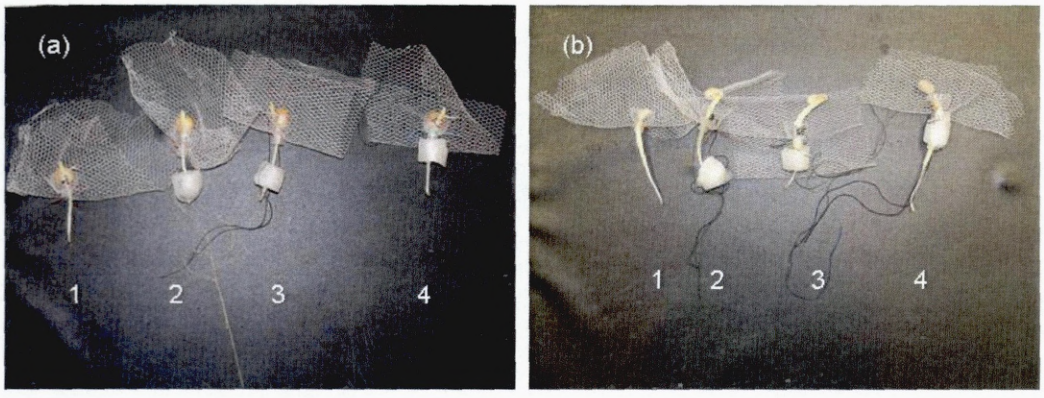


**Figure 7-8: Maize (a) and lupin (b) seedlings with 1.5–2.5 cm long primary roots, parts of the root are covered with 1 cm plastic tubes (diameter 1.2 cm) equipped with moist cotton wool and a control treatment (1, no tube). The root is either covered at the root tip (2), 1 cm above the root tip (3) or below the seed (4).**

In a second experiment, maize and lupin roots were covered with plastic tubes of different diameter and length: length 2 cm, diameter 0.6 cm; length 1 cm, diameter 0.8 cm and length 0.6 cm and diameter 1.2 cm and a control treatment with no cover. The tubes were filled with moist cotton wool surrounding the primary root (Figure 7-9).

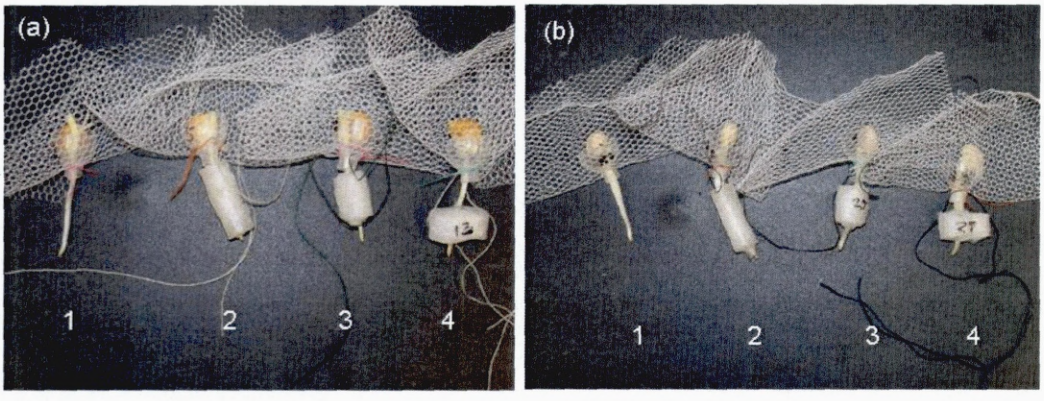


**Figure 7-9: Maize (a) and lupin (b) seedlings with 1.5 –2.5 cm long primary roots; roots are placed in tubes of 0.6 cm (2, diameter 1.2 cm) 1 cm (3, diameter 0.8 cm) or 2 cm length (4, diameter 0.6 cm) equipped with moist cotton wool and a control treatment (1, no tube).**

Maize and lupin seedlings were then placed randomly in the growth chamber at 20 °C for 48 h in darkness. As with the experiments conducted in the aeroponic system, root and shoot elongation rates were determined after 48 h.

The cotton wool insert in each tube was weighed before and after saturation and the amount of water added was determined. Cotton wool was weighed again after 48 h of growth to determine the water uptake.

## 7.3 Results

### 7.3.1 Experiments in the aeroponic system

The uniformity of mist distribution in the aeroponic system was tested by growing maize and lupin for 24 h. Root elongation rates of maize and lupin showed no significant differences in the horizontal ($p = 0.778$) or vertical directions ($p = 0.458$; Figure 7-10).

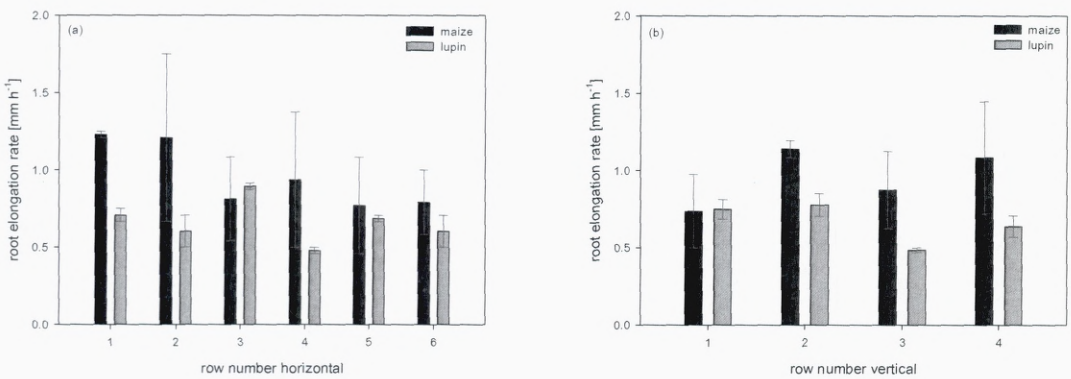


**Figure 7-10: Average root elongation rates per row [mm $h^{-1}$] of maize in aeroponic system in horizontal (a) and vertical (b) direction. Data are means ±SE. Horizontal direction n = 2; vertical direction n = 3.**

Examples of seedlings covered with 1 cm of sealed plastic tube after 48 h are shown in Figure 7-11). Maize roots covered at the tip buckled, while lupin roots covered at root tip grew straight, but the diameter of the root was greater compared to the other treatments.

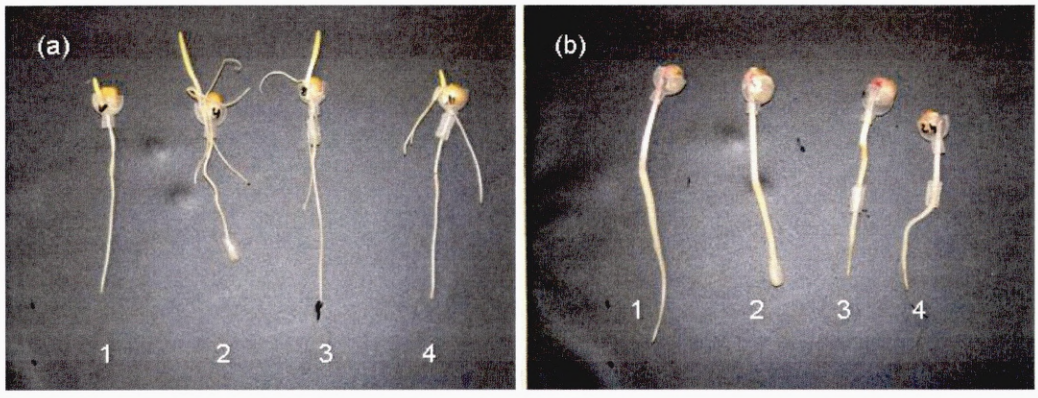


**Figure 7-11: Maize (a) and lupin (b) seedlings after 48 h in aeroponic chamber; parts of primary roots are covered with 1 cm plastic tubes and a control treatment with no coverage (1). The root is either covered at the root tip (2), 1 cm above the root tip (3) or below the seed (4). The ends of the tube are sealed with Nescofilm.**

Root elongation rate of maize and lupin was slowest when the root tip was placed in 1 cm long tubes, but differences between treatments were not significant ($p = 0.172$; Figure 7-12). Lupin root elongation ($0.42 \pm 0.06$ mm $h^{-1}$) was significantly slower than that of maize ($0.98 \pm 0.12$ mm $h^{-1}$; $p < 0.001$).

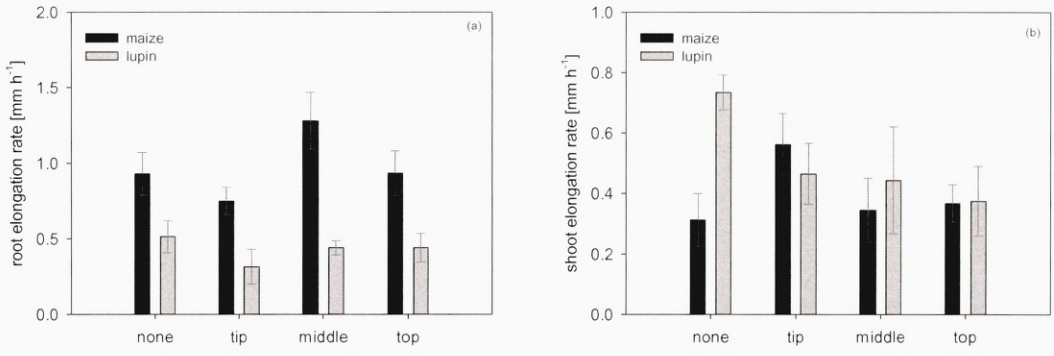


**Figure 7-12: Root (a) and shoot (b) elongation rates of maize and lupin in aeroponic system. Parts of primary roots were covered with 1 cm plastic tubes and a control treatment with no coverage. The root is either covered at the root tip (tip), 1 cm above the root tip (middle) or below the seed (top). Data are means ±SE (n =3).**

Shoot elongation rate of the maize control (0.31 ±0.09 mm $h^{-1}$) was significantly smaller than that of the lupin control (0.73 ±0.06 mm $h^{-1}$; p = 0.005; Figure 7-12). Overall shoot elongation of seedlings was not influenced by coverage of different areas of the root (p = 0.384).

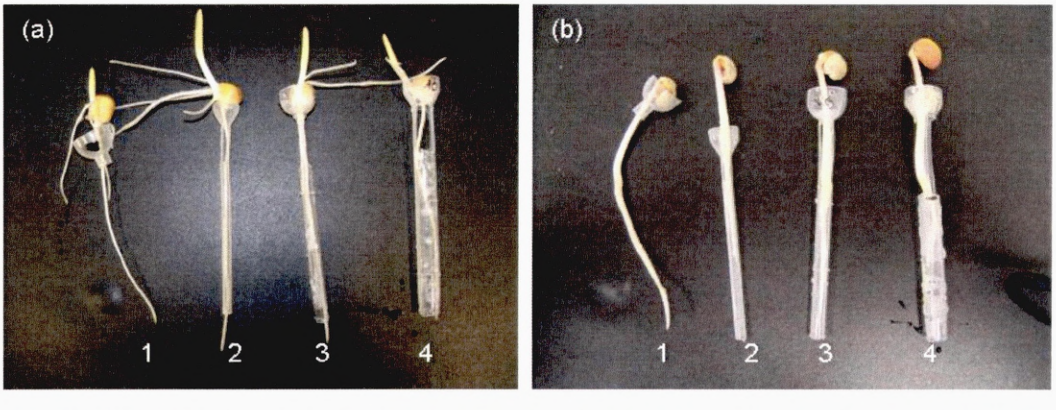


**Figure 7-13: Maize (a) and lupin (b) seedlings after 48 h in aeroponic chamber with 1.5–2.5 cm long primary roots; roots grown down in tubes of 2 mm (2), 4 mm (3) and 6 mm (4) diameter and a control treatment (1, no tube).**

Maize roots grown down tubes of three different diameters were oriented down the tube walls, while lupin roots were centred in the tubes (Figure 7-13).

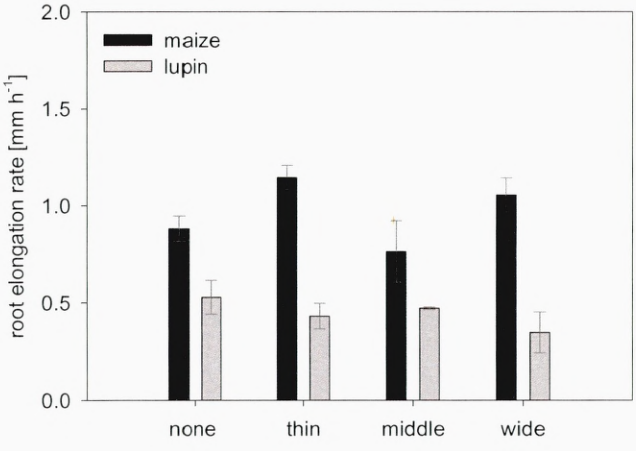


**Figure 7-14: Root elongation rates of maize and lupin roots placed in aeroponic system in tubes of different diameter (2 mm, 4 mm and 6 mm) and a control treatment with no tube in aeroponic system after 48 h.**

Root elongation of lupin was slower ($0.44 \pm 0.06$ mm $h^{-1}$) than of maize ($0.96 \pm 0.04$ mm $h^{-1}$) but tube diameter did not affect root elongation rate ($p = 0.384$, Figure 7-15).

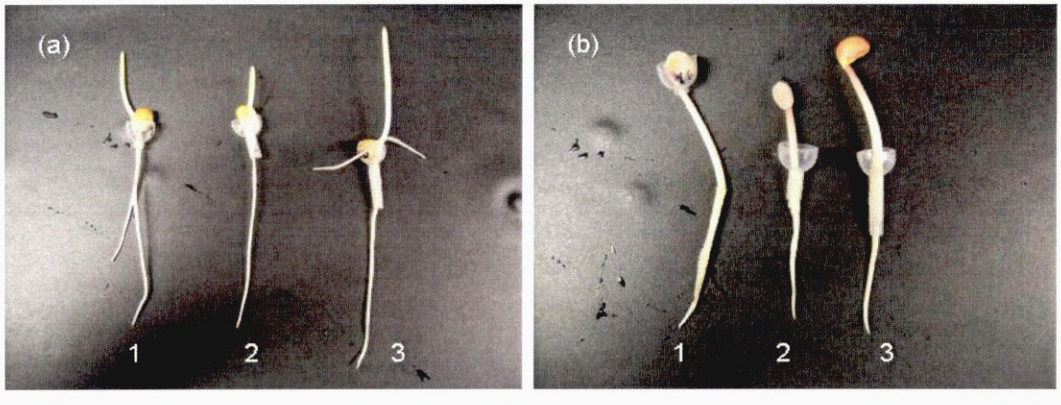


**Figure 7-15: Maize (a) and lupin (b) seedlings after 48 h in aeroponic chamber; roots are placed in tubes (4 mm diameter) of 1 cm (2) or 2 cm length (3) equipped with moist cotton wool and a control treatment not covered (1).**

Roots of maize and lupin seedlings grown for 48 h in tubes filled with moist cotton wool of 1 cm and 2 cm length had similar diameter and length as the control (Figure 7-15).

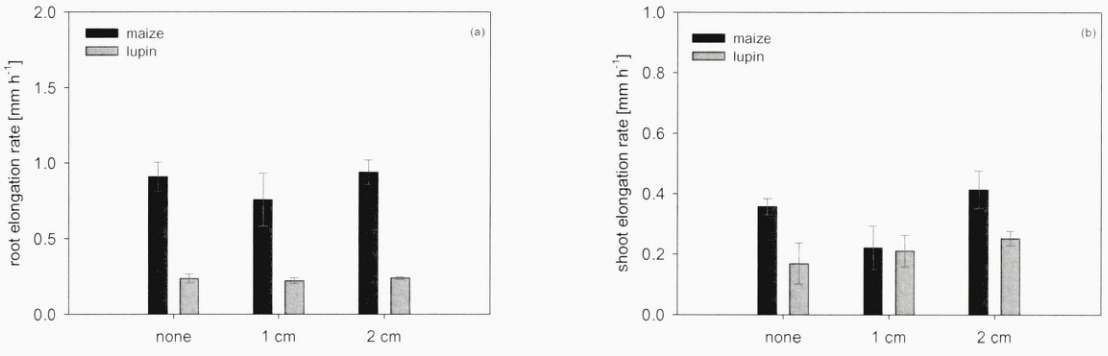


**Figure 7-16: Root elongation rates of maize and lupin roots during 48 h in aeroponic system placed in tubes of different length (1 cm and 2 cm) and equipped with moist cotton wool and a control treatment with no tube. Data are means ±SE (n = 4).**

Root and shoot elongation rates of maize and lupin were not affected by contact with cotton wool (Figure 7-16), but elongation rates of lupin (root 0.24 ±0.03 mm $h^{-1}$; shoot 0.22 ±0.03 mm $h^{-1}$) were significantly less ($p < 0.001$) than those of maize (root 0.87 ±0.07 mm $h^{-1}$; shoot 0.33 ±0.04 mm $h^{-1}$).

## 7.3.2 Experiments above the water surface

Maize and lupin roots grown for 48 h above a water surface are shown in Figure 7-17. Roots of seedlings with no cover and those covered at root tips were shorter than roots covered closer to the seed.

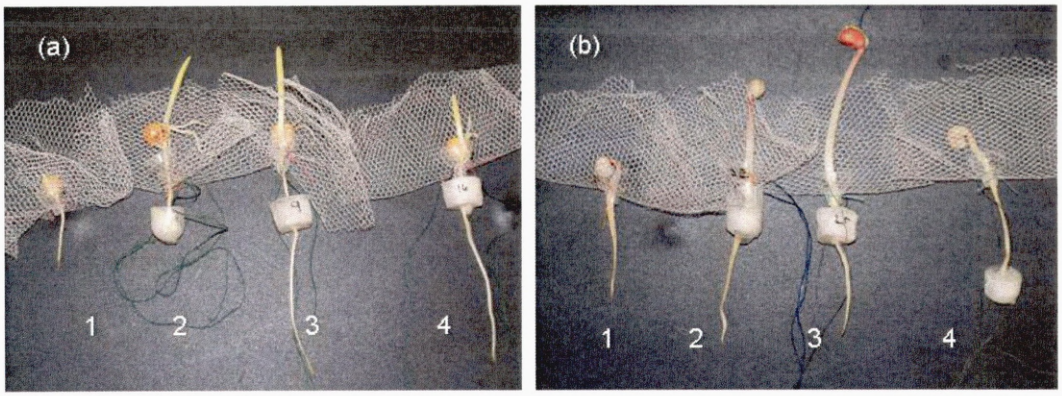


**Figure 7-17: Maize (a) and lupin (b) seedlings after 48 h above water surface; roots are placed in tubes of 1 cm (diameter 1.2 cm) equipped with moist cotton wool and a control treatment (no tube). The root is either covered at the root tip (2), 1 cm above the root tip (3) or below the seed (4).**

Roots of maize and lupin were thickened a few mm from the root tip when the root tip was covered. An example is shown in Figure 7-18.

**Figure 7-18: Lupin seedling after 2 days grown above water surface when root tip was covered in cotton wool.**

Roots of maize and lupin elongated significantly faster when supplied with water through cotton wool ($p < 0.001$; Figure 7-19) than when no water was supplied through cotton wool.

Roots elongated slower when they were covered with moist cotton wool at the root tip (maize 0.25 ±0.03 mm $h^{-1}$; lupin 0.14 ±0.02 mm $h^{-1}$) than when the cotton wool was placed directly below the seed (maize 0.99 ±0.03 mm $h^{-1}$; lupin 0.22 ±0.02 mm $h^{-1}$) or 1 cm above the root tip (maize 0.84 ±0.13 mm $h^{-1}$; lupin 0.31 ±0.07 mm $h^{-1}$).

Maize roots elongated faster than those of lupin when covered with moist cotton wool (Figure 7-19; $p < 0.001$). Maize shoots did not elongate when not in contact with moist cotton wool, but shoot elongation rates of maize were similar for all three cotton wool treatments ($p = 0.514$). Shoot elongation rate of lupin was significant slower with cotton wool at the tip than when water was supplied further along the root axis ($p = 0.007$; Figure 7-19).

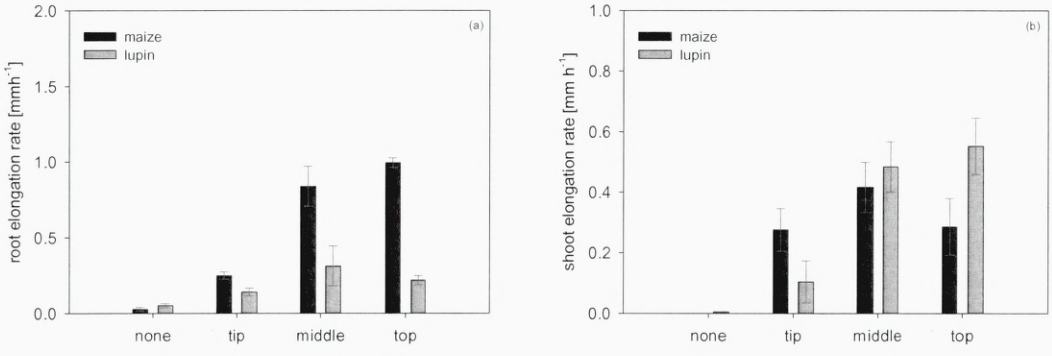


**Figure 7-19: Maize (a) and lupin (b) seedlings after 48 h grown above water surface; roots were placed in tubes of 1 cm (diameter 1.2 cm) equipped with moist cotton wool and a control treatment (no tube). The root is either covered at the root tip (tip), 1 cm above the root tip (middle) or below the seed (top).**

Roots in contact with moist cotton wool in tubes of different diameter were longer than the control treatment, but roots of the three cotton wool treatments looked the same (Figure 7-20).

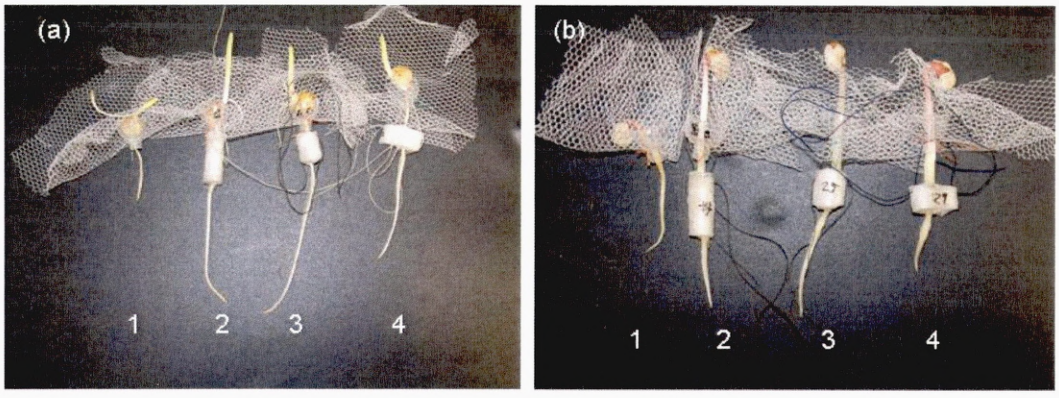


**Figure 7-20: Maize (a) and lupin (b) seedlings after 48 h above water surface; roots are placed in tubes of 0.6 cm (2, diameter 1.2 cm) 1 cm (3, diameter 0.8 cm) or 2 cm length (4, diameter 0.6 cm) equipped with moist cotton wool and a control treatment (1, no tube).**

Root elongation rates were significant greater when roots were in contact with moist cotton wool ($p < 0.001$), but the area of root surface in contact had no effect. Root elongation of maize was faster when in contact with moist cotton wool than lupin but slightly slower when the root had no contact with moist cotton wool (Figure 7-21).

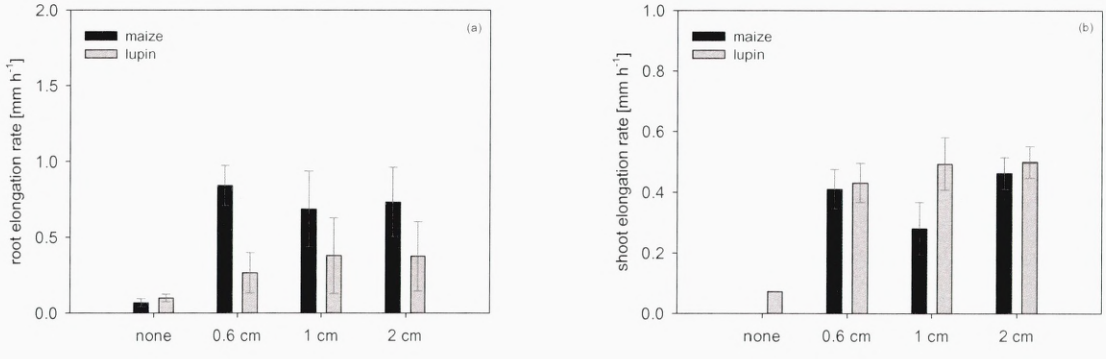


**Figure 7-21: Maize (a) and lupin (b) seedlings after 48 h above water surface; roots are placed in tubes of 0.6 cm (diameter 1.2 cm) 1 cm (diameter 0.8 cm) or 2 cm length (diameter 0.6 cm) equipped with moist cotton wool and a control treatment (1, no tube).**

There was no maize shoot elongation found, when seedlings had no contact with moist cotton wool. The area covered by cotton wool did not affect shoot elongation rate of either plant ($p = 0.502$; Figure 7-21).

**Table 7-1: Weight of dry cotton wool insert in tubes of 0.6 cm (diameter 1.2), 1 cm (diameter 0.8 cm) and 2 cm (diameter 0.6 cm) length; water added to cotton wool; amount of water left in cotton wool after 48 h and calculated water loss from cotton wool.**

| Plant | Treatment | Weight cotton wool [mg] | Weight water added to cotton wool [mg] | Weight water at end of experiment [mg] | Water loss [mg] |
|---|---|---|---|---|---|
| Maize | 2 cm | 58.53 | 752 | 400.6 | 351.4 |
| | | ±1.53 | ±8.39 | ±52.73 | ±58.49 |
| Maize | 1 cm | 58.6 | 707.33 | 297.33 | 410 |
| | | ±1.24 | ±19.23 | ±86.61 | ±83.82 |
| Maize | 0.6 cm | 58.34 | 738.98 | 315.05 | 423.93 |
| | | ±1.08 | ±20.30 | ±82.97 | ±87.89 |
| Lupin | 2 cm | 59.93 | 690.5 | 190.2 | 500.3 |
| | | ±0.33 | ±16.58 | ±49.24 | ±40.92 |
| Lupin | 1 cm | 59.03 | 655.25 | 178.4 | 476.85 |
| | | ±1.40 | ±9.94 | ±80.22 | ±79.40 |
| Lupin | 0.6 cm | 58.13 | 721.25 | 335.73 | 385.53 |
| | | ±1.21 | ±26.26 | ±52.28 | ±33.09 |

The amount of water added to dry cotton wool did not differ between the treatments ($p = 0.66$), but for lupin was slightly less than for maize ($p = 0.008$). The water content of cotton wool after 48 h was similar for all treatments ($p = 0.843$), which indicates that maize took up slightly more water than lupin.

## 7.4 Discussion

*Aeroponic system and chamber for root growth above water surface*

In this study an aeroponic system was built to study effects of contact area between root and water on root elongation. The mist distribution in the aeroponic system was tested by comparing elongation of maize and lupin at different locations in the chamber. No significant differences in root elongation were measured suggesting that the mist distribution was uniform.

The droplets produced in the aeroponic system were between 5 μm and 10 μm in diameter similar to a system used by Jarstfer and Sylvia (1995). They tested three different mister units and found the ultrasonic device failed to provide enough free moisture at the root surface so that the root growth was poor. Roots in the aeroponic used in this study showed well moistened root surface and plant growth did not appear to be limited by water stress.

The water temperature increased because the mister unit released heat. Even though water was circulated from the aeroponic tank into a water reservoir outside the aeroponic system temperature still varied by three degrees from the growth cabinet temperature. Temperature in the chamber where plants were grown above a water surface was less variable. This must be considered when comparing results from these two experimental systems, because plant growth is quite sensitive to changes in temperature (Vincent and Gregory, 1989).

*Roots covered with plastic tube and moist cotton wool at different positions*

The main objective of this chapter was to find a method for investigating the importance of contact area between root and water for root and shoot elongation. First it was tested if root and shoot elongation is affected when different parts of the root are not in contact with water. Parts of maize and lupin roots were covered at different positions with a sealed plastic tube. In this study it was not possible to completely avoid contact between the root and solid phase (seal of tube), but the contact area between Nescofilm and root was proportionately very small. Maize and lupin root and shoot elongation was not affected by smaller root surface area in contact with water, as long as there was direct contact) nor position of coverage. These results were similar to those results obtained of seedlings grown above the water surface, where water was supplied through moist cotton wool which was placed at three different positions. There were no differences in root and shoot elongation when the cotton wool was placed 1 cm above the root tip or at the more basal position, but when the cotton wool was placed at the root tip, roots elongated significantly slower. These differences in root elongation were due rather to mechanical impedance than to differences in root water uptake along the root axis, as indicated by thickening of the root diameter. These results suggest that root and shoot elongation rate is not affected by the part of the root in contact with the water. It is likely that the part of root covered in cotton wool was almost completely in contact with a continuous film of water.

The roots measured in this study were relatively young; in older roots the elongation rates might be affected differently by the part of the root in contact with water. Sanderson

(1983) and Varney and Canny (1993) measured water uptake along roots and found greatest water uptake 4 to 5 cm from the root tip with slower water uptake rates further along the root axis, possibly because and suberization in older tissue had slowed water uptake in the 1 to 2 weeks old seedlings.

Because root elongation rate was not affected by the position the plastic tube and cotton wool was placed, in following experiments no differentiation between positions of coverage were made.

*Roots in contact with cotton wool water reservoirs of different length*

The water loss from different length of cotton wool reservoirs (Table 7-1) indicated that, regardless of the root length covered with cotton wool and therefore of the contact area between water and root, water uptake was not significantly affected ($p = 0.843$). Water uptake per unit length was approximately 3 times greater for the shorter reservoir than the long: Presumably this is because water transport at the soil–root interface was not limiting uptake. Limitation to water flow may occur to radial and axial flow, as water may travel both apoplastically and symplastically through the root. For example, permeability of cell membranes may change with the activity of water channel proteins (aquaporins). Aquaporins have the ability to change their permeability to water in a short period of time (few hours to 2–3 days) in response to many stimuli (Javot and Maurel, 2002).

Root water uptake via vapour transport was probably negligible the distance between seedling and water surface was 10 to 20 cm depending on the growth rate (while vapour

transport is more important at small distances of a few mm; Owen, 1952). This was also indicated by the very slow root and shoot elongation rate of lupin and no shoot elongation of maize, when roots were not supplied with water through cotton wool. Seedlings probably used water stored in the seeds during the germination process for root and shoot growth, rather than uptake via vapour transport.

It was of interest to determine whether contact of roots with the solid phase affected root and shoot elongation, when the total root surface has access to water. Roots were placed in tubes of different diameter and exposed to the mist in the aeroponic system (Figure 7-5). It was initially assumed that they would change direction in the tube due to circumnutation (spiral movement of root tip) and so have greater contact the smaller the diameter of the tube. However, roots tracked down one side of the tube once they contacted the tube wall, instead of changing direction. Therefore the roots in tubes of different diameter had similar contact with the tube wall. Root elongation rate of roots in tubes of different diameter were the same, but contact with the solid phase was probably similar too (Figure 7-13).

In another experiment contact between root and solid phase was provided by saturated cotton wool. The plants were placed in the aeroponic system, where parts of the root not covered with moist cotton wool were exposed to the mist, so that the whole root surface was in contact with water, but had different amounts of contact with the solid phase. Root and shoot elongation rates were not affected by contact with cotton wool, this indicating that contact with the growth medium was not important when water availability is good.

*Growth responses of maize and lupin in comparison*

Root elongation rates of lupin were smaller than of maize throughout all experiments but shoot elongation of lupin was similar to shoot elongation of maize. This is probably caused by genetically differences of the two species, rather then by different water uptake rates of the two species. Similar water uptake was suggested by similar water losses from the cotton wool for maize and lupin. Although, smaller axial resistances and greater hydraulic conductivities were reported for lupin compared to cereals (Hamblin and Tennant,1987; Gallardo et al., 1996) Plants used in experiments of Hamblin and Tennant (1987) and Gallardo et al. (1996) were transpiring so that a greater hydraulic conductivity in axial flow direction was increasing the water uptake and the lower axial resistance of lupin roots could explain the greater water uptake rates by lupin compared to cereals, while in this experiment axial flow was less important, because of non–transpiring plants.

## 7.5 Summary

This Chapter summarizes different experiments which were conducted to find a method to determine the affects of the portion of the root in contact with liquid and solid phase when water availability is not limiting root and shoot growth.

Two different systems were used. Maize and lupin seedlings were placed in either an aeroponic system or above a water surface and supplied with water through moist cotton wool.

Contact of roots with water grown in the aeroponic system was hindered by covering parts of the roots with plastic tubes. No differences in root and shoot elongation rates were found when the plastic tubes were placed close to the seed or close to the root tip. Seedlings above the water surface were supplied with water through moist cotton wool at different positions and had similar elongation rates to the seedlings from the experiment in the aeroponic system, with no differences in contact position, except when placed at the root tip, but in this case roots showed signs of mechanical impedance.

Different positions of contact between the root and a solid phase was provided with moist cotton wool placed at different lengths along the root. When roots were sufficiently supplied with water the amount of contact with the solid phase did not affect root and shoot elongation rates.

Overall, root and shoot elongation was not affected by contact of the root with liquid phase or solid phase, when water was not limiting root growth.

# 8 General Discussion

## 8.1 *Effect of root–particle contact on root and shoot elongation in drying soils*

In this thesis several experiments were conducted to investigate the effects of root–particle contact on root and shoot elongation. A method was developed to determine root–soil contact in 3-D in different media. The method allowed the quantification of root–particle contact with 3 % accuracy. Moreover, hairless mutants were used to investigate the role of root–soil contact in root elongation. From these studies it was concluded that root–soil contact is important for root and shoot elongation when water is limiting growth but only when roots are not mechanically impeded. It was also found that lupin is less sensitive to changes in matric potential and penetrometer resistance than maize, but both maize and lupin showed a linear correlation between root elongation rate and the distance between the root hair zone and root tip.

Soil and plant properties which increase root–soil contact will become more important with climate change and adaption in land management from conventional to no tillage. No-tillage soils have greater soil strength and less pore volume with smaller pores than conventional tilled soils.

### 8.1.1 Root–particle contact and water distribution using X-ray microtomography

A method was developed to determine root–particle contact in 3-D using X-ray microtomography. The accuracy was tested using model systems of known contact areas. Root–particle contact was successfully quantified (accuracy about 3 %) from 3-D volumetric images for maize and lupin roots grown in soil (<2 mm) and vermiculite, as

well as in soil sieved to four aggregate fractions (4–2 mm, 2–1 mm, 1–0.5 mm and <0.5 mm). Until now root–soil contact has only been determined in 2-D from thin sections (Kooistra et al., 1992; Van Noordwijk et al., 1992; Veen et al., 1992). X-ray tomography was used by Carminati et al. (2009) to determine air gap dynamics around the lupin roots in wetting and drying cycles, but root–soil contact was not quantified.

Greater root–particle contact was found in soil than in vermiculite. The greater root–particle contact in soil was probably caused by the smaller size of the aggregates compared to the size of the vermiculite particles. This is supported by the findings of root–particle contact in soil of various aggregate sizes where root–soil contact decreased with increasing aggregate size. Lupin had greater contact with the aggregates in soil (sieved to <2 mm) and with the vermiculite particles than maize, but no significant differences between maize and lupin were determined in soils of different aggregate fractions. The root–soil contact might have been affected by the part of the root used to quantify the contact area, because lupin roots have a tapered shape and therefore a greater diameter further away from the root tip might have compressed the growth medium more and caused greater root–particle contact. However, the growth medium had greater effects on root–particle contact than plant species.

Promising work on water visualization was obtained in Chapter 3. The water content in a porous medium was quantified with 8–11 % accuracy and first steps for quantifying root–water contact were examined using a contrast enhancer. Root elongation was not significantly affected by the contrast enhancer, which will be helpful for future work in visualising and quantifying root water uptake. Other studies have focussed on

determining water distribution in soils without considering roots (Tippkötter et al., 2009; Mooney, 2002; Wildenschild et al., 2002). Wildenschild et al. (2002) also used a contrast enhancer to visualize water in coarse sand and were able to determine the air–water interfacial contacts using a medial axis analysis. Mooney (2002) determined the water flow pattern in undisturbed soil by scanning samples at field capacity and again after a wetting cycle. Water flow characteristics were similar to macropore structure.

### 8.1.2 Effects of particle size and bulk density

Fundamental knowledge of root and shoot growth responses to decreasing matric potential were obtained by Sharp and co workers (Sharp et al., 1988; Sharp et al., 2004; Spollen and Sharp, 1991; Voetberg and Sharp, 1991) who studied maize grown in vermiculite. The present results showed that root elongation rates decreased with decreasing matric potential in both soil and vermiculite. This agrees with several researchers (Sharp et al., 1988; Taylor and Ratliff, 1969; Veen and Boone, 1990). However root elongation was significantly slower in vermiculite than in soil (up to 50 to 60 %). This was probably caused by greater root–particle contact in soil than in vermiculite although effects of pH might have affected root elongation rates as well. No significant effect of pH on root elongation of maize and lupin was found for pH between 5.2 and 6.9. That greater root–particle contact is beneficial for root and shoot elongation was also shown with the results in soil with different aggregate sizes. Root and shoot elongation rates decreased by up to 34 % in coarser aggregates and root–particle contact was less in coarse aggregates than in fine aggregates. Good root–particle contact in very in the coarsest soil. Carminati et al. (2009) showed that lupin roots in drying soils shrank

in diameter and lost contact with the soil, which might be a mechanism to stop the plant from losing water to the dry soil.

Good root–soil contact is only advantageous when soil strength is not limiting root elongation. It was originally hypothesized that root elongation rate will increase initially as bulk density increases because of greater root–particle contact and then decrease because of mechanical impedance. However, root elongation rate decreased consistently with increasing bulk density in the range measured because penetrometer resistance increased constantly. These results confirmed findings of other researchers, such as Stirzaker et al. (1996), Veen et al. (1992), Mirreh and Ketcheso (1973) and Taylor and Ratliff (1969). Root–soil contact also probably increased from the lowest bulk density to the highest (Kooistra et al., 1992).

That root–particle contact affected root elongation rate was also suggested by the experiment in humid air, where root elongation of maize and lupin was slower than in soil and vermiculite. In this experiment root elongation was observed without direct contact of the root surface with the water, even though vapour transport would be slower than for a narrower gap between water and the root surface (Owen, 1952).

Comparison of maize and lupin root elongation rates in soil was examined in Chapter 4, where seedlings were placed on top of the soil in a petri dish and in Chapter 6, where seedlings were placed in the centre of a column filled with soil. Greater root elongation rates were found when the seedlings were surrounded by soil; greater root–particle contact in the cores probably led to the faster elongation rates.

Root and shoot elongation rates were measured for repacked cores with relatively uniform soil conditions. In the field cracks and biopores (large continuous pores made by soil fauna or previous roots) provide a more variable environment for root growth with large variations in root–soil contact, so that growth responses to soil physical stresses may differ to those found under controlled conditions (Bengough et al., 2011; Passioura, 1991; Volkmar, 1996). Root–particle contact may become more important in the field when transpiring plants are grown beyond the seedling stage and seed reserves of nutrients and water are exhausted. This is especially so for diffusion–limited nutrients, such as phosphorus. Gahoonia and Nielsen (2003) showed that barley wildtype (with root hairs) continued growth in soil where phosphorous availability was limiting plant growth, while the hairless mutant died after 30 days. The role of root hairs in increasing root–soil contact within subsoil biopores has also been noted by White and Kirkegaard (2010).

### 8.1.3 Effects of root hairs on root and shoot elongation

To test further whether root–particle contact affects root elongation, hairless mutants of maize and barley and their wildtypes were used (Chapter 5 and 6). It was hypothesized that wildtype root and shoot elongation would be faster than those of the hairless mutants. A well–studied hairless barley mutant and its wildtype were used (Gahoonia and Nielsen, 1997; Gahoonia and Nielsen, 2003) together with a maize wildtype and hairless mutant (Hochholdinger et al., 2004). The barley wildtype elongated up to 27 % faster than its hairless mutant in soil and vermiculite and root elongation of the hairless maize mutant was also slower than that of the wildtype, although this difference was not significantly

different at p >0.05. There was no evidence of pleiotropic effects on elongation in barley root mutants. Elongation rates were slower for the maize mutants than for the wildtype under well watered conditions so that pleiotropic effects could not be excluded. Greater root and shoot elongation rates of the wildtype may have been caused by a greater root–particle contact compared to the hairless mutant.

### 8.1.4 Comparison of maize and lupin root and shoot elongation in various growth media at different matric potentials

Lupin root and shoot elongation was less sensitive than maize to decreases in matric potential (by approximately 8 %) and increases in mechanical impedance (by approximately 30 %). The reason for this may be that lupin probably stores more water during the germination process, and borderlike cells exuded along the flanks of lupin roots might have built a bridge between root and soil particles and therefore increased root–particle contact, while maize only exude border cells and mucilage at the root tip (Figure 6-4). Furthermore those sloughed borderlike cells might have had a lubricating effect and reduced mechanical impedance in compacted soil (Iijima et al., 2004).

Root elongation rates of both maize and lupin were linearly correlated to the distance between the root hair zone and the root tip. The correlation for maize was slightly better than that for lupin, and probably results from the greater sensitivity towards soil physical stresses. This relationship will be useful for prediction of elongation rates of plants grown under field conditions. Dynamic variables such as root elongation are difficult to determine for excavated roots and are often estimated from repeated observations (differences in root length) (Pagès et al. 2009). A rather complex experimental design is

needed to distinguish between individual differences in root growth or effects of soil conditions on root growth.

The experiments conducted showed less sensitivity of root and shoot elongation to soil physical conditions by young maize seedlings compared to lupin seedlings suggesting that lupin seedlings may establish better than maize in dry and hard soils. Lupin is considered to be more resistant towards mechanical impedance in very hard soils (Materechera et al, 1991). However, it is important to note that in mature plants, lupin has other mechanisms to postpone dehydration during drought, such as a deep rooting system, stomatal closure to reduce water demand at a high leaf water potential and drought escape (French and Buirchell, 2005).

## *8.2 Future Research*

In this thesis the root and shoot elongation at various matric potentials in different growth media was investigated, focussing on the role of root–particle contact.

- In most of the experiments seedlings were grown in repacked soil (sieved) or vermiculite. Measurements of root and shoot elongation rates and root–particle contact in more structured soil would be the next step in understanding root–soil contact for plant growth in field conditions. This could be achieved either by applying different wetting and drying cycles to repacked soils or collecting undisturbed soil cores from a field site.
- The non–transpiring seedlings used in this study were grown for up to four days in darkness, with the seedlings were dependent largely on stored water and

nutrients (Kaydan and Yagmur, 2008). Older plants may become more sensitive to a decrease in root soil contact and in matric potential, especially when plants are transpiring. Root–soil contact and root and shoot elongation rates of plants should be studied under a wide range of conditions (different ages and soil physical stresses) to determine if the sensitivity changes with time.

- The results in this thesis suggest that good root–particle contact is important for root and shoot elongation. Greater root–particle contact allows faster transport of water and nutrients between the root and the growth medium. To test this further it would be of interest to visualize and quantify water uptake of roots in soil. Therefore the method for visualising water in porous media needs to be developed further to quantify the dynamics of soil water distribution and root–water contact around roots.
- Hairless mutants and their wildtypes were used to investigate the effects of root hairs on root and shoot elongation in growth media of various particle/aggregate sizes at different matric potentials. Root hairs should increase root–soil contact, but actual measurements of root–particle contact of the wildtype and the hairless mutant were not conducted. High–resolution imaging of root hairs in soil would allow root–soil contact to be quantified.

# 9 References

Abrol I P and Palta J P 1970 A Study of Effect of Aggregate Size and Bulk Density on Moisture Retention Characteristics of Selected Soils. Agrochimica 14, 157-165.

Alexander K G and Miller M H 1991 The Effect of Soil Aggregate Size on Early Growth and Shoot-Root Ratio of Maize (Zea-Mays L). Plant and Soil 138, 189-194.

Amemiya M 1965 The Influence of Aggregate Size on Soil Moisture Content-Capillary Conductivity Relations1. Soil Science Society of America Journal 29, 744-748.

Asseng S, Aylmore L, MacFall J, Hopmans J, Gregory P, Smit A, Bengough A, Engels C, Van Noordwijk M, Pellerin S and van de Geijn S 2000 Computer-assisted tomography and magnetic resonance imaging. Root methods: A handbook. Springer-Verlag Berlin Heidelberg, 345-363.

Atkinson B S, Sparkes D L and Mooney S J 2009 The impact of soil structure on the establishment of winter wheat (*Triticum aestivum*). European Journal of Agronomy 30, 243-257.

Atwell B J 1988 Physiological-Responses of Lupin Roots to Soil Compaction. Plant and Soil 111, 277-281.

Atwell B J 1990a The effect of soil compaction on wheat during early tillering. New Phytologist 115, 37-41.

Atwell B J 1990b The effect of soil compaction on wheat during early tillering. II. Concentrations of cell constituents. New Phytologist 115, 37-41.

Atwell B J 1990c The effect of soil compaction on wheat during early tillering. III. Fate of carbon transported to the roots. New Phytologist 115, 43-49.

Atwell B J and Newsome J C 1990 Turgor Pressure in Mechanically Impeded Lupin Roots. Australian Journal of Plant Physiology 17, 49-56.

Aylmore L A G 1993 Use of Computer-Assisted Tomography in Studying Water-Movement Around Plant-Roots. Advances in Agronomy 49, 1-54.

Bates T R and Lynch J P 1996 Stimulation of root hair elongation in Arabidopsis thaliana by low phosphorus availability. Plant Cell and Environment 19, 529-538.

Bengough A G and McKenzie B M 1997 Sloughing of root cap cells decreases the frictional resistance to maize (Zea mays L) root growth. Journal of Experimental Botany 48, 885-893.

Bengough A G and Mullins C E 1990 Mechanical Impedance to Root-Growth - A Review of Experimental-Techniques and Root-Growth Responses. Journal of Soil Science 41, 341-358.

Bengough A G and Mullins C E 1991 Penetrometer Resistance, Root Penetration Resistance and Root Elongation Rate in 2 Sandy Loam Soils. Plant and Soil 131, 59-66.

Bengough A G, Bransby M F, Hans J, McKenna S J, Roberts T J and Valentine T A 2006 Root responses to soil physical conditions; growth dynamics from field to cell. Journal of Experimental Botany 57, 437-447.

Bengough A G, Croser C and Pritchard J 1997 A biophysical analysis of root growth under mechanical stress. Plant and Soil 189, 155-164.

Bengough A G, de Kroon H and Visser E J 2003 Root growth and function in relation to soil structure, composition, and strength. Root ecology 151-171.

Bengough A G, Mackenzie C J and Elangwe H E 1994 Biophysics of the Growth-Responses of Pea Roots to Changes in Penetration Resistance. Plant and Soil 167, 135-141.

Bengough A G, McKenzie B M, Hallett P D and Valentine T A 2011 Root elongation, water stress, and mechanical impedance: a review of limiting stresses and beneficial root tip traits. Journal of Experimental Botany 62, 59-68.

Boone F R 1988 Weather and Other Environmental-Factors Influencing Crop Responses to Tillage and Traffic. Soil & Tillage Research 11, 283-324.

Brady D J, Wenzel C L, Fillery I R P and Gregory P J 1995 Root-Growth and Nitrate Uptake by Wheat (Triticum-Aestivum L) Following Wetting of Dry Surface Soil. Journal of Experimental Botany 46, 557-564.

Bruand A, Cousin I, Nicoullaud B, Duval O and Begon J C 1996 Backscattered electron scanning images of soil porosity for analyzing soil compaction around roots. Soil Science Society of America Journal 60, 895-901.

Campbell G S 1988 Soil-Water Potential Measurement - An Overview. Irrigation Science 9, 265-273.

Carminati A, Vetterlein D, Weller U, Vogel H J and Oswald S E 2009 When Roots Lose Contact. Vadose Zone Journal 8, 805-809.

Clark L J and Barraclough P B 1999 Do dicotyledons generate greater maximum axial root growth pressures than monocotyledons? Journal of Experimental Botany 50, 1263-1266.

Clark L J, Whalley W R and Barraclough P B 2003 How do roots penetrate strong soil? Plant and Soil 255, 93-104.

Clark L J, Whalley W R, Dexter A R, Barraclough P B and Leigh R A 1996 Complete mechanical impedance increases the turgor of cells in the apex of pea roots. Plant Cell and Environment 19, 1099-1102.

Croser C, Bengough A G and Pritchard J 1999 The effect of mechanical impedance on root growth in pea (Pisum sativum). I. Rates of cell flux, mitosis, and strain during recovery. Physiologia Plantarum 107, 277-286.

Croser C, Bengough A G and Pritchard J 2000 The effect of mechanical impedance on root growth in pea (Pisum sativum). II. Cell expansion and wall rheology during recovery. Physiologia Plantarum 109, 150-159.

Crossett R N, Campbell D J and Stewart H E 1975 Compensatory Growth in Cereal Root Systems. Plant and Soil 42, 673-683.

Culligan K A, Wildenschild D, Christensen B S B, Gray W G, Rivers M L and Tompson A F B 2004 Interfacial area measurements for unsaturated flow through a porous medium. Water Resources Research 40, 1-12.

DaSilva A P, Kay B D and Perfect E 1994 Characterization of the Least Limiting Water Range of Soils. Soil Science Society of America Journal 58, 1775-1781.

Davies W and Bacon M 2003 Adaptation of roots to drought. Springer-Verlag New York Inc.; Springer-Verlag GmbH & Co. KG, pp. 192.

Deka R N, Wairiu M, Mtakwa P W, Mullins C E, Veenendaal E M and Townend J 1995 Use and Accuracy of the Filter-Paper Technique for Measurement of Soil Matric Potential. European Journal of Soil Science 46, 233-238.

Dexter A R 1987 Compression of Soil Around Roots. Plant and Soil 97, 401-406.

Dexter A R and Tanner D W 1973 Response of Unsaturated Soils to Isotropic Stress. Journal of Soil Science 24, 491-502.

Donald R G, Kay B D and Miller M H 1987 The Effect of Soil Aggregate Size on Early Shoot and Root-Growth of Maize (Zea-Mays-L). Plant and Soil 103, 251-259.

Duliu O G 1999 Computer axial tomography in geosciences: an overview. Earth-Science Reviews 48, 265-281.

Eavis B W 1972 Soil Physical Conditions Affecting Seedling Root Growth 1. Mechanical Impedance, Aeration and Moisture Availability As Influenced by Bulk Density and Moisture Levels in A Sandy Loam Soil. Plant and Soil 36, 613-622.

Evans C E and Etherington J R 1991 The Effect of Soil-Water Potential on Seedling Growth of Some British Plants. New Phytologist 118, 571-579.

Ewens M and Leigh R A 1985 The Effect of Nutrient Solution Composition on the Length of Root Hairs of Wheat (Triticum-Aestivum L). Journal of Experimental Botany 36, 713-724.

Findenegg G R 1987 A Comparative-Study of Ammonium Toxicity at Different Constant Ph of the Nutrient Solution. Plant and Soil 103, 239-243.

Fraser T E, Silk W K and Rost T L 1990 Effects of Low Water Potential on Cortical Cell Length in Growing Regions of Maize Roots. Plant Physiology 93, 648-651.

French R J and Buirchell B J 2005 Lupin: the largest grain legume crop in Western Australia, its adaptation and improvement through plant breeding. Australian Journal of Agricultural Research 56, 1169-1180.

Gahoonia T S and Nielsen N E 1997 Variation in root hairs of barley cultivars doubled soil phosphorus uptake. Euphytica 98, 177-182.

Gahoonia T S and Nielsen N E 2003 Phosphorus (P) uptake and growth of a root hairless barley mutant (bald root barley, brb) and wild type in low- and high-P soils. Plant Cell and Environment 26, 1759-1766.

Gallardo M, Eastham J, Gregory P J and Turner N C 1996 A comparison of plant hydraulic conductances in wheat and lupins. Journal of Experimental Botany 47, 233-239.

Gardner C M K, Bell J P, Cooper J D, Dean T J, Hodnett M G, and Gardner N 1991 Soil water content. In KA Smith and CE Mullins (eds.). Soil analysis: Physical methods, Marcel Dekker Inc. New York, 1-73.

Gee G W, Campbell M D, Campbell G S and Campbell J H 1992 Rapid Measurement of Low Soil-Water Potentials Using A Water Activity Meter. Soil Science Society of America Journal 56, 1068-1070.

Genc Y, Huang C Y and Langridge P 2007 A study of the role of root morphological traits in growth of barley in zinc-deficient soil. Journal of Experimental Botany 58, 2775-2784.

Gilroy S and Jones D L 2000 Through form to function: root hair development and nutrient uptake. Trends in Plant Science 5, 56-60.

Goss M J 1977 Effects of Mechanical Impedance on Root-Growth in Barley (Hordeum-Vulgare-L) 1. Effects on Elongation and Branching of Seminal Root Axes. Journal of Experimental Botany 28, 96-111.

Greacen E L and Oh J S 1972 Physics of Root Growth. Nature-New Biology 235, 24-25.

Greacen E, Walker G and Cook P 1989 Procedure for the filter paper method of measuring soil water suction. CSIRO Division of Soils. Divl. Rep. No. 108, 7.

Gregory P J 2006 Plant roots: Growth, activity, and interaction with soils. Wiley-Blackwell, Oxford.

Gregory P J, Hutchison D J, Read D B, Jenneson P M, Gilboy W B and Morton E J 2003 Non-invasive imaging of roots with high resolution X-ray micro-tomography. Plant and Soil 255, 351-359.

Hamblin A and Tennant D 1987 Root Length Density and Water-Uptake in Cereals and Grain Legumes - How Well Are They Correlated. Australian Journal of Agricultural Research 38, 513-527.

Harris K, Young I M, Gilligan C A, Otten W and Ritz K 2003 Effect of bulk density on the spatial organisation of the fungus Rhizoctonia solani in soil. FEMS microbiology ecology 44, 45-56.

Heeraman D A, Hopmans J W and Clausnitzer V 1997 Three dimensional imaging of plant roots in situ with x-ray computed tomography. Plant and Soil 189, 167-179.

Herkelrath W N, Miller E E and Gardner W R 1977 Water-Uptake by Plants .2. Root Contact Model. Soil Science Society of America Journal 41, 1039-1043.

Hill J N S and Sumner M E 1967 Effect of bulk density on moisture characteristics of soils. Soil Science 103, 234-238.

Hochholdinger F, Park W J, Sauer M and Woll K 2004 From weeds to crops: genetic analysis of root development in cereals. Trends in Plant Science 9, 42-48.

Hofer R M 1991 Root hairs. Plant Roots: The Hidden Half, Marcel Dekker, New York 129-148.

Holford I C R 1997 Soil phosphorus: Its measurement, and its uptake by plants. Aust. J. Soil Res. 35, 227-239.

Iijima M, Griffiths B and Bengough A G 2000 Sloughing of cap cells and carbon exudation from maize seedling roots in compacted sand. New Phytologist 145, 477-482.

Iijima M, Higuchi T and Barlow P W 2004 Contribution of root cap mucilage and presence of an intact root cap in maize (Zea mays) to the reduction of soil mechanical impedance. Annals of Botany 94, 473-477.

Islam A K M S, Edwards D G and Asher C J 1980 Ph Optima for Crop Growth - Results of A Flowing Solution Culture Experiment with six Species. Plant and Soil 54, 339-357.

Itoh S and Barber S A 1983 Phosphorus Uptake by Six Plant-Species As Related to Root Hairs. Agronomy Journal 75, 457-461.

Jarstfer A G and Sylvia D M 1995 Aeroponic culture of VAM fungi. Mycorrhiza: Structure, function, molecular biology and biotechnology. A Varma and Hock B (eds) Mycorrhiza. Springer-Verlag Berlin Heidelberg, 427-441.

Javot H and Maurel C 2002 The role of aquaporins in root water uptake. Annals of Botany 90, 301-313.

Jupp A P and Newman E I 1987 Morphological and Anatomical Effects of Severe Drought on the Roots of Lolium-Perenne L. New Phytologist 105, 393-402.

Kaestner A, Schneebeli M and Graf F 2006 Visualizing three-dimensional root networks using computed tomography. Geoderma 136, 459-469.

Kaydan D and Yagmur M 2008 Germination, seedling growth and relative water content of shoot in different seed sizes of triticale under osmotic stress of water and NaCl. African Journal of Biotechnology 7, 2862-2868.

Ketcham R A and Carlson W D 2001 Acquisition, optimization and interpretation of X-ray computed tomographic imagery: applications to the geosciences. Computers & Geosciences 27, 381-400.

Kirby J M and Bengough A G 2002 Influence of soil strength on root growth: experiments and analysis using a critical-state model. European Journal of Soil Science 53, 119-127.

Kirkegaard J A, So H B and Troedson R J 1992 The Effect of Soil Strength on the Growth of Pigeonpea Radicles and Seedlings. Plant and Soil 140, 65-74.

Kooistra M J, Schoonderbeek D, Boone F R, Veen B W and Van Noordwijk M 1992 Root-Soil Contact of Maize, As Measured by A Thin-Section Technique .2. Effects of Soil Compaction. Plant and Soil 139, 119-129.

Kramer P J and Boyer J S 1995 Water relations of plants and soils. Academic Press, San Diego.

Lapen D R, Topp G C, Edwards M E, Gregorich E G and Curnoe W E 2004 Combination cone penetration resistance/water content instrumentation to evaluate cone penetration-water content relationships in tillage research. Soil & Tillage Research 79, 51-62.

Leong E C, He L and Rahardjo H 2002 Factors affecting the filter paper method for total and matric suction measurements. Geotechnical Testing Journal 25, 322-333.

Lipiec J, Walczak R, Witkowska-Walczak B, Nosalewicz A, Slowinska-Jurkiewicz A and Slawinski C 2007 The effect of aggregate size on water retention and pore structure of two silt loam soils of different genesis. Soil & Tillage Research 97, 239-246.

Loades K W, Bengough A G, Bransby M F and Hallett P D 2010 Planting density influence on fibrous root inforcement of soils. Ecological Engineering 36, 276-284.

Logsdon S D, Parker J C and Reneau R B 1987 Root-Growth As Influenced by Aggregate Size. Plant and Soil 99, 267-275.

Lontoc-Roy M, Dutilleul P, Prasher S O, Han L W, Brouillet T and Smith D L 2006 Advances in the acquisition and analysis of CT scan data to isolate a crop root system from the soil medium and quantify root system complexity in 3-D space. Geoderma 137, 231-241.

Madsen H B, Jensen C R and Boysen T 1986 A Comparison of the Thermocouple Psychrometer and the Pressure Plate Methods for Determination of Soil-Water Characteristic Curves. Journal of Soil Science 37, 357-362.

Materechera S A, Dexter A R and Alston A M 1991 Penetration of Very Strong Soils by Seedling Roots of Different Plant-Species. Plant and Soil 135, 31-41.

McCully M E 1999 Roots in soil: Unearthing the complexities of roots and their rhizospheres. Annual Review of Plant Physiology and Plant Molecular Biology 50, 695-718.

Mirreh H F and Ketcheso J W 1972 Influence of Soil Bulk Density and Matric Pressure on Soil Resistance to Penetration. Canadian Journal of Soil Science 52, 477-483.

Mirreh H F and Ketcheso J W 1973 Influence of Soil Water Matric Potential and Resistance to Penetration on Corn Root Elongation. Canadian Journal of Soil Science 53, 383-388.

Misra R K, Alston A M and Dexter A R 1988 Root-Growth and Phosphorus Uptake in Relation to the Size and Strength of Soil Aggregates.1. Experimental Studies. Soil & Tillage Research 11, 103-116.

Mooney S J 2002 Three-dimensional visualization and quantification of soil macroporosity and water flow patterns using computed tomography. Soil Use and Management 18, 142-151.

Nye P H 1994 The Effect of Root Shrinkage on Soil-Water Inflow. Philosophical Transactions of the Royal Society of London Series B-Biological Sciences 345, 395-402.

Or D and Wraith J M 2002 Soil water content and water potential relationships. In AW Warrick (ed.) Soil physics companion. CRC Press, Washington, DC, 49-84

Owen P C 1952 The Relation of Water Absorption by Wheat Seeds to Water Potential. Journal of Experimental Botany 3, 276-290.

Pagès L, Serra V, Draye X, Doussan C and Pierret A 2009 Estimating root elongation rates from morphological measurements of the root tip. Plant and Soil 1-10.

Passioura J B 1991 Soil Structure and Plant-Growth. Aust. J. Soil Res. 29, 717-728.

Perret J S, Al-Belushi M E and Deadman M 2007 Non-destructive visualization and quantification of roots using computed tomography. Soil Biology & Biochemistry 39, 391-399.

Pierret A, Kirby M and Moran C 2003 Simultaneous X-ray imaging of plant root growth and water uptake in thin-slab systems. Plant and Soil 255, 361-373.

Premalal B and Deen B 2006 Response of early corn (Zea mays L.) growth to soil aggregate size. Advances in Geoecology 38, 195-202.

Read D B and Gregory P J 1997 Surface tension and viscosity of axenic maize and lupin root mucilages. New Phytologist 137, 623-628.

Richards B G and Greacen E L 1986 Mechanical Stresses on An Expanding Cylindrical Root Analog in Antigranulocytes Media. Aust. J. Soil Res. 24, 393-404.

Rieger M and Litvin P 1999 Root system hydraulic conductivity in species with contrasting root anatomy. Journal of Experimental Botany 50, 201-209.

Rogasik H, Crawford J W, Wendroth O, Young I M, Joschko M and Ritz K 1999 Discrimination of soil phases by dual energy x-ray tomography. Soil Science Society of America Journal 63, 741-751.

Sanderson J 1983 Water-Uptake by Different Regions of the Barley Root - Pathways of Radial Flow in Relation to Development of the Endodermis. Journal of Experimental Botany 34, 240-253.

Schnall J A and Quatrano R S 1992 Abscisic-Acid Elicits the Water-Stress Response in Root Hairs of Arabidopsis-Thaliana. Plant Physiology 100, 216-218.

Schneider E C and Gupta S C 1985 Corn Emergence As Influenced by Soil-Temperature, Matric Potential, and Aggregate Size Distribution. Soil Science Society of America Journal 49, 415-422.

Segal E, Kushnir T, Mualem Y and Shani U 2008 Water uptake and hydraulics of the root hair rhizosphere. Vadose Zone Journal 7, 1027-1034.

Sharp R E 2002 Interaction with ethylene: changing views on the role of abscisic acid in root and shoot growth responses to water stress. Plant Cell and Environment 25, 211-222.

Sharp R E and Davies W J 1985 Root-Growth and Water-Uptake by Maize Plants in Drying Soil. Journal of Experimental Botany 36, 1441-1456.

Sharp R E and Davies W J 1989 Regulation of Growth and Development of Plants Growing with A Restricted Supply of Water. Plants Under Stress 39, 71-93.

Sharp R E, Hsiao T C and Silk W K 1990 Growth of the Maize Primary Root at Low Water Potentials .2. Role of Growth and Deposition of Hexose and Potassium in Osmotic Adjustment. Plant Physiology 93, 1337-1346.

Sharp R E, LeNoble M E, Else M A, Thorne E T and Gherardi F 2000 Endogenous ABA maintains shoot growth in tomato independently of effects on plant water balance: evidence for an interaction with ethylene. Journal of Experimental Botany 51, 1575-1584.

Sharp R E, Poroyko V, Hejlek L G, Spollen W G, Springer G K, Bohnert H J and Nguyen H T 2004 Root growth maintenance during water deficits: physiology to functional genomics. Journal of Experimental Botany 55, 2343-2351.

Sharp R E, Silk W K and Hsiao T C 1988 Growth of the Maize Primary Root at Low Water Potentials .1. Spatial-Distribution of Expansive Growth. Plant Physiology 87, 50-57.

Sharp R E, Wu Y J, Voetberg G S, Saab I N and LeNoble M E 1994 Confirmation That Abscisic-Acid Accumulation Is Required for Maize Primary Root Elongation at Low Water Potentials. Journal of Experimental Botany 45, 1743-1751.

Sibley J and Williams D 1990 A new filter material for measuring soil suction. Geotechnical Testing Journal 13, 381-384.

Soille P 2003 On the morphological processing of objects with varying local contrast. Springer-Verlag Berlin Heidelberg pp. 61.

Spollen W G and Sharp R E 1991 Spatial-Distribution of Turgor and Root-Growth at Low Water Potentials. Plant Physiology 96, 438-443.

Spollen W G, LeNoble M E, Samuels T D, Bernstein N and Sharp R E 2000 Abscisic acid accumulation maintains maize primary root elongation at low water potentials by restricting ethylene production. Plant Physiology 122, 967-976.

Sponchiado B N, White J W, Castillo J A and Jones P G 1989 Root-Growth of four Common Bean Cultivars in Relation to Drought Tolerance in Environments with Contrasting Soil Types. Experimental Agriculture 25, 249-257.

Steudle E 2000 Water uptake by roots: effects of water deficit. Journal of Experimental Botany 51, 1531-1542.

Steudle E and Peterson C A 1998 How does water get through roots? Journal of Experimental Botany 49, 775-788.

Stirzaker R J, Passioura J B and Wilms Y 1996 Soil structure and plant growth: Impact of bulk density and biopores. Plant and Soil 185, 151-162.

Stone J A and Wires K C 1990 Water-Content and Soil Core Volume on Brookston Clay Loam. Canadian Journal of Soil Science 70, 255-258.

Tamboli P M, Larson W E and Amemiya M 1964 Influence of Aggregate Size on Soil Moisture Retention. Iowa Academy of Science Proceedings 71, 103-108.

Tang C X, Kuo J, Longnecker N E, Thomson C J and Robson A D 1993 High Ph Causes Disintegration of the Root Surface in Lupinus-Angustifolius L. Annals of Botany 71, 201-207.

Tang C, Longnecker N E, Greenway H and Robson A D 1996 Reduced root elongation of Lupinus angustifolius L by high pH is not due to decreased membrane integrity of cortical cells or low proton production by the roots. Annals of Botany 78, 409-414.

Taylor H M and Ratliff L F 1969 Root Elongation Rates of Cotton and Peanuts As A Function of Soil Strength and Soil Water Content. Soil Science 108, 113-119.

Tinker P B 1976 Roots and Water - Transport of Water to Plant Roots in Soil. Philosophical Transactions of the Royal Society of London Series B-Biological Sciences 273, 445-461.

Tippkötter R, Eickhorst T, Taubner H, Gredner B and Rademaker G 2009 Detection of soil water in macropores of undisturbed soil using microfocus X-ray tube computerized tomography (μCT). Soil & Tillage Research 105, 12-20.

Tracy S, Roberts J, Black C, McNeill A, Davidson R and Mooney S 2010 The X-factor: visualizing undisturbed root architecture in soils using X-ray computed tomography. Journal of Experimental Botany 61, 311-313.

Van Noordwijk M, Kooistra M, Boone F, Veen B and Schoonderbeek D 1992 Root-soil contact of maize, as measured by a thin-section technique. I. Validity of the method. Plant and Soil 139, 109-118.

Varney G T and Canny M J 1993 Rates of Water-Uptake Into the Mature Root-System of Maize Plants. New Phytologist 123, 775-786.

Vaz C M P, Bassoi L H and Hopmans J W 2001 Contribution of water content and bulk density to field soil penetration resistance as measured by a combined cone penetrometer-TDR probe. Soil & Tillage Research 60, 35-42.

Veen B W and Boone F R 1990 The Influence of Mechanical Resistance and Soil-Water on the Growth of Seminal Roots of Maize. Soil & Tillage Research 16, 219-226.

Veen B W, Van Noordwijk M, Dewilligen P, Boone F R and Kooistra M J 1992 Root-Soil Contact of Maize, As Measured by A Thin-Section Technique .3. Effects on Shoot Growth, Nitrate and Water-Uptake Efficiency. Plant and Soil 139, 131-138.

Vincent C D and Gregory P J 1989 Effects of Temperature on the Development and Growth of Winter-Wheat Roots .1. Controlled Glasshouse Studies of Temperature, Nitrogen and Irradiance. Plant and Soil 119, 87-97.

Voetberg G S and Sharp R E 1991 Growth of the Maize Primary Root at Low Water Potentials .3. Role of Increased Proline Deposition in Osmotic Adjustment. Plant Physiology 96, 1125-1130.

Volkmar K M 1996 Effects of biopores on the growth and N-uptake of wheat at three levels of soil moisture. Canadian Journal of Soil Science 76, 453-458.

Watt M, McCully M E and Kirkegaard J A 2003 Soil strength and rate of root elongation alter the accumulation of Pseudomonas spp. and other bacteria in the rhizosphere of wheat. Functional Plant Biology 30, 483-491.

Whalley W R, Bengough A G and Dexter A R 1998 Water stress induced by PEG decreases the maximum growth pressure of the roots of pea seedlings. Journal of Experimental Botany 49, 1689-1694.

Whalley W R, Clark L J and Dexter A R 1994 The Temperature-Dependence of the Maximum Axial Growth Pressure of Roots of Pea (Pisum-Sativum L). Plant and Soil 163, 211-215.

White N A, Hallett P D, Feeney D, Palfreyman J W and Ritz K 2000 Changes to water repellence of soil caused by the growth of white-rot fungi: studies using a novel microcosm system. Fems Microbiology Letters 184, 73-77.

White P F 1990 Soil and Plant Factors Relating to the Poor Growth of Lupinus Species on Fine-Textured, Alkaline Soils - A Review. Australian Journal of Agricultural Research 41, 871-890.

White R and Kirkegaard J 2010 The distribution and abundance of wheat roots in a dense, structured subsoil - implications for water uptake. Plant, Cell and Environment 33.

Whiteley G M, Hewitt J S and Dexter A R 1982 The Buckling of Plant-Roots. Physiologia Plantarum 54, 333-342.

Whitmore A P and Whalley W R 2009 Physical effects of soil drying on roots and crop growth. Journal of Experimental Botany 60, 2845-2857.

Wildenschild D, Hopmans J W, Vaz C M P, Rivers M L, Rikard D and Christensen B S B 2002 Using X-ray computed tomography in hydrology: systems, resolution, and limitations. Journal of Hydrology 267, 285-297.

Witmuss H D and Mazurak A P 1958 Physical and chemical properties of soil aggregates in Brunizem soil. Soil Sci Soc Amer Proc 22, 1-5.

Worrall V S and Roughley R J 1976 Effect of Moisture Stress on Infection of Trifolium-Subterraneum L by Rhizobium-Trifolii Dang. Journal of Experimental Botany 27, 1233-1241.

Wu Y J and Cosgrove D J 2000 Adaptation of roots to low water potentials by changes in cell wall extensibility and cell wall proteins. Journal of Experimental Botany 51, 1543-1553.

Wu Y J, Sharp R E, Durachko D M and Cosgrove D J 1996 Growth maintenance of the maize primary root at low water potentials involves increases in cell-wall extension properties, expansin activity, and wall susceptibility to expansins. Plant Physiology 111, 765-772.

Wu Y J, Spollen W G, Sharp R E, Fry S C and Hetherington R 1993 Root-Growth Maintenance at Low Water Potentials - Increased Activity of Xyloglucan Endotransglycosylase. Journal of Cellular Biochemistry 24, 607-615.

Wu Y J, Spollen W G, Sharp R E, Hetherington P R and Fry S C 1994 Root-Growth Maintenance at Low Water Potentials - Increased Activity of Xyloglucan Endotransglycosylase and Its Possible Regulation by Abscisic-Acid. Plant Physiology 106, 607-615.

Wuest S B 2002 Water transfer from soil to seed: The role of vapor transport. Soil Science Society of America Journal 66, 1760-1763.

Wuest S B, Albrecht S L and Skirvin K W 1999 Vapor transport vs. seed-soil contact in wheat germination. Agronomy Journal 91, 783-787.

Yapa L G G, Fritton D D and Willatt S T 1988 Effect of Soil Strength on Root-Growth Under Different Water Conditions. Plant and Soil 109, 9-16.

Young I M, Crawford J W and Rappoldt C 2001 New methods and models for characterising structural heterogeneity of soil. Soil & Tillage Research 61, 33-45.

Zimmermann H M and Steudle E 1998 Apoplastic transport across young maize roots: effect of the exodermis. Planta 206, 7-19.